STUDIES ON THE CELL WALL OF DINOFLAGELLATE RESTING CYSTS:

MORPHOLOGICAL DEVELOPMENT, ULTRASTRUCTURE,

AND CHEMICAL COMPOSITION

by

John Peter Kokinos

B.S., Stanford University (1982)
M.S., Stanford University (1988)

SUBMITTED IN PARTIAL FULFILLMENT OF THE
REQUIREMENTS FOR THE DEGREE OF

DOCTOR OF PHILOSOPHY

at the

MASSACHUSETTS INSTITUTE OF TECHNOLOGY

and the

WOODS HOLE OCEANOGRAPHIC INSTITUTION

June 1994

©John P. Kokinos 1994

Signature of Author _____
Joint Program in Oceanography,
Massachusetts Institute of Technology /
Woods Hole Oceanographic Institution

Certified by _____
Donald M. Anderson
Thesis Supervisor

Accepted by _____
Hal Caswell
Chairman, Joint Committee for Biological Oceanography,
Massachusetts Institute of Technology /
Woods Hole Oceanographic Institution

STUDIES ON THE CELL WALL OF DINOFLAGELLATE RESTING CYSTS:

Morphological Development, Ultrastructure, and Chemical Composition

by

JOHN PETER KOKINOS

Submitted in partial fulfillment of the requirements
for the degree of Doctor of Philosophy

ABSTRACT

This thesis presents a series of investigations on the specialized cell covering of a dormant stage (the resting cyst) in the life cycle of the marine dinoflagellate *Lingulodinium polyedra*. These cell walls, along with those of resting cysts formed by many other dinoflagellate species, are resistant to degradation and persist in the depositional environment. Selective preservation of these materials has created a rich dinoflagellate fossil record (extending back ~225 million years) which has shown great utility in biostratigraphic applications. By elucidating the nature of resting cyst walls and directly observing their development in laboratory cultures, the research presented here addresses several long-standing questions regarding both the paleontology and biology of dinoflagellates.

Although resting cyst formation has been reported in other extant species, this thesis documents for the first time the morphological development of resting cysts having "fossilizable", morphologically complex cell walls. In laboratory cultures of *L. polyedra*, resting cyst formation is an extremely rapid phenomenon; the transition from thecate, actively swimming planozygote to spine-bearing, morphologically mature hypnozygote occurs within 10-20 minutes. The basic mechanism consists of dramatic cell expansion resulting from the widening of an interstice between the planozygotic cytoplasm and a balloon-like membrane external to the theca. Key morphological events in the development of the distinctive *L. polyedra* resting cyst cell covering occur within this interstice. These include early dissociation and outward migration of the theca, formation of the resistant endophragm, and growth of spines from globules on the surface of the cytoplasm. The level of morphological maturity attained by the encysting cell depends primarily on how much development occurs before rupture of the expanding outer membrane. If rupture is premature, a wide variation of resting cyst morphology may occur, particularly with respect to the size, number, and distribution of processes.

The direct observation of these developmental events has shed much light on several issues regarding resting cyst morphogenesis. First, growth of *L. polyedra* resting cyst spines is clearly centrifugal (i.e. growing radially outward). Although not necessarily representative of spine growth in all species, this mode of formation provides a useful preliminary framework for interpreting some of the "histrichosphaerid" morphologies present in the fossil record. Second, in this species at least, the theca plays no direct role in influencing the morphology of spines. Finally, considerable variation in spine morphology is possible within one biologically-defined species. This last point has considerable significance for cyst-based taxonomy, and strongly suggests that several of the fossil morphotypes traditionally designated as separate species of *Lingulodinium* are, in fact, synonymous.

Ultrastructural examination of *L. polyedra* resting cysts formed in laboratory culture has shown, for the first time, the fine structure of the cell walls enclosing a living, paleontologically-significant resting cyst. Unfortunately, difficulties associated with fixation and infiltration of these thick-walled structures precluded an in-depth investigation of the ultrastructural dynamics underlying the morphological development described above. Preliminary results, however, confirm earlier speculation that only the outermost wall of the *L. polyedra* resting cyst is normally preserved in the fossil record. This outer wall (including spines) appears constructed of closely appressed structural units, an ultrastructural style apparently widespread among species related to *L. polyedra*.

The resistant cell walls of *L. polyedra* resting cysts were isolated from laboratory cultures and chemically characterized by an extensive array of analytical techniques. Both thermal (pyrolysis) and chemical (CuO oxidation) dissociation of this material yielded suites of products consistent with a macromolecular substance composed significantly of aromatic components. In addition, the relative abundance of carboxylated phenols among resting cyst CuO oxidation products indicated that aromatic structural units in the dinoflagellate material may be largely carbon-carbon linked, probably directly through aromatic nuclei. Such a "condensed" arrangement may be, in part, responsible for the remarkable resistance of the dinoflagellate resting cyst wall biopolymer. Overall, the aromatic signature of *L. polyedra* resting cyst wall material can be clearly distinguished from that of both pollen wall "sporopollenin" and classical lignin.

Although some short chain carboxylic acids are generated during CuO oxidation, there is little evidence obtained by dissociation techniques to suggest the significant presence of extended polymethylenic elements in this macromolecular substance. As a result, the dinoflagellate material appears fundamentally different from the highly aliphatic "algaenans" recently identified in the cell wall of several chlorophyte species. Interestingly, pyrolysis (Py-GC/MS) of resting cyst wall material produced an abundance of prist-1-ene, strongly suggesting the presence of bound tocopherols which may play an important structural role in the resistant cell wall biopolymer. Lipid analysis of *L. polyedra* culture extract revealed a series of even carbon numbered fatty acids (C_{14} - C_{24}), as well as sterols (including dinosterol and cholesterol), and a full suite of tocopherols. These compounds are present during construction of the resistant outer wall of the resting cyst, and could function as precursors to the resting cyst wall biopolymer. Another possibility, given the strong aromaticity predicted by the results of pyrolysis and CuO oxidation, is some contribution by aromatic amino acids in an analogous fashion to lignin biosynthesis.

The extensive chemical characterization of the outermost cell wall of *L. polyedra* resting cysts reported in this thesis provides the first rigorous analysis of "fossilizable" biopolymer(s) produced by an extant dinoflagellate. Furthermore, these analyses represent an unprecedented level of chemical characterization of a resistant algal cell wall biopolymer, and clearly demonstrate the unique nature of the *L. polyedra* resting cyst wall. As a result, this work provides the first chemical data to justify the term "dinosporin", previously proposed to distinguish the highly resistant material comprising dinoflagellate resting cyst walls from other resistant cell wall biopolymers.

Thesis supervisor: Donald M. Anderson

ACKNOWLEDGMENTS

On a personal note, I wish to extend a very warm thanks to my many colleagues in the Anderson Lab. In particular, Bruce Keafer and Dave Kulis have been sounding boards for matters both professional and personal, and have taught me many things about science and life. Post docs Bob Miller and Greg Doucette made valuable contributions to my research and also provided diversions by inviting me over for some much appreciated time with their families. Thanks to my fellow dino students Peter Franks, Chris Scholin, Gires

v

TABLE OF CONTENTS

CHAPTER 3, Continued.

CHAPTER 4. THE RESISTANT OUTER WALL OF RESTING CYSTS
OF THE MARINE DINOFLAGELLATE *Lingulodinium polyedra*:
ULTRASTRUCTURE AND CHEMICAL COMPOSITION 147

LIST OF FIGURES

CHAPTER 3

LIST OF TABLES

LIST OF PLATES

CHAPTER 1

Introduction

The dinoflagellates comprise a class of microscopic algae which are widely distributed in both marine and freshwater environments. As a group, these typically single-celled organisms show an extraordinary level of sophistication and diversity in form, structure, nutritional regime, habitat, and life history (see Spector, 1984, and Taylor, 1987). Although once considered to be among the most primitive of all eukaryotes, the dinoflagellates apparently did not emerge until rather late in protistan evolution according to recent, rRNA-based phylogenies (e.g. Gunderson et al., 1987; Lenaers et al., 1989). Dinoflagellates are perhaps best known as biflagellated, free-swimming cells which are often present in great abundance among the plankton where they play a key role in primary production.

This thesis focuses on the ability of some dinoflagellates to enter into a dormant or resting stage as a part of their life cycle. These resting stages are generally thought to occur as a consequence of sexual reproduction: two motile gametes fuse to form a motile zygote (the planozygote) which, after a period of maturation, loses its motility, and synthesizes a new cell covering. The resulting nonmotile cell (called a hypnozygote, or resting cyst) then behaves as a passive particle, eventually sinking to the bottom of the water column. After a period of dormancy, resting cysts germinate, and the emerging motile cells return to the plankton.

Of particular relevance to this study are those species which develop thick and morphologically complex cell coverings during the encystment process. These coverings protect the enclosed cell during dormancy and often display a variety of specialized structural and compositional features. In some dinoflagellate species, the resting cyst cell wall incorporates an extremely resilient and chemically inert biopolymer which allows these structures to resist degradation. Selective preservation of this highly refractory organic

3

material in depositional environments has yielded a rich fossil record of dinoflagellate resting cysts which extends back at least 225 million years.

In recent decades, fossil dinoflagellates have attracted considerable attention due primarily to their utility in biostratigraphic studies, particularly those relating to petroleum exploration. This practical application has been the impetus for intensive morphological and biostratigraphical investigation of fossil dinoflagellates in both academic and industrial laboratories. One consequence of these micropaleontological studies has been a growing interest in the biology of resting cyst formation. Although the extensive resting cyst taxonomy developed by paleontologists is based almost exclusively on morphological details of the fossilized cell walls, the origin and variability of these details are largely unknown. Unfortunately, although recent advances in the ability to culture dinoflagellates in the laboratory have set the stage for biological studies of encystment, little has been done with those few extant dinoflagellates which produce geologically preservable resting cysts.

Research objectives

The primary aim of the research presented here was the exploration of the nature and development of resting cyst cell walls in cultures of a paleontologically relevant extant dinoflagellate species. I define "paleontologically relevant" species as those modern forms which produce resting cysts having morphologies similar to, or representative of, important fossil taxa. A selected list of extant species which fall into this category is provided in Table 1.1. Although several of these species were initially considered as possible experimental organisms for this study, the results described here all derive from investigation of *Lingulodinium* ("*Gonyaulax*") *polyedra*. This autotrophic marine dinoflagellate is widely distributed in coastal environments and the motile cells are well known for several phenomena, including an ability to bioluminesce and the potential to form large blooms. Over twenty strains of *L. polyedra* were established by germinating

4

TABLE 1.1. A selected list of paleontologically significant living dinoflagellates. Cyst/theca relationships from Wall and Dale, 1968, 1969, 1971; and Dale, 1976.

Biological Name	Paleontological Name of Resting Cyst
Gonyaulax digitalis	*Spiniferites bentori*
Gonyaulax scrippsae	*Spiniferites bulloideus*
Gonyaulax spinifera group (undifferentiated)	*Bitectatodinium tepikiense* *Nematosphaeropsis* spp. *Planinosphaeridium membranaceum* *Tectatodinium* spp. *Spiniferites* (several spp.) (*Impagidinium* spp.?)
Lingulodinium polyedra (formerly *Gonyaulax polyedra*)	*Lingulodinium machaerophorum*
Peridinium limbatum	(no separate cyst name)
Protoceratium reticulatum (formerly *Gonyaulax grindleyi*)	*Operculodinium centrocarpum*
Pyrodinium bahamense	*Polysphaeridium zoharyi*
Pyrophacus vancampoae	*Tuberculodinium vancampoae*

isolated cysts in the laboratory. These cultures proved fairly robust, and many were capable of forming resting cysts.

Since it is the resting cyst wall which ultimately contributes to the fossil record, these cell coverings are the focus of the investigations described in subsequent chapters. In brief, I have attempted to examine the *L. polyedra* resting cyst cell covering from three perspectives: morphological development, ultrastructure, and chemical composition. Although these themes were originally selected to address questions arising from the study of the dinoflagellate fossil record, the results of this work are also significant to the biology of the dinoflagellates, particularly in regards to mechanisms of encystment.

Previous Investigations

For general discussion concerning the previous study of both fossil and modern dinoflagellate cysts, the reader is referred to reviews by Evitt (1961, 1970, 1985), Wall (1970, 1971), Sarjeant (1974), Reid and Harland (1977), Williams (1977), Reid (1978), Tappan (1980), Dale (1983), Loeblich and Loeblich (1984), Goodman (1987), Taylor (1987), Harland (1988), and Fensome et al. (1993).

Morphological development. At the beginning of my thesis research, very little information concerning the morphological changes occurring during hypnozygote development existed in the literature. Although reports of the presence of cysts in both laboratory cultures and natural plankton samples are not uncommon, direct observation of the entire planozygote to hypnozygote transition appears to be a very rare event. Early reports of encystment (e.g. Claparede and Lachmann,1859; Wesenberg-Lund, 1908; Huber and Nipkow, 1922, 1923; Entz, 1925, 1931) are often difficult to evaluate, in part because species under investigation consisted mostly of freshwater *Ceratium* whose cyst stages may not even be true hypnozygotes. Tappan (1980) provides a good review of these early observations. More useful are recent life cycle studies (Table 1.2) which

6

TABLE 1.2. *Recent life cycle studies commenting on the planozygote to hypnozygote transition through direct observation.*

Species	Study
Ceratium cornutum	von Stosch, 1965
Gloeodinium montanum	Kelly and Pfiester, 1990
Gonyaulax monilata	Walker and Steidinger, 1979
Gonyaulax tamarensis (*Alexandrium tamarense*)	Turpin et al., 1978
	Anderson, 1980
Gymnodinium catenatum	Blackburn et al., 1989
Gymnodinium pseudopalustre	von Stosch, 1973
Gyrodinium uncatenum	Coats et al., 1984
Peridinium balticium	Liu and Zhang, 1987
Peridinium cinctum	Pfiester, 1975
	Spector et al., 1981
	Pfiester, 1984
Peridinium cunningtonii	Sako et al., 1984
Peridinium gatunense	Pfiester, 1977
Peridinium inconspicuum	Pfiester et al., 1984
Peridinium limbatum	Pfiester and Skvarla, 1980
Peridinium penardii	Sako et al., 1987
Peridinium volzii	Pfiester and Skvarla, 1979
Peridinium willei	Pfiester, 1976
Protogonyaulax catenella (*Alexandrium catenatum*)	Yoshimatsu, 1981
Scrippsiella trochoidea	Watanabe et al., 1982
Wolozynskia apiculata	von Stosch, 1973

comment on the planozygote to hypnozygote transition as observed in laboratory cultures or isolated field populations. Documentation of life cycle stages in these investigations is generally at the level of the light microscope although SEM micrographs are used occasionally. Table 1.3 lists studies which describe an inferred developmental sequence based on observations of morphotypes in samples of natural populations.

Tables 1.2 and 1.3 together include 26 studies covering 22 species. Although these investigations make important contributions to our general understanding of sexual reproduction in dinoflagellates, they contain little information which is relevant to the developmental interpretation of fossil cyst morphology. From this perspective, the available data is lacking in two aspects. First, nearly all species investigated produce hypnozygotes with no geologically preservable components and/or relatively simple morphologies (i.e. lacking the distinctive features--processes or spines, multiple preservable walls, reflections of thecal plates, etc.--commonly used in cyst based taxonomy). Second, accounts of resting cyst development typically fail to provide documentation at the level required by those who take resting cyst morphology seriously. Descriptions of the planozygote to hypnozygote transition tend to be very brief, often limited to one or two sentences, and the quality and quantity of photographs is often frustrating. In some cases, only changes in the character of the cytoplasm are mentioned, with little or no reference to the morphogenesis of the cyst wall. Furthermore, most investigators make no comment concerning the time involved for hypnozygote development. One very interesting exception to the general lack of detailed descriptions of development is von Stosch's (1973) report of resting cyst formation in *Gymnodinium pseudopalustre*, an unarmored freshwater species. Surprisingly, the encysment mechanism of *L. polyedra* , described for the first time in this thesis, is remarkably similar, though much more dramatic.

Ultrastructure. Ultrastructural studies of dinoflagellate cysts, both living and fossil, are listed in Table 1.4. As with the morphological studies discussed above,

8

TABLE 1.3. Studies inferring developmental sequence of hypnozygote (no direct observation).

Species	Study
Ceratium furcoides	Hickel, 1988a
Ceratium rhomvoides	Hickel, 1988b
Peridinium limbatum	Evitt and Wall, 1968
Wolozynskia tylota	Bibby and Dodge, 1972

ultrastructural investigations of living cysts tend to involve species with little relevance to the fossil record, and typically provide only isolated "snapshots" of cyst ultrastructure with limited application to the interpretation of the actual developmental process. An excellent study by Chapman et al. (1982) describes encystment in *Ceratium hirundinella*, a freshwater species which forms an (asexual) vegetative cyst lacking any geologically preservable components. Hypnozygotic cysts examined by Bibby and Dodge (1972), Dürr (1979), Doucette et al. (1989), and Fritz et al. (1989) have relatively simple morphologies of only minor interest to paleontologists. Gao et al. (1989) provide a fascinating look at encystment ultrastructure, but the species under investigation (*Scrippsiella* sp.) forms an outer cyst wall composed in part of calcite; such forms contrast with the organic-walled cysts which dominate the fossil record. TEM micrographs showing fossil cyst ultrastructure have been published by Jux (1968 and later) and von Benedek (1972). These studies provide an interesting glimpse at the fine structure of geologically preserved cyst walls but are unable to show the relationship between these walls and the cells which produced them. With one exception, the ultrastructural investigations cited above utilized traditional TEM methods. Recognizing the difficulties associated with applying these techniques to dinoflagellate resting cysts, Dürr (1979) successfully employed freeze fracture methods to investigate the ultrastructure of the cyst of *Peridinium cinctum*.

Chemical composition. Prior to the chemical investigations in this thesis, the composition of "organic-walled" dinoflagellate resting cysts was largely unknown. Because these structures commonly co-occur with pollen and spores in fossil assemblages, paleontologists and biologists have traditionally referred to preservable resting cyst wall material as sporopollenin or "sporopollenin-like" (e.g. Eisenack, 1963; Atkinson et al., 1972; Bujak and Davies, 1983; Evitt, 1985; Taylor, 1987; Hemsely and Scott, 1991). A few investigators, however, have noted differences between these fossil materials. Correia (1971) noted that when palynomorphs were exposed to increasing temperatures, pollen and spores seemed to show color changes at different rates than dinoflagellates and acritarchs.

TABLE 1.4. Ultrastructural investigations of dinoflagellate cysts.

Species	Study
Living Cysts	
Alexandrium tamarense (*Gonyaulax tamarensis*)	Fritz et al., 1989
	Doucette et al., 1989
Ceratium hirundinella	Chapman et al., 1982
Peridinium cinctum	Durr, 1979
Scrippsiella sp.	Gao et al., 1989
Wolozynskia tylota	Bibby and Dodge, 1972
Unidentified species	Buck et al., 1992
Fossil Cysts	
Apteodinium spiridoides	von Benedek, 1972
Bitectatodinium tepikiense	Jux, 1976
Cordosphaeridium inodes	Jux, 1968a
Hystrichosphaera bentori (*Spiniferites bentorii*)	Jux, 1968b
Hystrichosphaeridium simplex (*Dapsilidinium simplex*)	Jux, 1971
Impletosphaeridium sp.	Jux, 1971
Lingulodinium machaerophorum	Jux, 1971
Oligosphaeridium abaculum	Jux, 1980
Operculodinium centrocarpum	Jux, 1976

Chaloner and Orbel (1971) centrifuged mixed fossil assemblages in a density gradient and observed that dinoflagellate resting cysts displayed a different distribution behavior than pollen and spores. Finally, Sarjeant (e.g. 1986) has reported that fossil dinoflagellates show a consistently different response to various stains when compared with fossil pollen. As a result, this author has proposed the term "dinosporin" to distinguish dinoflagellate resting cyst wall material from that of pollen and spores.

Scope of the thesis

Together, the investigations described in this thesis explore each of the themes presented above. **Chapter 2** provides a detailed account of the morphological development of *Lingulodinium polyedra* resting cysts in laboratory culture. The basic mechanism consists of rapid cell expansion resulting from the widening of an interstice between the planozygotic cytoplasm and a membrane external to the theca. Key morphological events in the development of the resting cyst wall occur within this interstice. These include early dissociation and outward migration of the theca, synthesis of the resistant endophragm, and centrifugal development of cyst processes. The level of morphological maturity attained by the encysting cell depends primarily on how much development takes place before rupture of the expanding outer membrane. If rupture is premature, a wide variation of resting cyst morphology may occur, particularly with respect to the size, number, and distribution of processes. From a paleontological perspective, these results are significant because considerable morphological variation is produced by a single, biologically defined species.

Chapter 3 describes results obtained from testing the hypothesis that the resistant cell wall biopolymer of *L. polyedra* resting cysts may be related to sporopollenin, the macromolecular substances found in the cell covering of higher plant pollen and spores. Resting cyst cell walls were isolated from laboratory cultures by sequentially treating

culture material by solvent extraction, saponification, and acid hydrolysis. For comparison, commercially obtained pollen standards of a gymnosperm (*Juniperus scopulorum*) and an angiosperm (*Quercus rubra*) were similary treated to isolate nearly pure exine fractions. At all stages of processing, residues were characterized by optical microscopy, FTIR microscopy, elemental analysis, "in source" pyrolysis--mass spectrometry (Py-MS), and pyrolysis--gas chromatography--mass spectrometry (py-GC/MS). These techniques allowed a unique chemical fingerprint to be established for each of the resistant cell wall residues. None of the isolated materials showed convincing evidence of a carotenoid-based structure, and therefore represent macromolecular substances distinct from traditionally defined sporopollenin. Overall, the analytical results described here suggest similarities between the isolated cell wall fractions, but also reveal essential differences--particularly between the dinoflagellate and pollen substances.

Chapter 4 accomplishes 3 goals. First, the results from additional chemical characterization (via cupric oxide [CuO] oxidation, lipid analysis, in-source pyrolysis desorption chemical ionization mass spectrometry [Py-(DCI)MS], and solid state ^{13}C nuclear magnetic resonance spectroscopy [^{13}C NMR]) of pollen and dinoflagellate resting cysts are presented. Second, the ultrastructure of the *L. polyedra* resting cyst wall is examined. Finally, chemical, morphological, and ultrastructural data obtained over the course of the thesis are synthesized to form an integrated model of resting cyst wall development.

Major conclusions and suggestions for future research are discussed in **Chapter 5**, and supplemental information is contained in the **Appendices**.

REFERENCES

Anderson, D. M., 1980. Effects of temperature conditioning on development and germination of *Gonyaulax tamarensis* (Dinophyceae) hypnozygotes. *Journal of Phycology*, Vol. 16, No. 2, p. 166-172.

Atkinson, A. W., Jr., Gunning, B. E. S., and John, P. C. L., 1972. Sporopollenin in the cell wall of *Chlorella* and other algae: Ultrastructure, chemistry, and incorporation of ^{14}C acetate, studied in synchronous cultures. *Planta*, Vol. 107, No. 1, p. 1-32.

Bibby, B. T., and Dodge, J. D., 1972. The encystment of a freshwater dinoflagellate: A light and electron-microscopical study. *British Phycological Journal*, Vol. 7, No. 1, p. 85-100.

Blackburn, S. I., Hallegraeff, G. M., and Bolch, C. J., 1989. Vegetative reproduction and sexual life cycle of the toxic dinoflagellate *Gymnodinium catenatum* from Tasmania, Australia. *Journal of Phycology*, Vol. 25, No. 3, p. 577-590.

Buck, K. R., Bolt, P. A., Bentham, W. N., and Garrison, D. L., 1992. A dinoflagellate cyst from Antarctic sea ice. *Journal of Phycology*, Vol. 28, No. 1, p. 15-18.

Bujak, J. P., and Davies, E. H., 1983. *Modern and Fossil Peridiniineae*. AASP Contribution Series Number 13. American Association of Stratigraphich Palynologists Foundation. 203 p.

Chaloner, W. G., and Orbell, G., 1971. A palaeobiological definition of sporopollenin. *In* Brooks, J., Grant, P. R., Muir, M., van Gijzel, P., and Shaw, G., (eds.), *Sporopollenin*, Proceedings of a symposium held at the Geology Department, Imperial College, London, 23-25 September, 1970, Academic Press, London. p. 273-294.

Chapman, D. V., Dodge, J. D., and Heaney, S. I., 1982. Cyst formation in the freshwater dinoflagellate *Ceratium hirundinella* (Dinophyceae). *Journal of Phycology*, Vol. 18, No. 1, p. 121-129.

Claparède, E., and Lachmann, J., 1859. Études sur les Infusoires et les Rhizopodes. *Mémoires Institut National Génevois*, Vol. 6 (1858), p. 392-484.

Coats, D. W., Tyler, M. A., and Anderson, D. M., 1984. Sexual processes in the life cycle of *Gyrodinium uncatenum* (Dinophyceae): A morphogenetic overview. *Journal of Phycology*, Vol. 20, No. 3, p. 351-361.

Correia, M., 1971. Diagenesis of sporopollenin and other comparable organic substances: Application to hydrocarbon research. *In* Brooks, J., Grant, P. R., Muir, M., van Gijzel, P., and Shaw, G., (eds.), *Sporopollenin*, Proceedings of a symposium held at the Geology Department, Imperial College, London, 23-25 September, 1970, Academic Press, London. p.569-620.

Dale, B., 1976. Cyst formation, sedimentation, and preservation: Factors affecting dinoflagellate assemblages in Recent sediments from Trondhheimsfjord, Norway. *Review of Palaeobotany and Palynology*, Vol. 22, p. 39-60.

_____, 1983. Dinoflagellate resting cysts: "benthic plankton". *In* Fryxell, G. A., (ed.), *Survival Strategies of the Algae*, Cambridge University Press, Cambridge, p. 69-136.

Doucette, G. J., Cembella, A. D., and Boyer, G. L., 1989. Cyst formation in the red tide dinoflagellate *Alexandrium tamarense* (Dinophyceae): Effects of iron stress. *Journal of Phycology*, Vol. 25, No. 4, p. 721-731.

Dürr, G., 1979. Elektronenmikroskopische untersuchungen am panzer von dinoflagellaten III. Die zyste von *Peridinium cinctum*. *Archives für Protistenkunde*, Band 122, Heft 1 & 2, p. 121-139.

Eisenack, A., 1963. Hystrichosphären. *Biological Reviews of the Cambridge Philosophical Society*, Vol. 38, No. 1, p. 107-139.

Entz, G., 1925. Über cysten and encystierung der Süsswasser-Ceratien. *Archives für Protistenkunde*, Band 51, Heft 1, p. 131-183.

_____, 1931. Analyse des wachstums und der teilung einer population sowie eines individuums des protisten *Ceratium hirundinella* unter den naturlichen verhaltnissen. *Archives für Protistenkunde*, Band 74, Heft 2, p. 310-361.

Evitt, W. R., 1961. Observations on the morphology of fossil dinoflagellates. *Micropaleontology*, Vol. 7, No. 4, p. 385-420.

_____, 1970. Dinoflagellates--A selective review. *Geoscience and Man*, Vol. 1, p. 29-45.

_____, 1985. *Sporopollenin Dinoflagellate Cysts: Their Morphology and Interpretation*. American Association of Stratigraphic Palynologists Foundation. 333 p.

Evitt, W. R., and Wall, D., 1968. Dinoflagellate studies IV. Theca and cyst of recent freshwater *Peridinium limbatum* (Stokes) Lemmermann. *Stanford University Publications, Geological Sciences*, Vol. XII, No. 2, p. 1-23.

Fensome, R. A., Taylor, F. J. R., Norris, G., Sarjeant, W. A. S., Wharton, D. I., and Williams, G. L., 1993. *A Classification of Living and Fossil Dinoflagellates*. Micropaleontology, Special Publication Number 7. Sheridan Press, Hanover, Pennsylvania. 351 p.

Fritz, L., Anderson, D. M., and Triemer, R. E., 1989. Ultrastructural aspects of sexual reproduction in the red tide dinoflagellate *Gonyaulax tamarensis*. *Journal of Phycology*, Vol. 25, No. 1, p. 95-107.

Gao Xiaoping, Dodge, J. D., and Lewis, J., 1989. An ultrastructural study of planozygotes and encystment of a marine dinoflagellate, *Scrippsiella* sp. *British Phycological Journal*, Vol. 24, No. 2, p. 153-165.

Goodman, D. K., 1987. Dinoflagellate cysts in ancient and modern sediments. *In* Taylor, F. J. R., (ed.), *The Biology of Dinoflagellates*, Botanical Monographs, Vol. 21, Blackwell Scientific Publishers, Oxford, p. 649-722.

Gunderson, J. H., Elwood, H., Ingold, A., Kindle, K., and Sogin, M. L., 1987. Phylogenetic relationships between chlorophytes, chrysophytes, and oomycetes. *Proceedings of the National Academy of Sciences*, Vol. 84, p. 5823-5827.

Harland, R., 1988. Dinoflagellates, their cysts and Quaternary stratigraphy. *The New Phytologist*, Vol. 108, No. 1, p. 111-120.

Hemsley, A. R., and Scott, A. C., 1991. The occurrence and significance of ultrastructure in fossil spores. *Microscopy and Analysis*, Issue 22, 3 p.

Heslop-Harrison, J., 1968. Pollen wall development. *Science*, Vol. 161, No. 3838, p. 230-237.

Hickel, B., 1988a. Sexual reproduction and life cycle of *Ceratium furcoides* (Dinophyceae) *in situ* in the Lake Plussse (F.R.). *Hydrobiologia*, Vol. 161, p. 41-48.

_____, 1988b. Morphology and life cycle of *Ceratium rhomvoides* nov. sp. (Dinophyceae) from the Lake Plussse (Federal Republic). *Hydrobiologia*, Vol. 161, p. 49-54.

Huber, G., and Nipkow, F., 1922. Experimentelle untersuchungen über die entwicklung von *Ceratium hirundinella* O. F. M. *Zeitschrift für Botanik*, Jahrg. 14, Heft 5, p. 337-371.

_____, and _____, 1923. Experimentelle untersuchungen über entwicklung und formbildung von *Ceratium hirundinella* O. F. Muller. *Flora oder Allgemeine Botanische Zeitung*, Band 116, Heft 1 & 2, p. 114-215.

Jux, U., 1968a. Über den feinbau der wandung bei *Cordosphaeridium inoides* (Klump 1953). *Palaeontographica*, Abt. B, Vol. 122, p. 48-54.

_____, 1968b. Über den feinbau der wandung bei *Hystrichosphaera bentori* Rossignol. *Palaeontographica*, Abt. B, Vol. 123, p. 147-152.

_____, 1971. Über den feinbau der wandungen einiger Tertiärer dinophyceen-zysten und acritarcha - *Hystrichosphaeridium, Impletosphaeridium, Lingulodinium*. *Palaeontographica*, Abt. B, Vol. 132, p. 165-174.

_____, 1976. Über den feinbau der wandungen bei *Operculodinium centrocarpum* (Deflandre and Cookson) Wall 1967 und *Bitectatodinium tepikiense* Wilson 1973. *Palaeontographica*, Abt. B, Vol. 155, p. 149-156.

_____, 1980. Über den feinbau der wandung bei *Oligosphaeridium abaculum* Davey 1979. *Palaeontographica*, Abt. B, Vol. 174, p. 1-6.

Kelly, I., and Pfiester, L. A., 1990. Sexual reproduction in the freshwater dinoflagellate *Gloeodinium montanum*. *Journal of Phycology*, Vol. 26, No. 1, p. 167-173.

Lenaers, G., Maroteaux, L., Michot, B., and Herzog, M., 1989. Dinoflagellates in evolution. A molecular phylogenetic analysis of large subunit ribosomal RNA. *Journal of Molecular Evolution*, Vol. 29, p. 40-51.

Liu Zhi-Li and Zhang Shu-Qun, 1987. Observation on the sexual reproduction of *Peridinium bipes* Stein (Dinophyceae). *Acta Botanica Sinica*, Vol. 29, p. 229-235.

Loeblich, A. R., III, and Loeblich, L. A., 1984. Dinoflagellate cysts. *In* Spector, D. L., (ed.), *Dinoflagellates*, Academic Press, Inc., Orlando, p. 443-480.

Pfiester, L. A., 1975. Sexual reproduction of *Peridinium cinctum* f. *ovoplanum* (Dinophyceae). *Journal of Phycology*, Vol. 11, No. 3, p. 259-265.

_____, 1976. Sexual reproduction of *Peridinium willei* (Dinophyceae). *Journal of Phycology*, Vol. 12, No. 2, p. 234-238.

_____, 1977. Sexual reproduction of *Peridinium gatunense* (Dinophyceae). *Journal of Phycology*, Vol. 13, No. 1, p. 92-95.

_____, 1984. Sexual Reproduction. *In* Spector, D. L., ed., *Dinoflagellates*. Academic Press, Inc., Orlando. p. 181-199.

_____, 1989. Dinoflagellate sexuality. *International Reviews of Cytology*, Vol. 114, p. 249-272.

Pfiester, L. A., and Skvarla, J. J., 1979. Heterothallism and thecal development in the sexual life history of *Peridinium volzii* (Dinophyceae). *Phycologia*, Vol. 18, No. 1, p. 13-18.

_____, and _____, 1980. Comparative ultrastructure of vegetative and sexual thecae of *Peridinium limbatum* and *Peridinium cinctum* (Dinophyceae). *American Journal of Botany*, Vol. 67, No. 6, p. 955-958.

Pfiester, L. A., Timpano, P., Skvarla, J. J., and Holt, J. R., 1984. Sexual reproduction and meiosis in *Peridinium inconspicuum* Lemmermann (Dinophyceae). *American Journal of Botany*, Vol. 171, No. 8, p. 1121-1127.

Reid, P. C., 1978. Dinoflagellate cysts in the plankton. *The New Phytologist*, Vol. 80, No. 1, p. 219-229.

Reid, P. C., and Harland, R., 1977. Studies of Quaternary dinoflagellate cysts from the North Atlantic. *American Association of Stratigraphic Palynologists Contribution Series* No. 5A, p. 147-169.

Sako, Y., Ishida, Y., Kadota, H., and Hata, Y., 1984. Sexual reproduction and cyst formation in the freshwater dinoflagellate *Peridinium cunningtonii*. *Bulletin of the Japaense Society of Scientific Fisheries*, Vol. 50, No. 5, p. 743-750.

Sako, Y., Ishida, Y., Nishijima, T., and Hata, Y., 1987. Sexual reproduction and cyst formation in the freshwater dinoflagellate *Peridinium penardii*. *Nippon Suisan Gakkaishi*, Vol. 53, No. 3, p. 473-478.

Sarjeant, W. A. S., 1974. *Fossil and Living Dinoflagellates*. Academic Press, London. 182 p.

_____, 1986. *Review of:* Evitt, W. R., (1985), *Sporopollenin Dinoflagellate Cysts*, AASP Foundation, 333 p. *Micropaleontology*, Vol. 32, No. 3, p. 282-285.

Spector, D. L., (ed.), 1984. *Dinoflagellates*. Academic Press, Inc., Orlando. 545 p.

Spector, D. L., Pfiester, L. A., and Triemer, R. E., 1981. Ultrastructure of the dinoflagellate *Perinium cinctum* f. *ovoplanum*. II. Light and electron microscopic observations on fertilization. *American Journal of Botany*, Vol. 68, No. 1, p. 34-43.

Tappan, H., 1980. *The Paleobiology of Plant Protists*. W. H. Freeman and Company, San Francisco. 1028 p.

Taylor, F. J. R., (ed.), 1987. *The Biology of Dinoflagellates*. Botanical Monographs, Vol. 21. Blackwell Scientific Publications, Oxford. 785 p.

Turpin, D. H., Dobell, P. E. R., and Taylor, F. J. R., 1978. Sexuality and cyst formation in Pacific strains of the toxic dinoflagellate *Gonyaulax tamarensis*. *Journal of Phycology*, Vol. 14, No. 2, p. 235-238.

von Benedek, P. N., 1972. Phytoplanktonten aus dem Mittel- und Oberoligozän von Tönisberg (Niederrheingebiet). *Palaeontographica*, Abt. B, Vol. 137, p. 1-71.

von Stosch, H. A., 1965. Sexualität bei *Ceratium cornutum* (Dinophyta). *Die Naturwissenschaften*, Jahrg. 52, Heft 5, p. 112-113.

_____, 1973. Observations on vegetative reproduction and sexual life cycles of two freshwater dinoflagellates, *Gymnodinium pseudopalustre* Schiller and *Woloszynskia apiculata* sp. nov. *British Phycological Journal*, Vol. 8, No. 2, p. 105-134.

Walker, L. M., and Steidinger, K. A., 1979. Sexual reproduction in the toxic dinoflagellate *Gonyaulax monilata*. *Journal of Phycology*, Vol. 15, No. 3, p. 312-315.

Wall, D., 1970. Quaternary dinoflagellate micropaleontology: 1959 to 1969. *Proceedings of the North American Paleontological Convention*, Part G, p. 844-866.

_____, 1971. Biological problems concerning fossilizable dinoflagellates. *Geoscience and Man*, Vol. 3, p. 1-15.

Wall, D., and Dale, B., 1968. Modern dinoflagellate cysts and evolution of the Perindiniales. *Micropaleontology*, Vol. 14, No. 3, p. 265-304.

_____, and _____, 1969. The "Hystrichosphaerid" resting spore of *Pyrodinium bahamense*, Plate, 1906. *Journal of Phycology*, Vol. 5, p. 140-149.

_____, and _____, 1971. A reconsideration of living and fossil *Pyrophacus* Stein, 1883 (Dinophyceae). *Journal of Phycology*, Vol. 7, p. 221-235.

Watanabe, M. M., Watanabe, M., and Fukuyo, Y., 1982. Encystment and excystment of red tide flagellates I. Induction of encystment of *Scrippsiella trochoidea*. Research Report from the National Institute for Environment, No. 30, (Japan). Eutrophication and Red Tides in the Coastal Marine Environment Progress Report 1979-1980, p. 27-42.

Wesenberg-Lund, C., 1908. *Plankton Investigations of the Danish Lakes-The Baltic Freshwater Plankton, Its Origin and Variation*. Gyldendalske Boghandel, Nordisk Forlag, Copenhagen. 389 p.

18

Williams, G. L., 1977. Dinocysts. Their classification, biostratigraphy and palaoeoecology. *In* Ramsay, A. T. S., (ed.), *Oceanic Micropalaeontology*, Vol. 2, Academic Press, New York, p. 1231-1325.

Yoshimatsu, S., 1981. Sexual reproduction of *Protogonyaulax catenella* in culture. I. Heterothallism. *Bulletin of the Plankton Society of Japan*, Vol. 28, No. 2, p. 131-139.

CHAPTER 2

Morphological development of resting cysts in cultures of the marine dinoflagellate *Lingulodinium polyedra* (= *L. machaerophorum*)

Abstract

The previously undescribed morphological development of resting cysts of the living marine dinoflagellate *Lingulodinium* ("*Gonyaulax*") *polyedra* has been observed in laboratory cultures. Referred to as *L. machaerophorum* in cyst-based taxonomy, this species has a fossil record extending back at least to the Early Eocene. In our cultures, planozygotes preparing to encyst showed a distinctive clear zone in the peripheral cytoplasm and often displayed a characteristic swimming behavior. The transition from motile planozygote to morphologically mature hypnozygote (resting cyst) took approximately 10-20 minutes. Encystment began with several events occurring simultaneously: (1) the cell stopped swimming and came to rest at the bottom of the observation chamber, (2) flagella were expelled from their respective thecal grooves, (3) localized swelling of a membrane external to the theca formed bubble-like protrusions on the surface of the cell, (4) the theca began to dissociate along one or more plate sutures, and (5) a single layer of globules appeared in the clear zone between the theca and cytoplasm. External protrusions then enlarged and merged to liberate a continuous membrane which surrounded the entire cell. Subsequent expansion of this membrane gave the encysting cell the appearance of an inflating balloon. In most cases, the outer membrane remained partially attached to the theca so that expansion caused thecal sections to pull away from the underlying globules and cytoplasm. As the outer membrane enlarged, globules on the surface of the cytoplasmic mass grew radially outward (i.e. centrifugally) beneath the dissociating theca to form processes. Morphological development of the resting cyst ended when the expanding membrane ruptured. The maximum lateral dimension attained by this membrane was about 2.5 times the diameter of the internal body of the cyst. In these cases, cysts developed the distinctive processes characteristic of *Lingulodinium*. Premature rupture of the balloon-like membrane, however, resulted in processes showing considerable variation in size and morphology. Based on the variability of process morphology observed in laboratory

23

cultures of *L. polyedra*, two morphotypes currently designated as separate species of the genus *Lingulodinium* are here synonymized with *L. machaerophorum*.

INTRODUCTION

The ability of some living dinoflagellate species to form cysts was first recognized during observations of natural phytoplankton samples over a hundred years ago. Since periods of rest or dormancy are common in the life cycles of microorganisms, these early reports attracted little attention outside the small group of botanists and zoologists interested in the dinoflagellates around the turn of the century. At this time, difficulties associated with keeping dinoflagellates alive in the laboratory had not been overcome and thus precluded any long-term studies of a single population. Field samples provided isolated glimpses of various life cycle stages, but their significance remained obscure. A good summary of these early observations can be found in Tappan (1980).

Two lines of research, both gaining momentum around the late 1950s and early 60s, began to focus the interest of a large number of investigators on the phenomenon of dinoflagellate encystment. First, studies by paleontologists (Evitt, 1961; Evitt and Davidson, 1964; Wall and Dale, 1968) made it clear that the vast majority of fossil dinoflagellates were actually the preserved remains of cysts and not the thecate, motile cells as was previously thought. Meanwhile, developments in culturing methods finally allowed biologists (e.g. von Stosch, 1964, 1972, 1973; Pfiester,1975, 1976, 1977) to observe the entire life cycle of dinoflagellates maintained in laboratory cultures. These investigations documented the fundamental role of encysted stages in the reproductive strategy of some species and suggested that it was the hypnozygotic resting cysts and not the asexual temporary cysts which were likely to contribute to the fossil record.

An important consequence of the paleontological and biological studies of this period was the development of both a conceptual framework and an experimental system for subsequent investigation of encystment among living dinoflagellates. To date, however, while notable contributions can be cited in some areas, many aspects of resting cyst formation in laboratory cultures remain unexplored. Complete life cycles are known

for only about 30 of the approximately 1500 named living dinoflagellate species (Pfiester, 1989). From a paleontological perspective, perhaps the greatest omission has been the lack of research directed towards the life cycles and modes of encystment of the few extant dinoflagellates which produce resting cysts identical to some of those found in the fossil record. These species (e.g. *Gonyaulax spinifera*, *Pyrodinium bahamense*, *Lingulodinium polyedra*) clearly represent the strongest link between the biology and paleontology of dinoflagellates.

In the present study, our primary objective was to directly observe and document the morphological development of resting cysts in cultures of a paleontologically significant living dinoflagellate. We selected *Lingulodinium polyedra* (Stein) Dodge 1989, a widely distributed autotrophic and bioluminescent species well known for its ability to form large blooms in coastal waters. Resting cysts of *L. polyedra*, referred to as *L. machaerophorum* in cyst-based terminology, have a rich fossil record extending back at least to the Early Eocene. *L. polyedra* grows well in laboratory culture and the vegetative cells have been a popular experimental system for investigation of algal cell cycles, bloom phenomena, circadian rhythms, bioluminescence, photosynthesis, physiology, morphology, and ultrastructure (see Taylor, 1987 for references).

Resting cysts of this species (Plate 2.1, Figure 1) consist of a spherical, cytoplasm-containing inner body covered by a continuous outer wall which bears numerous hollow spines. These cells were first described by Nordli (1951) who deduced their taxonomic affinity after noting an association with *L. polyedra* thecal fragments in plankton samples taken from Oslo fjord in Norway. Shortly thereafter, similar hystrichosphaerid forms were identified in plankton tow material and natural sediments by Erdtman (1954), Mckee et al. (1959), Evitt and Davidson (1964), and Evitt (1967). Direct confirmation of the cyst/theca relationship in this species was provided by Wall and Dale (1968) who, in a series of laboratory experiments, germinated individual resting cysts isolated from natural sediments to yield the thecate, motile form of *L. polyedra*. Since that time, many investigators have

encountered resting cysts of this species in studies of cyst distribution in modern estuarine and marine environments.

Fossil representatives of *L. polyedra* were first described (as *Hystrichosphaeridium machaerophorum*) by Deflandre and Cookson (1955) from Miocene strata in Australia. Subsequently, Wall (1967) made this species the type for the new genus *Lingulodinium*. Dodge (1989) considered the cyst-based genus *Lingulodinium* to have priority in his taxonomic reassignment of modern *Gonyaulax polyedra*, thus combining previously separate biological and paleontological nomenclature for a single species.

To place the description of resting cyst development contained in this paper in a biological context, it is instructive to briefly review a general model of the dinoflagellate life cycle. In this model, a typical thecate dinoflagellate is unicellular, biflagellate and swims freely in water. The motile stage is haploid, and reproduction consists of simple vegetative division. When subjected to environmental stress, cells may form asexual temporary cysts which revive when favorable conditions return. Occasionally, and for reasons not well understood, vegetatively dividing cells produce gametes which fuse to form a diploid motile zygote (the planozygote). Except for being larger in size, planozygotes often closely resemble vegetative cells. In some species, however, the planozygote ultimately loses motility, sheds its theca, and develops one or more new wall layers to become a hypnozygote, or resting cyst. After a period of obligate dormancy, hypnozygotes germinate and the excysting cell undergoes a meiotic division, but the exact timing and nature of this division are not always clear. The resulting daughter cells are motile and resume vegetative growth to complete the life cycle. For more detailed treatment of dinoflagellate reproduction, the reader is referred to summaries in Tappan (1980), Walker (1984), Pfiester (1984, 1989), and Pfiester and Anderson (1987).

In spite of the numerous investigations involving living *L. polyedra* and related species, their life cycles are incompletely known. Previous morphological studies of living *L. polyedra* have reported on aspects of asexual reproduction (Kofoid, 1911; Dürr and

Netzel, 1974; Dürr, 1979), germination of hypnozygotes (Wall and Dale, 1968),

development of newly excysted cells (Lewis and Burton, 1988), and formation of

temporary cysts (Marasovic, 1989). Resting cyst development, however, while certainly

one of the most dramatic transitions in the life cycle of this species, is described in this

paper for the first time.

MATERIALS AND METHODS

Experimental organism

All observations were made with isolates GpES-13, GpES-17, and GpES-19 of

Lingulodinium polyedra (syn. *Gonyaulax polyedra*). The original cultures were

established by J. P. Kokinos in March, 1990 using cysts isolated from sediments collected

at Essvik Station 1 (90 m), Gullmar Fjord, Sweden. Each strain was started from a single

cyst; cultures were not axenic.

Culture medium

All stock and experimental cultures employed ES medium (Provasoli, 1968;

Harrison et al., 1980) modified according to M. Clement Durand (written communication,

1986), with additional minor changes incorporated by our laboratory. Our medium (termed

ES-DK) differs from Provasoli's original recipe as follows: (1) Substituting 12.3 mg of

anhydrous $MnSO_4$ for 16.4 mg tetrahydrate $MnSO_4$ in the preparation of 400 mL of P_{II}

metals primary stock, (2) Adding one third less distilled water in the preparation of ES-DK

working stock, (3) Eliminating Tris, (4) Substituting Guillard's (1975) f/2 vitamin

preparation and enrichment protocol (0.5 mL of f/2 vitamin working stock added to 1 L

seawater), and (5) Adding 9.3 mL ES-DK working stock (rather than the 20 mL specified by Provasoli) to 1L autoclaved/0.22 μm filtered seawater. Table 2.1 describes final concentrations of major nutrients, trace metals, and vitamins in 1 L of ES-DK. In general, medium preparation procedures were identical to those described in Anderson et al. (1984) except that glassware was not treated with Surfasil.

Culturing procedures

Experimental cultures were inoculated with cells in mid- to late-exponential growth to yield an initial concentration of approximately 300 cells per mL. The growth stage of batch cultures was loosely monitored by measuring in vivo fluorescence at 2-day intervals. All cultures were kept at 20° C. Irradiance was provided by Cool-White fluorescent bulbs at approximately 250 $\mu E \cdot m^{-2} \cdot s^{-1}$ PAR. A 14:10 h L:D cycle was used for all experimental and stock cultures.

Observation

Small volumes of culture were removed aseptically from culture tubes in a laminar flow hood using 3 mL autoclaved glass pipettes and placed into microscope slide chambers. For preliminary observation at 100 to 200x, Palmer-Maloney slides were employed. However, to permit use of higher power objectives with shorter working distances, allow precise focusing of the substage condenser, and minimize spherical aberration due to depth of the water sample, special observation chambers were constructed using spacers cut from plastic coverslips (American Scientific Products diSPo Slips, M6100), parafilm "M" (American Can Company), cellophane tape (3M, Scotch Brand Tape 3750-G), or plastic film (Saran Wrap, DowBrands Inc.). Spacers were fixed to standard 1 x 3" glass microscope slides by either self-adhesion (cellophane tape), gentle

29

TABLE 2.1. Final Composition of ES-DK Medium

	mg/L	Concentration (µM)
Major Nutrients		
1. $NaNO_3$	32.55	[N] = 382.99
2. Glycerophosphate of Na	4.65	[P] = 14.35
Trace Metals		
1. EDTA (Na_2) (2 sources)	3.860	[EDTA] = 10.37
2. $Fe(NH_4)_2(SO_4)_2 \cdot 6H_2O$	1.632	[Fe] = 4.16
3. $FeCl_3 \cdot 6H_2O$	0.114	[Fe] = 0.422
4. H_3BO_3	2.651	[B] = 42.88
5. $MnSO_4$	0.286	[Mn] = 1.89
6. $ZnSO_4 \cdot 7H_2O$	0.051	[Zn] = 0.177
7. $CoSO_4 \cdot (x)H_2O$	0.011	[Co] = 0.071
Vitamins (cf. Guillard, 1975)		
1. Thiamin $\cdot$ HCl	0.1	0.296
2. Biotin	0.5 µg	0.002
3. B_{12}	0.5 µg	3.7×10^{-4}
Seawater	1L	

30

heating (parafilm), or a thin layer of Silicon stopcock grease (coverslips, plastic film). Evaporation of medium during observation of cells was reduced by covering chambers with glass coverslips (Corning No. 1 1/2). All light microscopy was carried out on a Zeiss Axioskop equipped with DIC (Nomarski) optics.

Photography

35 mm black and white photography was accomplished using a Zeiss MC 100 camera system and Kodak Technical Pan film. SVHS format video employed an Optronics CS-450 camera/camera control system, Sony Trinitron Super Fine Pitch monitor, Panasonic TL (Time Lapse) SVHS AG-6720A video camera recorder, and 3M Blackwatch ST-120 SVHS videotape.

RESULTS

Timing and Observation of Life Cycle Stages

When inoculated with cells in mid-exponential growth, cultures of *L. polyedra* showed a brief lag phase of typically less than 2 days. Maximum growth rate during exponential phase was approximately 0.7 div./day. *In vivo* fluorescence peaked approximately 3 weeks after inoculation and maximum cell densities (up to 16,000 cells/mL) were recorded 4-5 days after the fluorescence peak. The actual growth limiting factor in batch culture tubes was not determined.

Several previously described life cycle events of *L. polyedra* were encountered in our study. Vegetative cell division occurred with the highest frequency during exponential growth but could be seen at just about any time except late in senescence. Continuous

31

observations of the entire division process were made twice; in both cases, dividing cells were initially thecate and motile. Early stages of cytoplasmic partitioning were visible while the parent theca was still intact. The general pattern of cell division appeared consistent with a typical gonyaulacoid desmoschisis; sutures opened along an oblique line and separated the theca into left anterior and right posterior halves. Each daughter cell retained one half of the parent theca and seemed to regenerate their missing halves as cytoplasmic division progressed. When daughter cells finally detached, newly generated and inherited thecal moieties could not be readily distinguished at low power. No shedding of parental thecal remnants was observed either while daughter cells were still joined or immediately after separation. In both episodes, division lasted approximately 1 hour and cells remained motile throughout the entire process.

Although what appeared to be temporary cysts were frequently encountered during our investigation, we did not witness the actual formation of these structures. In some culture tubes, ecdysed thecae were abundant and typically showed some degree of dissociation in the vicinity of the mid-dorsal precingular plate (Kofoid 3'; Taylor-Evitt 4), presumably to allow escape of a temporary cyst.

In general, syngamy was first noted a day or two beyond the point of peak fluorescence. Gametes (average size : 30-40 μm length; 25-30 μm width) appeared smaller than typical vegetative cells (38-45 μm length; 35-45 μm width), were lighter in color, and often showed a simpler outline (pentagonal in dorsoventral view). In a few cases, larger cells seemed to be fusing, but none of these pairs were observed to complete the process. A typical fusion episode took about 45 minutes and involved one or more intervals during which the fusing cells were non-motile and rested on the chamber bottom. During the present investigation, we did not observe any process which could be clearly interpreted as gametogenesis. In most culture tubes, the small gamete-like cells formed a considerable percentage of the swimming population starting about the time of the fluorescence peak.

Development of the resting cyst.

Resting cyst formation was best observed 5 to 12 days after the fluorescence peak, although in at least two instances it was noted as early as mid-exponential phase. Our description of this process is based on 28 observations of encystment; 13 of these encompassed the entire morphological transition from active planozygote to hypnozygote. The developmental sequence from loss of motility to morphologically mature resting cyst took approximately 10 to 20 minutes. To facilitate description, we divide the encystment process into the following 4 stages: (I) Pre-expansion (cell still motile), (II) Initiation, (III) Cell expansion, and (IV) Rupture of the outer membrane.

I. **Pre-expansion.** This stage encompasses all encystment-related events occurring while the cell is still motile, i.e. planozygotic. With the light microscope, the first detectable evidence signaling commencement of resting cyst formation was the presence of a prominent zone of differentiation in the planozygote peripheral cytoplasm (Plate 2.1, Figure 2). In our cultures, planozygotes could be distinguished from cells in other motile life-cycle stages primarily by their large size (up to 60 μm length, 50 μm width) and darker color, but in some cases (using high magnification), wide growth bands and/or duel longitudinal flagella could be detected. At low power (100x), the differentiated zone appeared as a colorless interstice positioned between the theca and a central mass of pigmented vesiculated cytoplasm. Where it was well developed, the zone was continuously visible at all angles during the swimming behavior of the planozygote suggesting that the interstice completely surrounded the cytoplasm (with the possible exception of the area near the flagellar insertion). At higher power (400x) with DIC contrast enhancement, some faint structure was visible in the clear zone; this consisted mostly of irregular lines (seen in optical cross section) which were roughly parallel to the curvature of the theca. In one specimen, particles in Brownian motion partially filled the interstice. Typically, the boundary between the clear zone and central cytoplasmic mass

33

was not smooth, being defined by the outermost extent of relatively large and rounded cytoplasmic vesicles (Plate 2.1, Figure 2). The irregular nature of this surface gave the clear zone of any given specimen a variable thickness, but that of a well developed interstice averaged ~5 μm.

It should be noted that not all planozygotes displaying the peripheral interstice went on to complete encystment. Specimens observed late in plateau phase often showed a similar feature but none were observed to fully encyst.

In some cases, planozygotes displayed a unique swimming behavior just prior to their hypnozygote transition. Cells would orient themselves with their polar (longitudinal) axis perpendicular to the bottom of the observation chamber and rotate slowly with very little lateral movement, either swimming upward (towards the viewer) or staying roughly at one level. These episodes would often be interrupted by short lateral swims, after which the cell would resume its slow rotation. This behavior, however, was only observed in Palmer-Maloney slides. The extremely shallow water column of the observation chambers used for higher magnification may have prevented planozygotes from adopting this behavior. Whether the "polar spin" is normal encystment behavior or something induced by our observational methods could not be determined.

II. Initiation. This stage includes those events representing the initial morphological changes accompanying the transition from planozygote to hypnozygote: loss of motility, initial expansion of cell membranes, dissociation of the theca, and the appearance of structures which later develop into cyst processes. In our cultures, these events were rapid and often difficult to observe as they occurred more or less simultaneously during the first 1-2 minutes of resting cyst formation.

Loss of motility. The loss of motility was usually abrupt; normal corkscrew swimming stopped and the cell drifted to the bottom of the observation chamber. In some cases, the swimming behavior of the planozygote became less energetic immediately before swimming totally ceased, but again, it is difficult to say whether this is normal behavior or

due to observation conditions (e.g.. high light intensity, cramped swimming space, etc.). On a few occasions, some flagellar motion continued for several seconds after the cell stopped swimming. In one case, final beating of the longitudinal flagella propelled the planozygote forward for a short distance along the bottom of the observation chamber while cell expansion began.

Fate of the flagella. Once the planozygote came to rest, the flagella were expelled from their respective thecal grooves. The absolute cessation of flagellar movement was often preceded by a highly exaggerated writhing. At this point, both longitudinal and transverse flagella commonly showed spherical swellings along their lengths which gave the appearance of beads on a string (e.g. Plate 2.2, Figures 3 and 7). These swellings were present during the last stages of flagellar movement and persisted after motion had stopped. Swellings consistently appeared more numerous and showed more variability in size on the transverse flagellum compared to the longitudinal flagella (Plate 2.2, Figure 10). The writhing movement often left flagella in a tangle; the transverse flagellum usually ending up more tightly tangled than the longitudinal flagella.

All flagella remained connected to the cell during at least the early stages of morphological development, but could be found detached around fully developed resting cysts. In some cases, flagella were observed to fragment during resting cyst development. Isolated flagella or flagellar fragments, still retaining the beads or swellings, were commonly encountered while scanning the bottom of a slide containing residue from an encysting population. Around newly encysted cells, flagella were visible at low focus; a typical arrangement consisted of a tangled transverse flagellum located at some distance from the intertwined longitudinal flagella (Plate 2.2, Figures 3 and 10). In this investigation, we saw no evidence suggesting the presence of a second transverse flagellum. (For a discussion of hypotheses and observations relating to the number of transverse flagella on dinoflagellate planozygotes, the reader is referred to Gao et al., 1989.)

Bulging of membranes external to the theca. Perhaps the most dramatic of the early developmental events is the initiation of cell expansion. One or more membranes external to the theca bulged outward forming blister-like protrusions on the surface of the encysting cell (Plate 2.1, Figure 3). The number, shape and location of initial bulges was variable from episode to episode; on any one specimen, these features were modified relatively quickly as encystment progressed (Plate 2.1, Figures 3-7). On some specimens, bulges seemed to be intratabular with respect to thecal plates. The outer membrane(s) appeared anchored along sutures while bulges developed over plate surfaces (Plate 2.1, Figure 6; Plate 2.2, Figure 4). As the encysting cell continued to expand, bulges appeared to grow outward, coalescing and extending laterally to cover more of the thecal surface (Plate 2.1, Figures 4-5). Eventually, expanding bulges merged to form larger protrusions surrounding the entire cell (Plate 2.1, Figures 6-7). At no time during cell expansion could the outer membrane be resolved into more than one component with the light microscope. As a result, we will refer to this structure as a single membrane in subsequent description.

Thecal dissociation. As bulging of the outer membrane progressed, the theca began to dissociate. Close inspection of the theca at this stage (and later) revealed that dissociation was often not random, but followed a broad pattern. Major breaks in the theca tended to occur in two places, namely along the upper and lower margins of the cingulum. In many cases, these breaks defined three thecal sections: an epithecal hemisphere composed of apical and precingular plates, a hypothecal hemisphere composed of postcingulars and antapical plates, and a cingular "strip" or band. Sections often remained connected locally (Plate 2.2, Figure 5). "Accessory" sutures occasionally opened to partially dissociate larger sections.

Thecae of encysting specimens were significantly different from those encountered on cells in other life cycle stages. The former seemed degraded and looked thinner, with greatly reduced ornament (Plate 2.2, Figures 2, 5, and 9). Margins of growth bands were

36

often visible, but intratabular areas showed only faint topography. At this stage, plates no longer behaved as rigid units, but instead showed some flexibility.

Although, in general, membrane bulges external to the dissociating theca enlarged and grew together, the original outer membrane never completely separated from the theca, remaining attached locally (Plate 2.1 Figures 6; Plate 2.2, Figure 4). Residual attachments often appeared confined along plate sutures. With continued expansion of the cell, the irregularly bulged external membrane became increasingly spherical, and moved away from the underlying cytoplasm (Plate 2.1, Figures 6-8). Because of the residual attachment sites to the dissociating theca, this outward movement pulled thecal sections away from the underlying cytoplasm (Plate 2.2, Figure 6).

Process globules. Simultaneous (or nearly so) with the appearance and early growth of external bulges and the dissociation of the theca, was the modification of the outer surface of the central cytoplasmic mass. During initiation, the irregular surface bounding the vesiculated cytoplasm of the planozygote became better defined (Plate 2.1, Figures 3-4). On this new surface appeared numerous colorless refractive globules in a single layer (Plate 2.1, Figures 4-7; Plate 2.2, Figure 4); the initial number and distribution of these globules varied between specimens. Normally, globules did not contact either the dissociating theca or the expanding outer membrane. On the average, globules measured about 5 μm in diameter.

In the third developmental stage (Expansion), globules extended radially outward to form the characteristic processes of *Lingulodinium* resting cysts. Before this extension, however, globules on some specimens clearly underwent modification in size, shape, and/or location. In some cases, globules completely detached from the cytoplasmic surface and became spherical bodies floating throughout the expansion zone in Brownian motion (Plate 2.3, Figure 1). Reattachment of free-floating globules to the developing cyst was not observed. Another form of modification involved larger initial globules changing into

smaller globules. On any given specimen, globules often varied in size at the beginning of process growth (Plate 2.1, Figure 7).

III. Spherical Expansion and Process Formation. Stage III begins when the outer wall approaches circularity in optical cross section and globules on the surface of the cytoplasm begin development into processes.

Cell geometry. During this stage, continued expansion of the outer membrane gave the encysting cell the appearance of an inflating balloon (Plate 2.1, Figures 7-12). Although this expansion tended to be laterally symmetric (i.e. outer membrane equidistant from the surface of the internal cytoplasmic mass), asymmetric geometries were observed early in the developmental sequence of some specimens. These latter episodes resulted when thecal sections adhered to the underlying cytoplasmic surface or globules. Since the outer membrane often remained partially attached to thecal sections, expansion became skewed and the cytoplasmic mass and outer membrane were not concentric. With continued inflation of the cell, however, the growing outer membrane eventually peeled recalcitrant thecal sections away from the cytoplasm to establish a more symmetric geometry.

In spite of this apparent shift from asymmetric to symmetric development, however, the inner cyst body and the outer wall were never truly concentric. Critical focus on encysting cells showed a consistent difference in vertical position of the equator of the outer membrane verses that of the internal cytoplasmic mass (e.g. Plate 2.1,. Figures 11 and 12). In this case, the equator of the outer membrane was always higher than that of the internal cytoplasmic mass, a vertical asymmetry probably caused by cyst formation and expansion pressure against the glass bottom of the observation chamber.

Contents of the expansion zone. During cell expansion, the widening zone between the cytoplasmic mass and the outer membrane typically showed the same optical character as the external medium (e.g. Plate 2.1, Figures 10 and 12). In two cases, however, what

38

appeared to be cytoplasmic particles vibrating in Brownian motion occupied a small portion of this space.

Process formation. Process formation involved two basic steps. First, centrifugally developing process shafts (i.e. growth initiates at the cytoplasmic surface and shafts grow outward) were deposited beneath the globules, and second, globules were modified to form process tips. Radial growth of processes did not occur immediately after appearance of the globules on the surface of the cytoplasm but commenced after a short interval of time, normally on the order of a few minutes. The first recognizable portion of a developing process appeared between a globule and the cytoplasmic surface (Plate 2.1, Figure 7). While proximal portions of the processes formed, globules persisted distally, initially maintaining their size, shape, and optical character (Plate 2.1, Figures 7-10). In some cases, the diameter of terminal globules decreased slightly as development proceeded.

Proximally, process shafts tended to be larger in diameter than the later-formed distal portions (Plate 2.1, Figures 10 and 11). As mentioned previously, not all globules were identical in size at the start of process development. Larger globules tended to yield wider though not necessarily longer processes. Once initiated, process formation appeared smooth and continuous, though not necessarily at the same rate for all processes on a given specimen. During early stages of growth, the rigid and structurally competent appearance of the partially-built process shafts contrasted sharply with the delicate bubble-like appearance of the distal globules (Plate 2.1, Figures 8 and 9). Surface features such as longitudinal striations - often visible on processes of morphologically-mature *L. polyedra* resting cysts - could be detected at the earliest phase of process material deposition; these features formed in a centrifugal fashion as an integral part of the process shaft.

Thecal interference. As mentioned above, process outgrowth typically was delayed for several minutes after globules first appeared on the surface of the cytoplasmic mass. Normally, this allowed for sufficient expansion of the outer membrane (at least laterally) to pull the dissociating theca away from the underlying globules before the initiation of

process deposition. As a result, process development usually occurred without contact with the theca (Plate 2.1, Figures 7-12). In some cases, however, portions of the dissociating theca did not move far enough to avoid contact with the outgrowing processes. (This was certainly true for the area of each encysting specimen in contact with the bottom of the observation chamber.) However, as long as the theca had room to move (i.e. not pinned between the inner body and the observation chamber bottom or sides), processes appeared to develop normally. It was not clear if process outgrowth pushed back the interfering sections of theca or if sections were pulled away by continued expansion of the outer membrane.

Modification of terminal globules. The final step in the development of process morphology began after deposition of process shaft material was complete and outer membrane expansion reached a maximum, both of which occurred at more or less the same time. As seen in optical section, the maximum diameter obtained by the outer wall was about 2 times the diameter of the inner body (Plate 2.1, Figure 10). At this point, modification of distal globules gave each process its final form. In most cases, modification of process tips occurred without contacting either remnants of the theca or the expanding outer wall. Observed globule modifications were of 3 basic types:

1. Globules constricted to form tapering extensions to the already-formed process shafts (Plate 2.1, Figures 9-10). These extensions often bore spinules which formed during collapse of the initially smooth, unornamented spherical globules. The first signs of spinule formation often could be observed while the globule was still spherical, appearing as irregularities on the surface. These irregularities then remained behind as topographic highs while the rest of the globule surface collapsed around them (Plate 2.1, Figures 10-12). Spinule presence and morphology was highly variable among different specimens but also between different processes occurring on a single specimen (Plate 2.2, Figure 1).

40

2. Globules deflated only sightly, retaining a spherical or bulbous shape (Plate 2.2, Figure 8) and developed a rigid appearance similar to that of the process shaft. Bulbous terminations were observed with or without spinule ornamentation.

3. Globules collapsed into irregularly shaped masses. These terminal structures did not appear as simple hollow extensions of the shaft, but served to give the process a more capitate appearance (Plate 2.2, Figures 11 and 12). During formation of these irregular structures, numerous faint particles of varying size and in Brownian motion could be seen localized near collapsing terminal globules. The origin of these particles was not observed

Free-floating globules (see above), if present, were modified in a fashion similar to and simultaneously with process tip globules. Detached globules collapsed into irregularly shaped particles which continued to vibrate in Brownian motion. After globule modification, the morphologically mature resting cyst was often observed to twitch and/or rotate slightly within the still-intact outer membrane. The mechanism for this movement could not be determined.

IV. Rupture of the outer membrane. The final stage of development involved rupture of the outer membrane and release of the newly-formed resting cyst. Rupture occurred suddenly, as in the popping of a balloon. In most cases, the outer membrane disintegrated immediately. Occasionally, however, portions of this membrane persisted for several seconds and could be seen collapsing onto the cyst processes (Plate 2.3, Figures 3 and 6). Whether occurring immediately after rupture or delayed, disintegration of the membrane was instantaneous, breaking into small and very faint particles which dispersed rapidly in the surrounding medium.

Rupture of the outer membrane allowed the back-migration of thecal sections which often came into contact with the processes. As a result, morphologically mature resting cysts encountered at the bottom of our culture vessels were often partially enclosed by or

41

closely associated with portions of the theca belonging to the original planozygote (Plate 2.2, Figures 1, 8, and 9).

Newly liberated resting cysts appeared morphologically mature and looked more or less identical to cysts recovered from natural sediments. The spherical inner body of a mature resting cyst typically measured about 50 µm in diameter; with well-formed processes, the total resting cyst diameter averaged about 70 µm. Continued observation of some specimens for up to 3 months revealed no additional changes in gross morphology. Resting cysts formed in our observation chambers typically showed one side bearing shorter, and in some cases bent, processes (Plate 2.1, Figure 1) presumably reflecting their impeded growth against the chamber bottom. Immediately after formation, the typical resting cyst cytoplasm appeared evenly colored brownish-grey with dispersed orange-red pigment. Within 24 hours, the cytoplasm appeared lighter, almost colorless, and orange red pigment seemed to be localized in a small number of patches. On some specimens, these patches were very well defined, to the point were they resembled mineral grains. Also developing within this time was the endospore, a thin clear band between the outermost cyst wall and the cytoplasm (e.g. Plate 2.3, Figure 7). In most specimens, this band was irregular in thickness and displayed a characteristic interference figure (reminiscent of a uniaxial cross) when viewed with crossed nicols at low magnification. Such an interference figure has been noted for other dinoflagellate cysts (Erdtman, 1954; Reid and Boalch, 1987). Particles in Brownian motion were commonly observed throughout the cytoplasm. Periodic examination of cysts over several months revealed that the orange-red bodies changed both in position and number over time.

Premature rupture of the outer membrane

In our observation chambers, encysting cells attaining full expansion, with subsequent formation of morphologically mature processes, were the exception rather than

the rule. In most cases, the outer membrane ruptured prematurely, before modification of process tip globules was complete.

The most visible result of premature rupture was the interruption of normal process development. If rupture occurred before the initial deposition of process material, globules tended to detach from the surface of the cytoplasm and disperse in the surrounding medium (Plate 2.3, Figure 1); the resultant "cyst" was sub-spherical and typically showed an irregular distribution of processes (Plate 2.3, Figure 3). In the present investigation, no attempts were made to determine the viability of such aberrant cysts. If rupture occurred during process shaft deposition, terminal globules completely collapsed leaving behind sharply truncated processes (Plate 2.3, Figures 3, 6, and 7). The premature collapse of terminal globules occurred in two different ways. (1) The initially smooth and spherical globules developed a granular surface texture which appeared to quiver as though surface granules were in Brownian motion. This was followed by rapid and complete deflation of the globule (globule material appeared to collapse into the process shaft) to yield a truncated process. (2) After rupture, terminal globules deflated smoothly while maintaining their spherical morphology (Plate 2.3, Figures 4-6). With the light microscope, we were unable to determine if truncated processes were distally open or closed.

DISCUSSION

In this paper, the morphological development of *L. polyedra* resting cysts is described for the first time. The basic mechanism consists of rapid cell expansion resulting from the widening of an interstice between the planozygotic cytoplasm and a membrane external to the theca. Key morphological events in the development of the resting cyst take place within this expanding interstice. These include early dissociation and outward migration of the theca, synthesis of the sporopollenin-like endophragm, and centrifugal

development of cyst processes. The level of morphological maturity attained by the encysting cell depends primarily on how much development occurs before rupture of the expanding outer membrane. If rupture is premature, a wide variation of resting cyst morphology may occur, particularly with respect to the size, number, and distribution of processes. From a paleontological point of view, these results are significant because considerable morphological variation is produced by a single biologically defined species.

Life cycle

Since the complete life cycle of *L. polyedra* has never been described, it seems appropriate to briefly comment on some of the life cycle stages, in addition to resting cyst formation, observed in our investigation. Vegetative cells in the process of asexual division were frequently encountered, particularly during exponential growth. The morphological details of desmoschisis appeared essentially consistent with previous descriptions by Dürr and Netzel (1974) and Dürr (1979) for this species. However, in the two complete episodes of asexual division we followed, daughter cells were not observed to shed their inherited thecal moieties as was reported by the latter author. Such shedding may have taken place after the physical separation of daughter cells, but we did not track cells beyond this point. It is interesting to note that most of the thecal material which accumulated at the bottom of our culture tubes consisted of relatively entire thecae. If cells routinely shed well-defined thecal "halves" during vegetative division, one would expect to encounter large numbers of these moieties in culture vessel residues. Although both Kofoid (1911) and Dürr and Netzel (1974) mention vegetative division among naked cells, no clear indications of this phenomenon were encountered during our study.

When batch culture growth became limiting (as indicated by maxima in fluorescence and cell density), morphologically distinct gametes appeared which were later observed fusing in pairs to form motile zygotes. Since experimental cultures in this investigation

were started from cysts, all mating types (if they exist) are assumed to be present in any given batch culture. As a result, it was not possible to determine if *L. polyedra* was homothallic (all gametes identical and capable of indiscriminate fusing) or heterothallic (mating types exist and "plus" and "minus" strains required for fusion; see Pfiester and Anderson, 1987). After a period of cell fusion, large, darker-colored cells with two longitudinal flagella and wide thecal growth bands began to form a significant percentage of the swimming population. We consider these cells to be planozygotes. As reported in this paper, planozygotes transformed directly into resting cysts. Since we did not follow individual cells throughout all stages of sexual reproduction (cf. Pfiester, 1975, 1976, 1977), a rigorous definition of the complete life cycle of *L. polyedra* is not possible at this time. Nevertheless, our observations strongly suggest a course of events consistent with the basic dinoflagellate sexual cycle model summarized by Dale (1983).

Cells appearing to be temporary or pellicle cysts were quite common in some of our cultures, although formation of these forms was not observed directly. In our study, there was no obvious connection between the occurrence of temporary cysts and any recognizable event in the sexual life cycle outlined above. This observation contrasts with the preliminary report of Marasovic (1991) which suggested that temporary cyst formation may be a precursor to resting cyst formation among natural populations. In our laboratory cultures, resting cysts of *L. polyedra* formed directly from actively swimming planozygotes without any pellicle or temporary cyst intermediates.

It is interesting to consider the implications surrounding the observation of resting cyst formation during early to mid log-phase growth of batch cultures. If our interpretation of the life cycle is accurate, encystment must be preceded by gametogenesis, syngamy, and planozygote maturation. These events, however, are commonly hypothesized to occur as a result of limitation following exponential growth (Anderson et al., 1984; Anderson and Lindquist, 1985; Pfiester and Anderson, 1987). One possible revision of this hypothesis might cast the first step towards resting cyst formation (namely gametogenesis) as a broad

response to several kinds of stresses - not necessarily involving limitation - which cells may experience in the batch culture environment. For example, early gametogenesis induced in a small percentage of cells by inoculation shock might be one explanation for the hypnozygote formation occasionally observed during log-phase growth.

Morphology of hypnozygote development

To date, most reports of dinoflagellate resting cyst formation mention the deposition of one or more new walls which surround the cytoplasm as the cell loses motility. In armored species, these layers form beneath the theca which tends to remain more or less intact until cyst formation is complete. The only published encystment mechanism among the dinoflagellates that approaches what we have observed for *L. polyedra* appears to be that of *Gymnodinium pseudopalustre*, an athecate, freshwater dinoflagellate whose life cycle was described by von Stosch (1973). Planozygotes of this species were observed to secrete an outer membrane (termed the preliminary wall by von Stosch) which, upon swelling, formed a "hyaline interstice" around the cytoplasm. Granules then formed on the surface of the cytoplasmic mass and these elongated outward into short, hair-like spines as the outer wall continued to expand to a maximum diameter (based on our interpretation of von Stosch's illustrations) of about 1.5 times the diameter of the inner body. Rupture of the preliminary wall liberated the hypnozygote. The entire sequence described by von Stosch lasted 9 minutes.

Although quite striking as a dynamic morphological phenomenon, resting cyst formation in *L. polyedra* was relatively difficult to observe in its entirety. The loss of planozygote motility and beginning of cell expansion is extremely rapid (on the order of seconds) and the chance of encountering this initiation event in a random low-magnification survey of lab cultures or natural populations is correspondingly low. In our investigation, planozygotes likely to encyst (showing a well developed peripheral interstice) were

46

identified and tracked under the microscope at 200x so that initiation events could be observed and documented. Tracking episodes lasting one to two hours were not uncommon and as a result considerable time was invested at the microscope. In addition, key encystment structures such as the balloon-like outer wall and process globules were usually very faint and required contrast enhancement and relatively high magnification for observation and photography. Given these difficulties, it is not surprising that detailed descriptions of dinoflagellate encystment have been rare in the literature.

Planozygote cytoplasm. Our account of the morphological development of resting cyst formation in *L. polyedra* begins with the observation of a zone of cytoplasmic differentiation beneath the planozygote theca. Although changes in the cell leading to the development of this peripheral interstice must begin at some point during planozygote maturation, the exact nature and timing of these events were not detectable with the light microscope. The actual mechanism of cytoplasmic differentiation was not observed in the present study but it is interesting to note that when multiple specimens showing the peripheral interstice could be seen simultaneously, some variability in zone definition and character was clearly visible. It is unknown whether these differences represented different stages of cytoplasmic differentiation or, alternatively, if differentiation occurred to different degrees in different specimens.

Regarding the significance of the peripheral zone, it seems likely that this feature represents consolidation and/or modification of cytoplasmic components in preparation for cyst formation. Extensive rearrangement of cytoplasm was noted during an ultrastructural investigation of encystment of freshwater *Woloszynskia tylota* by Bibby and Dodge (1972). Similar observations were reported in studies of *Scrippsiella* sp. (Gao et al, 1989) and *Alexandrium tamarense* (Fritz et al., 1989; Doucette et al, 1989). In an investigation of the fine structure of the *L. polyedra* cell surface, Dürr and Netzel (1974) mention but do not illustrate the presence of a "hyaline zone" around the cytoplasm of cells preparing for

ecdysis. This suggests that a peripheral interstice is not unique to planozygotes but may signal the reorganization of cytoplasm during other life cycle stages as well.

Theca. Degradation of thecal cellulose has been observed by Netzel and Dürr (1984) during vegetative division of *Peridinium cinctum*. In our study of *L. polyedra*, cellulose degradation clearly occurs prior to and/or during dissociation of the theca during resting cyst formation. Again, the precise timing and nature of this phenomenon could not be determined. Intuitively, a reduction in the rigidity of the thecal plates seems consistent with an encysting cell trying to shed its planozygotic amphiesma. Our observations suggest some sort of enzymatic dissolution of the theca. Severe reduction of all surface features indicates that dissolution is not localized with respect to any part of the thecal plates. One hypothesis to explain thecal degredation might invoke resorption of cellulose just prior to encystment in order to build reserves which later are used in the deposition of the cellulosic endospore. Our report of thecal degradation during encystment contrasts with Dale's (1983, p. 103) observation that "thecal plates attached to fully developed cysts [of *L. polyedra*] usually show no evidence of decay".

Outer membrane. This feature appears homologous to the "preliminary wall" described by von Stosch (1973). At the level of the light microscope, it is difficult to correlate the bulging outer membrane with any specific amphiesmal component described in ultrastructural studies of *L. polyedra* (Schmitter, 1971; Gaudsmith and Dawes, 1972; Sweeny, 1976; Dürr 1979; Lewis and Burton, 1988). At the very least, it seems safe to assume that this membrane incorporates the plasmalemma, but it may be possible that other membranes are involved as well. In some encystment sequences, initial bulging was clearly intratabular; i.e. the outer membrane remained temporarily anchored along thecal sutures while bulges formed over plate areas. Although connections between outer membrane and theca are largely broken during the early stages of cell expansion, some degree of "connectedness" persists throughout encystment. These remnant attachments allow the expanding outer membrane(s) to pull thecal sections away from the underlying

cytoplasm and process globules. One way to explain these observations is that expansion may initiate *within* amphiesmal vesicles. If this is so, bulges exterior to the theca are bound by both the plasmalemma and the outer vesicular membrane (see Loeblich, 1970; Dodge and Crawford, 1970; Morrill and Loeblich, 1983; Höhfeld and Melkonian, 1992; and Bricheux et al., 1992 for amphiesmal ultrastucture). Elucidation of these ultrastructural details will require future investigation at the level of the electron microscope.

Cell expansion. A model of outer membrane expansion invoking a simple sphere increasing in diameter from 50 to 125 μm, gives an increase in cell volume of roughly 16x, this occurring in less than 20 minutes. There are three hypotheses which may account for this phenomenon: (1) Soluble compounds from outside the cell are transported across the outer membrane; (2) Volume increases "internally" either by alteration of existing cytoplasmic contents or the production of new material; and (3) A combination of internal and external sources. As noted previously, the optical character of the material filling the space between the cytoplasmic mass and outer membrane appears identical to that of the external medium, suggesting that the expanding "balloon" may be filled with fluid pumped from the cell's exterior environment. Interestingly, von Stosch (1973) mentioned a mass of "coagulum" adhering to a newly formed resting cyst of *G. pseudopalustre* and speculated that it represented the remnants of material filling the space between the outer ("preliminary") wall and inner body. There was no obvious release of such material during rupture of the outer wall in our investigation of *L. polyedra*.

Endophragm formation. The precise nature and timing of endophragm formation are unclear. Close examination of photographed sequences show the cytoplasmic mass to be more or less irregular in shape without a well-defined boundary layer throughout the initiation stage of encystment. At the level of the light microscope, a wall-like layer surrounding the cytoplasm first becomes detectable near the time of preliminary globule development. Globules, however, are clearly present (although perhaps not fixed in terms of size and location) before this "proto-endophragm" becomes

well defined suggesting some overlap in the formation of periphragm (i.e. processes) and endophragm. According to von Stosch (1973), spine growth and "exospore secretion" occur concurrently during encystment of *G. pseudopalustre*. As with other aspects of encystment, a more detailed description of wall formation requires investigation at the level of the electron microscope.

Globules. Process globules presumably derive from the cytoplasmic mass, although this origin was not visibly obvious during the flurry of activity accompanying the initiation of the planozygote to hypnozygote transition. The structure, composition, and contents of the globules as well as their exact relationship to the developing cyst processes are unknown. With the light microscope, globules appear as bubbles which form the terminal structures of hollow processes. What drives the outward migration of the globules? Is this movement solely the result of adding process shaft material beneath the globules or perhaps a response to physical forces such as pressure acting within the cell?

The dynamic nature of globule shape, size, and position during the early stages of cyst formation suggests that process distribution and/or morphology are not fixed until expansion of the cell is well underway. The degree to which distribution and morphology are directly controlled by the cell as opposed to "generic physical mechanisms" (buoyancy, surface tension, adhesion, etc.; see Newman and Comper, 1990) is unknown.

Processes. In the terminology of cyst morphology, processes on the cyst of *L. polyedra* represent an outer wall layer referred to as the periphragm. On fully developed cysts, the material which forms these processes is visually similar to that of the endophragm and both layers respond similarly to chemical treatments such as acetolysis. Our observations on the morphology of spine development prompt questions regarding the chemical and ultrastructural details of cyst wall formation. For example, what is the source of the sporopollenin-like material which ultimately forms the chief structural component of the processes? Is it newly synthesized during the relatively rapid deposition of spines or

are precursors formed and stored in the planozygote so that the dynamics described in this report represent merely an assembly phase?

During process elongation, it is clear that the composition and/or structure of the terminal globules differ from that of the process shaft. This is supported by the reaction of these features to premature rupture of the outer membrane - terminal globules collapse and disappear while process shafts appear unaffected. At which point do process shafts and terminal structures become chemically indistinguishable and what is the nature of this transition? During uninterrupted encystment episodes (i.e. those that escape premature rupture), any unattached free-floating globules undergo collapse simultaneously with the modification of terminal globules into process tips which occurrs at least several minutes before rupture of the outer membrane. This suggests that some kind of signal, acting throughout the entire region between the inner cyst body and the outer wall, triggers the structural and chemical modification of terminal globules into terminal process structures.

Variability of process length. Resting cysts formed in our laboratory cultures occasionally showed reduced processes on one side of the inner body. This presumably relates to cyst formation as cells rested against the bottom of the various culture vessels employed in this study. In contrast, resting cysts recovered from sediments display a more even distribution of long and short processes suggesting that cyst formation in natural waters occurs while cells are in soft sediments or still suspended in the water column. In the absence of external obstruction, expansion of the outer membrane and subsequent process development is likely to be symmetrical.

Rupture of the outer membrane. Thus far, outer membrane rupture has been referred to as either "normal" (i.e. releasing a morphologically mature resting cyst) or premature. Details relating to how the outer membrane actually expands and what causes it to rupture are unknown. In most encystment sequences, rupture of the outer membrane appears to be the result of this feature reaching its physical limit of expansion although this certainly does not rule out a mechanism involving some kind of physical and/or chemical

51

disruption. Regarding the physical integrity of the outer wall, it is noteworthy that encysting cells in the late stages of expansion, in spite of their delicate appearance under the microscope, were occasionally observed to withstand being rammed by swimming cells.

As to the causes of premature rupture, an important question concerns whether cells are "internally" predisposed towards this phenomenon (e.g. early rupture due to aberrant physiological state of the cell) or whether the cause is external and due to a more immediate physical and/or chemical "disruptant" in the culture environment. In our study, there was no obvious correlation between any visual character of an encysting cell and its disposition to premature rupture. All observed episodes of encystment involved cells resting against the bottom of covered, motionless chambers suggesting that turbulence is not a necessary factor for premature rupture. Other possible disruptants might include heat from microscope illumination, salinity changes due to evaporation, pH imbalance, bacterial metabolites, and other contaminants in the culture medium.

Surveys of cysts collected from the bottom of our culture tubes often showed a relatively high proportion of the population bearing truncated processes (Plate 2.3, Figure 7). This indicates that premature rupture is significant in both the tube environment and the microscope chamber. Resting cysts of *L. polyedra* recovered from natural sediments also occasionally show incomplete development of processes indicating that premature rupture of the outer wall occurs during encystment of natural populations. A more precise statement concerning the frequency of this phenomenon in natural settings will require a quantitative analysis of resting cysts from sediments. The identity and viability of naturally occurring cysts with truncated processes has been confirmed by germinating such cysts in the laboratory, identifying the motile stages, inducing resting cyst formation, and observing the range of cyst morphology produced (unpublished observations).

Morphological variability (Evolutionary vs environmental control)

Resting cysts formed in our cultures showed an interesting range of morphology, particularly with respect to the number, distribution, and character of processes. Typical processes were 5-10 μm long and tapered distally from a fibrous base to a bluntly rounded point bearing short spinules. Process length varied widely, sometimes on a single specimen, and shapes ranged from conical to slightly lagenate. Terminations varied from relatively sharp points to irregular fist-like structures while others showed abrupt truncations. Some specimens lacked spines completely.

Given the degree of morphological variability of cysts formed in our cultures, it is interesting to consider similar forms encountered both in modern natural sediments and the fossil record. Traditionally, classification of dinoflagellate cysts rests primarily upon interpretation of their morphology. As a result, cyst "species" represent morphotypes whose true biological affinities are often unknown. The definition of how much morphological variability is validly encompassed by any given taxon is largely subjective in nature and highly dependent on the background, experience, and philosophy of the taxonomist.

Lentin and Williams (1989) list 11 species and 4 subspecies of resting cysts which have been assigned to the genus *Lingulodinium* as applied to fossil dinoflagellates. Several of these forms appear very similar to the type species (*L. machaerophorum*) but are distinguished on the basis of the processes; indeed, Islam (1983b) cites process morphology as "one of the main criteria for specification in *Lingulodinium*". The variation in process number, distribution, and morphology shown by resting cysts produced in our cultures of *L. polyedra* suggests that one need not invoke additional species/subspecies to account for morphotypes such as those just mentioned. As a result, we propose the synonymy of several forms (see Systematic Paleontology, below). Although the suggestion that process morphology (particularly length) may not always be an optimal

53

criterion for the delineation of cyst species is certainly not new, our study lends considerable weight to this notion by providing a look at the magnitude of process variability encountered in laboratory populations.

Many investigators have suggested that some morphological variability displayed by resting cysts of *L. polyedra* may be environmentally controlled. The bulbous process terminations described by Wall et al (1973) on *L. machaerophorum* recovered from Black Sea sediments seemed to correlate with low salinity (estuarine) environments. Turon (1984) also correlated reduced process length in this species with lower salinity. A similar suggestion was made by Dale (1988) regarding the shorter spine length shown by some *Operculodinium centrocarpum* and *Spiniferites bulloideus* from recent sediments of the Baltic region. Other variations in fossil *Lingulodinium* morphology have been noted by many investigators. Processes occasionally appear slightly flattened or bladed and, in terms of ornament, can be smooth, granular, or fibrous. Similarly, the number of paraplates involved in archeopyle formation varies from one to at least five, and may be as high as nine in some cases (J. H. Wrenn, written communication, 1987). The ability to correlate specific morphologies to environmental conditions would greatly enhance the paleoenvironmetal application of fossil dinoflagellates. To firmly establish such correlations, if they exist, requires morphological analysis of resting cyst assemblages produced in laboratory cultures grown under different environmental conditions. This approach was successfully adopted by Sandgren (1983) in a study of the effects of temperature on the morphology of chrysophycean resting cysts.

Previous models of resting cyst morphogenesis

Observations of multilayered hypnozygote development in living dinoflagellate species (e.g. Pfiester, 1975 and later) have generally confirmed earlier speculation (Evitt and Wall, 1968) that wall layers form in a centripetal sense, i.e. outer layers form first and

54

inner layers later. The development of spines, processes and other major elements of surface relief (high ridges, septa, etc.), however, has long been a topic of debate, particularly in the paleontological literature (e.g. Dale, 1983; Gocht, 1983, 1987; Evitt, 1985; Sarjeant et al., 1987). Evitt (1961, 1985) discussed three hypotheses: (1) process formation is purely centripetal, beginning distally and proceeding inward as the protoplast contracts (Dale, 1983, refers to this as the "contractional growth hypothesis"); (2) processes are elongated in a purely centrifugal fashion, growing outward from the surface of the protoplast; and (3) process growth combines both centripetal and centrifugal mechanisms; tips form in contact with the theca and subsequent outward elongation proceeds by addition of material to process bases. A fourth hypothesis has been proposed by G. Gaines (oral communication, 1989) who suggested that process growth in some species is neither centripetal nor centrifugal but occurs simultaneously along the entire length of the process as it polymerizes in a mucoid layer between protoplast and outermost wall.

Although he did not observe process development, Nordli (1951) speculated that *L. polyedra* spines grew outward from the central body. This opinion was also expressed by Dale (1983) who inferred centrifugal spine formation based on comparison of planozygote and hypnozygote volume in both plankton tow and cultured material. The results of the present study clearly demonstrate that processes of the *L. polyedra* resting cyst develop in a centrifugal sense. As mentioned above, a similar mechanism was documented by von Stosch (1973) during observation of encystment by *Gymnodinium pseudopalustre*.

Although it is tempting to speculate, based on observations of these two very different extant species, that centrifugal growth may be the general mechanism of surface relief development in dinoflagellate resting cysts, we believe that such a conclusion is not warranted at this time. Processes on resting cysts of both *L. polyedra* and *G. pseudopalustre* are randomly distributed (i.e. nontabular) over the central cyst body and a given specimen of either species often displays processes of significantly different length .

This situation contrasts sharply with resting cysts of many other species both fossil and

modern which clearly show tabular arrangements of surface relief, and morphology

consistent with a developmental model invoking a rigid outer wall and centripetal growth.

After careful morphological analysis of fossil specimens, Evitt (1985) favored a centripetal

mechanism (at least in part) for many species. Some biological evidence for the potential

significance of contractional growth during dinoflagellate encystment has been provided by

Blackburn et al (1989) who documented the reduced size of the *Gymnodinium catenatum*

hypnozygote (a "proximate" cyst) relative to the planozygote. Finally, it is interesting to

consider Gaines' hypothesis which is based on unpublished observations of encystment

among living species of *Gonyaulax* and *Polykrikos*. In summary, we believe that the

existence of multiple developmental mechanisms among a group as diverse as the

dinoflagellates is entirely possible and it remains for continued investigation of encystment

in living species to shed more light on this issue.

SYSTEMATIC PALEONTOLOGY

Division PYRRHOPHYTA Pascher 1914

Class DINOPHYCEAE Fritsch 1935

Order PERIDINIALES Haeckel 1894

Family GONYAULACACEAE Lindemann 1928

Genus *Lingulodinium* Wall 1967 emend. Wall et al. 1973

Lingulodinium machaerophorum (Deflandre & Cookson) Wall 1967

Plates 2.1, figures 1-12; Plate 2.2, figures 1-12; Plate 2.3, figures 1-7

Baltisphaeridium funginum Morgenroth, 1966, p. 17, plate 3, figures 7-8.

Lingulodinium funginum (Morgenroth) Islam, 1983b, p. 341, plate 3, figures 10.

Lingulodinium sadoense Matsuoka, 1983, p. 124, plate 10, figures 1a-c, 2-3, 4a-b, 6-7.

Comments. *Lingulodinium machaerophorum* is the resting cyst stage of the extant dinoflagellate *L. polyedra*. Based on the range of resting cyst morphology observed during germination and culturing studies of *L. polyedra*, the above cyst-based species are here synonymized with *L. machaerophorum*. Islam (1983b) stated that *L. funginum* "differs from other species of *Lingulodinium* in possessing mushroom-like or distally truncate processes". Both of these process types were common on our culture-produced resting cysts. *L. sadoense* (Matsuoka, 1983) was distinguished from *L. machaerophorum* in having larger but fewer processes. This morphotype, while rare in our cultures, was common in natural sediment samples examined during the early stages of this project; germination of these forms yielded motile cells of *L. polyedra*.

Other morphotypes now designated as separate species of the genus *Lingulodinium* may well be synonymous with *L. machaerophorum*, but it is difficult to rigorously assess this possibility with the descriptions currently available in the literature. Among those species deserving restudy are *L. brevispinosum* Matsuoka and Bujak, 1988; *L. pycnospinosum* Benedek and Sarjeant, 1981; *L. siculum* Wall et al., 1973; *L. strangulatum* Islam, 1983a; and *L. varium* Sütö-Szentai, 1986. Although the exact process types described for these species were not directly observed in our *L. polyedra* cultures, they nevertheless appear to fall within the range of possible process morphology produced by the developmental sequence described above. From this perspective, further cyst germination and laboratory culture investigations of *L. polyedra* are warranted.

REFERENCES CITED

ANDERSON, D. M., KULIS, D. M., and BINDER, B. J.
    1984   Sexuality and cyst formation in the dinoflagellate *Gonyaulax tamarensis*:
                cyst yield in batch cultures. *Journal of Phycology* 20 (3): 418-425.

ANDERSON, D. M., and LINDQUIST, N. L.
    1985   Time-course measurements of phosphorus depletion and cyst formation in
                the dinoflagellate *Gonyaulax tamarensis* Lebour. *Journal of Experimental
                Marine Biology and Ecology*, 86 (1): 1-13.

BENEDEK, P. N., and SARJEANT, W. A. S.
    1981   Dinoflagellate cysts from the Middle and Upper Oligocene of Tönisberg
                (Niederrheingebiet): A morphological and taxonomic restudy. *Nova
                Hedwigia*, 35 (2+3): 313-356.

BIBBY, B. T., and DODGE, J. D.
    1972   The encystment of a freshwater dinoflagellate: a light and electron-
                microscopical study. *British Phycological Journal*, 7 (1): 85-100.

BLACKBURN, S. I., HALLEGRAEFF, G. M., and BOLCH, C. J.
    1989   Vegetative reproduction and sexual life cycle of the toxic dinoflagellate
                Gymnodinium catenatum from Tasmania, Australia. *Journal of Phycology*,
                25 (3): 577-590.

BRICHEUX, G., MAHONEY, D. G., and GIBBS, S. P.
    1992   Development of the pellicle and thecal plates following ecdysis in the
                dinoflagellate *Glenodinium foliaceum*. *Protoplasma*, 168 (3-4): 159-171.

DALE, B.
    1983   Dinoflagellate resting cysts: "benthic plankton". *In:* Fryxell, G. A. (ed.),
                Survival strategies of the algae. Cambridge University Press, Cambridge,
                p. 69-136.
    1988   Low salinity dinoflagellate cyst assemblages from Recent sediments of the
                Baltic region [Abstract]. *Abstracts of the 7th International Palynological
                Congress*, Brisbane, Australia, August 28-September 2, 1988, p. 33.

DEFLANDRE, G., and COOKSON, I. C.
    1955   Fossil microplankton from Australian Late Mesozoic and Tertiary
                sediments. *Australian Journal of Marine and Freshwater Research*, 6 (2):
                242-313.

DODGE, J. D.
    1989   Some revisions of the Family Gonyaulacaceae (Dinophyceae) based on a
                scanning electron microscope study. *Botanica Marina*, 32 (4): 275-298.

DODGE, J. D., and CRAWFORD, R. M.
    1970   A survey of thecal fine structure in the Dinophyceae. *Botanical Journal of
                the Linnean Society*, 63 (1): 53-67.

DOUCETTE, G. J., CEMBELLA, A. D., and BOYER, G. L.
  1989   Cyst formation in the red tide dinoflagellate *Alexandrium tamarense*
            (Dinophyceae): effects of iron stress. *Journal of Phycology*, 25 (4): 721-
            731.

DÜRR, G.
  1979   Elektronenmikroskopische untersuchungen am panzer von dinoflagellaten I.
            Gonyaulax polyedra. Archives für Protistenkunde, Band 122, Heft 1 & 2:
            55-87.

DÜRR, G., and NETZEL, H.
  1974   The fine structure of the cell surface in *Gonyaulax polyedra* (Dinoflagellata).
            Cell and Tissue Research, 150 (1): 21-41.

ERDTMAN, G.
  1954   On pollen grains and dinoflagellate cysts in the Firth of Gullmarn, SW.
            Sweden. *Botaniska Notiser*, Häfte 2: 103-111.

EVITT, W. R.
  1961   Observations on the morphology of fossil dinoflagellates.
            Micropaleontology, 7 (4): 385-420.
  1967   Dinoflagellate studies II. The archeopyle. *Stanford University
            Publications, Geological Sciences*, 10 (3): 1-83.
  1985   *Sporopollenin dinoflagellate cysts. Their morphology and interpretation.*
            American Association of Stratigraphic Palynologists Foundation, Dallas,
            333 p.

EVITT, W. R., and DAVIDSON, S. E.
  1964   Dinoflagellate studies I. Dinoflagellate cysts and thecae. *Stanford
            University Publications, Geological Sciences*, 10 (1): 1-12.

EVITT, W. R., and WALL, D.
  1968   Dinoflagellate studies IV. Theca and cyst of Recent freshwater *Peridinium
            limbatum* (Stokes) Lemmermann. *Stanford University Publications,
            Geological Sciences*, 12 (2): 1-23.

FRITZ, L., ANDERSON, D. M., and TRIEMER, R. E.
  1989   Ultrastructural aspects of sexual reproduction in the red tide dinoflagellate
            Gonyaulax tamarensis. Journal of Phycology, 25 (1): 95-107.

GAO XIAOPING, DODGE, J. D., and LEWIS, J.
  1989   An ultrastructural study of planozygotes and encystment of a marine
            dinoflagellate, *Scrippsiella* sp. *British Phycological Journal*, 24 (2): 153-
            165.

GAUDSMITH, J. T., and DAWES, C. J.
  1972   The ultrastructure of several dinoflagellates with emphasis on *Gonyaulax
            polyedra* Stein and *Gonyaulax monilata* Davis. *Phycologia*, 11 (2): 123-
            132.

GOCHT, H.
  1983   Morphogenetische deutung und bezeichnung ausgewählter merkmale bei
            dinoflagellaten-zysten. [Morphogenetic interpretation and terminology of

selected dinoflagellate cyst features.] *Neues Jahrbuch für Geologie und Paläontologie; Monatshefte*, Heft 5: 257-276.

1987 Morphogenetische deutung und bezeichnung ausgewahlter merkmale bei dinoflagellaten-zysten: nachtrage. [Morphogenetic interpretation and terminology of selected dinoflagellate cyst features. Additions] *Neues Jahrbuch für Geologie und Paläontologie; Monatshefte*, Heft 12: 705-725.

GUILLARD, R. R. L.

1975 Culture of phytoplankton for feeding marine invertebrates. *In*: Smith W. L., and Chanley, M. H. (eds.), *Culture of marine inverteberate animals*. Plenum Publishing Corporation, New York, p. 29-60.

HARRISON, P. J., WATERS, R. E., and TAYLOR, F. J. R.

1980 A broad spectrum artificial seawater medium for coastal and open ocean phytoplankton. *Journal of Phycology*, 16 (1): 28-35.

HÖHFELD, I., and MELKONIAN, M.

1992 Amphiesmal ultrastructure of dinoflagellates: a reevaluation of pellicle formation. *Journal of Phycology*, 28 (1): 82-89.

ISLAM, M. A.

1983a Dinoflagellate cysts from the Eocene of the London and the Hampshire Basins, southern England. *Palynology*, 7: 71-92.

1983b Dinoflagellate cyst taxonomy and biostratigraphy of the Eocene Bracklesham Group in southern England. *Micropaleontology*, 29 (3): 328-353.

KOFOID, C. A.

1911 Dinoflagellata of the San Diego Region, IV. The genus *Gonyaulax*, with notes on its skeletal morphology and a discussion of its generic and specific characters. *University of California Publications in Zoology*, 8 (4): 187-286.

LENTIN, J. K., and WILLIAMS, G. L.

1989 Fossil dinoflagellates: index to genera and species, 1989 edition. *American Association of Stratigraphic Palynologists, Contribution Series*, No. 20, 473 p.

LEWIS, J., and BURTON, P.

1988 A study of newly excysted cells of *Gonyaulax polyedra* (Dinophyceae) by electron microscopy. *British Phycological Journal*, 23 (1): 49-60.

LOEBLICH, A. R., III

1970 The amphiesma or dinoflagellate cell covering. *Proceedings of the North American Paleontological Convention*, Chicago, September, 1969, Vol. 2, Part G: 867-929.

MARASOVIC, I.

1989 Encystment and excystment of *Gonyaulax polyedra* during a red tide. *Estuarine, Coastal and Shelf Science*, 28 (1): 35-41.

1991 Preliminary observations on the relationship between temporary and resting cysts of *Lingulodinium polyedra* (Stein) comb. nov. [Abstract]. *Abstracts and Participants, Fifth International Conference on Toxic Marine*

Phytoplankton, Newport, Rhode Island, October 28-November 1, 1991, p. 77.

MATSUOKA, K.
    1983   Late Cenozoic dinoflagellates and acritarchs in the Niigata District, central Japan. *Palaeontographica*, Abteilung B, 187: 89-154.

MATSUOKA, K., AND BUJAK, J. P.
    1988   Cenozoic dinoflagellate cysts from the Navarin Basin, Norton Sound, and St. George Basin, Bering Sea. *Bulletin of the Faculty of Liberal Arts, Nagasaki University, Natural Science*, 29 (1): 1-147.

McKEE, E. D., CHRONIC, J., and LEOPOLD, E. B.
    1959   Sedimentary belts in lagoon of Kapingamarangi Atoll. *Bulletin of the American Association of Petroleum Geologists*, 43 (3): 501-562.

MORGENROTH, P.
    1966   Mikrofossilien und konkretionen des nordwesteuropäischen untereozäns. *Palaeontographica*, Abteilung B, 119:1-53.

MORRILL, L. C., and LOEBLICH, A. R., III
    1983   Ultrastructure of the dinoflagellate amphiesma. *International Review of Cytology*, 82: 151-180.

NETZEL, H., and DÜRR, G.
    1984   Dinoflagellate cell cortex. *In*: Spector, D. L. (ed.), *Dinoflagellates*. Academic Press, Inc., Orlando, p. 43-105.

NEWMAN, S. A., and COMPER, W. D.
    1990   'Generic' physical mechanisms of morphogenesis and pattern formation. *Development*, 110 (1): 1-18.

NORDLI, E.
    1951   Resting spores in *Goniaulax polyedra* Stein. *Nytt Magasin for Naturvidenskapene*, Bind 88: 207-212.

PFIESTER, L. A.
    1975   Sexual reproduction of *Peridinium cinctum* f. *ovoplanum* (Dinophyceae). *Journal of Phycology*, 11 (3): 259-265.
    1976   Sexual reproduction of *Peridinium willei* (Dinophyceae). *Journal of Phycology*, 12 (2): 234-238.
    1977   Sexual reproduction of *Peridinium gatunense* (Dinophyceae). *Journal of Phycology*, 13 (1): 92-95.
    1984   Sexual reproduction. *In*: Spector, D. L. (ed.), *Dinoflagellates*. Academic Press, Inc., Orlando, p. 181-199.
    1989   Dinoflagellate sexuality. *International Reviews of Cytology*, 114: 249-272.

PFIESTER, L. A., and ANDERSON, D. M.
    1987   Dinoflagellate reproduction. *In*: Taylor, F. J. R. (ed.), *The biology of dinoflagellates*. Botanical Monographs, Vol. 21. Blackwell Scientific Publications, Oxford, p. 611-648.

PROVASOLI, L.
1968   Media and prospects for the cultivation of marine algae. *In*: Watanabe, A., and Hattori, A. (eds.), *Cultures and collections of algae*. Proceedings of the U. S.-Japan Conference, Hakone, September 12-15, 1966. The Japanese Society of Plant Physiologists. p. 63-75.

REID, P. C., and BOALCH, G. T.
1987   A new method for the identification of dinoflagellate cysts. *Journal of Plankton Research*, 9 (1): 249-253.

ROSSIGNOL, M.
1964   Hystrichosphères du Quaternaire en Méditerranée Orientale, dan les sédiments Pléistocènes et les boues marines actuelles. *Revue de Micropaléontologie*, 7 (2): 83-99.

SANDGREN, C. D.
1983   Morphological variability in populations of chrysophycean resting cysts. I. Genetic (interclonal) and encystment temperature effects on morphology. *Journal of Phycology*, 19 (1): 64-70.

SARJEANT, W. A. S., LACALLI, T., and GAINES, G.
1987   The cysts and skeletal elements of dinoflagellates: speculations on the ecological causes for their morphology and development. *Micropaleontology*, 33 (1): 1-36.

SCHMITTER, R. E.
1971   The fine structure of *Gonyaulax polyedra*, a bioluminescent marine dinoflagellate. *Journal of Cell Science*, 9 (1): 147-173.

SÜTÖ-SZENTAI, M.
1986   A magyarorszagi pannoniai (s.l.) rétegosszlet mikroplankton vizsgálata. *Folia Comloensis*, 2: 25-45.

SWEENEY, B. M.
1976   Freeze fracture studies of the thecal membranes of *Gonyaulax polyedra*: circadian changes in the particles of one membrane face. *Journal of Cell Biology*, 68 (3): 451-461.

TAPPAN, H.
1980   *The Paleobiology of Plant Protists*. W. H. Freeman and Company, San Francisco, 1028 p.

TAYLOR, F. J. R. (editor)
1987   *The biology of dinoflagellates*. Botanical Monographs, Vol. 21. Blackwell Scientific Publications, Oxford, 785 p.

TURON, J.-L.
1984   Le palynoplancton dans l'environnement actuel de L'Atlantique Nord-Oriental. Evolution climatique et hydrologique depuis le dernier maximum glaciaire. *Memoires de l'Institut de Geologie du Bassin d'Aquitaine*, Universite de Bordeaux, No. 17: 313 p.

VON STOSCH, H. A.
  1964   Zum problem der sexuellen fortpflanzung in der Peridineengattung
            Ceratium. Helgoländer Wissenschaftliche Meeresuntersuchungen, 10 (1-4):
            140-152.
  1972   La signification cytologique de la "cyclose nucléaire" dans le cycle de vie
            des dinoflagellés. *Bulletin de la Société Botanique de France, Mémoires.*
            Colloque sur les cycles sexuels et l'alternance des generations chez les
            algues, November 13-14, 1970, Paris, France: 201-212.
  1973   Observations on vegetative reproduction and sexual life cycles of two
            freshwater dinoflagellates, *Gymnodinium pseudopalustre* Schiller and
            Woloszynskia apiculata sp. nov. *British Phycological Journal*, 8 (2): 105-
            134.

WALKER, L. M.
  1984   Life histories, dispersal, and survival in marine, planktonic dinoflagellates.
            In: Steidinger, K. A., and Walker, L. M. (eds.), *Marine plankton life cycle
            strategies*. CRC Press, Inc., Boca Raton, Florida, p. 20-34.

WALL, D.
  1967   Fossil microplankton in deep-sea cores from the Caribbean Sea.
            Palaeontology, 10 (1): 95-123.

WALL, D., and DALE, B.
  1968   Modern dinoflagellate cysts and evolution of the Peridiniales.
            Micropaleontology, 14 (3): 265-304.

WALL, D., DALE, B., and HARADA, K.
  1973   Descriptions of new fossil dinoflagellates from the Late Quaternary of the
            Black Sea. *Micropaleontology*, 19 (1): 18-31.

PLATE 2.1

Morphological development of *L. polyedra* resting cysts. All figures 500x. Figures 3-12 show a single specimen at successive stages during the transition from planozygote to hypnozygote: Figures 3-6 represent Stage II (Initiation), while Figures 7-12 illustrate Stage III (Expansion).

Figure 1.   Living resting cyst (hypnozygote) of *L. polyedra* produced in laboratory culture. Optical section. Note that processes appear hollow and distally closed; some (e.g. at 3 and 4 o' clock) bear distal spinules.

Figure 2.   Planozygote in dorsoventral view, Stage I (Pre-expansion). Optical section showing zone of differentiation in peripheral cytoplasm.

Figure 3.   Planozygote immediately after loss of motility. Outer membrane (external to the theca) beginning to bulge outward. Note longitudinal flagella at upper right of cell.

Figure 4.   A few moments later, slightly lower focus. Dissociation of theca visible at lower left. Also note transverse flagellum (which has been expelled from the cingulum) at top of cell, and first appearance of globules on surface of cytoplasm (~1 o' clock).

Figure 5.   Growth of bulges. Expansion of outer membrane begins to pull thecal sections away from underlying cytoplasm (lower right).

Figure 6.   Continued cell expansion, bulges merging to define a continuous membrane distinct from the theca and cytoplasm. Note "residual" connections between theca and membrane (e.g. 9 and 11 o' clock) which appear to occur at thecal plate boundaries. At this stage, thecal sections are no longer in contact with the cytoplasm. Cytoplasmic mass approaches circularity (in optical section) and shows globules more or less evenly distributed on the surface.

Figure 7.   Stage III. Outer membrane nearly circular in optical section; globules on the surface of the cytoplasm begin development into processes. Note initiation of process shaft formation between globules and cytoplasmic surface (~7-8 o' clock).

Figure 8.   Continued expansion of outer membrane occurring simultaneously with deposition of process shafts. Note that (1) thecal sections do not contact developing processes, and (2) globules remain spherical as process shafts grow outwards.

Figure 9.   Cell at same point as Figure 8, lower focus.

Figure 10.   Maximum extent of cell expansion. Development of process shafts complete. Most processes still bear a terminal globule.

Figure 11.   Slightly lower focus of fully expanded cell. Note that boundary of outer membrane is out-of-focus, while the internal cyst shows a clear optical section (c.f. Figure 10). This relationship reflects the

65

lack of concentricity induced by the occurrence of resting cyst
formation on the bottom of the viewing chamber.

Figure 12.   Modification of terminal globules. Spherical globules are beginning
to collapse to form process tips. Incomplete or uneven collapse
results in terminal spinules which are characteristic of spines of
Lingulodinium resting cysts.
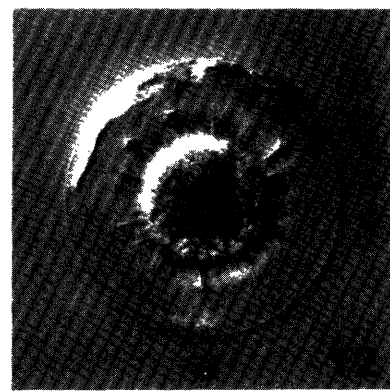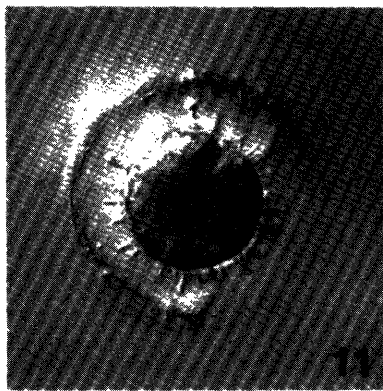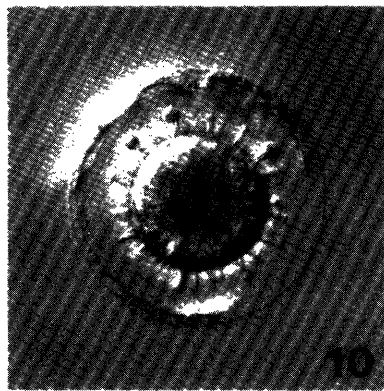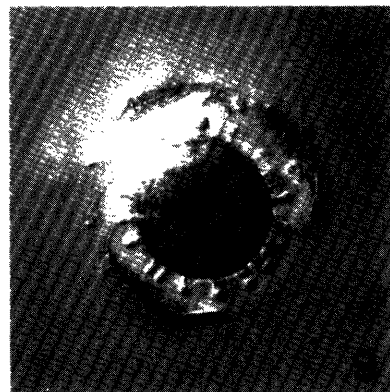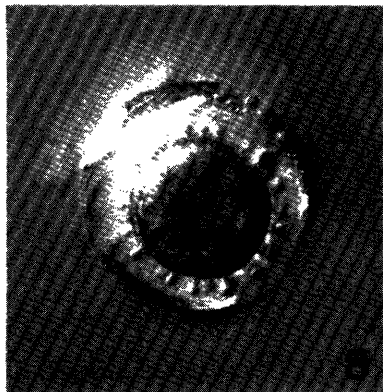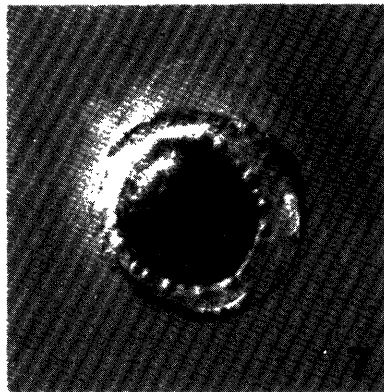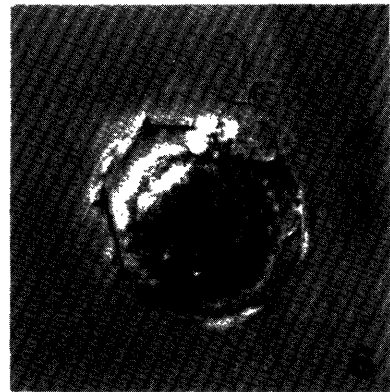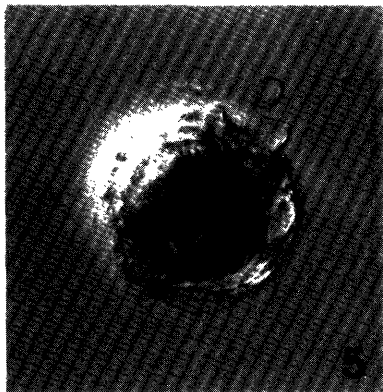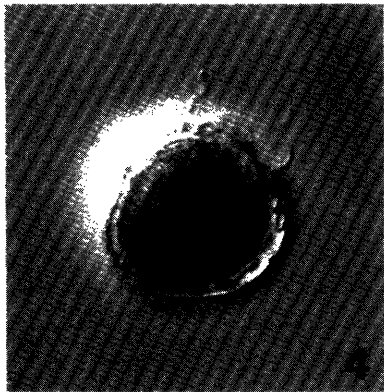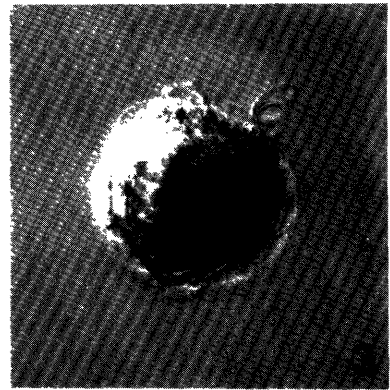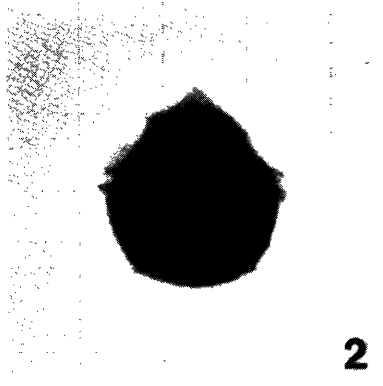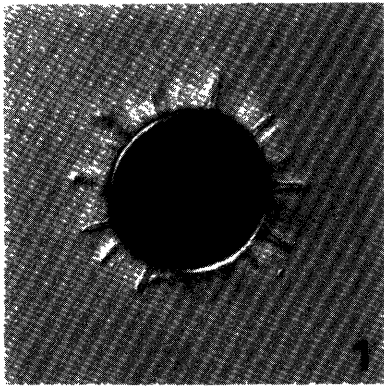
PLATE 2.2

Morphological development of *L. polyedra* resting cysts. All figures 500x. Figures 1-3 represent a continuation of the developmental sequence illustrated in Plate 2.1, Figures 3-12.

Figure 1.   Resting cyst immediately after rupture of outer membrane. Approximately equatorial focus. Note variability of process morphology. Remnants of planozygotic theca to the left of the cell. At this stage, resting cyst lacks an endospore.

Figure 2.   Same speciman as Figure 1, high focus on remnants of the epitheca. Note reduced plate ornament.

Figure 3.   Same specimen as Figure 1, low focus on planozygotic flagella. Duel longitudinal flagella at ~2 o' clock; single transverse flagellum at ~11 o' clock. Note various swellings along each of the flagella, those on the transverse flagellum appear more numerous and variable in size (see also Figure 10). Planozygotic theca to the left, showing wide growth bands.

Figure 4.   Specimen during Stage II (initiation) of resting cyst formation; view approximately dorsoventral, with apex to the upper right. Bulging outer membrane appears anchored along plate sutures, particularly those between cingular and adjacent (anterior and posterior) plates (e.g. ~3-4 o'clock). This specimen also clearly shows the globule layer on the cytoplasmic surface, as well as longitudinal flagella at ~6 o' clock.

Figure 5.   High focus on a cell during Stage III (expansion). Mid-dorsal portion of epitheca is more or less intact and remains loosely attached to cingular plates. Hypotheca is underneath the developing cyst (out-of-focus). Again, note significantly reduced intratabular ornament.

Figure 6.   Optical section (equatorial focus) of cell nearing the end of expansion. Thecal sections appear connected to outer membrane at various points including those at 9, 10, and 11 o' clock. Development of processes proceeding independantly of theca.

Figure 7.   High focus on cell immediately after rupture of outer membrane. Note single transverse flagellum with regularly spaced swellings.

Figure 8.   Equatorial focus on resting cyst showing an assortment of process morphologies. Note bulbous terminations at 1 and ~3 o' clock. Planozygotic theca to the left of cell.

Figure 9.   Same specimen as Figure 8; lower focus. Note (1) wide growth bands on the theca, and (2) isolated transverse flagellum at 12 o' clock.

Figure 10.   Resting cyst immediately after rupture of outer membrane. Low
              focus on flagella: single transverse flagellum at ~2-3 o' clock;
              tangled longitudinal flagella at ~5 o' clock.

Figure 11.   Multiple process morphologies present on a single resting cyst.
              Compare bases of processes at 1 and 2 o' clock.

Figure 12.   Same specimen as Figure 11; slightly lower focus. Again, note
              variability of process morphology. Spine at ~12 o' clock shows
              widely flaired base, and irregular "fist-like" termination. Spines at 2
              and 3 o' clock have more compact bases, but the former is capitate
              and lacks spinules, while the latter is acuminate and bears spinules.
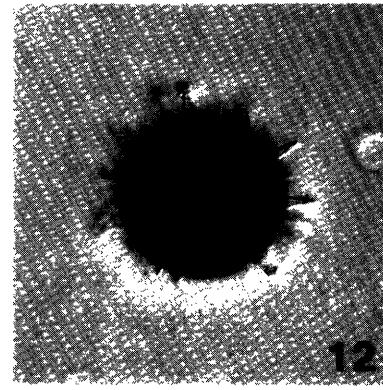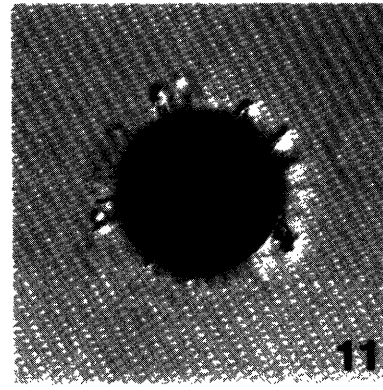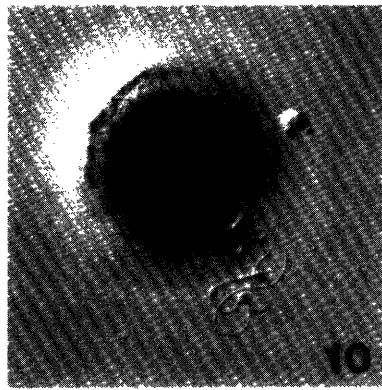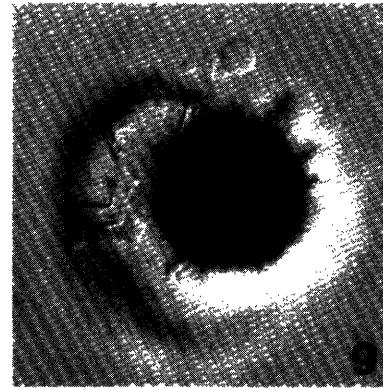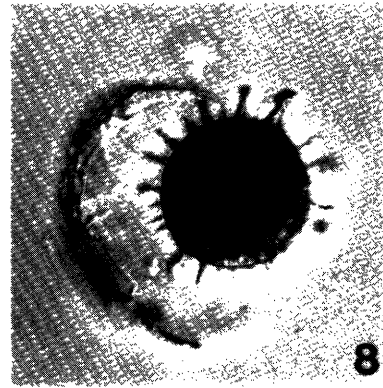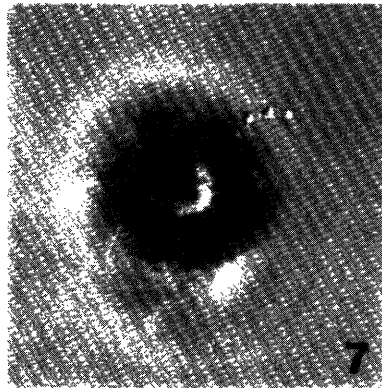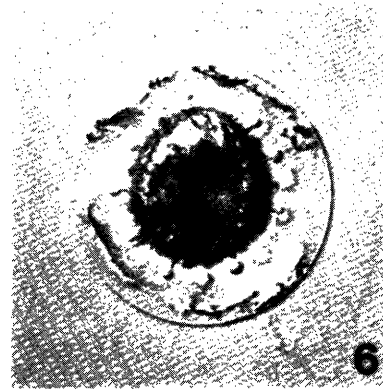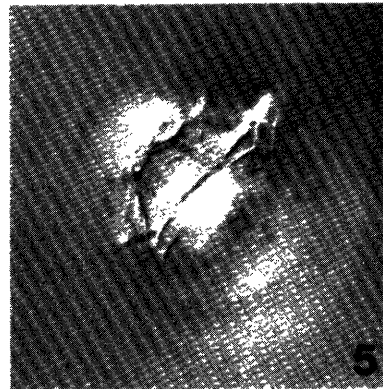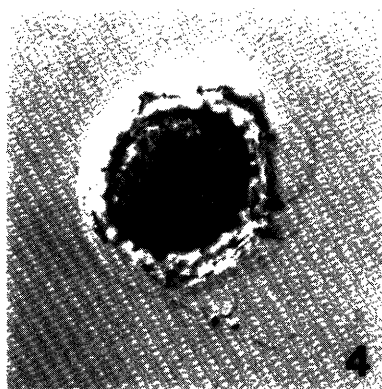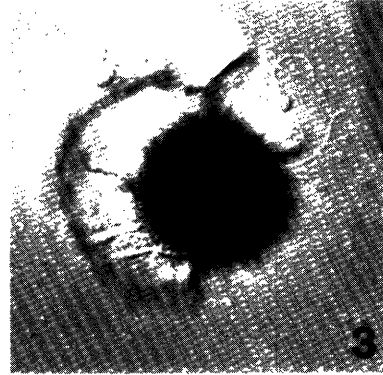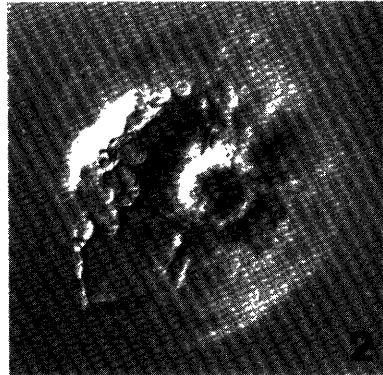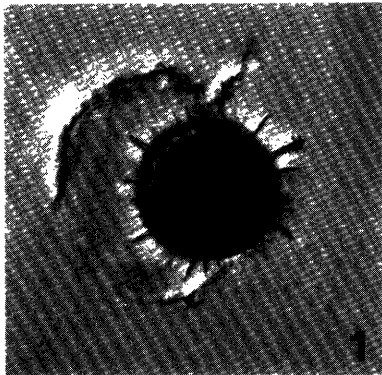
PLATE 2.3

Morphological development of *L. polyedra* resting cysts. All figures 500x. Sequences shown in Figures 1-3 and 4-6 illustrate two aberrations of resting cyst formation as observed in labratory cultures.

Figures 1-3 = globule detachment.

Figure 1.   Specimen during initiation (Stage II) phase of development. Note detached globules free-floating in expansion zone.

Figure 2.   Cell during expansion (Stage III) phase. In equatorial focus, region of cytoplasmic surface between ~11 and 3 o' clock lacks developing processes.

Figure 3.   Immediately after rupture (premature) of outer membrane. Note: (1) outer membrane is still visible, (2) membrane shows residual attachment to the theca (e.g. 11 and 1 o' clock), (3) premature rupture of membrane resulted in truncation of spines (e.g. 7-8 o' clock), and (4) final distribution of spines on cyst surface is highly uneven.

Figures 4-6 = premature rupture of outer membrane.

Figure 4.   Specimen during expansion (Stage III) phase, just prior to rupture of the outer membrane.

Figure 5.   Immediately after membrane rupture, membrane still visible. Terminal globules on processes at ~8 and 9 o' clock maintain spherical morphology while rapidly deflating (c.f. Figure 4).

Figure 6.   Moments after rupture, terminal globules fully deflated leaving sharply truncated processes.

Figure 7.   Collection of culture-produced resting cysts showing an assortment of process morphologies. Also note (1) well-developed endospore shown by specimen on the far left, and (2) darker colored mass (accummulation body?) adjacent to the wall of the "empty" resting cyst at top of photo.
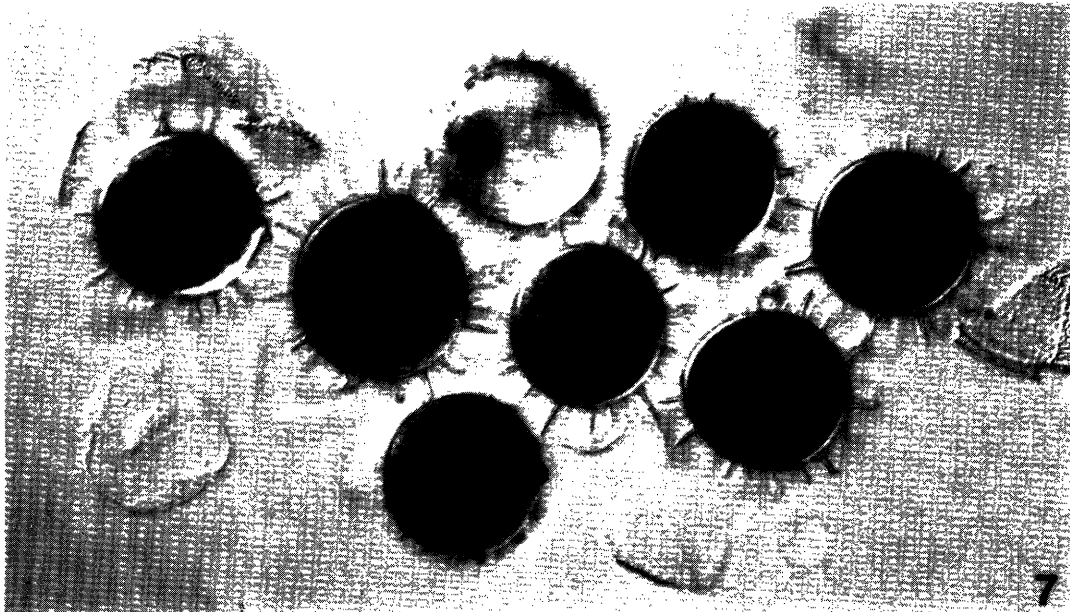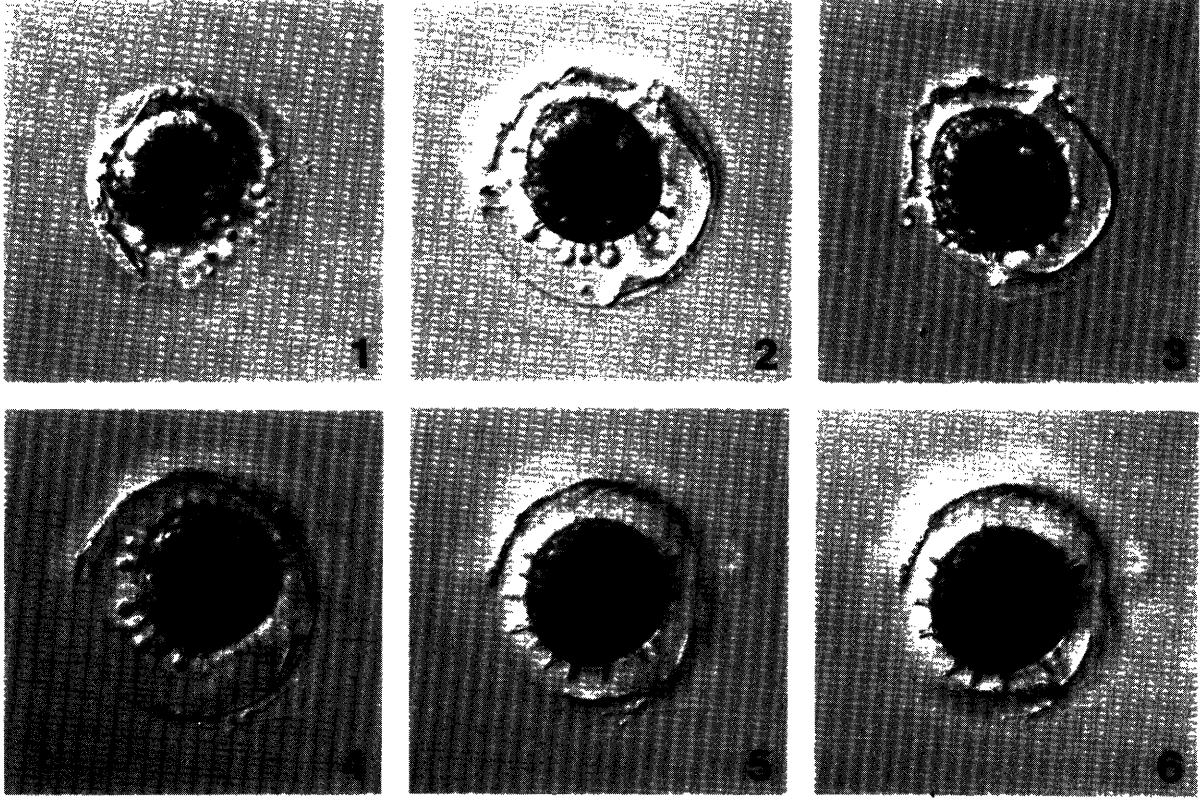
CHAPTER 3

A comparative study of resistant cell wall biopolymers from resting cysts of the marine dinoflagellate *Lingulodinium polyedra* and pollen of *Juniperus* and *Quercus*

ABSTRACT

Although recent studies of a number of species within the green algae have made substantial contributions to our understanding of the distribution and composition of highly resistant cell wall biopolymers, other algal groups are largely unstudied from this perspective. Among the dinoflagellates (Division Pyrrhophyta, Class Dinophyceae), several species are well known for their ability to form thick, geologically-preservable cell walls. The remarkable physical and chemical resistance of these structures is traditionally thought to derive from the presence of sporopollenin. In the present investigation, we test this assumption by comparing resistant cell walls isolated from the resting cysts of a marine dinoflagellate (*Lingulodinium polyedra*) to "traditional" sporopollenins derived from the pollen cell walls of a gymnosperm (*Juniperus scopulorum*) and an angiosperm (*Quercus rubra*). Isolation of nearly pure cell wall fractions was achieved by sequentially treating initial materials by solvent extraction, saponification, and acid hydrolysis. At each stage of processing, residues were characterized by optical microscopy, FTIR microscopy, elemental analysis, "in-source" pyrolysis--mass spectrometry (Py-MS), and Curie-point pyrolysis--gas chromatography--mass spectrometry (Py-GC/MS). These techniques allowed a unique chemical fingerprint to be established for each of the resistant cell wall residues. None of the isolated materials showed convincing evidence of a carotenoid-based structure, and therefore probably represent macromolecular substances distinct from traditionally-defined sporopollenin. Cell walls of both pollens and *L. polyedra* resting cysts appeared largely aromatic in composition; however, the suite of aromatic products generated by pyrolysis of the dinoflagellate residues was clearly different from those of the pollens. In addition to this aromatic signature, Juniper pollen walls showed the presence of an aliphatic biopolymer. Analysis of *L. polydera* resting cyst cell walls yielded no strong evidence for the presence of aliphatic components aside from the liberation of prist-1-ene during pyrolysis. The abundance of this latter compound, however, implies the presence

of bound tocopherols which may play an important structural role in the cell wall of dinoflagellate resting cysts. Overall, the non-hydrolyzable macromolecular substance isolated from *L. polyedra* resting cyst walls appears fundamentally different from "algaenan", the highly aliphatic resistant biopolymer reported to comprise the cell walls of many green algae.

INTRODUCTION

Over the last decade, there has been a growing appreciation of the importance of highly resistant biomacromolecules as components of sedimentary organic matter. Several recent investigations (e.g. Largeau et al., 1984; Brunner and Honegger, 1985; Nip et al., 1987; Burczyk and Dworzanski, 1988; Goth et al., 1988; Tegelaar et al., 1989; Derenne et al., 1991; Gatellier et al, 1993) have made noteworthy contributions to our present understanding of these substances by elucidating their chemical composition, distribution among living organisms, potential for survival during sedimentation and diagenesis, and contribution to the organic matter preserved in the fossil record. A current review of progress in this field is provided by de Leeuw and Largeau (1993).

Perhaps the best known of these highly resistant biopolymers belong to the group of compounds collectively referred to as sporopollenin. This term was coined by Zetzsche et al. (1931) to describe the highly resistant substance present in the exine of the pollen wall and the exosporium of a large number of spore walls. Attempts to understand the nature of these resistant cell walls first appeared in the literature early in the 19th century (John, 1814; Braconnot, 1829). An intensive investigation of sporopollenin chemistry and biochemistry using modern analytical techniques was initiated in the 1960's by Brooks and co-workers (Brooks et al., 1971; Brooks and Shaw, 1978). Based on extensive chemical and cytochemical analysis they concluded that sporopollenin was an oxidative polymer of carotenoids or carotenoid esters. At that time, the term sporopollenin was widely used to describe resistant cell walls (usually defined as those capable of withstanding acetolysis) identified among several species of algae and fungi (Brooks et al., 1971; Atkinson et al., 1972).

More recent studies, however, have suggested that at least two revisions of these earlier conclusions are in order. First, the "carotenoid hypothesis" may not be generally applicable to all pollen and spore cell walls. Prahl et al. (1985, 1986) found that

sporopollenin accumulation in the anthers of *Cucurbita pepo* was not significantly affected by severe inhibition of carotenoid biosynthesis. Guilford et al (1988) examined the chemical structure of sporopollenin from diverse sources using high resolution solid state ^{13}C NMR spectroscopy and concluded that precursors to sporopollenin biosynthesis consisted largely of saturated compounds such as fatty acids. Finally, several investigators (Schultze Osthoff and Weimann, 1987; Herminghaus et al., 1988; Wehling et al., 1989; Mulder et al., 1992) found that degradation of pollen sporopollenins by various means tended to yield significant amounts of phenolic compounds, products which are inconsistent with a parent structure composed entirely of carotenoid precursors.

Another aspect of the earlier paradigm which appears to require reconsideration is the application of the term sporopollenin, with its connotation of a specific chemical composition, to materials produced by organisms other than higher plants. Many recent studies have focused on resistant cell walls found among the green algae (Largeau et al., 1984, 1985; Burczyk, 1987a,b; Goth et al, 1988; Kadouri et al., 1988; Derenne et al., 1989, 1990; 1991; 1992). For all species investigated thus far, the isolated resistant cell wall substances were found to consist mainly of highly aliphatic macromolecules with long polyalkyl chains as major structural elements. Such a structure stands in sharp contrast to the carotenoid-based sporopollenin model formulated earlier. As a result, Tegelaar et al. (1989) introduced the term "algaenan" to distinguish this highly aliphatic resistant biopolymer from traditional sporopollenin.

Although much has been done to characterize the resistant biomacromolecules produced by chlorophyte algae, other algal groups remain largely unstudied from this perspective. Among the dinoflagellates (Division Pyrrhophyta, Class Dinophyceae), a number of species produce highly resistant cell walls. The selective preservation of these materials in depositional environments has yielded a rich fossil record of dinoflagellates which extends back at least 225 million years (Evitt, 1985). In recent decades, fossil dinoflagellates have attracted considerable attention due to their utility in biostratigraphic

studies, particularly those relating to petroleum exploration (Williams and Bujak, 1985; Goodman, 1987). Although a small number of dinoflagellate fossils are calcareous or silicious, the vast majority are non-mineral in composition. These latter forms are routinely extracted from consolidated sediment samples using standard palynological maceration techniques (i.e. digestion of rock minerals with concentrated HF and HCl; see Gray, 1965, and Barss and Williams, 1973) which typically leave the preserved cell walls morphologically unaltered. Because fossil pollen and spores often co-occur with dinoflagellates in the resulting residues, it has become commonplace among paleontologists and biologists to classify organic dinoflagellate fossil material under the general umbrella of sporopollenin (Eisenack, 1963; Chaloner and Orbell, 1971; Atkinson et al., 1972; Bujak and Davies, 1983; Evitt, 1985, Taylor, 1987, Hemsley and Scott, 1991) although its composition is largely unknown.

Studies of the highly resistant biopolymers formed by living dinoflagellates are complicated by the fact that these materials seem to be produced only by a small minority of extant species, and then only during specific stages of the life cycle. Dinoflagellate life histories tend to be rather complex and are relatively poorly known; a complete life cycle has been documented for only about 30 of the ~1500 known living species (Pfiester, 1989). Since the present study often refers to stages in the dinoflagellate life cycle, we provide a brief review here. A typical dinoflagellate is unicellular, biflagellate and swims freely in water. At this stage, many dinoflagellate species are characterized by an armor (the theca) of cellulosic plates which encloses the cell. The motile stage is haploid, and reproduction consists of simple vegetative division. When subjected to environmental stress, motile cells may form non-motile asexual temporary cysts (also known as pellicle cysts) which revert to the motile form when favorable growth conditions return. Occasionally, and for reasons not well understood, vegetatively dividing cells produce gametes which fuse to form a diploid motile zygote (the planozygote). Except for being larger in size, planozygotes often closely resemble vegetative cells. In some species,

however, the planozygote ultimately loses motility, sheds its theca, and develops one or more new wall layers to become a hypnozygote, or resting cyst. After a period of obligate dormancy, hypnozygotes germinate and the excysting cell undergoes a meiotic division. However, the exact timing and nature of this division are not always clear. The resulting daughter cells are motile and resume vegetative growth to complete the life cycle. For more detailed treatment of dinoflagellate reproduction, the reader is referred to previous reviews in Tappan (1980), Walker (1984), Pfiester (1984, 1989), and Pfiester and Anderson (1987).

Among the dinoflagellates, sporopollenin-like materials are believed to occur mainly in the walls of the resting cyst, although some reports (Swift and Remson, 1970; Morrill and Loeblich, 1981) claim the motile stage and/or temporary cyst wall may contain similar substances based on the resistance of some cellular features to acetolysis. Fossil dinoflagellates are now recognized to be almost exclusively the preserved walls of hypnozygotes (Evitt, 1961; 1985).

In the present investigation, we collected resting cysts produced in cultures of the marine dinoflagellate *Lingulodinium polyedra* and compared their resistant cell walls to those isolated from pollen (i.e. "classical" sporopollenin) of a gymnosperm (*Juniperus scopulorum*) and an angiosperm (*Quercus rubra*). Materials were analyzed by (1) optical microscopy, (2) FTIR microscopy, (3) elemental analysis, (4) in source (DEI) pyrolysis--mass spectrometry [Py-MS], and (5) Curie-point pyrolysis--gas chromatography--mass spectrometry [Py-GC/MS]. With these techniques, a unique chemical fingerprint was established for each of our samples. Ultimately, neither the cell walls of the pollens nor those of *L. polyedra* resting cysts showed convincing evidence of a carotenoid-based structure, and therefore probably represent substances distinct from traditionally-defined sporopollenin. Furthermore, aside from the generation of prist-1-ene during pyrolysis, no aliphatic components were detected during analysis of the dinoflagellate material. These

results indicate that the resistant biopolymers comprising *L. polyedra* resting cyst walls may be fundamentally different than the algaenans of the chlorophyte algae.

EXPERIMENTAL

Biological materials and culturing conditions

Laboratory cultures of *Lingulodinium polyedra* were established and maintained as described in Chapter 2. All dinoflagellate material utilized in the present study derived from a single strain (GpES-19). Although cultures were not axenic, examination under the microscope revealed any bacterial mass to be negligible. The majority of resting cyst production in batch cultures occurred during the 2 weeks following peak cell density (i.e. starting about 3.5-4 weeks after inoculation). After cyst production was complete, cultures tubes were stored under the same conditions used for actively growing cultures. To collect enough dinoflagellate material for analysis, 50 culture tubes (inoculated between April and November, 1991) were harvested using a teflon policeman to gently scrape culture residue from tube bottoms. Loostened materials were transfered to centrifuge tubes, washed 5 times in Milli-Q water, briefly sonified, washed again 5 times, and then freeze dried. Pollen of *Juniperus scopulorum* (Rocky Mountain Juniper) and *Quercus rubra* (Northern Red Oak) were obtained from Sigma (Sigma Chemical Company, St. Louis, MO, U.S.A.). Both pollens were microscopically examined for purity prior to analysis.

Isolation of resistant cell walls

Resistant cell wall materials were isolated using a 3-step procedure (solvent extraction, saponification, acid hydrolysis) shown schematically in Figure 3.1.
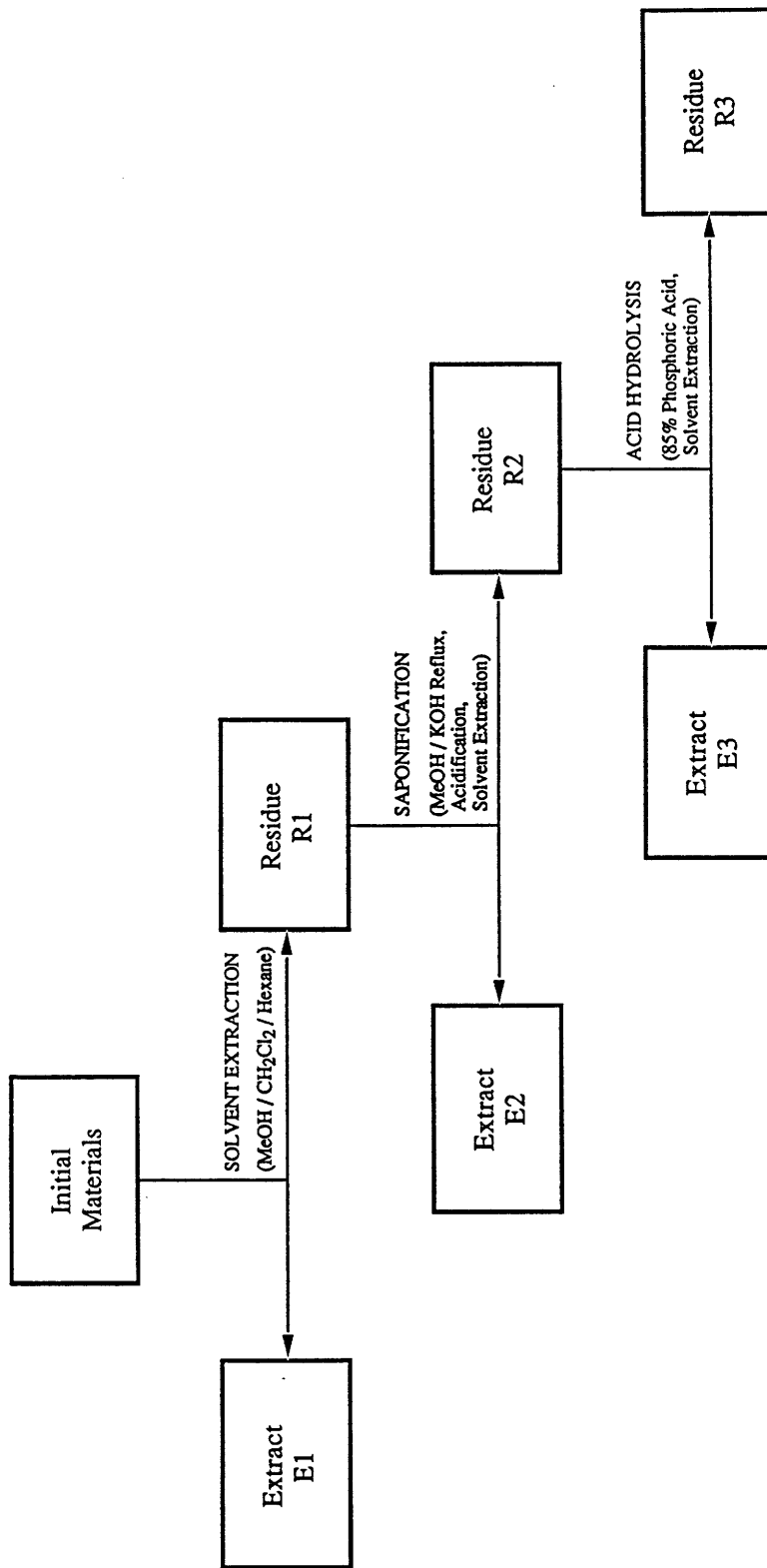
FIGURE 3.1 Schematic illustration of procedures used to isolate resistant cell wall fractions.

Solvent extraction. Samples were sequentially extracted ultrasonically at room temperature with a mixture of methanol (MeOH) and dichloromethane (CH_2Cl_2) (1/1, v/v, 2x) and CH_2Cl_2 / hexane (4/1, v/v, 2x). After each extraction, the insoluble residues were recovered by centrifugation, yielding residues R1; extraction supernatants were combined and concentrated for each sample resulting in extracts E1.

Saponification. R1 residues were refluxed for 6 hours in 6% KOH in MeOH/H_2O (9/1, v/v). After saponification, reflux mixtures were acidified to pH 4 by additions of 2N HCl/MeOH (1/1, v/v). Residues were separated by centrifugation and supernatants transferred to a separatory funnel. The residues were then ultrasonically extracted using H_2O (100%), MeOH / H_2O (1/1, v/v), MeOH (100%), MeOH / CH_2Cl_2 (1/1, v/v), and CH_2Cl_2 / hexane (4/1, v/v). Each time, supernatants were combined in the separatory funnels. After final extraction (CH_2Cl_2 / hexane), funnel contents separated into a bottom organic phase and an upper aqueous phase. Organic phases were removed, and the aqueous phases back-extracted with CH_2Cl_2 (2x). All CH_2Cl_2 fractions were combined to yield extracts E2. Aqueous layers were left standing over a small volume of residual CH_2Cl_2 in separatory funnels; fine suspended materials in the aqueous phase collected at the CH_2Cl_2 / aqueous layer interface. These materials were collected and archived as E2 "fluffs".

Acid hydrolysis. R2 residues were heated to 55°C in 85% phosphoric acid for 13 days without stirring. Insoluble residues were then separated by filtration (polycarbonate membrane; pore size, 0.4 μm) and extracted as above. The filtrate and all solvent extraction supernatants were combined and partitioned in separatory funnels as described above; these procedures resulted in extracts E3, residues R3, and E3 "fluffs".

Optical microscopy. Initial materials and residues R1, R2, and R3 of resting

cyst and pollen materials were optically characterized using a Zeiss Axioskop equipped

with Differential Interference Contrast (DIC). A Zeiss MC-100 camera system and Kodak

Technical Pan film were used for photomicrography.

FTIR microscopy. Infrared transmission spectra were acquired on a

Nicolet/Spectra-Tech IRμs/SIRM (scanning infrared microprobe) from $600 - 4000$ cm^{-1}

using a triangular apodization function and a resolution of 4 cm^{-1}. Objectives were either

32x (0.65 NA) or 15x (0.58 NA) Reflachromat (reflecting Cassegrainian type) and the

condensor was a 10x (0.71 NA) Reflachromat. The detector was a liquid-nitrogen-cooled,

narrow-band MCT. Sample spectra were obtained by co-adding a number of scans (128

for high signal-to-noise samples and 256 or 512 for small, low signal-to-noise samples)

and ratioing the sample scans to the background scans. Samples were prepared by placing

a small amount of material on a BaF$_2$ or KCl plate. A second salt plate was placed on top

of the first and the entire arrangement was housed in a micro-compression cell. The sample

could then be flattened until it became transparent (~5-15 μm in thickness). A small crystal

of KBr was also placed in the cell and used for background spectra. All samples were

doubly apertured (above the sample to define the sampling area and below to eliminate stray

light effects) with variable rectangular apetures. Sample sizes varied from 20 x 20 to 100 x

100 μm. For each of the dinoflagellate residues, spectra were obtained from the walls of a

single, isolated, empty resting cyst to distinguish this material from other cellular debris in

the samples. Pollen spectra were obtained from clumps of residue representing resistant

cell walls plus any cytoplasmic materials present in the sample. A recent review of FTIR

microscopy is provided by Katon and Sommer (1992).

Elemental analysis. C, H, and N contents for all residues were obtained on a

Perkin Elmer 2400 CHN Elemental Analyzer. The limited quantities of our residues,

particularly those derived from dinoflagellate cultures, generally precluded duplicate analyses. Oak Initial and R1 residues, however, were analyzed in triplicate, and showed less than 1% variation between measurements, despite large differences in sample size.

"In-source" pyrolysis--mass spectrometry (Py-MS). "In-source" pyrolysis--mass spectrometry was performed on a JEOL DX-303 double focusing mass spectrometer equipped with a resistively heated platinum filament Desorption Electron Ionization (DEI) probe. Samples (1 to 5 μg) were applied to the filament as a MeOH suspension. The filament was heated at 2 A min^{-1} ($\sim$20°C sec^{-1}) up to 1.5 A ($\sim$800°C). Electron Impact (EI) spectra (16eV) were acquired over mass ranges varying from either 20-750 amu to 50-2000 amu, at a scan cycle time of 1 sec. The source temperature was 180°C. An extensive description of Py-MS methods is given by Boon (1992).

Multivariate analysis of averaged spectra summed over the entire acquisition period was carried out on a Sun SparcStation using a modified version of the ARTHUR package (Infometrix, Seattle, WA). Pyrolysis-MS analysis of all residues was performed in triplicate to allow both factor and discriminant analysis of the resulting data.

Curie-point pyrolysis--gas chromatography--mass spectrometry [Py-GC/MS]. Py-GC/MS analysis was performed using a Horizon Curie-Point Pyrolysis unit, a Hewlett Packard HP 5890 Series II gas chromatograph, and a VG AutoSpec Q mass spectrometer. Samples (15-100 μg) were pyrolyzed for 2 or 5 sec on wires with a Curie temperature of either 610°C or 770°C under a helium head pressure of 15 psi. Gas chromatographic separation was achieved on a fused silica column (Restec, 60 m x 0.32 mm I.D.) coated with a methylsilicone (R_{tx-1}) stationary phase (film thickness, 0.5 μm). The GC was programed from 35°C (5 min.) at initial temperature to 320°C (20 min.) at final temperature at 3°C min^{-1}. Electron Impact (EI) mass spectra (55eV) were acquired over a scan range of 35 to 500 Da at a scan rate of 0.6 sec/decade and resolution of 2000.

RESULTS

Optical Microscopy

Plate 3.1 shows the appearance of dinoflagellate and pollen materials before and after each stage of the treatments used to isolate the resistant walls for analysis. Unprocessed residue from culture tubes of *Lingulodinium polyedra* consisted chiefly of empty thecae at various stages of dissociation, but also contained cellular debris from all stages of the life cycle including resting cysts, intact motile cells (both vegetative and planozygotic), gametes, ecdysed cells, temporary cysts, and various dispersed cytoplasmic components (Plate 3.1, Figure 1). The spherical, spine-bearing resting cysts of this species are morphologically distinct from other life cycle stages (see Chapter 2). Initial washing, freeze-drying, and solvent extraction of the dinoflagellate material resulted in an R1 residue showing no significant changes in visual composition, aside from the physical disruption and dispersion of cellular materials (Plate 3.1, Figure 4). Formerly intact resting cysts and other cell types were largely disrupted, thecae tended to dissociate into individual plates, and cytoplasmic materials were widely dispersed. Similarly, saponification did little to change the basic visual composition of the residues (Plate 3.1, Figure 7). After acid hydrolysis, however, the character of the residue changed dramatically (Plate 3.1, Figure 10a). Dinoflagellate R3 consisted almost entirely of random-sized sheets of resting cyst walls, clearly identifiable by their characteristic "fibrous" wall texture, archeopyle sutures, and spines. Resting cyst walls at this stage appeared light amber in color, a noticable change from the greyish translucence shown in R2 (pre acid-hydrolysis) residues. Co-occurring with the wall material in the R3 residues were small (generally <10 μm) globular to irregularly shaped masses of uncertain origin (Plate 3.1, Figure 10b). Although a minor component of the overall residue (< ~3%, visual estimation), these masses were clearly

different from the wall material. No walls or membranes from other life cycle stages could be identified in the dinoflagellate R3.

Initial Juniper pollen consisted of intact, viable cells (Plate 3.1, Figure 2); in fact, a large percentage of these grains germinated during microscopic observation while in a wet mount. Juniper pollen cells were spherical with no obvious apertures; typical grains showed patches of granular ornament on the outer surface of the exine. Solvent extracted cells (Plate 3.1, Figure 5) appeared identical to the initial materials, and indeed some R1 cells actually germinated during observation. Examination of Juniper R2 showed saponification and subsequent extractions to have ruptured most of the cells and removed most of the cytoplasmic materials (Plate 3.1, Figure 8). All remaining cytoplasmic components appeared to be eliminated by acid hydrolysis. A small amount of granular material was present in R3 material (Plate 3.1, Fig. 11) and may represent a portion of the granular exine ornament which sheared off during processing. As with the dinoflagellate residue, acid hydrolysis noticeably darkened the Juniper pollen cell walls.

Oak pollen initial materials again consisted of intact cells, although none were observed to germinate. These cells were oblate in general morphology and tricolpate with respect to apertures (Plate 3.1, Figure 3). The solvent extracted residue (R1, Plate 3.1, Figure 6) showed general retention of pollen grain morphology although many cells were ruptured and appeared to have lost cytoplasm. Saponification and subsequent extraction of this material caused further rupture of cells and removal of cytoplasmic components (Plate 3.1, Figure 9). At this stage (R2), a thin wall or membrane was still visible in the colpi of some specimens. These membranes disappeared during acid hydrolysis so that Oak R3 (Plate 3.1, Figure 12) consisted entirely of the tricolpate outer walls (typically torn and/or distorted) showing a characteristic fibrous texture. As with both the dinoflagellate and Juniper materials, acid hydrolysis imparted a darker color to the isolated Oak R3 pollen walls.

FTIR spectra of dinoflagellate and pollen materials at all stages of the isolation protocol are shown in Figures 3.2 to 3.4, and illustrate the evolution of functional group chemistry as a result of solvent extraction, saponification, and acid hydrolysis.

A single empty *L. polyedra* resting cyst isolated from the initial dinoflagellate culture material (after washing and freeze-drying) yielded the spectrum shown in Figure 3.2a. The broad band centered at 3380 cm^{-1} represents hydroxyl groups (primarily phenolic, alcoholic, and/or carboxylic OH, but any remaining free water would also contribute to this absorbance). A sharp absorption at 2929 cm^{-1}, and a weaker one at about 2855 cm^{-1}, relate to CH_2 and/or CH_3 groups. At slightly lower wavenumbers, the very weak and broad absorbance centered at about 2700 cm^{-1} probably results from the presence of carboxylic acid dimers. The carbonyl stretch in carboxylic acid gives rise to the absorbance at 1702 cm^{-1}, while nearby bands at 1654 and 1560 cm^{-1} probably relate to amide C=O and amide N-H bonding, respectively. Absorptions in the interval from about 1450 to 1200 cm^{-1} are difficult to assign with any certainty aside from that at 1374 cm^{-1} which likely relates to CH_2 and/or CH_3 groups. Finally, the strong absorption with a maximum at 1077 cm^{-1} indicates a C-O stretch in carboxylic acids.

The spectrum of an empty resting cyst isolated from R1 residue (Fig. 3.2b) was essentially identical to the initial spectrum aside from small shifts in the wavenumbers of some absorbances, resolution of additional minor bands in the 1100 to 1160 cm^{-1} region, and a decrease in the relative intensity of the CO band at 1063 cm^{-1}. Similarly, the spectrum of post-saponification resting cyst walls (Fig. 3.2c) shows no real change except for some loss of definition of absorbances at 1700 and 1560 cm^{-1}.

A spectrum obtained from sheets of resting cyst walls from *L. polyedra* R3 is shown in Fig 3.2d. The OH and CO absorptions were still prominent (3415 and 1063 cm^{-1}) but significantly reduced relative to the sharp CH_2 and/or CH_3 absorptions at 2929
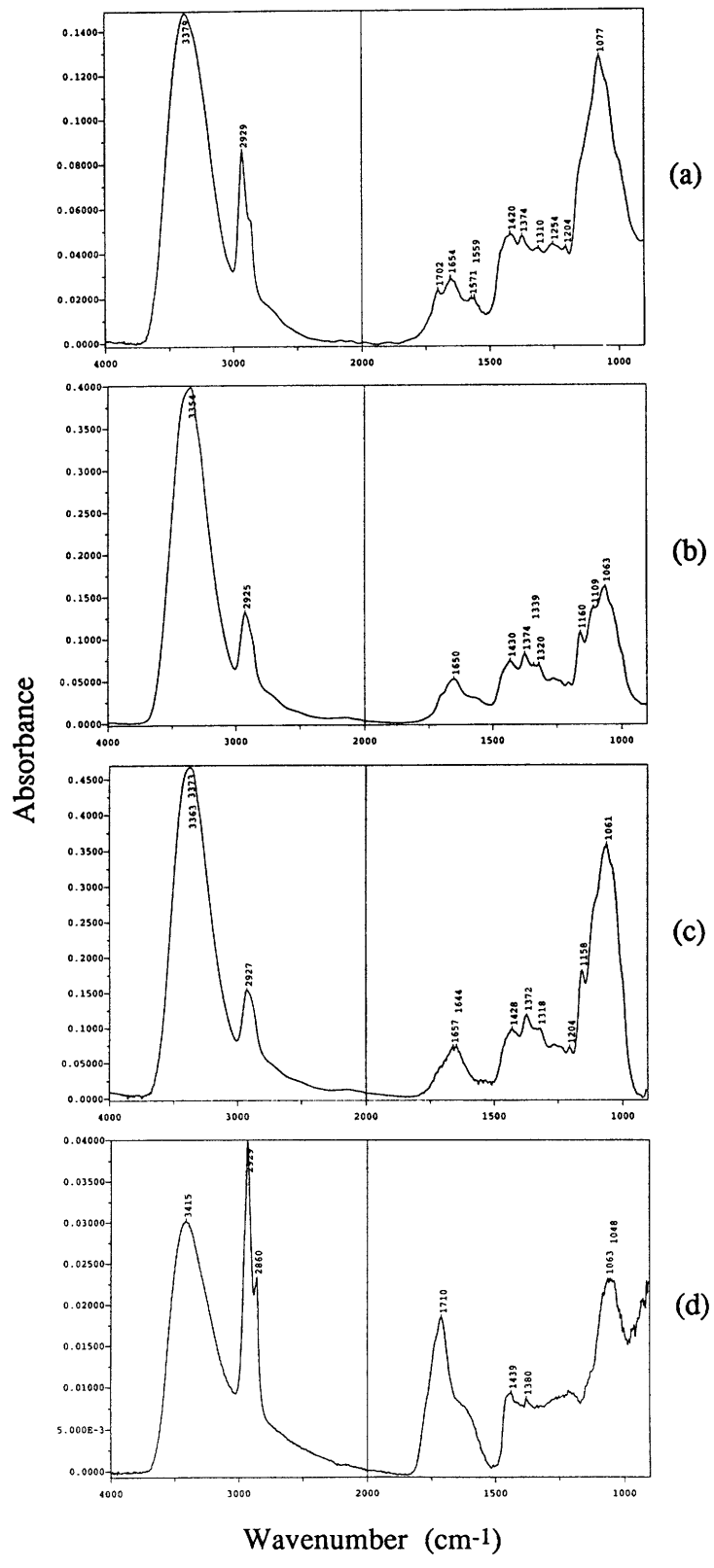
FIGURE 3.2 FTIR spectra of single, empty resting cysts isolated from dinoflagellate residues: (a) Initial, (b) R1, (c) R2, (d) R3.

and 2860 cm^{-1}. A strong absorption at 1710 cm^{-1} indicates the presence of C=O groups, possibly from carboxylic acids. This band shows a broad shoulder in the vicinity of 1630 cm^{-1} which may be due to aromatic C=C, although other groups (free water, amide C=O) could make some contribution.

Wide OH and CO absorption bands (3371 and 1075 cm^{-1}) are also present in the spectrum obtained from unprocessed Juniper pollen (Fig. 3.3a) as are bands relating to CH$_2$ and/or CH$_3$ (2931 and 2860 cm^{-1}) and COOH (weak response at ~2700 cm^{-1}). Additional features of the initial Juniper material include a band at 1727 cm^{-1} relating to ester groups, and a strong absorption at 1657 cm^{-1} possibly due to amide C=O and/or any free water.

Solvent extracted Juniper pollen yielded a spectrum (Fig. 3.3b) which was virtually identical to that of the initial material. After saponification, however, some differences could be noted (Fig. 3.3c). OH and CO absorbances (3375 and 1077 cm^{-1}) were reduced relative to the CH$_2$ and/or CH$_3$ bands at 2935 and 2861 cm^{-1}. In addition, the ester band noted previously (~1725 cm^{-1}) was not visible in the Juniper R2 spectrum. Instead, this region was dominated by an absorption at 1683 cm^{-1}, possibly relating to the presence of amide groups. Notches in the shoulder of this band (~1580 cm^{-1}) probably represent aromatic C=C. The sharp band at 1517 cm^{-1} is difficult to assign, but is also shown in the spectrum obtained from Juniper R3 (Fig. 3.3d). Aside from the presence of this latter feature, the Juniper R3 spectrum is essentially the same as that of Dinoflagellate R3 (Fig. 3.2d).

As evidenced by FTIR microscopy, the evolution of Oak pollen functional group chemistry was similar to that just described for the Juniper materials. A spectrum of Oak Initial material (Fig. 3.4a) showed OH and CO bands at 3300 and 1067 cm^{-1}, CH$_2$ + CH$_3$ bands at 2929 and 2856 cm^{-1}, and a weak COOH absorption at about 3050 cm^{-1}. The presence of esters was suggested by the inflection at ~1750 cm^{-1}. A very prominent band
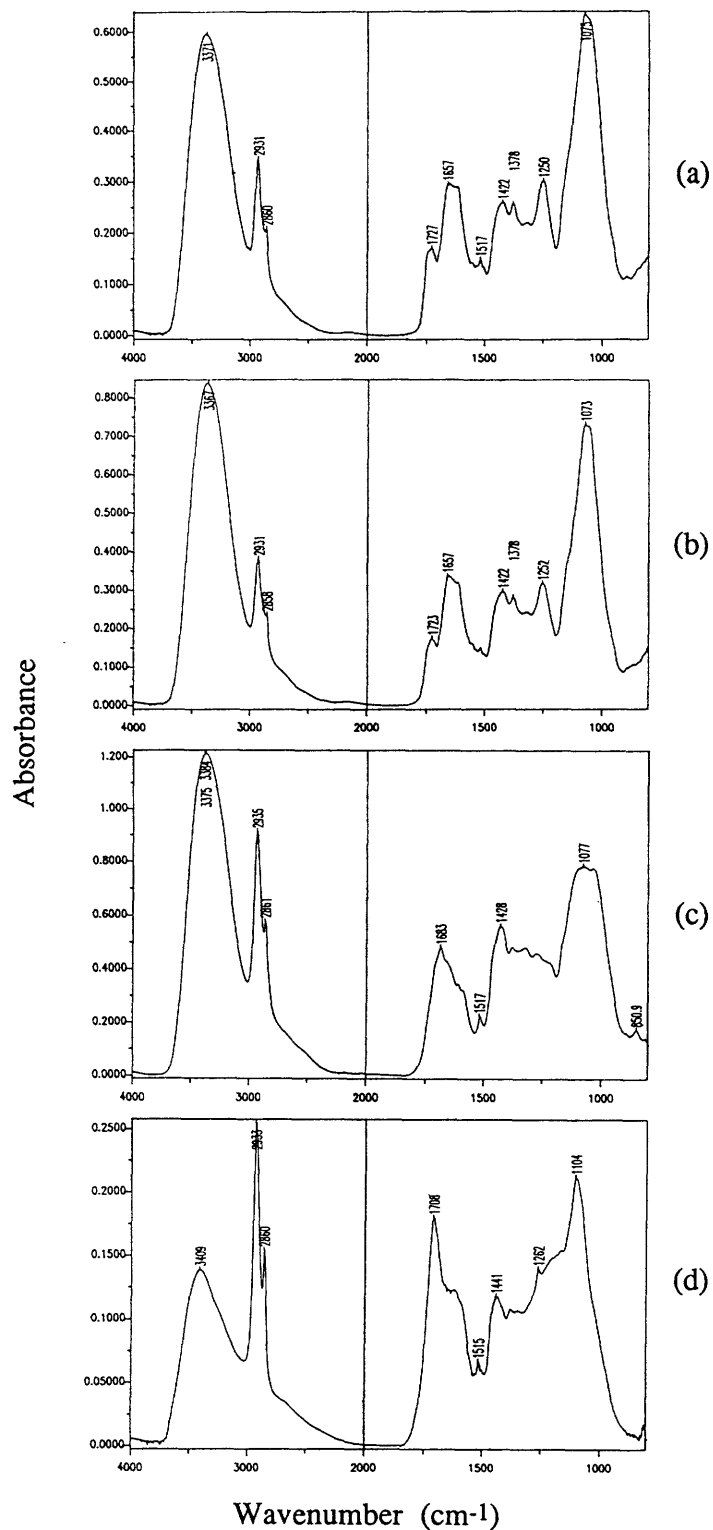
FIGURE 3.3 FTIR spectra of Juniper residues: (a) Initial, (b) R1, (c) R2, (d) R3.
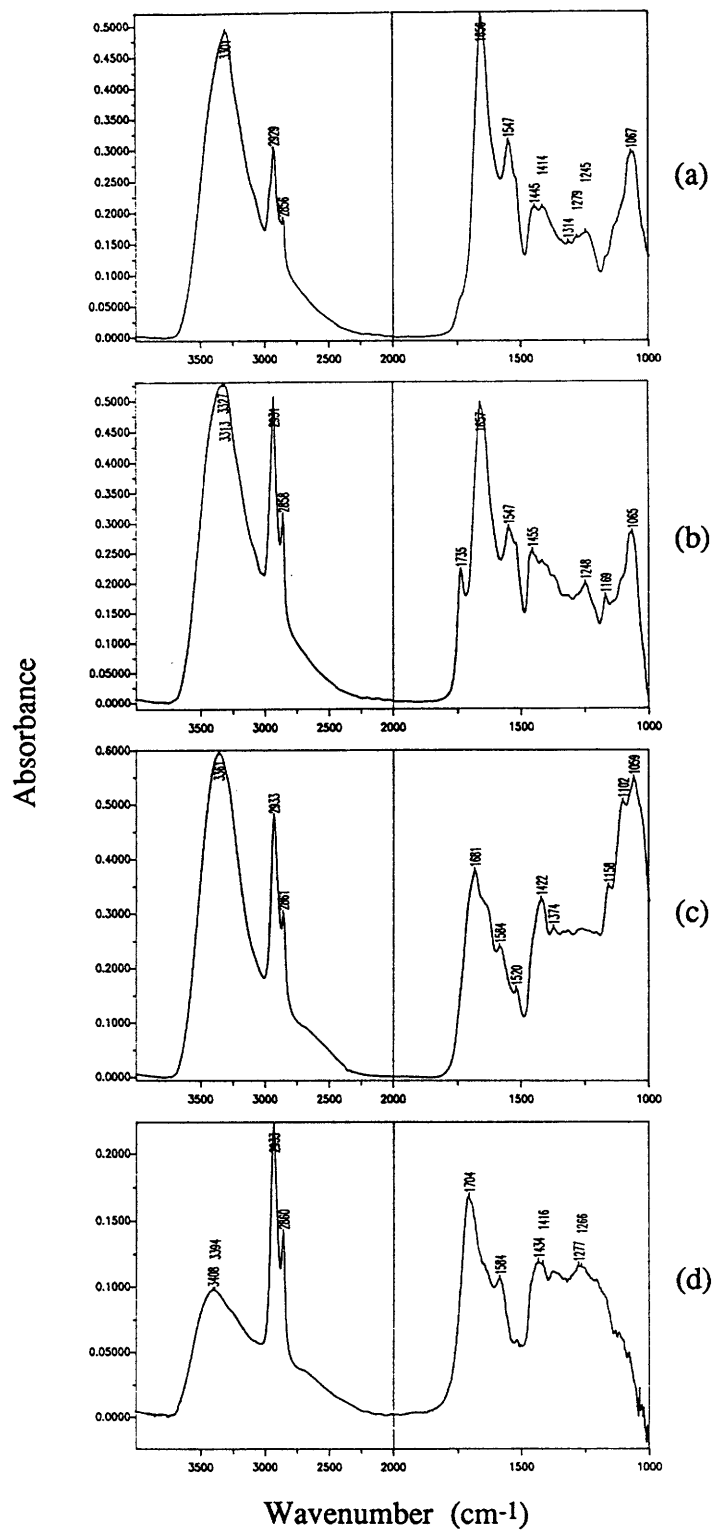
FIGURE 3.4 FTIR spectra of Oak residues: (a) Initial, (b) R1, (c) R2, (d) R3.

94

at 1656 cm^{-1} and another at 1547 cm^{-1} probably relate to amide groups (and/or free water), while the notch at ~1520 cm^{-1} may result from the presence of CO_2.

In the Oak R1 spectrum (Fig. 3.4b), OH and CO bands diminish in relative intensity while the ester band (1735 cm^{-1}) becomes better defined, but otherwise solvent extraction does not appear to have caused significant functional group changes. Saponification of Oak R1 eliminated the ester peak and produced a strong band at 1681 cm-1 (Fig. 3.4c). These and other changes yielded an Oak R2 spectrum almost identical to that of Juniper R2. Similarly, acid hydrolysis had the same effects on the Oak material as it did for Juniper. The only real difference in the spectrum of Oak R3 residue (relative to that for Juniper R3) is the lack of a well defined CO absorbance in the 1060 cm^{-1} region (Fig. 3.4d).

Elemental Analysis

Values for % carbon, hydrogen, and nitrogen in dinoflagellate and pollen materials are shown in Table 3.1. Approximate values for % oxygen are also included, but these were arrived at by difference and therefore probably represent overestimates of the amount of oxygen present. No determination of ash content was attempted in this investigation. Atomic ratios were calculated using the above elemental data and are included in Table 3.1.

Initially, the percentage of carbon in all three materials assayed to 43-48%. These values showed no meaningful change throughout solvent extraction and saponification treatments, but increased significantly (to 52-58%) as a result of acid hydrolysis. The dinoflagellate material showed a similar trend in percentage of hydrogen (i.e. no significant changes in initial values until acid hydrolysis). Although a marked decrease in % nitrogen was observed in the Dinoflagellate R3, this trend was not as clearly shown by the pollens.

95

TABLE 3.1. Elemental Analysis

		Initial	R 1	R 2	R 3
L. polyedra	%C:	43.12	44.02	41.66	52.73
	%N:	10.06	12.53	8.14	1.25
	%H:	4.60	4.77	4.40	8.64
	*%O:	42.22	38.68	45.80	37.38
	H/C:	1.270	1.293	1.254	1.948
	O/C:	0.735	0.658	0.826	0.530
	N/C:	0.200	0.244	0.166	0.020
Juniper	%C:	43.37	44.23	47.47	58.69
	%N:	1.27	1.63	7.95	3.43
	%H:	4.72	4.75	4.94	5.80
	*%O:	50.64	49.39	39.64	32.08
	H/C:	1.295	1.278	1.241	1.176
	O/C:	0.876	0.838	0.626	0.410
	N/C:	0.025	0.032	0.144	0.050
Oak	%C:	48.12	46.60	42.11	57.08
	%N:	5.94	6.19	1.04	0.59
	%H:	5.14	4.87	4.42	5.77
	*%O:	40.80	42.34	52.43	36.56
	H/C:	1.270	1.243	1.246	1.201
	O/C:	.0.636	0.682	0.935	0.481
	N/C:	0.106	0.114	0.021	0.009

* Calculated by difference

Total Ion Current (TIC) profiles. TIC thermal evolution profiles resulting from direct mass spectrometry of dinoflagellate materials are shown in Fig. 3.5. Pyrolysis of unprocessed culture residue (Fig. 3.5a) yielded three maxima in the TIC trace: the first results from thermal desorption (evaporation) of compounds, and the other two at higher temperatures from thermal dissociation (pyrolysis). After solvent extraction, the desorption maximum was no longer visible (Fig. 3.5b). Saponification further modified the TIC profile by eliminating the secondary pyrolysis maximum (Fig. 3.5c). Pyrolysis of R3 materials (i.e. after acid hydrolysis) yielded the single TIC peak shown in Fig. 3.5d. Although similar in basic outline to Fig. 3.5c, the R3 TIC peak showed two significant differences: (1) the R3 TIC maximum occurred at a higher temperature (scan 41, representing a temperature of ~800°C), relative to that of R2 (scan 38), and (2) the R3 TIC peak is narrower. Thus, acid hydrolysis selectively removed those compounds represented by the lower temperature portion of the TIC curve in Fig. 3.5c.

A similar evolution in TIC profile was demonstrated by the pollen materials. Figures 3.6 and 3.7 show these profiles for Juniper and Oak, respectively. Note that the temperature of maximum evolution for the R3 residues was similar for all three samples (scan 41, ~800°C).

Summed Spectra. The average spectrum of initial dinoflagellate culture material summed over scans 15-50 (Fig. 3.8a) was largely dominated by ions representing polysaccharide fragments (e.g. m/z 57, 60, 73, 98, 126, & 163). Other prominant ions at m/z 271, 287, 316, 366, and 384 suggest the presence of sterols, while those at m/z 213, 239, & 256 reflect free and bound fatty acids. A series of tocopherols are suggested by ions at m/z 402, 416, & 430; ions at m/z 522, 550 & 578 probably relate to the presence of diglyceride units.
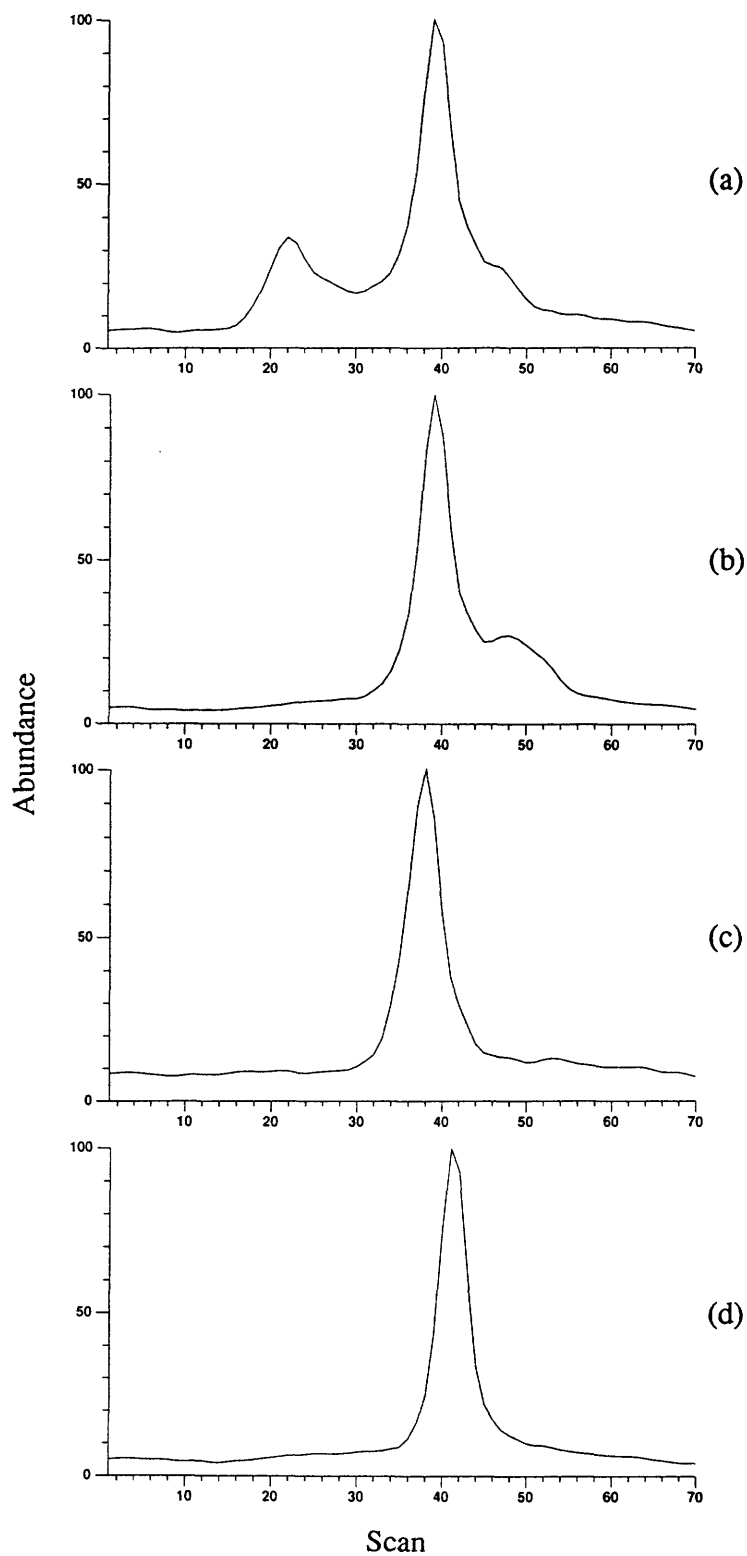
FIGURE 3.5 Total ion current (TIC) profiles from Py-MS analysis
of dinoflagellate materials: (a) Initial, (b) R1, (c) R2, (d) R3.
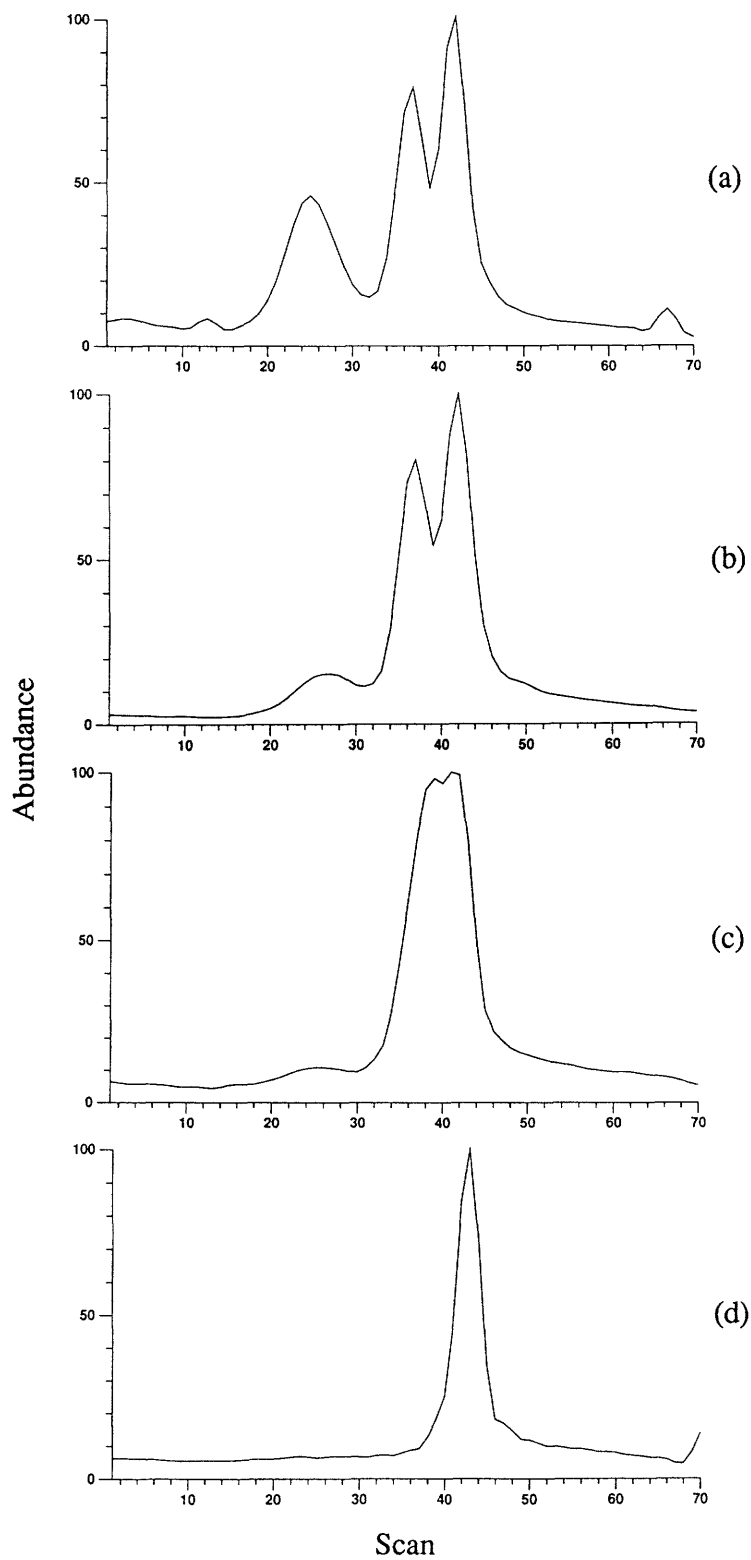
FIGURE 3.6 Total ion current (TIC) profiles from Py-MS analysis of Juniper materials: (a) Initial, (b) R1, (c) R2, (d) R3.
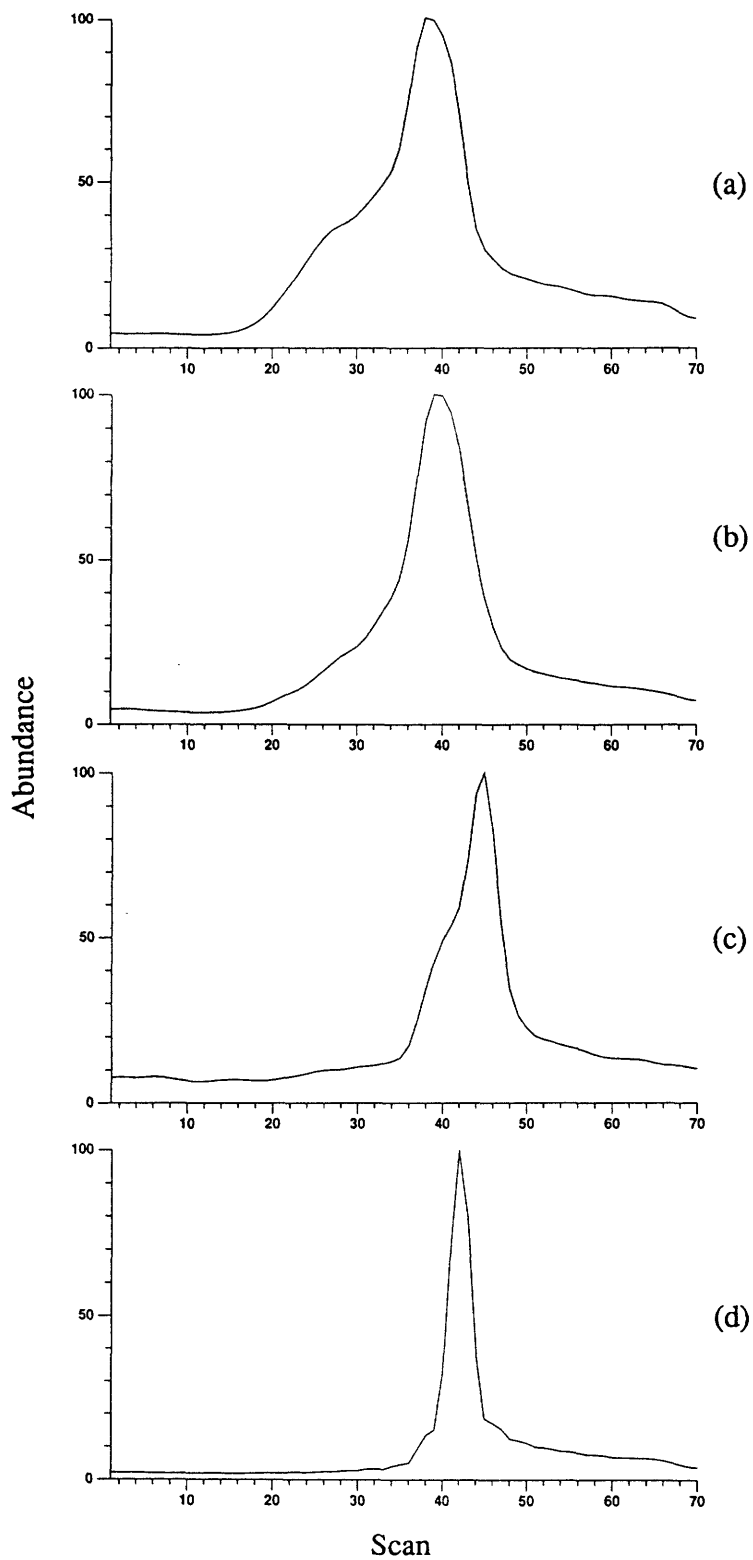
FIGURE 3.7 Total ion current (TIC) profiles from Py-MS analysis
of Oak materials: (a) Initial, (b) R1, (c) R2, (d) R3.

Ions of polysaccharide fragments again dominated the summed spectrum of dinoflagellate residue R1 (Fig. 3.8b) implying the resistance of parent polysaccharides to solvent extraction. Sterols, however, were largely removed, with the possible exception of some residual dehydrated sterol suggested by the ion at m/z 366. Fatty acids also continue to contribute to the spectrum as shown by the presence of ions at m/z 228, 239, & 256. The spectrum of dinoflagellate R2 (Fig. 3.8c) is very similar to that of R1 indicating that post-saponification residue still consists mainly of polysaccharides. Ions at m/z 149, 167, & 279 probably represent phthalate (plasticizer) contamination, while that at m/z 446 most likely relates to instrument background contributions (vacuum pump oil).

Py-MS of the dinoflagellate material after acid hydrolysis yielded a complex spectrum (Fig. 3.8d) showing a bias towards ions of low mass number. The polysaccharide signature present in Initial, R1, and R2 spectra could no longer be detected at this stage. Of those assignable, the most abundant ion (m/z 44) represents CO_2, presumably derived from carboxylic acid groups. Ions at m/z 224, 252, & 280 may relate to aliphatic fragments in the C_{16} to C_{24} range, while others (m/z 110, 120, & 122) are suggestive of phenolic compounds.

Ions dominating the Py-MS spectrum of initial Juniper material (m/z 73, 87, 102, & 116) indicate the presence of soluble sugars in the unprocessed pollen (Fig. 3.9a). Others (e.g. m/z 256, 262, 264, 280, 308, & 336) relate to fatty acids; diglyceride components are indicated by ions at m/z 576, 600, & 618 and point to longer chain fatty acids. Ions at m/z 414 (M^+) and m/z 396 (M^+ - H_2O) most likely represent the C_{29} higher plant sterol, ß-sitosterol.

The elimination of polysaccharides, fatty acids, and sterols from the Juniper pollen as a result of the sequential chemical treatments (solvent extraction, saponification, and acid hydrolysis) was similar to that observed for the dinoflagellate material. Py-MS of the final residue (R3) yielded the mass spectrum shown in Fig. 3.9b. The general profile of low m/z ions indicated here resembles that of the Dinoflagellate R3 spectrum, but suggests
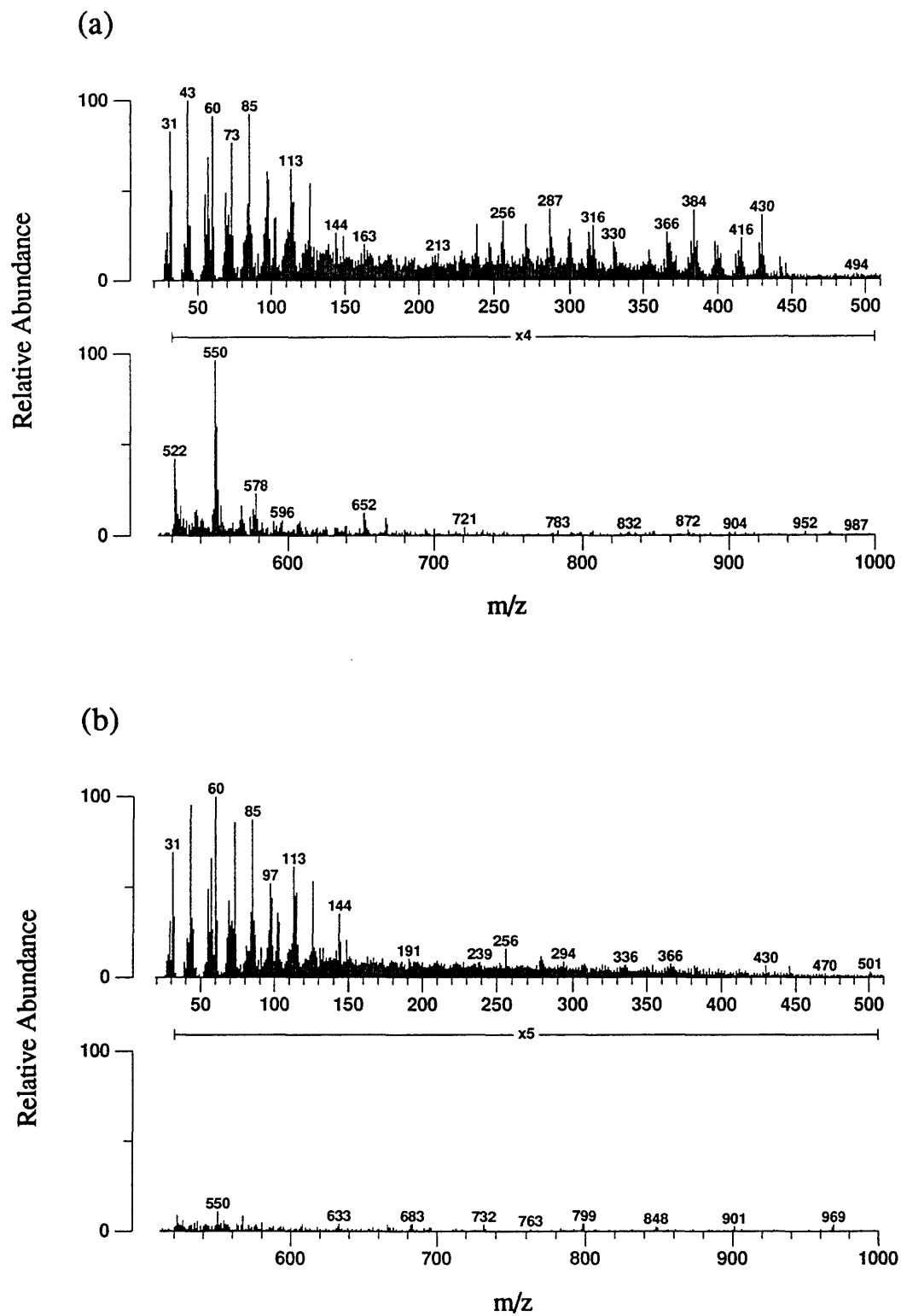
FIGURE 3.8 Average summed mass spectra from Py-MS analysis of dinoflagellate materials: (a) Initial, (b) R1. Note scale magnification starting at *m/z* 520.

(c)

(d)
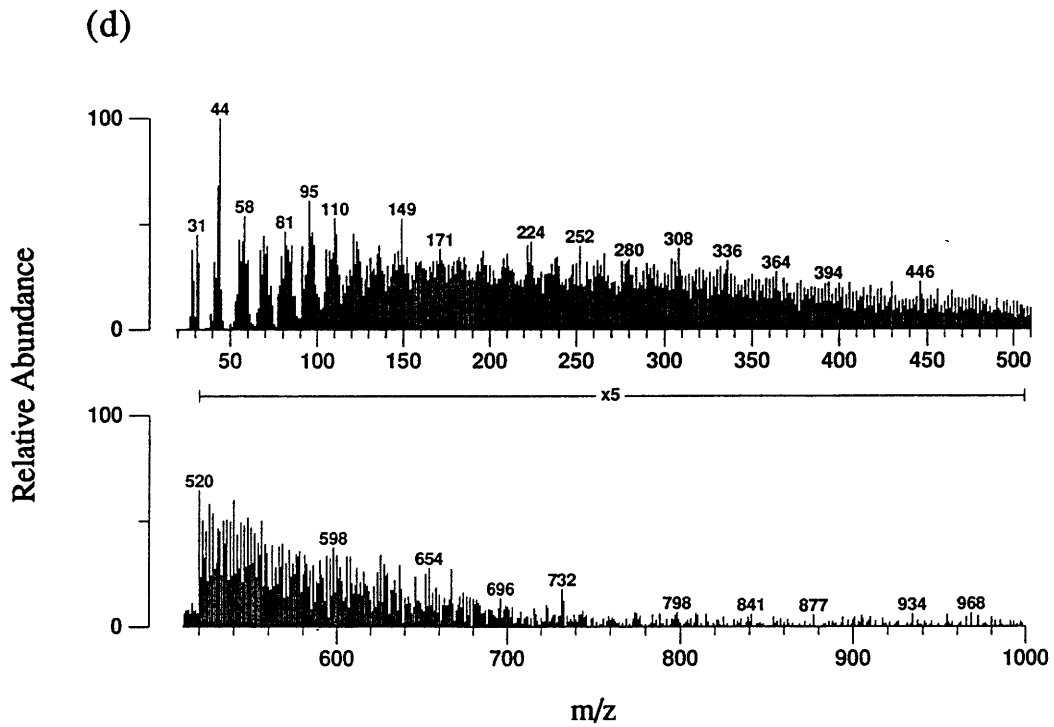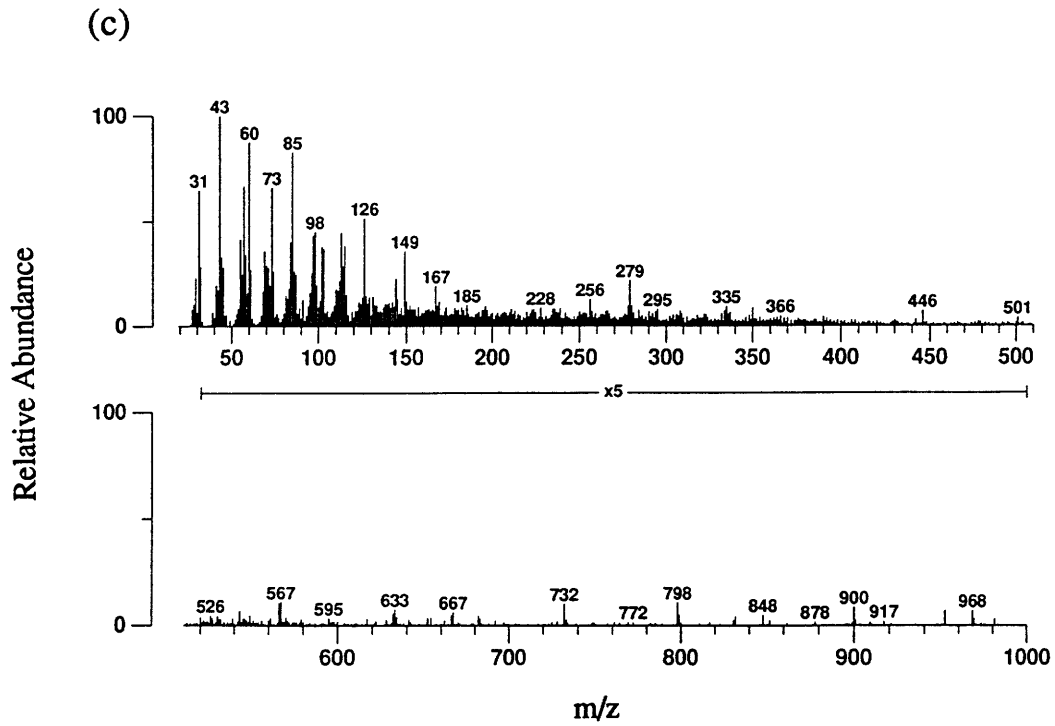
FIGURE 3.8, continued: (c) R2, (d) R3.

103
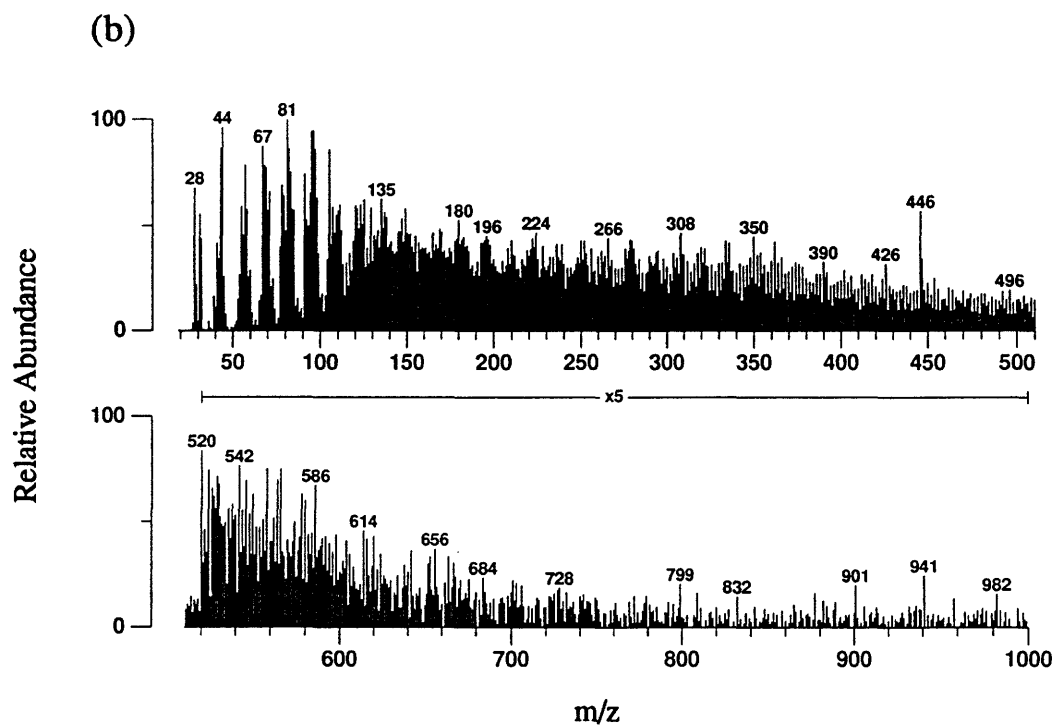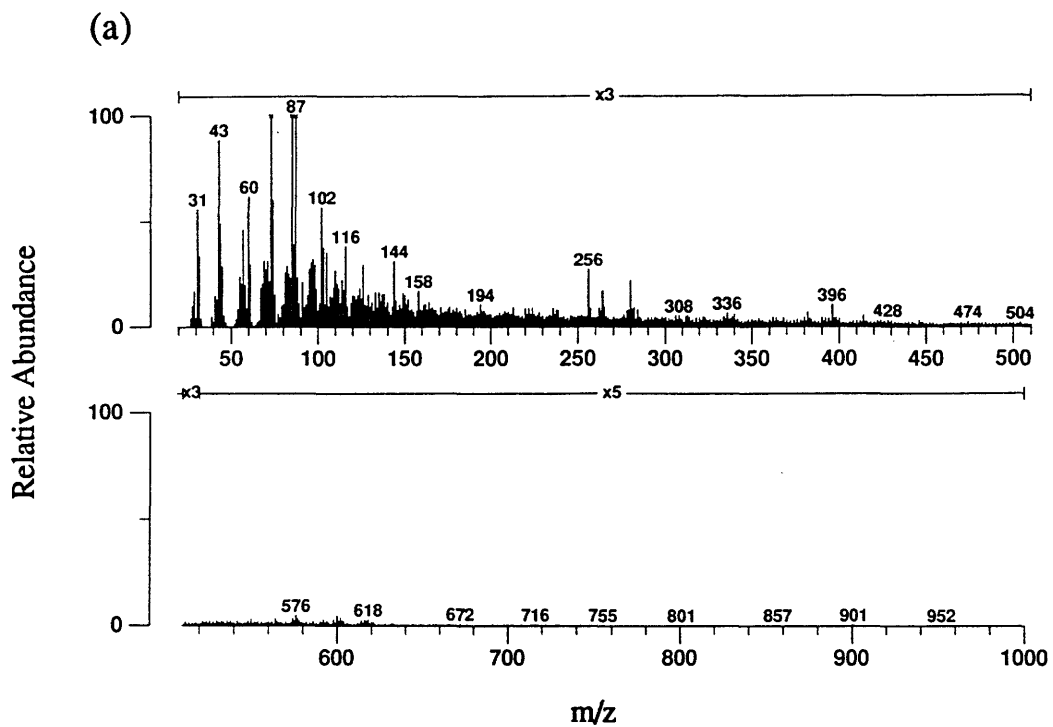
FIGURE 3.9 Average summed mass spectra from Py-MS analysis
of Juniper materials: (a) Initial, (b) R3.
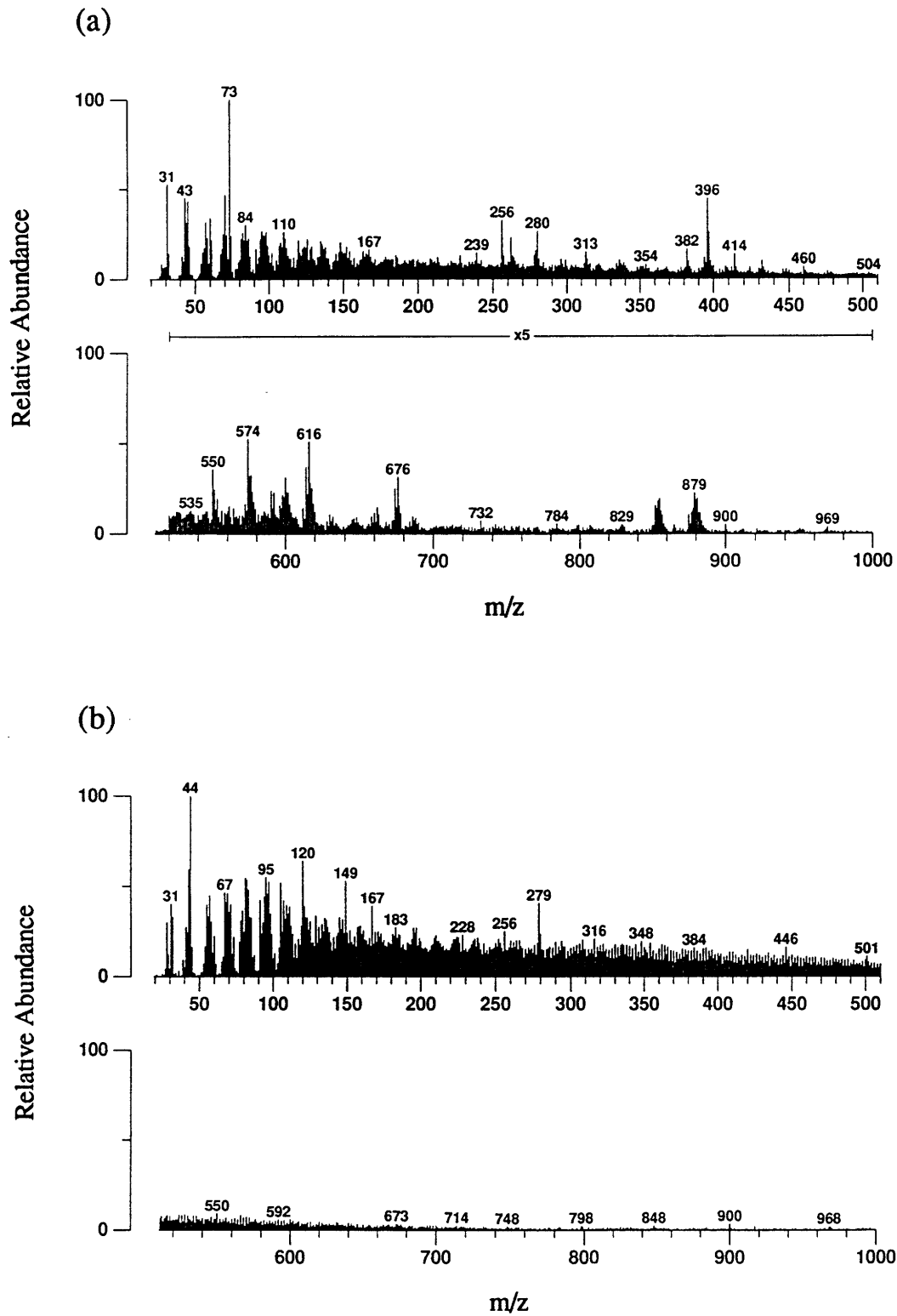
FIGURE 3.10 Average summed mass spectra from Py-MS analysis
of Oak materials: (a) Initial, (b) R3.

105

greater relative abundance of long chain aliphatic components. Ions at m/z 196 and 224 may indicate alkene fragments, but most other ions are difficult to assign with confidence.

Characteristic ions in the Py-MS spectrum of unprocessed Oak pollen (Fig. 3.10a) include m/z 73 (soluble sugars); m/z 239, 256, 280, 313, & 354 (fatty acids); m/z 676 & 732 (wax esters); and m/z 829, 879, & 900 (triglycerides). A protein component is suggested by m/z 84.

In contrast to the dinoflagellate and Juniper materials, Oak residue R3 (i.e. after saponification and acid hydrolysis) still contained some lipid material, as evidenced by the fatty acid signal at m/z 256 (Fig. 3.10b). Also noteworthy in the Oak R3 Py-MS spectrum is the mass peak at m/z 120, possibly suggesting the presence of acetophenone (M^+) or p-coumaric acid (M^+ - CO_2). Decarboxylation of this latter compound could also, in part, contribute to the prominant CO_2 signal at m/z 44.

Multivariate analysis of Py-MS data. To identify variables that would reflect the chemical differences between our materials, summed mass spectra for each of the samples were input into the FOM-PYROMAP statistical package for multivariate data reduction. Nine principal components (PC's) cummulatively accounted for 86% of the total variance in the data set (Table 3.2). Subsequent discriminant analyses of triplicate runs allowed refinement of these PC's and yielded new independent variables (discriminant functions) which are shown in Table 3.3. Each discriminant function (DF) was mathematically reconstructed into a "mass spectrum" of covarying mass peaks. The relative dissimilarity of dinoflagellate, Juniper, and Oak materials at each stage of the isolation procedure are represented in the plot of discriminant function sample scores (DF 1 and 2) shown in Fig. 3.11. Sample distribution within the score plot depends on the degree of Py-MS similarity relative to positive and negative DF 1 spectra (horizontal axis) and positive and negative DF 2 spectra (vertical axis). These mathematically reconstructed spectra, reflecting the discriminant loadings, are shown in Figs. 3.12 and 3.13.

TABLE 3.2. Principal Components

	PC1	PC2	PC3	PC4	PC5	PC6	PC7	PC8	PC9
Eigenvalue:	318.163	89.010	63.803	44.105	21.485	17.482	12.798	11.276	0.484
% Variation Preserved (Each) :	46.7	13.1	9.4	6.5	3.2	2.6	1.9	1.7	1.2
% Variation Preserved (Cumulative):	46.7	59.8	69.2	75.6	78.8	81.4	83.2	84.9	86.1

107

TABLE 3.3. Discriminant Functions

	DF1	DF2	DF3	DF4	DF5	DF6	DF7	DF8	DF9
Eigenvalue:	152.325	91.739	56.354	188.915	24.454	20.348	23.020	18.956	10.492
% Variation Preserved (Each) :	22.4	13.5	8.3	27.7	3.6	3.0	3.4	2.8	1.5
% Variation Preserved (Cumulative):	22.4	35.8	44.1	71.9	75.4	78.4	81.8	84.6	86.1

108
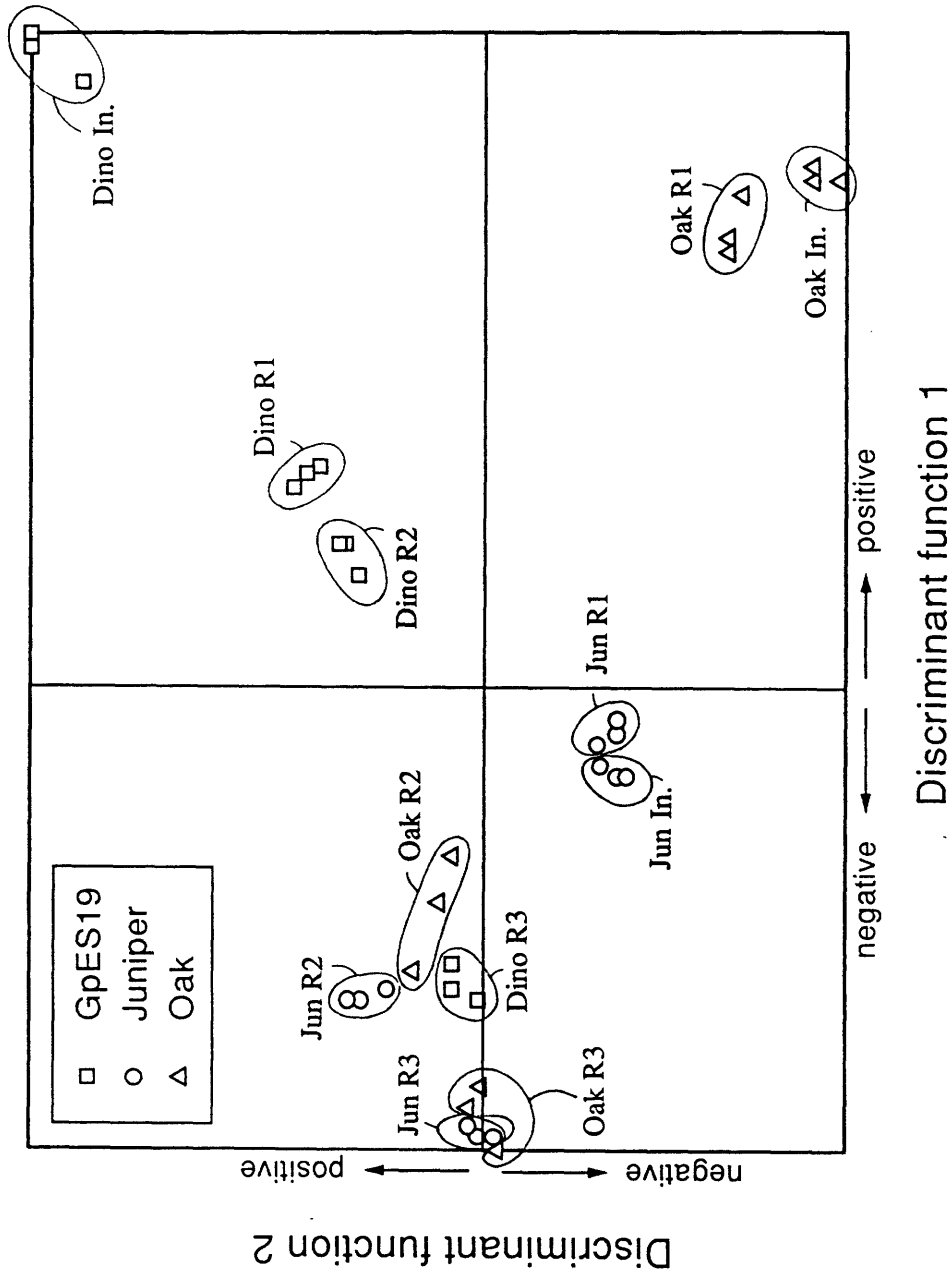
FIGURE 3.11 Plot of Discriminant Function sample scores (DF 1 and 2).
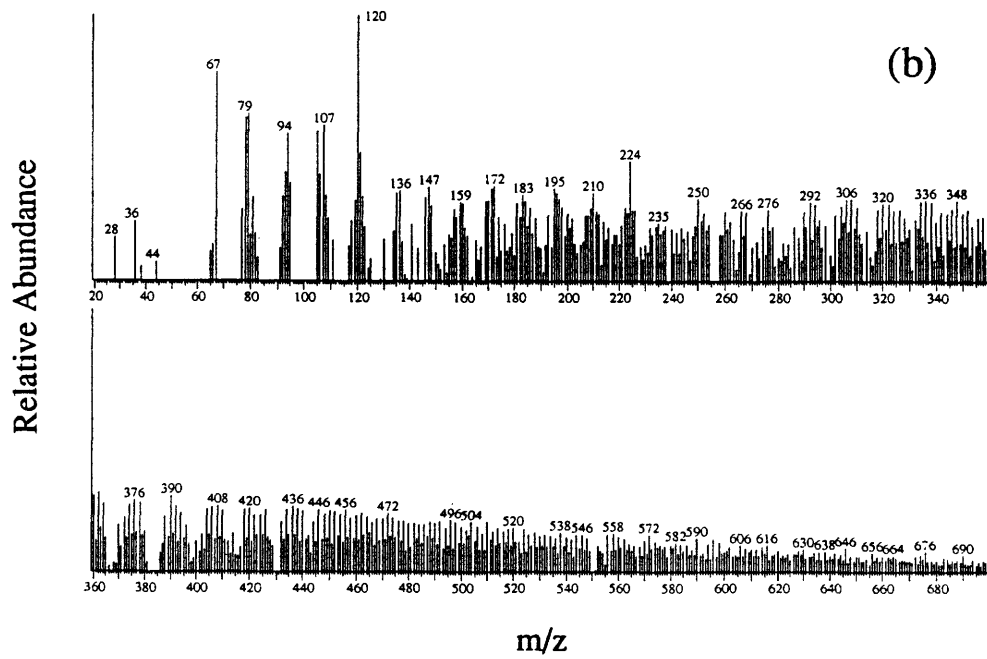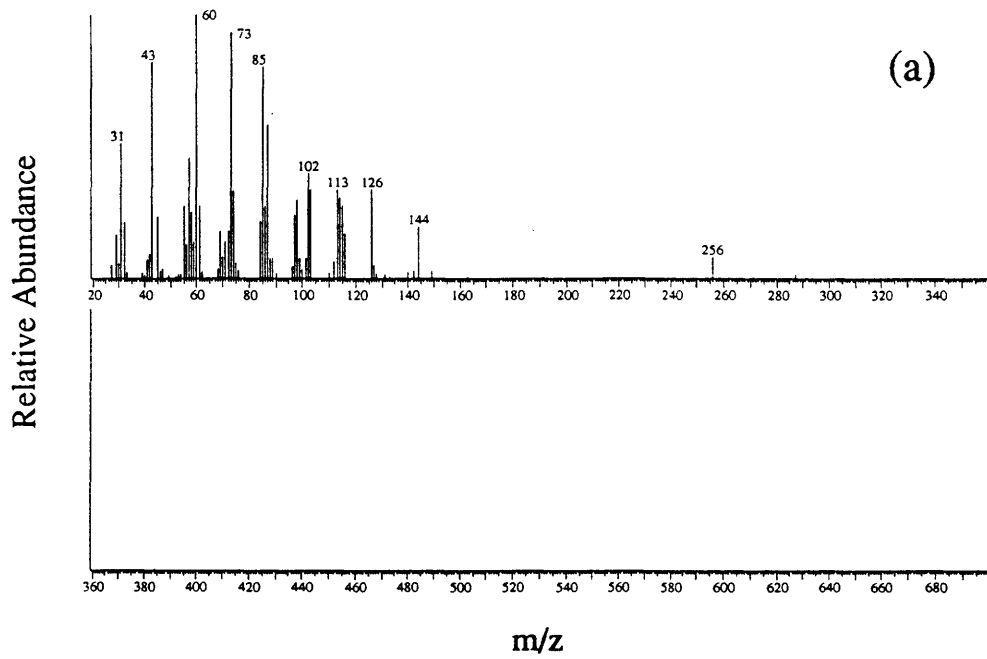
FIGURE 3.12 Discriminant Function 1 spectra: (a) DF 1+, (b) DF 1-.
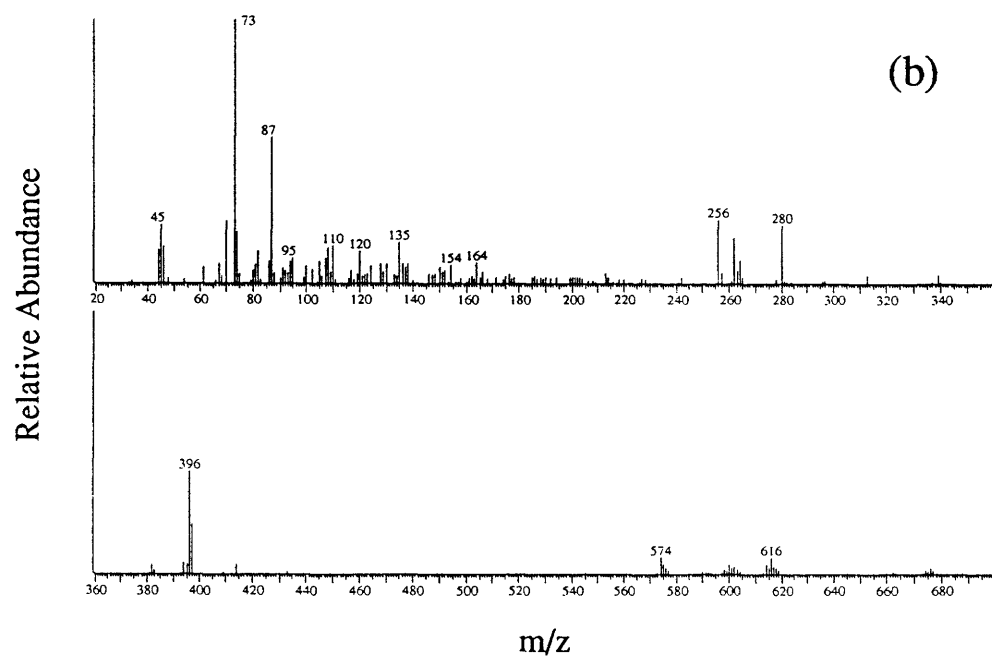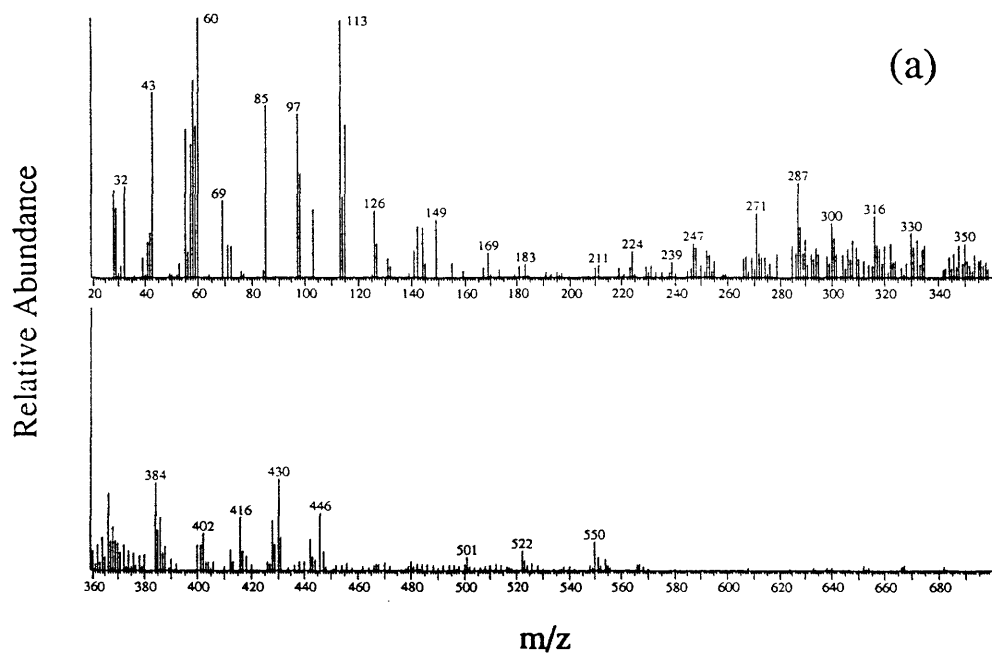
FIGURE 3.13 Discriminant Function 2 spectra: (a) DF 2+, (b) DF 2-.

The positive DF 1 (DF 1+) spectrum is relatively uncomplicated and clearly represents a polysaccharide signature, indicated by peaks at m/z 57, 60, 73, 85, 98, and 126. Ion specificity appears much more obscure in the complex assemblage of the negative DF 1 (DF 1-) spectrum; one exception is the strong mass peak at m/z 120 which may be correlated to relatively high amounts of p-coumaric acid in each of the R3 residues. The DF 2+ spectrum also shows a partial contribution from polysaccharide ions (m/z 60, 113, 85, 126), but also contains a strong sterol signature (m/z 271, 287, 316, 366, 384). Ions characteristic of tocopherols (m/z 402, 416, 430) and diglyceride molecular ions (m/z 522, 550) can also be identified. Prominent in the DF 2- spectrum is a strong mass peak at m/z 73 which likely relates to soluble sugars. A fatty acid component is also suggested by ions at m/z 256 and 280.

As reflected by their location in the DF score plot (Fig. 3.11), starting materials for the dinoflagellate, Juniper, and Oak samples showed significant chemical differences. The position of Dinoflagellate Initial material indicates strong correlation with both DF 1+ and DF 2+. In contrast, Oak Initial material shows a strong affinity to DF 1+ and DF 2-. Juniper Initial material is only only weakly correlated to these discriminant functions, but does show some association with DF 1- and DF 2-. Changes in chemical composition as a result of solvent extraction, saponification, and acid hydrolysis procedures are illustrated by changes in DF scores for R1, R2, and R3 residues. Solvent extraction did little to change the Py-MS character of the pollens, but had a noticable effect on the dinoflagellate materials. The reverse is true for saponification, which had no major impact on the dinoflagellate residue but caused large shifts in DF scores of the pollens. Interestingly, as a result of these shifts, R2 residues of Juniper and Oak show clustering in the score plot, suggesting similarity in composition at this stage. After acid hydrolysis, all residues clustered on the extreme left of the score plot (indicating strong correlation to DF 1-), but showed relatively neutral correlation with respect to DF 2.

Total ion current chromatograms from Curie-point Py-GC/MS analysis of Dinoflagellate Initial, Dinoflagellate R3, Juniper R3, and Oak R3 residues are shown in Figures 3.14-3.17. Selected peaks are identified in Tables 3.4; these identifications are based largely on comparison of individual peak mass spectra to those in both the literature and standard MS libraries. Recognition of homologous series was aided by mass chromatography of characteristic ions.

Prominent in the TIC trace of Dinoflagellate Initial (Fig. 3.14) are peaks representing polysaccharide pyrolysis fragments, including both early-eluting compounds (lower molecular weight furans, furanones, and pyrans), and later-eluting compounds including 1,4-dideoxy-D-*glycero*-hex-1-enopyranos-3-ulose and, most abundantly, levoglucosan. Aromatic compounds such as toluene (Peak #14) and phenol (Peak #39) were minor products. A major component (Peak #79) is identified as a $C_{16:0}$ fatty acid, while spectra obtained for several high molecular weight peaks (collectively #89) suggest the presence of sterols.

Peaks representing sterols and fatty acids are not detectable in the Dinoflagellate R3 Py-GC/MS TIC chromatogram shown in Figure 3.15. The strong polysaccharide signature of the initial dinoflagellate material has also been significantly reduced, but not eliminated entirely as indicated by the continued presence of furan and furanone peaks. Pyrolysis of the R3 material produced a more prominent and extensive series of aromatic compounds including naphthalenes, indanes, indenes, and benzaldehydes as well as alkylbenzenes and phenols. The strong signal at Peak #76 was identified as prist-1-ene.

The Juniper R3 Py-GC/MS TIC chromatogram (Fig. 3.16) was marked by a well defined homologous series of *n*-alkanes and *n*-alk-1-enes ranging from C_7 to C_{28}. Other peaks corresponded to primarily aromatic compounds (alkylbenzenes, alkylphenols, methyl phenols, indanes, indenes, naphthalenes, and benzaldehyde). This strong aromatic

113
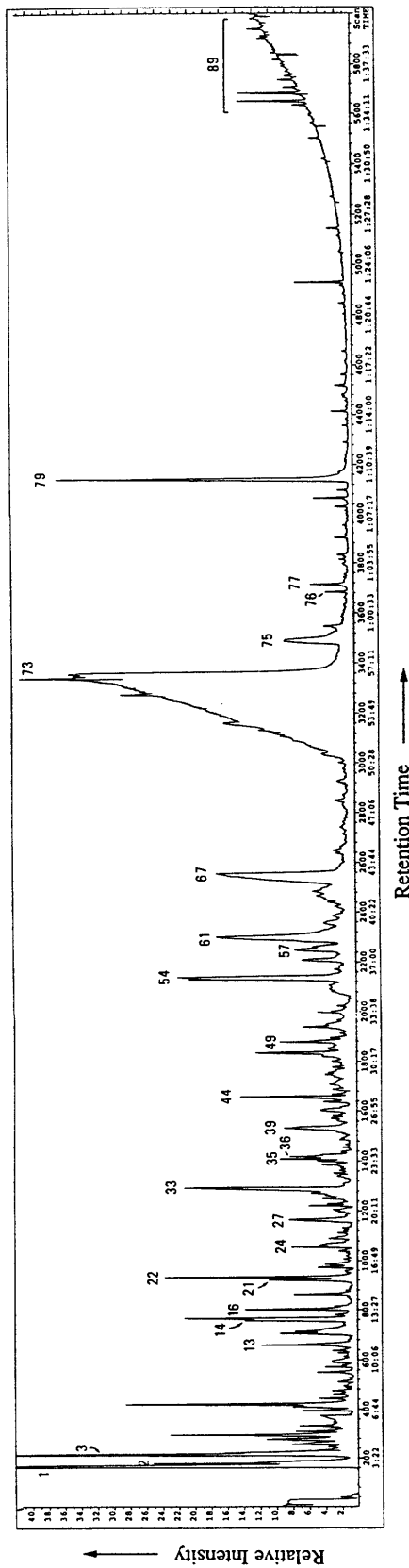
FIGURE 3.14 Total ion current (TIC) chromatogram from Curie-point Py-GC/MS analysis of Dinoflagellate Initial residue. Peak numbers correspond to compounds listed in Table 3.4.

114
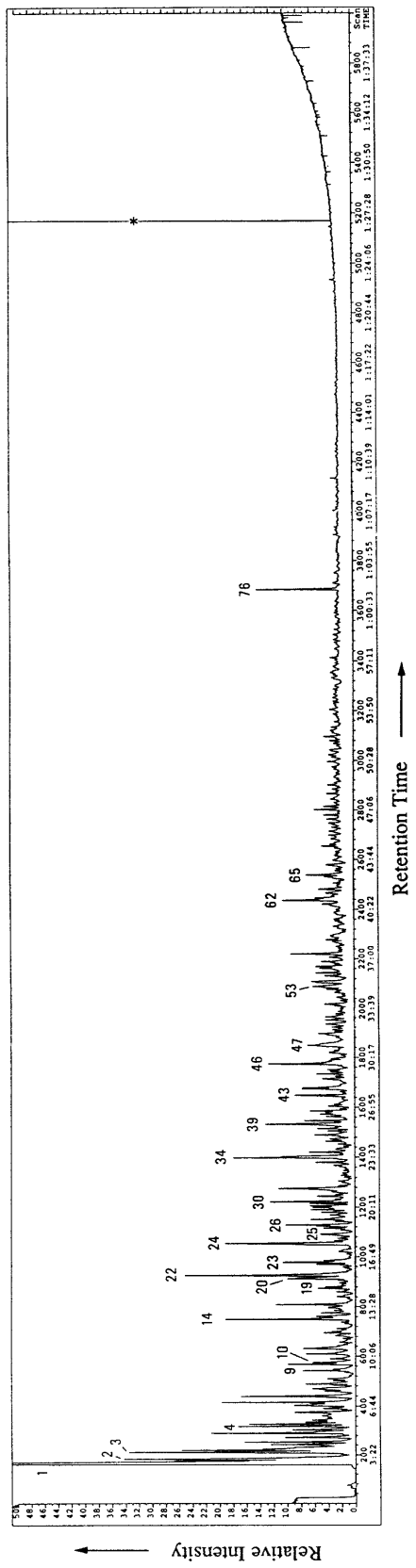
FIGURE 3.15 Total ion current (TIC) chromatogram from Curie-point Py-GC/MS analysis of Dinoflagellate R3 residue. Peak numbers correspond to compounds listed in Table 3.4. (Asterisk denotes instrument noise spike.)
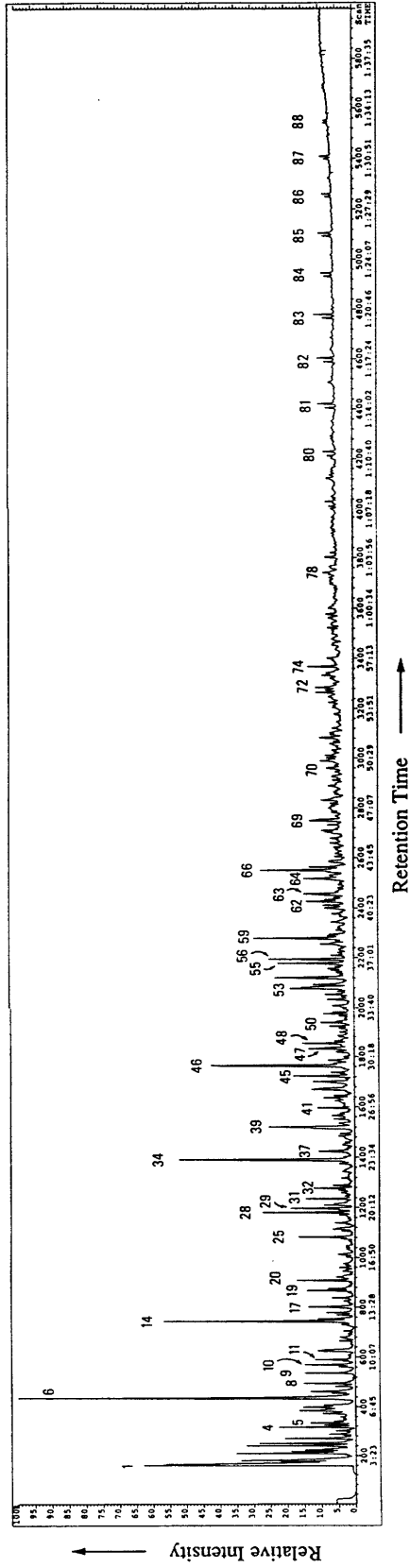
FIGURE 3.16 Total ion current (TIC) chromatogram from Curie-point Py-GC/MS analysis of Juniper R3 residue. Peak numbers correspond to compounds listed in Table 3.4.

116
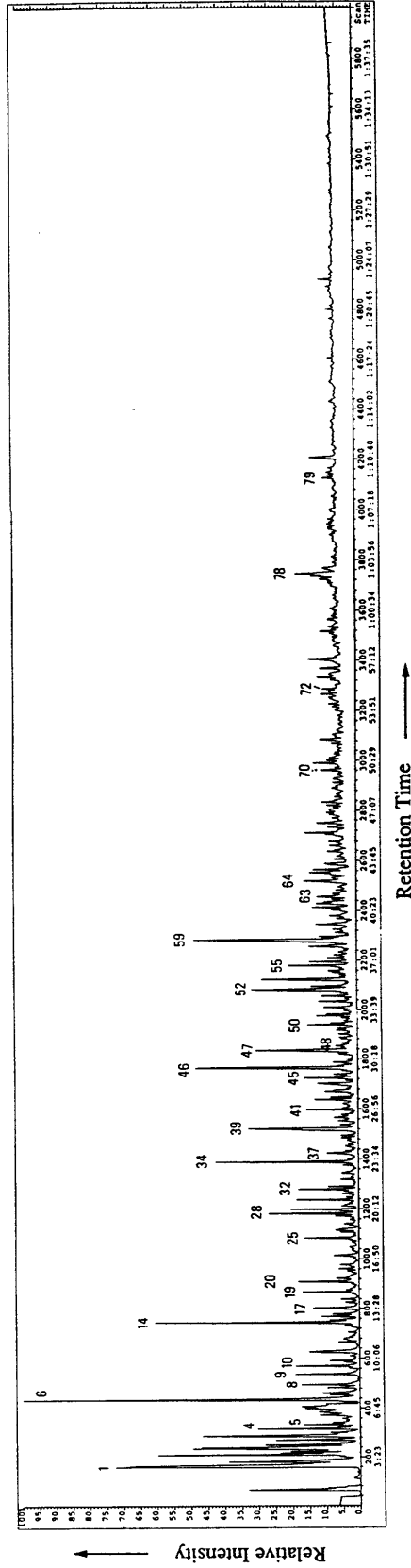
FIGURE 3.17 Total ion current (TIC) chromatogram from Curie-point Py-GC/MS analysis of Oak R3 residue. Peak numbers correspond to compounds listed in Table 3.4.

117

TABLE 3.4. Py-GC/MS data on *L. polyedra* Initial, *L. polyedra* R3, Juniper R3, and Oak R3. Compound numbers refer to the peak numbers in Figures 3.14 - 3.17.

Compound Number	Compound Name
1	carbon dioxide
2	nC4 alkene + alkane
3	nC5 alkene + alkane
4	nC6 alkene
5	nC6 alkalkane
6	benzene
7	cyclopenadiene
8	cyclohexane
9	nC7 alkene
10	nC7 alkane
11	heptatirene
12	unknown
13	alkylfuran ?
14	toluene
15	methylcyclohexane
16	cyclopentanone
17	heptatriene
18	furaldehyde
19	nC8 alkene
20	nC8 alkane
21	cyclopentanone
22	furaldehyde
23	methylvinylfuran
24	C3-furan
25	ethylbenzene
26	1,3 + 1,4-dimethylbenzene
27	furan-2-one
28	styrene
29	1,2-dimethylbenzene
30	C4-furan ?
31	nC9 alkene
32	nC9 alkane
33	hydroxycyclopent-2-ene-1-one
34	benzaldehyde
35	methyl furaldehyde
36	methyl pyranone
37	n-propyl benzene
38	C3-benzene
39	phenol
40	C3-benzene
41	nC10 alkene
42	nC10 alkane
43	hydroxymethylcyclopentanone
44	hydroxymethylcyclopentanone
45	indene
46	acetophenone
47	methylphenol

TABLE 3.4. Continued

Compound Number	Compound Name
48	methoxyphenol
49	levoglucosenone + hydroxymethylpyranone
50	nC11 alkene
51	nC11 alkane
52	C1 benzaldehyde + C3 phenol
53	C5 benzene + methylindene
54	unknown
55	napthalene
56	C1 methoxyphenol
57	dianhydrolucopyranose
58	nC12 alkene
59	dihyrobenzofuran
60	nC12 alkane
61	5-hydroxymethyl-2-furaldehyde
62	dihyroinden-1-one
63	C2-methoxyphenol
64	2-methylnapthalene
65	C2-dihydroindene
66	methoxyphenylethanone
67	1,4-dideoxy-D-glycero-hex-1-enpyranos-3-ulose
68	1-methylnaphthalene
69	unknown phenol
70	C2-naphthalene
71	C8-benzene
72	fluorene
73	levoglucosan
74	benzophenone
75	anhydro-ß-D-glucofuranose
76	prist-1-ene
77	C14:0 fatty acid
78	phenanthrene
79	C16:0 fatty acid
80	nC20 alkene + alkane
81	nC21 alkene + alkane
82	nC22 alkene + alkane
83	nC23 alkene + alkane
84	nC24 alkene + alkane
85	nC25 alkene + alkane
86	nC26 alkene + alkane
87	nC27 alkene + alkane
88	nC28 alkene + alkane
89	sterols

signature was also reflected in the TIC trace of Oak R3 (Fig. 3.17); in fact, nearly all of the aromatic compound peaks in the Juniper R3 chromatogram had exact counterparts in the Oak R3 chromatogram. The latter trace, however, failed to show the extended alkane/alkene homologous series characteristic of the Juniper R3 material. In the Oak R3 TIC chromatogram, this series could only be indentified from C_7 to C_{13}.

DISCUSSION

This investigation compares resistant cell wall biopolymers derived from two very different cell types: the first, resting cysts of a unicellular marine alga (a dinoflagellate); and the second, pollen from terrestrial seed plants. Both types commonly occur together as morphologically distinctive structures in the fossil record and traditionally have been considered similar in composition. To test this assumption, we employed a three-step procedure aimed at isolating resistant cell wall materials from (1) dinoflagellate resting cysts (*Lingulodinium polyedra*), (2) gymnosperm pollen (*Juniperus scopulorum*), and (3) angiosperm pollen (*Quercus rubra*), for optical and chemical analysis. After each step, residues were characterized by a variety of methods to evaluate the effects of chemical treatments. Analysis of final residues suggests similarities between these resistant materials, but also reveals essential differences--particularly between the dinoflagellate and pollen substances.

Assessment of isolation methods

A critical component of studies exploring the resistant walls of plant cells is the nature of the isolation procedure. An ideal protocol would meet two objectives, (1) isolate a pure residue of the cell wall material by elimination of all other cellular (and extracellular)

120

substances, and (2) accomplish this isolation without modification of wall chemistry. The extent to which these objectives can both be met is currently difficult to assess. Early investigations of pollen and spores often accomplished wall isolation using relatively drastic chemical techniques such as acetolysis (i.e. boiling in acetic anhydride / concentrated sulfuric acid, ~9/1, v/v, for ~10-20 min.; see Erdtman, 1961). Although generally yielding "clean" wall preparations, this technique has more recently been suspected to alter the composition of the walls to such an extent as to make original components difficult or impossible to identify. Berkaloff et al. (1983) concluded that acetolysis resulted in partial acetylation of hydroxyl groups which greatly complicated IR analysis and subsequent use of spectra for comparative purposes. Furthermore, acetolysis of unextracted materials can produce artifacts due to the condensation of carotenoids and other lipids into resistant clumps which, again, may hamper analysis by IR and other methods (Brunner and Honegger, 1985). Direct acetolysis of our dinoflagellate and pollen materials (see Appendix 2) yielded substances having FTIR and Py-MS characteristics very different from those of the R3 residues described in this report.

To avoid the drawbacks of direct acetolysis, many recent studies (e.g. Berkaloff et al., 1983; Largeau et al., 1984, 1985; Burczyk, 1987a,b; Puel et al., 1987; Burczyk and Dworzanski, 1988; Guilford et al., 1988; Kadouri et al., 1988; Derenne et al., 1989, 1990, 1991) have employed succesive chemical treatments patterned to various degrees after those of Zetzsche et al. (1931) and Shaw and Yeadon (1966). Typically, these treatments consist of (1) solvent extraction, (2) saponification via KOH reflux, and (3) acid hydrolysis (phosphoric acid), designed to liberate free (lipid), esterified, and more tightly-bound components respectively. Many of the investigations employing such an approach have sought to elucidate the nature of resistant biopolymers among the green algae. To allow comparison of our results to these studies, we adopted the above treatments, basing details on the scheme provided by Tegelaar (1990). It should be noted, however, that an alternative isolation strategy, the use of enzymes to remove unwanted cellular materials, has

been applied by some pollen investigators (Schulze Osthoff and Wiermann, 1987; Wehling et al., 1989; Mulder et al., 1992) and shows great potential for obtaining pure cell wall fractions while avoiding aggressive acid/base treatments altogether.

Modification of residues during isolation treatments

Solvent extraction. Our solvent extraction procedure was aimed at the release of free lipids. Since these materials typically comprise only a few percent of the cellular biomass, we did not see significant changes in bulk parameters such as optical character and elemental composition. In contrast, one might predict that removal of long chain fatty acids via solvent extraction could impact FTIR spectra to some extent by reducing any aliphatic signature. Both Dinoflagellate and Juniper R1 FTIR spectra show a weaker CH_2 + CH_3 absorbance (relative to the wide OH band at ~3360 cm^{-1}) compared to the corresponding spectra of unprocessed materials (Figs. 3.2 & 3.3). The Oak R1 FTIR spectrum, however, shows the opposite trend.

Py-MS mass spectra of all three R1 residues indicate a significant reduction of fatty acids, sterols, free tocopherols, and diglycerides as a result of solvent extraction. This is supported by the corresponding TIC traces which show the loss of the low temperature thermal desorption event. As pointed out earlier, solvent extraction had little effect on the position of pollens in the discriminant function (DF 1 and 2) score plot, while the dinoflagellate materials showed a significant shift from Initial to R1 positions. One interpretation of this difference between samples might invoke the degree of cytoplasm exposure in the initial materials. Microscopic examination of materials before processing revealed the majority of dinoflagellate cells to be showing evidence of wall rupture (chiefly the vegetative stages, but some resting cysts had fully- to partially-developed archeopyles), while pollen cells were generally intact. As a result, pollens were much less affected by extraction and sonification. The fact that Juniper pollen could actually germinate after

122

solvent extraction and sonification testifies to the remarkable physical and chemical resistance of these cells.

An additional and/or alternative explanation for the different responses of our samples to solvent extraction relates to differences in the percentage of total original biomass that is lipid. If the dinoflagellate material were higher in % lipid relative to the pollens, a more marked change would be observed as a result of solvent extraction.

Saponification. Reflux in KOH, followed by acidification and extraction, was employed to cleave ester bonds and remove the released hydrolysis products. Saponification of Dinoflagellate R1 had no significant impact on the visual character of this material. Similarly, virtually no change could be detected with FTIR analysis of the R2. Although the TIC trace resulting from Py-MS of Dinoflagellate R2 shows some modification of the high temperature pyrolysis peak, little change could be detected in the mass spectrum relative to that of R1. Consequently, the position of Dinoflagellate R2 in the DF score plot shows very little change.

In contrast to the algal material, both pollens show a relatively dramatic response to saponification and subsequent extractions. Visual inspection indicated that these treatments induced significant rupturing of pollen cells. FTIR spectra of both pollen R2's showed the loss of the ester functional group signature (appearing near 1730 cm^{-1} in the R1 spectra). As a result of this and other changes, the FTIR spectra of post-saponification pollen materials are essentially identical. TIC thermal evolution profiles from Py-MS analysis of R2 pollen materials show the maxima of pyrolysis product evolution shifting to higher scan numbers (i.e. higher temperatures) while the Py-MS mass spectra from these analyses indicated significant reduction of fatty acid and lipid peaks. Correspondingly, both pollens show a marked shift in the DF score plot from R1 to R2. Also, as pointed out earlier, pollen R2 residues occupy the same locus in the score plot, again suggesting (along with the FTIR data) compositional and structural similarity of pollen materials at this stage.

Acid Hydrolysis. Acid hydrolysis was employed to remove polysaccharides (by cleavage of glycosidic linkages) and proteinaceous materials (by cleavage of peptide bonds). Since the bulk of the dinoflagellate material up to this point consisted of cellulosic thecal plates, we anticipated drastic results from treatment with phosphoric acid. Indeed, optical analysis of Dinoflagellate R3 showed complete removal of thecal plates and all other cellular components with the exception of the peculiar globular/irregular bodies noted above.

This major change in visual character was reflected in results from other analyses of the dinoflagellate residue, all of which documented the substantial removal of polysaccharides during acid hydrolysis. Elemental analysis of Dinoflagellate R3 showed major changes in bulk composition. FTIR analysis of isolated sheets of resting cyst wall material indicated a significant decrease in OH peak intensity, consistent with the loss of polysaccharides from the cell wall. Similarly, both the high temperature shift of the Py-MS TIC profile maximum and the elimination or partial reduction of specific mass peaks from the Py-MS spectrum suggest major changes in the composition of the dinoflagellate material, again consistent with removal of polysaccharides.

The response of pollen R2 residues to acid hydrolysis paralleled that of the dinoflagellate material. As observed under the microscope, non-exine materials were more or less eliminated from R3 residues. FTIR spectra of these final residues showed the same reduction of OH absorbances as those for Dinoflagellate R3, while C, H, and N percentages showed significant changes consistent with the removal of carbohydrates. Py-MS spectra of pollen R3 residues also showed loss of peaks corresponding to polysaccharide fragments.

Direct gravimetric assessment of R3 residue yields was avoided in the present study due to the limited quantity of final product (especially of the dinoflagellate material) available after acid hydrolysis. Subsequent processing of additional dinoflagellate and pollen materials, however, allowed estimation of final residue yields. After solvent

extraction, saponification, and acid hydrolysis, these residues comprised approximately 8% and 1-2% (on a dry weight basis) of the initial Juniper pollen and *L. polyedra* culture materials, respectively. The difference in these values may reflect the heterogeneous population of cell types present in the initial dinoflagellate culture debris; resting cysts accounted for <~5% (visual estimation) of this material and therefore the final yield of resting cyst cell walls was substantially less than that of the pollens.

Overall, our results show that solvent extraction, saponification, and acid hydrolysis treatments had the intended effect of sequentially removing characterizable biochemicals from dinoflagellate and pollen materials. Perhaps the best visual summary of the evolution of residue composition throughout our successive treatments is provided by the Py-MS discriminant function (DF 1 and 2) score plot (Fig. 11). Although initial materials are widely separated, succesive treatments ultimately drive DF scores along paths which are somewhat predictable (from a biochemical perspective) by consideration of materials removed at each stage.

Assessment of processing artifacts

Mass chromatography. As mentioned earlier, a second consideration of the isolation protocol concerns the possibility that resistant cell wall materials themselves become chemically modified during one or more of the isolation treatments. Ideally, the structure and composition of R3 residues are an accurate reflection of the parent biopolymers. If this is the case, characteristics of the R3 residues should be present, though perhaps not as prominent, in the initial materials.

To test this assumption at a chemical level, we employed mass chromatography of characteristic ions in the dinoflagellate R3 residue to selectively enhance the signal of specific pyrolysis products in the Py-GC/MS chromatogram of the dinoflagellate initial materials. The partial summed (composite) chromatograms shown in Figure 3.18 were
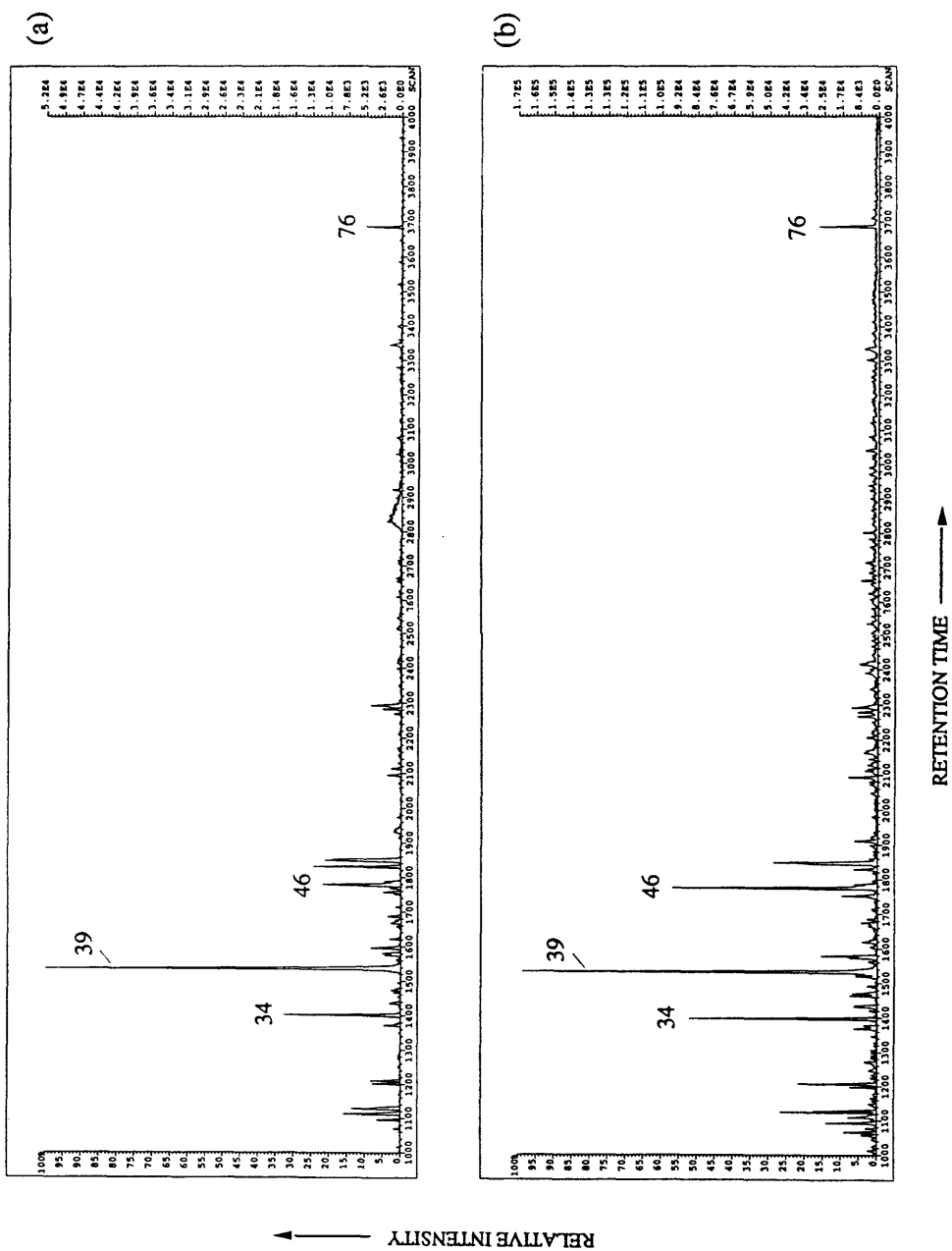
FIGURE 3.18 Partial summed (composite) mass chromatograms from Curie-point Py-GC/MS analysis of Dinoflagellate Initial (a), and R3 (b) residues. Peak numbers correspond to compounds listed in Table 3.4 (34 = benzaldehyde, 39 = phenol, 46 = acetophenone, 76 = prist-1-ene).

126

generated via mass chromatography of ions of m/z 94.07 + 106.08 + 108.09 + 120.1 + 126.19 + 266.36. In these chromatograms, peaks characteristic of the products liberated during R3 pyrolysis (Fig. 3.18b: 34 = benzaldehyde; 39 = phenol; 46 = acetophenone, 76 = prist-1-ene) are clearly revealed in the initial dinoflagellate materials (Fig. 3.18a). The occurrence of the characteristic pyrolysis products both before and after application of the isolation treatments suggests that resistant biopolymers originally present in the *L. polyedra* resting cyst wall were unaltered by the isolation protocol.

Comparison of R3 residues

Optical Microscopy. Under the light microscope, R3 residues consisted almost entirely of isolated resting cyst walls or pollen exines and were morphologically identical in appearance to residues obtained from the same starting materials but isolated by acetolysis (unpublished results). Regardless of processing method, however, dinoflagellate final residues contained the unusual globular to irregularly shaped masses described earlier. The size and morphology of these bodies suggest a relationship to small globular masses, termed accummulation bodies, occurring in the cytoplasm of some living dinoflagellate species (Taylor, 1968; Schmitter, 1971, 1989; Bibby and Dodge, 1972). These structures can be detected within motile cells, but are most obvious in resting cysts. Although the function of accummulation bodies is unknown, many workers have hypothesized a role in subcellular digestion (e.g. Fritz et al., 1989). The brownish to reddish orange color typical of these bodies has been considered to suggest the presense of concentrated carotenoids (see Evitt, 1985), an interesting hypothesis in light of earlier proposals linking the "fossilizability" of dinoflagellate resting cyst walls to the presence of a "carotenoid-derived" sporopollenin substance.

Structures virtually identical to accummulation bodies are commonly associated with fossilized dinoflagellate cyst walls (including those of fossil *L. polyedra*) and often

have a characteristic species-dependent appearance (Evitt, 1985). Since *L. polyedra* resting cysts forming in our laboratory cultures showed one or more prominent orange-pigmented accummulation bodies (Chapter 2), it is tempting to link these structures to those found in our R3 residue. An unambigious correlation, however, will likely involve further examination, perhaps analyzing cellular structures with transmission electron microscopy before and after all isolation steps.

The lack of recognizable pellicle structures in both Dinoflagellate R3 and in acetolyzed dinoflagellate material (unpublished data) was surprizing, given the statement by Morrill and Loeblich (1981, p. 321) that the pellicular layer of *Gonyaulax* (now *Lingulodinium*) *polyedra* is resistant to acetolysis. Table 1 of these authors, however, lists two strains of *L. polyedra* tested, but only one is indicated to have yielded resistant pellicles. These results may indicate that pellicle resistance is strain-specific. In the present investigation, we expected any surviving pellicular layers in the dinoflagellate R3 materials to be visible during detailed observations with contrast enhancement microscopy, since (1) initial dinoflagellate culture material contained large numbers of vegetative cells, all of which presumably contained a pellicle layer, and (2) both acetolysis and our 3-step isolation protocol darkened resistant wall layers enhancing their visibility under the microscope. Overall, based on our optical characterization of Dinoflagellate R3, we conclude that this residue consists almost entirely (>97%) of isolated walls of *L. polyedra* resting cysts.

FTIR. In this study, FTIR microscopy yielded a unique perspective on R3 materials since it could be performed on optically identified, isolated particles rather than on total residue. As noted earlier, spectra produced by FTIR analysis of R3 residues were virtually indistinguishable. All showed absorbances indicative of abundant aliphatic CH_2 and/or CH_3, carboxylic acid C=O, and hydroxyl groups, features which suggest the presence of long chain fatty acids. Interestingly, our R3 FTIR profiles very closely resemble published IR spectra of *Lycopodium* spore cell walls (Rouxhet et al., 1980;

128

Berkaloff et al., 1983; Puel et al., 1987; Geisert et al., 1987). Atkinson et al. (1972) also

illustrate an IR spectrum of *Lycopodium* spores, but unfortunately resistant materials were

obtained by acetolysis, and hence the spectrum is difficult to interpret. An IR spectrum of

pollen wing (*Pinus mugo*) sporopollenin isolated with enzymatic treatments has been

reported by Schulze Osthoff and Wiermann (1987). This spectrum extends to lower

wavenumbers than we were able to obtain under micro-FTIR conditions (625 vs. ~950

cm^{-1}), but where comparable, very closely matches that of our dinoflagellate, Juniper, and

Oak R3 residues. These authors note peaks at 1625, ~1600, ~1500, 1430, and 830 cm^{-1}

as being indicative of the presence of aromatic compounds. Our R3 spectra all show

similar features in comparable regions (shoulder in the 1600-1625 cm^{-1} region, peak

around 1430-1440 cm^{-1}, weak and variably expressed response at ~1515 cm^{-1}), and thus

suggest the presence of aromatic structural components in both the dinoflagellate and pollen

materials. Puel et al. (1987) isolated sporopollenin from another species of *Pinus* (*P.

silvestris*) by successive solvent extraction, saponification, and acid hydrolysis; IR analysis

of this material yielded a spectrum identical to that of *P. mugo*.

Several studies have been published which describe IR spectra of resistant outer

walls isolated from algal species outside of the Dinophyceae. Many of these (Atkinson et

al., 1972; Good and Chapman, 1978; Konig and Peveling, 1980; Devries et al., 1983;

Delwiche et al., 1989) employed acetolysis as the isolation mechanism and therefore results

are not directly comparable to those reported here. Investigations by Berkaloff et al,

(1983), Puel et al. (1987), and Burczyk (1987), however, isolated resistant cell wall

biopolymers from various green algae using techniques similar to those of the present

study. In the first two of these investigations, IR spectra were compared to those obtained

from traditional sporopollenins (*Pinus* pollen and *Lycopodium* spores). Differences

between algal and spore/pollen materials were notable, especially concerning oxygen

distribution and degree of unsaturation. On the strength of these IR comparisons, both

Berkaloff et al (1983) and Puel et al. (1987) conclude that resistant cell wall materials

derived from *Prototheca* and *Botryococcus* are distinct in structure and composition from "traditional" sporopollenins. This conclusion is provocative given the results of the present investigation. Our FTIR results indicate that *L. polyedra* resting cyst walls are more similar in terms of functional group chemistry to "classical sporopollenins" than to resistant cell wall materials derived from other algae--in this case, freshwater chlorophytes.

Elemental Analysis. In contrast to the FTIR data, results from our elemental analysis seem to suggest differences between pollen and dinoflagellate materials. The H/C ratio for Dinoflagellate R3 is nearly 2, pointing toward a highly aliphatic structure--an observation somewhat consistent with the FTIR results, but contradictory to pyrolysis data (see below). Both pollens, however, show R3 H/C ratios closer to 1, suggesting a more condensed (aromatic) structure. This lack of agreement between FTIR and elemental analysis is difficult to interpret, but may derive from a biasing of CHN measurements due to water absorption. Given the very limited quantity of dinoflagellate R3 available for elemental analysis, even a small amount of absorbed water could have interferred with final results, giving higher H/C values. Alternatively, residual polysaccharides in the dinoflagellate R3 materials might also serve to artificially elevate the H/C ratio.

As mentioned earlier, the %O values included in Table 3.1 were not obtained by direct measurement but were calculated by difference and may include some bias. Interestingly, if these values are used to calculate O/C atomic ratios, dinoflagellate R3 materials classify as "Type I" kerogens (Tissot and Welte, 1984) and, on this level, appear analogous to the aliphatic biopolymers found among some of the green algae (e.g. *Botryococcus braunii*).

Pyrolysis. In our study, Py-MS and Py-GC/MS analyses provided the strongest criteria for detailed comparison of R3 residue structure and composition. Although pyrolysis liberates only a subset of the macromolecular building blocks, recent studies have illustrated that the fragments generated are structurally representative of the parent macromolecule(s) (Larter and Horsfield, 1993).

130

An unexpected feature of the Dinoflagellate R3 Py-GC/MS TIC chromatogram was the abundance of peaks representing lower molecular weight furans. Since optical microscopy indicated the complete removal of cellulosic thecal materials during acid hydrolysis, we anticipated any polysaccharide signature generated during pyrolysis of R3 materials to be greatly reduced or eliminated entirely. Furthermore, it is unusual to see lower molecular weight polysaccharide products when no evidence of corresponding higher molecular weight products (e.g. levoglucosan) could be detected.

Interpretations of this phenomenon might draw on one or more of a number of hypotheses. First, the presence of furan peaks may indicate a residual polysaccharide component in the dinoflagellate R3 residue which is independant of the original thecal plate materials. Many investigations have described a relatively thick cellulosic layer (the endospore) which is incorporated in the cell covering of some dinoflagellate resting cysts (see Evitt, 1985). Such wall layers are a prominent feature of *L. polyedra* resting cysts, and can be easily detected with both light and electron microscopy (Chapters 2 and 4, respectively). If polysaccharides in this layer are tightly bound to the overlying resistant cell wall and manage to survive acid hydrolysis, furan products may be among those products generated by pyrolysis. Note that the possibility of residual polysaccharides in dinoflagellate R3 materials was also mentioned earlier, in the discussion of the results of elemental analysis.

Other hypotheses to explain furan production during dinoflagellate R3 pyrolysis invoke artifacts of acid hydrolysis. For example, strong dehydration during acid hydrolysis may have led to "charring" which could be responsible for furan generation during subsequent pyrolysis (J. J. Boon, personal communication). Melanoidins are another potential artifact of acid hydrolysis conditions. These acidic polymers are believed to result from sugar/amino acid condensation reactions (Larter et al., 1981) and also may yield furans upon pyrolysis. To evaluate these latter hypotheses, it would be interesting to compare (via Py-GC) the R3 materials obtained in this study to those isolated with

131

alternative methods (e.g. enzymatic treatments) which do not employ aggressive acid hydrolysis.

Another noteworthy feature of the dinoflagellate R3 chromatogram is the prominient peak representing prist-1-ene [2,6,10,14-Tetramethyl pentadec-1-ene]. This compound has been encountered in investigations of resistant wall biopolymers of the green algae (Goth et al., 1988) and also appears ubiquitous in pyrolysates of marine kerogens (Larter et al, 1979), although exactly why is not clear. There has been considerable interest in the origin of this pyrolysis product in geochemical samples (e.g. Goossens et al., 1984), and tocopherols and chlorophylls have both been suggested as possible sources. Based on the prominence of tocopherols in the associated lipid extract of the dinoflagellate materials (unpublished results) and the lack of chlorophyll pigmentation associated with *L. polyedra* cell walls, a tocopherol origin seems more likely for the prist-1-ene encountered in the present study. In this case, the prominence of prist-1-ene strongly suggests that this compound forms an integral part of the *L. polyedra* resting cyst wall, but a non-wall source (accummulation bodies?) cannot be dismissed at this time. Prist-1-ene was not detected in either Juniper or Oak pollen R3 residues.

Although FTIR and elemental analysis both suggest an aliphatic structure for Dinoflagellate R3, Py-GC/MS analysis of this material shows, with the exception of prist-1-ene, no clear indication of aliphatic components. The TIC chromatogram does contain, however, peaks of aromatic compounds (alkylbenzenes, alkylphenols, napthalenes, indanes, indenes, and benzaldehydes) and points to a partially condensed macromolecular structure.

Direct comparison of our Py-GC and Py-GC/MS results to those obtained in other studies is restricted by the relatively few reports in which these techniques have been applied to sporopollenin, algaenan and similar substances. Regarding the resistant cell wall materials of algae, Py-GC data is available only for the freshwater chlorophytes *Botryococcus braunii* (Largeau et al., 1984, 1985; Kadouri et al., 1988; Derenne et al.,

1989, 1990), *Chlorella fusca* (Derenne et al., 1992), *Scenedesmus obliquus* (Burczyk and Dworzanski, 1988), *S. quadricauda* (Derenne et al., 1991), and *Tetraedron minimum* (Goth et al., 1988), and the marine chlorophyte *Nanochlorum eucaryotum* (Derenne et al., 1992). The results of these investigations, while differing in minor detail, all strongly indicate macromolecular structures comprised chiefly of long (up to C_{30}) polymethylenic chains. This highly aliphatic character is typified by pyrolysates of *S.obliquus* and *B. braunii* both of which are dominated by a homologous series of *n*-alkanes/alkenes of chain length C_{13}-C_{32}, and show striking similarities to pyrolysis products of polyethylene (Burczyk and Dworzanski, 1988). In contrast, pyrolysis of *Lycopodium clavatum* spore sporopollenin yields markedly different products devoid of a clear aliphatic signature (Burczyk and Dworzanski, 1988). To date, all studies of resistant wall substances among the green algae have stressed the fundamental differences between "algaenan" structure (highly aliphatic macromolecule(s), based on a network of long polymethylenic chains) and that of more traditional, allegedly carotenoid-derived sporopollenin.

To confirm the absence of polymethylenic components in our dinoflagellate resting cyst material, we performed Py-GC/MS analysis of the R3 residue at a higher Curie-point temperature (770°C) and for longer duration (5 sec.). These pyrolysis conditions, designed to expose the most refractory aliphatic networks, yielded no meaningful changes in the overall TIC profile. Thus, we conclude that the resistant biopolymer in *L. polyedra* resting cyst walls shows substantial structural differences compared to the aliphatic algaenans.

Py-GC/MS chromatograms of both Juniper R3 and Oak R3 residues show strong and nearly identical distributions of aromatic pyrolysis products. As mentioned previously, the Juniper R3 chromatogram is also characterized by a homologous series of *n*-alkanes/alkenes. On the basis of Py-GC/MS analysis, therefore, pollens can be clearly distinguished from the dinoflagellate resting cyst material. The aromatic character of the Juniper and Oak pollen residues is consistent with the results of several recent investigations of sporopollenin of *Pinus mugo* (a gymnosperm) and *Corylus avellana* (an

133

angiosperm) (Schulze Osthoff and Wiermann, 1987; Herminghaus et al., 1987; Wehling et al., 1989; and Mulder et al., 1992). Using a variety of methods (IR analysis, chemolysis, and "in-source" Py-MS), these studies each report that phenolic compounds (e.g. p-coumaric acid, p-hydroxybenzoic acid, vanillic acid, vanillin, p-hydroxybenzaldehyde, and ferulic acid) are important structural components of sporopollenin.

In two investigations (Wehling et al., 1989; and Mulder et al., 1992), some attention was focused on the identification and potential structural role of p-coumaric acid as elucidated by "in-source" Py-MS techniques. In Py-MS (16 eV) spectra of Pinus pollen wing material, this compound showed a molecular ion at m/z 164 and a major fragment ion $(M^+ - CO_2)$ at m/z 120. This latter mass peak (but not the former) is highly visible in our Oak R3 Py-MS mass spectrum, and is detectable though less prominent in both Juniper and Dinoflagellate R3 mass spectra. This mass also has a significant loading on the DF 1- mass spectrum which strongly correlates to all R3 residues in the DF score plot. The m/z 120 mass peak may, therefore, suggest the presence of p-coumaric acid in both the dinoflagellate and pollen materials. However, acetophenone (MW 120), was identified in the Py-GC/MS analysis of all three R3's and could also be responsible for this ion in the Py-MS spectra. Further work is necessary to clarify this point.

It is difficult to account for our analytical results by invoking sporopollenin substances built exclusively of carotenoid precursors. Two studies of synthetic sporopollenin (prepared by polymerization of carotenoids) have shown that phenolic compounds are released only in negligible amounts during potash-fusion, nitrobenzene oxidation, and AlI3 degradation (Herminghaus et al., 1987; Wehling et al., 1989). In contrast, significant amounts of phenolic compounds were detected in the same studies when these techniques were applied to Pinus and Corylus sporopollenins. Similarly, in the present investigation, the type and amount of phenolic and other aromatic moieties resulting from Py-GC/MS and Py-MS analyses of dinoflagellate and pollen materials are inconsistent with the "traditional" carotenoid-based sporopollenin structure.

134

In summary, the results from this investigation point to some general similarities in composition between resistant cell wall materials of resting cysts of one species of marine dinoflagellate and those of two types of terrestrial plant pollen. However, there is also strong evidence for essential differences between these biopolymers, particularly at the molecular level. That these substances might be different is not a new idea; however, most of the previous comparisons of this nature are based on indirect observations and stem from the study of dinoflagellate and pollen/spore cell walls recovered from the fossil record. Chaloner and Orbell (1971) found that dinoflagellate resting cysts showed a different distribution behavior than pollen and spores when mixed fossil assemblages were centrifuged in a density gradient. Data presented by Correia (1971) suggested that, when exposed to increasing temperatures, pollen and spores show color changes at different rates than dinoflagellates and acritarchs. Finally, Sarjeant (1986) has commented that fossil dinoflagellates show a consistently different response to various stains when compared with fossil pollen.

On the basis of these stain tests, the latter author has proposed the taxonomically-restricted term "dinosporin" to distinguish dinoflagellate resting cyst wall material from that of pollen and spores. This term has been recently adopted by Fensome et al. (1993) in their extensive suprageneric classification of modern and fossil dinoflagellates, and will likely find wide usage among dinoflagellate biologists and paleontologists. The proposal and use of "dinosporin" is interesting in light of our results which suggest that dinoflagellate resting cyst material may indeed be distinct from both the traditional "sporopollenins" of higher plant pollen and spores and the aliphatic "algaenans" found amongst the green algae.

This report represents the first study which provides a detailed comparison of the chemical composition of extant pollen and dinoflagellate resting cyst wall materials using modern analytical techniques. It is emphasized, however, that definitive statements of the precise nature and structure of these complex macromolecular substances are not yet

135

possible. Investigation of additional dinoflagellate, pollen, and spore species using multiple, complementary techniques to isolate and characterize resistant materials are necessary steps towards the structural elucidation of sporopollenins, algaenans, dinosporins, and allied biopolymers.

CONCLUSIONS

1. Successive treatment of initial dinoflagellate and pollen materials by solvent extraction, saponification, and acid hydrolysis had the intended effect of sequentially and predictably removing characterizable biochemicals. These procedures yielded final residues consisting almost entirely of isolated resistant cell walls.

2. No convincing evidence for a carotenoid-based structure was detected during analysis of either dinoflagellate or pollen resistent cell wall materials.

3. The resistant cell walls of both pollens and *L. polyedra* resting cysts appeared largely aromatic in composition. Pyrolysis of isolated Juniper and Oak wall materials yielded nearly identical distributions of aromatic products.

4. In addition to the aromatic signature, Juniper pollen walls also showed the significant presence of an aliphatic biopolymer.

5. The class of "traditional" sporopollenins (exine materials of pollen and spores) appears to encompass some compositional heterogeneity.

6. The suite of aromatic products generated during pyrolysis of *L. polyedra* resting cyst walls is less extensive and distinct from that of the pollens.

7. Pyrolysis of isolated resting cyst walls produced an abundance of prist-1-ene. This strongly suggests the presence of bound tocopherols which may play an important structural role in the cell wall of *L. polyedra* resting cysts.

8. The resistant macromolecular substance isolated from *L. polyedra* resting cyst walls appears fundamentally different from "algaenan", the highly aliphatic resistant biopolymer reported to comprise the cell walls of many green algae.

REFERENCES

Atkinson, A. W., Jr., Gunning, B. E. S., and John, P. C. L., 1972. Sporopollenin in the cell wall of *Chlorella* and other algae: Ultrastructure, chemistry, and incorporation of ^{14}C acetate, studied in synchronous cultures. *Planta*, Vol. 107, No. 1, p. 1-32.

Barss, M. S, and Williams, G. L., 1973. Palynology and nannofossil processing techniques. *Geological Survey of Canada, Paper 73-26*, p. 1-25.

Berkaloff, C., Casadevall, E., Largeau, C., Metzger, P., Peracca, S., and Virlet, J., 1983. The resistant polymer of the walls of the hydrocarbon-rich alga *Botryococcus braunii*. *Phytochemistry*, Vol. 22, No. 2, p. 389-397.

Bibby, B. T., and Dodge, J. D., 1972. The encystment of a freshwater dinoflagellate: A light and electron microscopical study. *British Phycological Journal*, Vol. 7, No. 1, p. 85-100.

Boon, J. J., 1992. Analytical pyrolysis mass spectroscopy: New vistas opened by temperature-resolved in-source PYMS. *International Journal of Mass Spectroscopy and Ion Processes*, Vol. 118/119, p. 755-787.

Braconnot, H., 1829. Über sporopolleninine. *Annales de Chimie et de Physique*, Vol. 2, p. 42-57.

Brooks, J., Grant, P. R., Muir, M., van Gijzel, P., and Shaw, G., (eds.), 1971. *Sporopollenin*. Proceedings of a symposium held at the Geology Department, Imperial College, London, 23-25 September, 1970. Academic Press, London. 718 p.

Brooks, J., and Shaw, G., 1978. Sporopollenin: A review of its chemistry, palaeochemistry and geochemistry. *Grana*, Vol. 17, p. 91-97.

Brunner, U. and Honegger, R., 1985. Chemical and ultrastructural studies on the distribution of sporopolleninlike biopolymers in six genera of lichen phycobionts. *Canadian Journal of Botany*, Vol. 63, No. 12, p. 2221-2230.

Bujak, J. P., and Davies, E. H., 1983. *Modern and Fossil Peridiniineae*. AASP Contribution Series Number 13. American Association of Stratigraphic Palynologists Foundation. 203 p.

Burczyk, J., 1987a. Biogenetic relationships between ketocarotenoids and sporopollenins in green algae. *Phytochemistry*, Vol. 26, No. 1, p. 113-119.

Burczyk, J., 1987b. Cell wall carotenoids in green algae which form sporopollenins. *Phytochemistry*, Vol. 26, No. 1, p. 121-128.

Burczyk, J. and Dworzanski, J., 1988. Comparison of sporopollenin-like algal resistant polymer from cell wall of *Botryococcus*, *Scenedesmus* and *Lycopodium clavatum* by GC-pyrolysis. *Phytochemistry*, Vol. 27, No. 7, p. 2151-2153.

Chaloner, W. G. and Orbell, G., 1971. A palaeobiological definition of sporopollenin. *In* Brooks, J., Grant, P. R., Muir, M., van Gijzel, P., and Shaw, G., (eds.),

Sporopollenin, Proceedings of a symposium held at the Geology Department, Imperial College, London, 23-25 September, 1970, Academic Press, London. p. 273-294.

Correia, M., 1971. Diagenesis of sporopollenin and other comparable organic substances: Application to hydrocarbon research. *In* Brooks, J., Grant, P. R., Muir, M., van Gijzel, P., and Shaw, G., (eds.), *Sporopollenin*, Proceedings of a symposium held at the Geology Department, Imperial College, London, 23-25 September, 1970, Academic Press, London. p. 569-620.

de Leeuw, J. W., and Largeau, C., 1993. A review of macromolecular organic compounds that comprise living organisms and their role in kerogen, coal, and petroleum formation. *In* Engel, M. H., and Macko, S. A., (eds.), *Organic Geochemistry*, Plenum Press, New York. p. 23-72.

Derenne, S., Largeau, C., Casadevall, E., and Berkaloff, C., 1989. Occurrence of a resistant biopolymer in the *L* race of *Botryococcus braunii*. *Phytochemistry*, Vol. 28, No. 4, p. 1137-1142.

Derenne, S., Largeau, C., Casadevall, E., and Sellier, N., 1990. Direct relationship between the resistant biopolymer and the tetraterpenic hydrocarbon in the lycopadiene race of *Botryococcus braunii*. *Phytochemistry*, Vol. 29, No. 7, p. 2187-2192.

Derenne, S., Largeau, C., Casadevall, E., Berkaloff, C., and Rousseau, B., 1991. Chemical evidence of kerogen formation in source rocks and oil shales via selective preservation of thin resistant outer walls of microalgae: Origin of ultralaminae. *Geochimica et Cosmochimica Acta*, Vol. 55, No. 4, p. 1041-1050.

Derenne, S., Largeau, C., Berkaloff, C., Rousseau, B., Wilhelm, C., and Hatcher, P. G., 1992. Non-hydrolysable macromolecular constituents from outer walls of *Chlorella fusca* and *Nanochlorum eucaryotum*. *Phytochemistry*, Vol. 31, No. 6, p. 1923-1929.

Delwiche, C. F., Graham, L. E., and Thomson, N., 1989. Lignin-like compounds and sporopollenin in *Coleochaete*, an algal model for land plant ancestry. *Science*, Vol. 245, No. 4916, p. 399-401.

de Vries, P. J. R., Simons, J., and van Beem, A. P., 1983. Sporopollenin in the spore wall of *Spirogyra* (Zygnemataceae, Chlorophyceae). *Acta Botanica Neerlandica*, Vol. 32, No. 1/2, p. 25-28.

Eisenack, A., 1963. Hystrichosphären. *Biological Reviews of the Cambridge Philosophical Society*, Vol. 38, No. 1, p. 107-139.

Erdtman, G., 1961. The Acetolysis Method. A revised description. *Svensk Botanisk Tidskrift*, Vol. 54, No. 4, p. 561-564.

Evitt, W. R., 1961. Observations on the morphology of fossil dinoflagellates. *Micropaleontology*, Vol. 7, No. 4, p. 385-420.

Evitt, W. R., 1985. *Sporopollenin Dinoflagellate Cysts: Their Morphology and Interpretation*. American Association of Stratigraphic Palynologists Foundation. 333 p.

139

Fensome, R. A, Taylor, F. J. R., Norris, G., Sarjeant, W. A. S., Wharton, D. I., and Williams, G. L., 1993. *A Classification of Living and Fossil Dinoflagellates.* Micropaleontology, Special Publication Number 7. Sheridan Press, Hanover, Pennsylvania. 351 p.

Fritz, L., Anderson, D. M., and Triemer, R. E., 1989. Ultrastructural aspects of sexual reproduction in the red tide dinoflAgellate *Gonyaulax tamarensis. Journal of Phycology*, Vol. 25, No. 1, p. 95-107.

Gatellier, J.-P. L. A., de Leeuw, J. W., Sinninghe Damsté, J. S., Derenne, S., Largeau, C., and Metzger, P., 1993. A comparative study of macromolecular substances of a Coorongite and cell walls of the extant alga *Botryococcus braunii. Geochimica et Cosmochimica Acta*, Vol. 57, No. 9, p. 2053-2068.

Geisert, M., Rose, T., Bauer, W., and Zahn, R. K., 1987. Occurrence of carotenoids and sporopollenin in *Nanochlorum eucaryotum* a novel marine alga with unusual characteristics. *BioSystems*, Vol. 20, No. 2, p. 133-142.

Good, B. H., and Chapman, R. L., 1978. The ultrastructure of *Phycopeltis* (Chroolepidaceae: Chlorophyta). I. Sporopollenin in the cell walls. *American Journal of Botany*, Vol. 65, No. 1, p. 27-33.

Goodman, D. K., 1987. Dinoflagellate cysts in ancient and modern sediments. *In* Taylor, F. J. R., (ed.), *The Biology of Dinoflagellates*, Botanical Monographs, Vol. 21, Blackwell Scientific Publishers, Oxford. p. 649-722.

Goossens, H., de Leeuw, J. W., Schenck, P. A., and Brassell, S. C., 1984. Tocopherols as likely precursors of pristane in ancient sediments and crude oils. *Nature*, Vol. 312, No. 5993, p. 440-442.

Goth, K., de Leeuw, J. W., Püttmann, W., and Tegelaar, E. W., 1988. Origin of Messel Oil Shale kerogen. *Nature*, Vol. 339, No. 6201, p. 759-761.

Gray, J., 1965. Techniques in palynology; Part III. *In* Kummel, B., and Raup, D. M., (eds.), *Handbook of Paleontological Techniques*, Freeman and Company, San Francisco, California. p. 469-706.

Guilford, W. J., Schneider, D. M., Labovitz, J., and Opella, S. J., 1988. High resolution solid state ^{13}C NMR spectroscopy of sporopollenins from different plant taxa. *Plant Physiology*, Vol. 86, No. 1, p. 134-136.

Herminghaus, S., Gubatz, S., Arendt, S., and Wiermann, R., 1988. The occurrence of phenols as degradation products of natural sporopollenin--a comparison with "synthetic sporopollenin". *Zeitschrift für Naturforschung*, Vol. 43c, No. 7/8, p. 491-500.

John, J. F., 1814. Über befruchtenstaube nebst eine analyse des tulpen pollens. *Journal für Chemie und Physik*, Vol. 12, p. 244-261.

Kadouri, A., Derenne, S., Largeau, C., Casadevall, E., and Berkaloff, C., 1988. Resistant biopolymer in the outer walls of *Botryococcus braunii, B* race. *Phytochemistry*, Vol. 27, No. 2, p. 551-557.

Katon, J. E. and Sommer, A. J, 1992. IR microspectroscopy. *Analytical Chemistry*, Vol. 64, No. 19, p. 931A-940A.

König, J., and Peveling, E., 1980. Vorkommen von sporopollenin in der zellwand des phycobionten *Trebouxia*. (Sporopollenin in the cell wall of the phycobiont *Trebouxia*.) *Zeitschrift für Pflanzenphysiologie (International Journal of Plant Physiology)*, Vol. 98, No. 5, p.459-464.

Largeau, C., Casadevall, E., Kadouri, A., and Metzger, P., 1984. Formation of *Botryococcus*-derived kerogens--Comparative study of immature torbanites and of the extant alga *Botryococcus braunii*. *Organic Geochemistry*, Vol. 6, p. 327-332.

Largeau, C., Derenne, S., Casadevall, E., Kadouri, A., and Sellier, N., 1985. Pyrolysis of immature Torbanite and of the resistant biopolymer (PRB A) isolated from the extant alga *Botryococcus braunii*. Mechanism of formation and structure of Torbanite. *Organic Geochemistry*, Vol. 10, No. 4-6, p. 1023-1032.

Larter, S. R., Solli, H., Douglas, A. G., De Lange, F., and de Leeuw, J. W., 1979. The occurrence and significance of prist-1-ene in kerogen pyrolysates. *Nature*, Vol. 279, No. 5712, p. 405-408.

Larter, S. R., Solli, H., and Douglas, A. G., 1981. Phytol-containing melanoidins and their bearing on the fate of isoprenoid structures in sediments. *In* Bjorøy, M., et al., (eds.), *Advances in Organic Geochemistry*, Proceedings of the 10th International Meeting on Organic Geochemistry, University of Bergen, Norway, 14-18 September 1981. p. 513-523.

Larter, S. R., and Horsfield, B., 1993. Determination of structural components of kerogens by the use of analytical pyrolysis methods. *In* Engel, M. H., and Macko, S. A., (eds.), *Organic Geochemistry*, Plenum Press, New York. p. 271-287.

Morrill, L. C., and Loeblich, A. R., III, 1981. The dinoflagellate pellicular wall layer and its occurrence in the division Pyrrhophyta. *Journal of Phycology*, Vol. 17, No. 4, p. 315-323.

Mulder, M. M., van der Hage, E. R. E., and Boon, J. J., 1992. Analytical *in source* pyrolytic methylation electron impact mass spectrometry of pheonolic acids in biological matrices. *Phytochemical Analysis*, Vol. 3, p. 165-172.

Nip, M., Tegelaar, E. W., de Leeuw, J. W., Schenck, P. A., and Holloway, P. J., 1986. A new non-saponifiable highly aliphatic and resistant biopolymer in plant cuticles. Evidence from pyrolysis and ^{13}C-NMR analysis of present-day and fossil plants. *Naturwissenschaften*, Vol. 73, No. 10, p. 579-585.

Pfiester, L. A., 1984. Sexual reproduction. *In* Spector, D. L., (ed.), *Dinoflagellates*, Academic Press, Inc., Orlando, Florida. p. 181-199.

Pfiester, L. A., 1989. Dinoflagellate sexuality. *International Reviews of Cytology*, Vol. 114, p. 249-272.

Pfiester, L. A. and Anderson, D. M., 1987. Dinoflagellate Reproduction. *In* Taylor, F. J. R., (ed.), *The Biology of Dinoflagellates*, Botanical Monographs, Vol. 21, Blackwell Scientific Publishers, Oxford. p. 611-648.

Prahl, A. K., Springstubbe, H., Grumbach, K., and Wiermann, R., 1985. Studies on sporopollenin biosynthesis: The effect of inhibitors of carotenoid biosynthesis on sporopollenin accumulation. *Zeitschrift für Naturforschung*, Vol. 40c, No. 9/10, p. 621-626.

Prahl, A. K., Rittscher, M., and Wiermann, R., 1986. New aspects of sporopollenin biosynthesis. *In* Mulcahy, D. L., Mulcahy, G. B., and Ottaviano, E., (eds), *Biotechnology and Ecology of Pollen*, Proceedings of the International Conference on the Biotechnology and Ecology of Pollen, 9-11 July 1985, University of Massachusetts, Amherst, Massachusetts, Springer-Verlag, New York. p. 313-318.

Puel, F., Largeau, C., and Giraud, G., 1987. Occurrence of a resistant biopolymer in the outer walls of the parasitic alga *Prototheca wickerhamii* (Chlorococcales): Ultrastructure and chemical studies. *Journal of Phycology*, Vol. 23, No.4, p. 649-656.

Rouxhet, P. G., Robin, P. L., and Nicaise, G., 1980. Characterization of kerogens and of their evolution by infrared spectroscopy. *In* Durand, B., (ed.), *Kerogen: Insoluble Organic Matter from Sedimentary Rocks*, Éditions Technip, Paris. p. 163-190.

Sarjeant, W. A. S., 1986. *Review of* Evitt, W. R., 1985, *Sporopollenin Dinoflagellate Cysts: Their Morphology and Interpretation. Micropaleontology*, Vol. 32, No. 3, p. 282-285.

Schmitter, R. E., 1971. The fine structure of *Gonyaulax polyedra*, a bioluminescent marine dinoflagellate. *Journal of Cell Science*, Vol. 9, No. 1, p 147-173.

Schmitter, R. E., 1989. Structure and function of globular bodies in dinoflagellate cells [Abstract]. *Fourth International Conference on Modern and Fossil Dinoflagellates, Marine Biological Laboratory, Woods Hole, Massachusetts, Program and Abstracts*, p. 92.

Schultze Osthoff, K. and Weirmann, R., 1987. Phenols as integrated compounds of sporopollenin from *Pinus* pollen. *Journal of Plant Physiology*, Vol. 131, No. 1/2, p. 5-15.

Shaw, G., and Yeadon, A., 1966. Chemical studies on the constitution of some pollen and spore membranes. *Journal of the Chemical Society*, Section C, Part 1, p. 16-22.

Swift, E., and Remson, C. C., 1970. The cell wall of *Pyrocystis* spp. (Dinococcales). *Journal of Phycology*, Vol. 6, No.1, p. 79-86.

Tappan, H.,1980. *The Paleobiology of Plant Protists*. W. H. Freeman and Company, San Francisco, California. 1028 p.

Taylor, D. L., 1968. *In situ* studies on the cytochemistry and ultrastructure of a symbiotic marine dinoflagellate. *Journal of the Marine Biological Association of the United Kingdom*, Vol. 48, No. 2, p. 349-366.

Taylor, F. J. R., (ed.), 1987. *The Biology of Dinoflagellates*. Botanical Monographs, Vol. 21. Blackwell Scientific Publications, Oxford. 785 p.

Tegelaar, E. W., de Leeuw, J. W., Derenne, S., and Largeau, C., 1989. A reappraisal of kerogen formation. *Geochimica et Cosmochimica Acta*, Vol. 53, No. 11, p. 3103-3106.

Tegelaar, E. W., 1990. Resistant biomacromolecules in morphologically characterized constituents of kerogen: A key to the relationship between biomass and fossil fuels. PhD thesis, Rijksuniversiteit Te Utrecht.

Tissot, B. P., and Welte, D. H., 1984. *Petroleum Formation and Occurrence*, Second Edition. Springer-Verlag, Berlin, 699 p.

Walker, L. M., 1984. Life histories, dispersal, and survival in marine, planktonic dinoflagellates. *In* Steidinger, K. A., and Walker, L. M., (eds.), *Marine Plankton Life Cycle Strategies*, CRC Press, Inc., Boca Raton, Florida. p 19-34.

Wehling, K., Niester, C., Boon, J. J., Willemse, M. T. M., and Wiermann, R., 1989. *p*-Coumaric acid--a monomer in the sporopollenin skeleton. *Planta*, Vol. 179, No. 3, p. 376-380.

Williams, G. L., and Bujak, J. P., 1985. Mesozoic and Cenozoic dinoflagellates. *In* Bolli, H. M., Saunders, J. B., and Perch-Nielsen, K., (eds.), *Plankton Stratigraphy*, Cambridge Earth Science Series, Cambridge University Press, Cambridge. p. 847-964.

Williams, G. L., Stover, L. E., and Kidson, E. J., 1993. Morphology and stratigraphic ranges of selected Mesozoic-Cenozoic dinoflagellate taxa in the northern hemisphere. *Geological Survey of Canada Paper 92-10*, p. 1-137.

Zetzsche, F., Kalt, P., Leichti, J., and Ziegler, E., 1931. Zur konstitution des lycopodiumsporinins des tasmins und des lange-sporonins. *Journal fuer Praktische Chemie*, Vol. 148, p. 67-84.

PLATE 3.1

Dinoflagellate *(L. polyedra* culture) and pollen samples at each stage of the isolation procedure. Figures 1-3 = initial materials, Figures 4-6 = R1 residues, Figures 7-9 = R2 residues, Figures 10-12 = R3 residues. All figures 250x.

Figure 1.   Unprocessed *L. polyedra* culture debris showing a living resting cyst (spiney sphere, just left of center) surrounded by empty thecae.

Figure 2.   Initial Juniper pollen *(Juniperus scopulorum)*. After a few moments in a wet mount, many grains were observed to germinate.

Figure 3.   Initial Oak pollen *(Quercus rubra)*.

Figure 4.   Dinoflagellate R1 (i.e. residue after sonification and solvent extraction). Culture debris disrupted and dispersed. Residue consists mostly of dissociated thecal plates; sheet of resting cyst wall (spines sheared off) visible at lower right.

Figure 5.   Juniper R1. Cells appear unchanged compared to initial pollen grains (Figure 2). Again, some of these cells germinated while being observed in a wet mount.

Figure 6.   Oak R1. As with the Juniper material, Oak pollen was relatively unchanged by solvent extraction. (Grains in photo are distorted due to cover glass pressure.)

Figure 7.   Dinoflagellate R2 (i.e. residue after saponification). Visually identical to the R1 residue (Figure 4). Note sheet of resting cyst wall at top of photo.

Figure 8.   Juniper R2. Cytoplasmic components partly removed.

Figure 9.   Oak R2. Cells largely ruptured, cytoplasmic components mostly removed.

Figure 10.   Dinoflagellate R3 (i.e. residue after acid hydrolysis)

(a)   The R3 consisted almost entirely of isolated sheets of resting cyst wall material. In most cases, spines have been sheared off during processing.

(b)   Irregular to globular bodies present in the dinoflagellate R3 (< 3%, visual estimation).

Figure 11.   Juniper R3. Cell walls were darkened by acid hydrolysis. Note also the presence of dark granular material believed to derive from the exine (see text).

Figure 12.   Oak R3. Cell walls mostly torn and/or distorted and darker in color relative to the R2 (Figure 9).
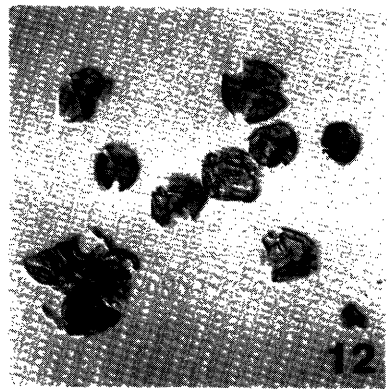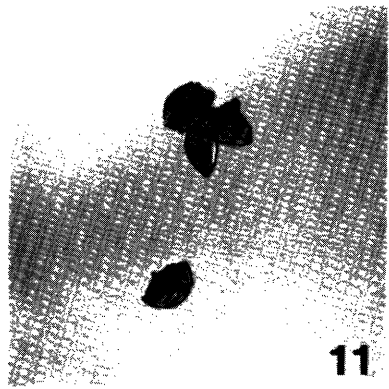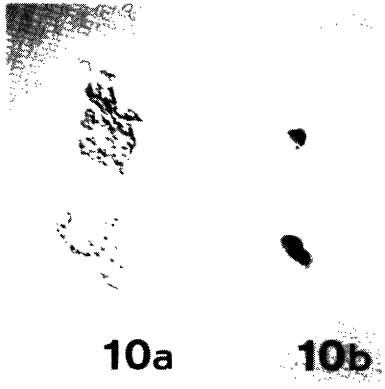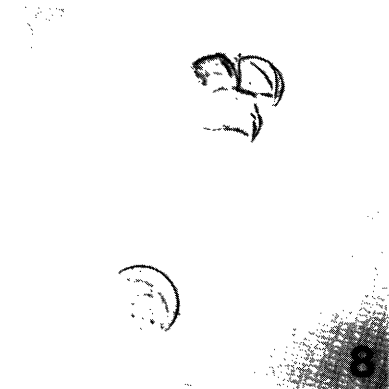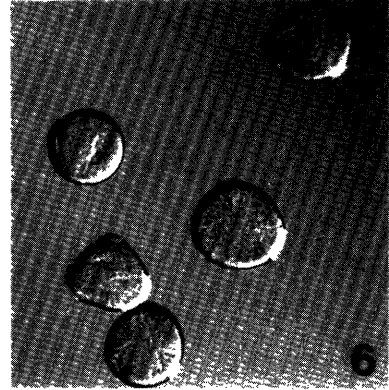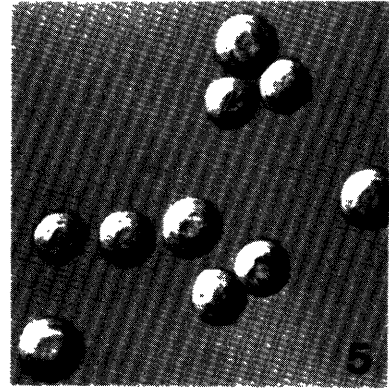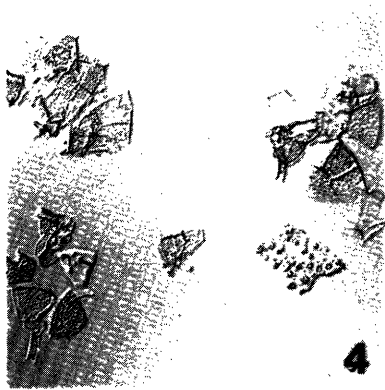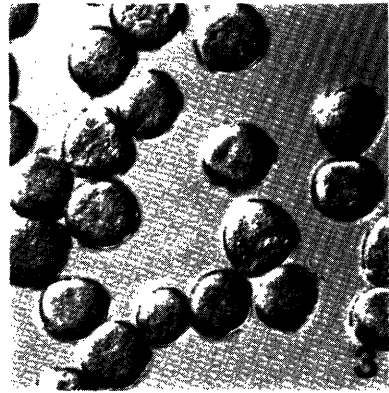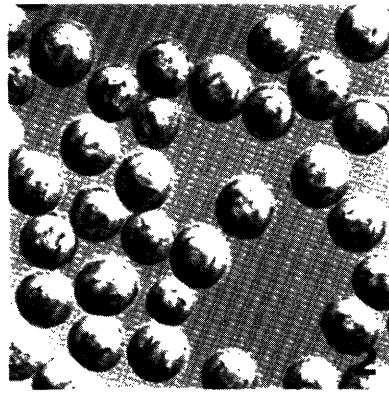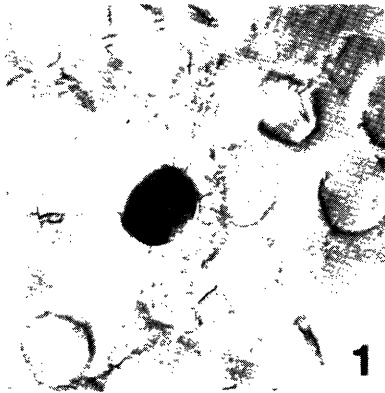
144

1

2

3

4

5

6

7

8

9

10a   10b

11

12

CHAPTER 4

The resistant outer wall of resting cysts
of the marine dinoflagellate *Lingulodinium polyedra*:
Ultrastructure and chemical composition

ABSTRACT

Resting cysts of the common marine dinoflagellate *Lingulodinium polyedra* are enclosed by a thick, multilayered cell wall which is both morphologically and compositionally distinct from the cell coverings present during other stages of the life cycle. In this species, the outermost layer of the resting cyst wall is composed of an extremely resistant organic material showing remarkable chemical and physical stability in the depositional environment. As a result, these selectivly preserved cyst walls are well represented in the fossil record and have been recovered from strata as old as the Early Eocene. In general, the rich fossil record of dinoflagellates appears to be dominated by forms composed of resistant substances similar to that of *L. polyedra*. The present study represents the second part in a series of investigations aimed at rigorously characterizing, for the first time, the "fossilizable" wall material enclosing the *L. polyedra* resting cyst. Transmission electron micrographs of the resistant outer layer reveal a structure of closely appressed and more or less elaborately branched masses rooted on a basel surface. Analysis of these wall layers via cupric oxide (CuO) oxidation strongly supports our earlier conclusion that this highly resistant material is composed partly of aromatic (phenolic) components which are most likely predominantly carbon-carbon linked. Although some short chain carboxylic acids are generated during CuO oxidation, there is little evidence to suggest the significant presence of extended polymethylenic elements in this macromolecular substance, which clearly sets it apart from the resistant aliphtic macromolecules identified in other phytoplankton. Lipid analysis of *L. polyedra* culture containing mostly vegetative cells revealed a series of sterols, even-carbon-number fatty acids, and an abundance of tocopherols, all of which (and especially the latter) are potential precursor materials available for resting cyst wall formation. Together with our earlier analyses, the results reported in this study represent an unprecedented level of chemical characterization of a resistant algal cell wall biopolymer. Overall, the macromolecular

substance in the cell walls of *L. polyedra* resting cysts appears fundamentally different from both carotenoid-based "sporopollenins" and aliphatic algaenans. Through these results, we provide the first chemically-based data to support the term "dinosporin", previously proposed to distinguish the highly resistant material comprising dinoflagellate resting cyst walls from other refractory cell wall biopolymers.

INTRODUCTION

Lingulodinium polyedra (Stein) Dodge 1989 is an autotrophic marine dinoflagellate widely distributed in coastal environments. As reported for a number of other dinoflagellate species, *L. polyedra* incorporates both a free-swimming planktic stage and a benthic resting stage in its life cycle. A typical motile cell is biflagellate, angular in outline, and enclosed by a robust theca composed of numerous cellulosic plates. Motile cells of this species are common constituents of neritic plankton assemblages and are well known for several phenomena, including an ability to bioluminesce and the potential to form large blooms (see for example Kofoid, 1911).

In the resting stage of the life cycle, cells (termed resting cysts) appear strikingly different from the motile forms. Resting cysts of *L. polyedra* consist of a spherical, cytoplasm-containing inner body which is covered by a continuous, non-mineral outer wall bearing numerous tapering spines. In this species, resting cysts form as a consequence of sexual reproduction (see Chapter 2): two free-swimming gametes fuse to form a motile zygote (the planozygote) which, after a period of maturation, sheds its cellulosic covering, loses its motility, and synthesizes a new cell covering. The non-motile cysts (hypnozygotes) then behave as passive particles, eventually sinking to the bottom of the water column. After a mandatory period of dormancy, resting cysts germinate, and the emerging motile cells return to the plankton, leaving behind the empty cyst capsules. A detailed account of resting cyst morphogenesis in laboratory cultures of *L. polyedra* can be found in Chapter 2. Readers interested in more complete summaries of dinoflagellate reproduction and life cycles should consult Pfiester (1989) and Pfiester and Anderson (1987).

L. polyedra is one of a small number of extant dinoflagellate species whose resting cyst walls persist in sediments long after cells have germinated. In some cases, the extraordinary physical and chemical resistance of these cell walls ultimately leads to their

preservation as fossils. As a group, dinoflagellates have a rich fossil record extending back at least 225 million years, and the vast majority of these fossils are the preserved walls of resting cysts (Evitt, 1961,1985). Resting cysts of *L. polyedra* (known as *L. machaerophorum* in paleontological taxonomy) are commonly encountered in strata ranging in age from the Early Eocene (~54 million years ago) to the present (Williams et al., 1993). Overall, fossil dinoflagellates have proved extremely valuable to micropaleontologists; the wide geographic distribution, high morphological diversity, and rapid evolution of dinoflagellates make their fossilized resting cysts ideal tools for biostratigraphy (Williams and Bujak, 1985; Goodman, 1987).

The remarkable resistance of some dinoflagellate resting cyst walls, including those of *L. polyedra*, has long invited questions concerning their chemical composition. Because these structures often co-occur with pollen and spores in fossil assemblages, paleontologists and biologists have traditionally referred to resting cyst wall material as sporopollenin or "sporopollenin-like" (e.g. Eisenack, 1963; Atkinson et al., 1972; Bujak and Davies, 1983; Evitt, 1985; Taylor, 1987, Hemsley and Scott, 1991). A few investigators, however, have noted differences between these fossil materials. Chaloner and Orbel (1971) found that dinoflagellate resting cysts showed a different distribution behavior than pollen and spores when mixed fossil assemblages were centrifuged in a density gradient. Data presented by Correia (1971) suggested that, when exposed to increasing temperatures, pollen and spores show color changes at different rates than dinoflagellates and acritarchs. Finally Sarjeant (e.g. 1986) has commented that fossil dinoflagellates show a consistently different response to various stains when compared with fossil pollen. Based on these stain tests, the latter author proposed the term "dinosporin" to distinguish dinoflagellate resting cyst wall material from that of pollen and spores.

To date, perhaps the greatest impediment to rigorous chemical characterization of dinoflagellate resting cyst wall material relates to the difficulties inherent in obtaining pure

wall fractions from either the fossil record or from cultures of modern cyst-producing species. In a previous investigation (Chapter 3), the successful isolation of such a fraction from laboratory cultures of *L. polyedra* was described. Detailed comparison of the composition of this material to similar fractions isolated from pollens of a gymnosperm (*Juniperus scopulorum*) and angiosperm (*Quercus rubra*) were undertaken via optical microscopy, FTIR microscopy, elemental analysis, *in-source* pyrolysis--(DEI) mass spectrometry, and pyrolysis--gas chromatography--mass spectrometry. These analyses suggested that, while cell walls of dinoflagellate resting cysts and pollen show some compositional similarity, there are several fundamental differences between these materials. Pyrolysis-GC/MS analysis of cell walls from both pollens and *L. polyedra* resting cysts yielded a strong aromatic signature, with some apparent similarities to that of lignin. Interestingly, the Py-GC/MS TIC chromatogram of the dinoflagellate material showed an abundance of prist-1-ene, thought to derive from tocopherols bound to the resting cyst wall biopolymer. Although prist-1-ene has also been detected in studies of isolated cell walls of a green alga (Goth et al., 1988), data from recent investigations of several chlorophyte species (e.g. Largeau et al., 1984, 1985; Geisert et al., 1987; Burczyk and Dworzanski, 1988; Kadouri et al., 1988; Derenne et al., 1989, 1990, 1991, 1992) clearly point to a cell wall biopolymer which is chiefly comprised of linear aliphatic chains. Thus, work to date suggests that the resistant cell walls of *L. polyedra* are comprised of a macromolecular substance distinct from both "traditional" sporopollenins (pollen and spores of higher plants; see Brooks and Shaw, 1978) and those found among the green algae.

In the present investigation, we further characterize the resting cyst cell wall of *L. polyera* using transmission electron microscopy (TEM) and gas chromatography--mass spectrometry (GC/MS) of cupric oxide (CuO) oxidation products. In addition, in-source pyrolysis desorption chemical ionization mass spectrometry [Py-(DCI)MS] of unprocessed dinoflagellate culture residue and GC/MS of extractable lipids are employed to characterize available biochemicals which could function as precursors to the resting cyst wall .

biopolymer. Analysis of Juniper and Oak pollen materials using CuO oxidation and solid state ^{13}C NMR spectroscopy allow further comparison of these materials to those of the resting cyst wall. Together, these approaches permit a more definitive statement of the nature of the biopolymer in the outer wall of *L. polyedra* resting cysts. When combined with our earlier observations on the morphological development of resting cysts (Chapter 2), our results allow some inferences to be made on the likely origin and mode of formation of this highly resistant biomacromolecule.

MATERIALS AND METHODS

Biological materials and culturing conditions.

Laboratory cultures of *Lingulodinium polyedra* were established and maintained as described in Chapter 2. All dinoflagellate material utilized in the present study derived from a single strain (GpES-19). Although cultures were not axenic, examination under the microscope revealed any bacterial mass to be negligible. The majority of resting cyst production in batch cultures occurred during the 2 weeks following peak cell density (i.e. starting about 3.5-4 weeks after inoculation). After cyst production was complete, culture tubes were stored under the same conditions used for actively growing cultures. 100 culture tubes (inoculated between April and November, 1991) were harvested using a teflon policeman to gently scrape culture residue from tube bottoms. Loosened materials were transferred to centrifuge tubes, washed 5 times in Milli-Q water, briefly sonified, washed again 5 times, and then freeze dried. For use as "sporopollenin" controls, pollen of *Juniperus scopulorum* (Rocky Mountain Juniper) and *Quercus rubra* (Northern Red Oak) were obtained from Sigma (Sigma Chemical Company, St. Louis, MO, U.S.A.). Both pollens were microscopically examined for purity prior to analysis.

Transmission electron microscopy.

Resting cysts (<1-2 weeks old) were collected from the bottom of culture tubes with a pasteur capillary pipette and fixed for ~3 hr at 4°C using 2.5% glutaraldehyde and 2.0% paraformaldehyde in 0.25 M PIPES buffer. Cells were subsequently washed 3 times in cold buffer (0.4 M PIPES + 0.1 M sucrose) and post-fixed for 1.5 hr at 4°C in 1% osmium tetroxide in 0.3 M PIPES and 0.4 M sucrose. Following post-fixation, cells were washed 4 times: twice in cold buffer (as above) and twice in cold Milli-Q H_2O. All fixatives and rinse buffers used prior to Milli-Q H_2O rinses were adjusted to a pH of 7.2 and osmolarity of ~1200 mOsm. After rinsing, cells were en bloc stained in saturated uranyl acetate for 1.5 hr at 4°C, washed 3 times in cold Milli-Q H_2O, and then encapsulated in 2% agarose (SeaPlaque low gelling temperature agarose; FMC Corporation, Rockland, Maine, U.S.A.) as follows: Cells were resuspended in molten agarose in 1.5 mL Eppendorf tubes, and then pelleted by gentle centrifugation. Tubes were placed on ice for ~20 min. to facilitate gelling of the agarose. The encapsulated cells were then recovered by cutting off the tips of the Eppendorf tubes and excising the pellet. Agarose portions (containing cells) thus obtained were submerged under cold Milli-Q H_2O in a petrie dish and dissected into small cubes (~1 mm^3). After transfer to vials, cubes were dehydrated in a graded ethanol series. Following dehydration, the agarose/cell cubes were infiltrated in Spurr resin (Spurr, 1969) over a period of 4 days. During this interval, infiltration vials were normally kept on a rotary mixer, but were moved periodically into a vacuum desiccator maintained at ~0.5 atm. Infiltrated agarose cubes were flat embedded in fresh Spurr resin (medium hardness formulation) and polymerization was achieved at 70°C for 12 hrs. Sections were cut on a Reichert Jung Ultracut E microtome, collected on uncoated copper grids, and examined (unstained) with a Zeiss 10CA transmission electron microscope.

Although not discussed in this chapter, a small number of *L. polyedra* resting cysts were fixed and embedded for transmission electron microscopy using a protocol developed for isolated cells. These methods are described in Appendix 1.

Isolation of restistant cell wall materials.

Isolation of resistant cell wall biopolymers was accomplished by processing initial materials in two batches, hereafter designated as I and II. In Batch I, half of the dinoflagellate culture material and approximately 1 g of each of the two pollens were subjected to a three step procedure (solvent extraction, saponification, acid hydrolysis) described in detail in Chapter 3. The remaining half of the dinoflagellate culture residue and about 0.7 g of Juniper pollen comprised the second batch of initial materials, which were treated according to a slightly abbreviated and modified version of the first protocol. This second protocol employed two major treatments (saponification and acid hydrolysis) as follows:

Saponification. Initial materials were refluxed for 6 hours in 6% KOH in MeOH/H_2O (9/1, v/v). After saponification, reflux mixtures were acidified to pH 4 by addition of 2N HCl/MeOH (1/1, v/v). Residues were separated by centrifugation and supernatants transferred into a separatory funnel. The residues were then ultrasonically extracted using H_2O (100%), MeOH / H_2O (1/1, v/v), MeOH (100%), MeOH / CH_2Cl_2 (1/1, v/v), and CH_2Cl_2 / hexane (4/1, v/v). Each time, supernatants (after centrifugation) were combined in the separatory funnels. After final extraction (CH_2Cl_2 / hexane), funnel contents separated into an organic phase (lower) and an aqueous phase (upper). Organic phases were removed, and the aqueous phases back-extracted with CH_2Cl_2 (2x). All CH_2Cl_2 fractions were combined to yield extracts (II)E1. Aqueous layers were left standing over a small volume of residual CH_2Cl_2 in separatory funnels; fine suspended

materials in the aqueous phase collected at the CH_2Cl_2 / aqueous layer interface. These materials were collected and archived as (II)E1 "fluffs".

Acid hydrolysis. Residues (II)R1 obtained above were refluxed under nitrogen for 2 hours in concentrated (95%) sulfuric acid. Insoluble residues were then separated by filtration (polycarbonate membrane; pore size, 0.4 μm) and extracted as above. The filtrate and all solvent extraction supernatants were combined and partioned in separatory funnels as described above; these procedures resulted in extracts (II)E2, residues (II)R2, and (II)E2 "fluffs".

Analytical techniques.

Cupric oxide oxidation. Alkaline CuO oxidation followed the procedure of Hedges and Ertel (1982), with some modification according to Goñi and Hedges (1992). Approximately 20 mg of pollen (I)R3 residue, or 2 mg of *L. polyedra* (II)R2 residue, was combined with ~1 g of CuO and 100 mg of $Fe(NH_4)_2(SO_4)_2 \cdot 6H_2O$ in a stainless steel minibomb and oxidized in the presence of 8% NaOH (~20 mL) for 3 hours. Four minibombs were enclosed in a larger reaction chamber which contained additional base and was fitted in an insulated heating sleeve controlled by a 02155-series platinum RTD temperature controller (Cole Parmer). The large reaction chamber was heated from room temperature to a final internal temperature of 155°C over an interval of 30 min. Internal and external temperatures were monitored with two 100W platinum RTD probes (Cole Parmer).

After oxidation, minibombs were cooled and opened, at which time recovery standards (*trans*-cinnamic acid and ethylvanillin) were added. Samples were transferred to centrifugation tubes and centrifuged for 10 min to separate the aqueous phase from the solid residue. The liquid from each tube was transferred to a separatory funnel while the solid residues were archived frozen. This procedure was repeated two more times to

ensure all hydrolyzed products were separated from the solid residue. Alkaline solutions in the separatory funnels were acidified to pH 1 by addition of ~5 mL of concentrated HCl. Acidified solutions were then extracted with ~50 mL of freshly distilled ether (3x) and the organic phases transferred to a round bottom flask. Anhydrous sodium sulfate (Na_2SO_4) was added during this step to capture any remaining water in the ether extract. The volumes of ether were subsequently reduced in a rotoevaporator, transferred to a sample vial (via an Na_2SO_4 column), and dried completely under a N_2 stream.

Dry extracts of the CuO reaction mixture were prepared for gas chromatography as detailed by Goñi and Hedges (1992). In summary, this involved dissolving extracts in pyridine (50-100 µL) and derivatizing with equal volumes of silylating agent (BSTFA + 1% TCMS; Regis Chemical Co.) for 60°C for 15 min..

Gas chromatography / mass spectrometry. GC/MS was performed using a Hewlett Packard HP 5890 Series II gas chromatograph and VG AutoSpec-Q mass spectrometer. On-column injection of the samples (0.5 µL) was accomplished by an HP 7673 autosampler, and chromatographic separation was achieved on a capillary column (J & W, 60 m x 320 µm I.D.) coated with a DB-1 stationary phase (film thickness, 0.25 µm). Carrier gas (He) supply was operated in constant mass flow mode with vacuum compensation. The GC was programmed from an initial temperature of 70°C (5 min.) to a final temperature of 320°C (20 min.) at 4°C min^{-1}. Electron Impact (EI) mass spectra (50 eV) were acquired over a scan range of 50 to 650 Da at a scan rate of 0.9 sec/decade and resolution of 2000. The GC/MS interface temperature was 320°C, and source temperature of the mass spectrometer was 250°C.

Lipid analysis. Concentrated (I)E1 extracts of dinoflagellate culture, Juniper, and Oak materials were prepared for GC and GC/MS in the following fashion: Anhydrous sodium sulfate (Na_2SO_4) was added to remove any residual water. Extracts were then filtered (Gelman Acrodisc teflon filters; pore size, 0.45 µm), combined with 2 mL of MeOH / HCl (95/5, v/v), and purged with N_2 before sealing sample vials with Mininert™

vial caps. Transesterification (methanolysis) was performed at 70°C (dri-bath) for 14 hr. On cooling, 1 mL of H_2O was added and the aqueous phase was extracted by shaking with hexane (4x, 1 mL) and diethylether (3x, 1 mL). Water was removed from the combined organic (upper) phases by passing over a Na_2SO_4 mini-column, and the resulting anhydrous extracts taken to dryness under N_2. After re-dissolving extracts in equal volumes of pyridine and Regisil (BSTFA + 1% TCMS), derivatization was performed at 60°C for 15 min. This combination of methanolysis followed by BSTFA derivatization converts free and bound fatty acids to corresponding methylesters, and alcohols to trimethylsilyl (TMS) -ethers. Analysis by gas chromatography / mass spectrometry was carried out as described above for CuO oxidation products.

In-source pyrolysis desorption chemical ionization mass spectrometry [Py-(DCI)MS]. Py-(DCI)MS analysis of dinoflagellate initial materials was performed on a JEOL SX-102A (B/E) mass spectrometer equipped with a resistively heated Pt/Rh filament Desorption Chemical Ionization (DCI) probe. Samples (1 to 5 µL) were applied to the filament as a MeOH suspension. The filament was heated at 2 A min^{-1} (~20°C sec^{-1}) up to 1.5 A (800°C). A soft ionization mode was employed to reduce fragmentation of sugar compounds. Ammonia Chemical Ionization (NH_3^+-CI) spectra were acquired over a mass range of 30-2000 amu, at a scan cycle time of 1.5 sec. The source temperature was 180 °C.

Solid state ^{13}C NMR Spectroscopy. Solid state ^{13}C NMR spectra of Juniper (II)R2 and Oak (I)R3 residues were acquired on a Chemagnetics M-100 spectrometer operating at a field strength of 2.35 Tesla, with a sample spinning rate of 3.3 KHz, pulse repetition time of 1 sec, contact time of 1 msec., and acquisition length of 0.5 K. Additional operational details are as described by Hatcher (1988).

RESULTS

Ultrastructure

Due to difficulties associated with fixative penetration and resin infiltration, successful microtomy and TEM observation of *L. polyedra* resting cysts was rare. As a result, the following comments are based on the examination of only three specimens and should be regarded as preliminary. Transmission electron micrographs illustrating the ultrastructure of *L. polyedra* resting cyst walls are shown in Plate 4.1. The cell covering is clearly multilayered, but a precise definition of the number of layers is somewhat subjective. In this investigation, we describe three layers, starting with the outermost.

Layer 1. The outermost layer (Layer 1) of the *L. polyedra* resting cyst is a prominent, electron-dense feature which shows a highly irregular variation in thickness from about 0.1 to 0.25 μm. This layer appears composed of closely appressed masses of irregular shape, ranging from sub-rounded to elaborately branched (Plate 4.1, Figures 2 and 3). Where individual masses are more or less distinct, their dimensions are in the range of 0.05 to 0.1 μm. In some regions of this layer, interstitial spaces may remain between the appressed bodies; locally, these spaces seem to form a network of connected channels. The inner boundary of Layer 1 appears relatively smooth and unbroken, and functions as a foundational surface upon which the appressed masses are rooted. Irregular protrusion of these bodies outward from the inner boundary creates the characteristic "fibrous" wall texture seen with the light microscope. No obvious differences could be noted in the structure of the wall between spines as opposed to those wall portions under the spines.

Although not optimally intersected by our thin sections, the spines of the *L. polyedra* resting cyst seem to be extensions of this wall of irregular appressed masses. Structural units of spine walls, however, appear more complex in morphology and are

difficult to define. Spine walls measured from ~0.08 to 0.15 μm in thickness. Within the population of resting cysts forming in our laboratory cultures, spine length was highly variable, ranging from zero (no discernable spines) to ~10 μm. Spines are hollow and, at the scale of light microscopy, distally closed. Cross sections of spine walls, however, seem to show small (< 0.05 μm) openings which may link the spine interior to the outside medium.

Layer 2 This layer directly underlies the spine-bearing outer wall and comprises the thickest component of the resting cyst cell covering. The thickness of this layer varied somewhat among the resting cysts encountered in our cultures, ranging from ~ 0.5 to 1.5 μm. In any given specimen, however, Layer 2 appears relatively uniform in thickness. Typically, this feature showed some evidence of stratification (Plate 4.1, Figures 2 and 3). In some cases, suggestions of internal lamination were visible in sections of intact wall. This lamination was less pronounced in other specimens, but mechanical disruption of some of these latter types during sectioning caused this portion of the wall to locally separate into laminae. When internal laminae were visible, an abrupt change in the definition of these features sometimes occurs within Layer 2 and divides this part of the cell wall into two zones which are roughly equal in thickness (Plate 4.1, Figures 1 and 2). The inner zone is marked by the presence of numerous patches (slightly darker than the surrounding material) which are elongated parallel to the wall to give the impression of faint laminae. The outer zone of Layer 2 appears more homogeneous in structure, but does show some variation in color as seen in TEM.

One of the specimens examined for this study showed two distinct features of note localized in the outer zone of Layer 2. The first of these was a discontinuous layer of irregular thickness (pinching-out laterally) occurring at or very near the interface between Layers 1 and 2 (Plate 4.1, Figures 1-4). This feature was typically lighter in color than the surrounding material, but contained darker, more or less densely-packed bodies. In some cases, these bodies were reminiscent of the units comprising Layer 1, but tended to be

smaller, less closely appressed, and were more regular in morphology (rounded to globular). Locally, this feature appeared to contact Layer 1, but in some cases Layer 2 material was clearly interposed.

Also noteworthy in the outer zone of Layer 2 was the presence of prominent electron dense bodies, here referred to as Endospore Inclusion Bodies (EIB) (Plate 4.1, Figures 1 and 3). Some appeared circular in section while others were more irregular. EIB's were approximately 1 μm in diameter; in any given section, up to about 8 could be visible and were irregularly distributed around the cell periphery. Internally, these features were heterogeneous in character, but structural details were difficult to discern (Plate 4.1, Figure 3). The presence of these bodies caused inward bulging of Layer 2, resulting in local thickenings of the cell covering (Plate 4.1, Figures 1 and 3). Within Layer 2, laminar features appeared to follow the contours imposed by the EIB so that no intersection of these features was observed. Although typically situated very near the contact with Layer 1, no clear connection between these wall components could be established. However, the discontinuous layers mentioned above occasionally appeared to impinge on the EIB (Plate 4.1, Figure 1).

Layer 3. Layer 3 was similar in appearance to the inner zone of Layer 2 except that defined lineations were finer and more continuous (Plate 4.1, Figure 2); locally, this gave the layer a distinct microlaminar structure. Layer 3 maintained a consistent thickness of ~0.2 μm. In one specimen, the boundary between Layers 2 and 3 was defined by a very prominent dark band. The nature of this feature was difficult to assess due to the thickness of our sections. Occasionally, a dark rounded body (~ 0.08 μm) appeared to be incorporated into this boundary. Interestingly, when improperly embedded specimens tore or dropped out of sections during microtomy, failure consistently occurred at the Layer 2 / Layer 3 interface.

Cytoplasm. In all specimens examined, the cytoplasm was dominated by the presence of large starch bodies, more or less oval in shape, with the longest dimension

measuring about ~3 μm (Plate 4.1, Figure 1). These features are easily detected via light microscopy (Chapter 2) and could be identified even as isolated bodies when culture debris was examined. Aside from these prominent storage bodies, very little else could be discerned in the resting cyst cytoplasm. Some structure could be detected within the interstitial space between the starch bodies, but these regions of our micrographs were generally obscure and difficult to interpret.

Cupric oxide (CuO) oxidation

Total ion current (TIC) chromatograms showing the results of GC/MS analysis of Juniper (I)R3, Oak (I)R3, and *L. polyedra* (II)R2 cupric oxide oxidation reaction products are shown in Figure 4.1; peak numbers correspond to tentative identification of compounds as listed in Table 4.1.

Overall, the pollen CuO reaction product mixtures are very similar, showing benzoic acid, butane-1,4-dioic acid, vanillin, vanillic acid, *p*-coumaric acid, and octadecanoic acid (Peaks #1, 2, 13, 24, 31, and 47, respectively) as major components. However, some differences can be detected. Tetradecanoic acid (Peak #28) and two unidentified peaks (#7, and #41) are present in the Oak chromatogram, but are either absent or barely detectable among the Juniper CuO products. Similarly, both *p*-hydroxybenzaldehyde (Peak #5) and hexadecanoic acid (Peak #36) are much more prominent in the Oak chromatogram compared with that of Juniper. This relationship also holds for the saturated and unsaturated C_{18} fatty acids (Peaks #44, #45, and #47). On the other hand, ferulic acid (Peak #38), which is present in small but significant amounts in the Juniper chromatogram, is difficult to detect in the Oak CuO products. Finally, the alkane series from C_{22} to C_{29} which appears in the Oak chromatogram (between scans 1380 and ~1900) is absent from the Juniper chromatogram. Interestingly, no syringyl
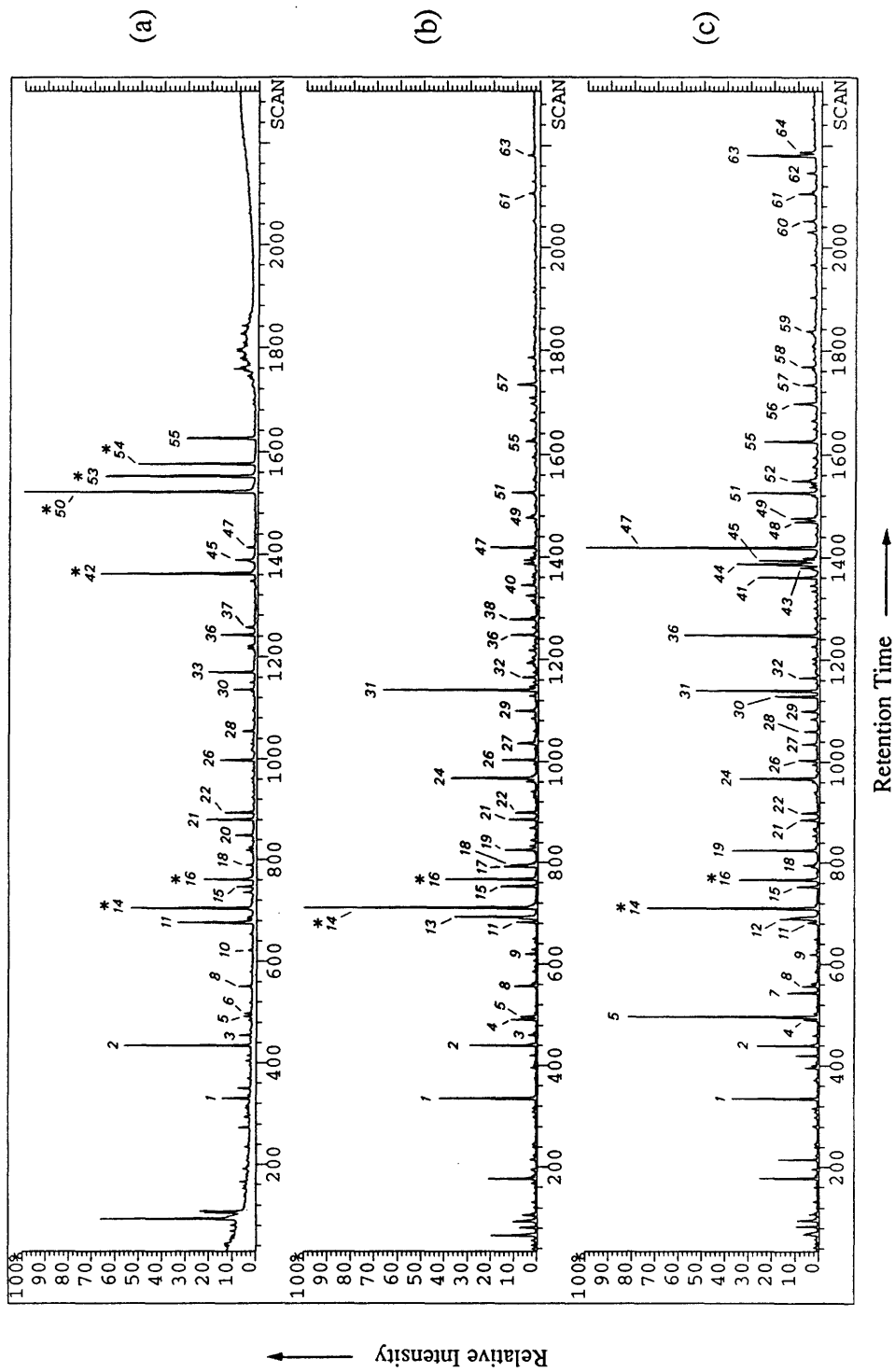
FIGURE 4.1 Total ion current (TIC) chromatograms showing CuO oxidation reaction products (TMS derivatives) as revealed by GC/MS: (a) *L. polyedra* (II)R2, (b) Juniper (I)R3, and (c) Oak (I)R3. Peak numbers correspond to compounds listed in Table 4.1. Asterisks denote internal standards.

164

TABLE 4.1. *CuO reaction products of Juniper (I)R3, Oak (I)R3, and* L. polydera *(II)R2 residues as revealed by GC/MS. Compound numbers refer to peak labels in Figures 4.1, 4.7, and 4.8. (I.S. = internal standard.)*

Compound Number	Compound Name
1	Benzoic Acid
2	Butane-1,4-dioic Acid
3	C4 diacid (branched)
4	2-Butene-1,4-dioic Acid
5	*p*-Hydroxybenzaldehyde
6	C9 FA
7	unknown
8	Pentane-1,5-dioic Acid
9	*p*-Hydroxyacetophenone
10	C10 FA
11	Hexane-1,6-dioic Acid
12	*o*-Hydroxybenzoic Acid
13	Vanillin
14	*trans*-Cinnamic Acid (I.S.)
15	*m*-Hydroxybenzoic Acid
16	Ethylvanillin
17	Acetovanillone
18	Heptane-1,7-dioic Acid?
19	*p*-Hydroxybenzoic Acid
20	C12 FA
21	Carboxy-hydroxybenzaldehyde
22	Octane-1,8-dioic Acid
23	Carboxy hydroxybenzaldehyde
24	Vanillic Acid
25	C14 alcohol
26	Nonane-1,9-dioic Acid + 2-Carboxy-4-hydroxybenzaldehyde
27	p-Hydroxyphenylglyoxylic Acid + 3,5-Dihydroxybenzoic Acid
28	Tetradecanoic Acid
29	Decane-1,10-dioic Acid
30	unknown
31	*p*-Coumaric Acid
32	Vanillylglyoxylic Acid
33	Di-OH C10 FA ?
34	C11 DA
35	C16:1 FA
36	Hexadecanoic Acid
37	Di-OH C11 FA ?
38	Ferulic Acid
39	C12 DA
40	unknown
41	unknown
42	C13 DA ? (I.S.)
43	n-alkane?
44	Octadecadienoic Acid
45	Octadecenoic Acid

TABLE 4.1. Continued

Compound Number	Compound Name
46	unknown
47	Octadecanoic Acid
48	C23 n-alkane
49	11,12-Dihydroxytetradecanoic Acid ?
50	unknown I.S.
51	unknown
52	C24 n-alkane
53	unknown I.S.
54	unknown I.S.
55	13,14-Dihydroxyhexadecanoic Acid
56	C26 n-alkane
57	7-Hydroxyhexadecane-1,16-dioic Acid + 8-Hydroxyhexadecane-1,16-dioic Acid.
58	C27 n-alkane
59	C28 n-alkane
60	unknown
61	unknown
62	unknown
63	unknown
64	unknown

(i.e. di-methoxy) components were detected in the products from either pollen.

Although the suite of CuO oxidation products in the *L. polyedra* chromatogram (Fig. 4.1a) shows some similarities to that of the pollen materials, substantial differences can be noted. With respect to aromatic products, methoxylated phenolic compounds (e.g. vanillin, Peak #13; vanillic acid, Peak #24; and acetovanillone, Peak #17), though prominent in the pollen chromatograms, are present in only trace amounts in that of the dinoflagellate material. Similarly, *p*-coumaric acid (Peak #31) is a major CuO product of the pollen residues but is barely detectable in the *L. polyedra* chromatogram. Other differences include *p*-hydroxybenzaldehyde (Peak #5) which is prominent among the Oak CuO products, reduced somewhat in the Juniper chromatogram, and virtually absent from the dinoflagellate material. *p*-Hydoxyacetophenone (Peak #9) is present in both pollen chromatograms but completely absent from that of the resting cyst cell wall residue. Although *para*, *ortho*, and *meta* isomers of hydroxybenzoic acid are present in all three samples, their distribution shows some variability; both pollen chromatograms display a bias towards the *p*- isomer, while the *m*- form is most abundant in the dinoflagellate material. Finally, carboxylated phenols (e.g. Peaks #21 and #26) appear to be more significant in the *L. polyedra* chromatogram.

Concerning aliphatic CuO oxidation products, while both pollens yielded a continuous series of di-acids extending up to at least C_{12}, the analogous series in the dinoflagellate chromatogram is strongly even-carbon-number dominated and abruptly truncates at C_{10}. Also noteworthy are the hydroxy C_{16} di-acids (Peak #57) which are not present among the dinoflagellate CuO products but readily detected in the pollen chromatograms. Finally, while dihydroxy C_{10} and C_{11} fatty acids (Peaks #33 and 37, respectively) appear in all three chromatograms (see Fig. 4.7), the dihydroxy C_{14} fatty acid (Peak #49) is present only in that of the pollens.

Solid state ^{13}C NMR spectra of Juniper (II)R2 and Oak(I)R3 residues are shown in Figure 4.2. The Juniper spectrum is dominated by a peak at 20-50 ppm (saturated carbons without heterosubstituents) with a sharp maximum at 30 ppm (CH_2 in polymethylenic chains) and a "notch" at 41 ppm (carbons adjacent to oxygen-bearing carbons). The small shoulder at about 54 ppm may relate to sp^3 carbons bonded to N and/or to methoxyl carbons. Another prominent peak occurs from 60-80 ppm with a sharp maximum at 72 which corresponds to alcohol and ether groups. Other oxygen functions are indicated by responses at 165-180 ppm (carboxyl, ester, and/or amide) and 200-210 ppm (carbonyl). Several peaks in the interval from 100 to 160 ppm (e.g. 103, 113, 130, and 148 ppm) indicate the presence of unsaturated C=C.

The ^{13}C NMR spectrum of Oak (I)R3 is very similar to that of the Juniper material, but the following differences can be noted: (1) At 41 ppm, the Oak spectrum shows only a very weak inflection rather than a notch. (2) The alcohol/ether response centered at 72 ppm is much less significant. (3) Oxygen function peaks at 165-180 ppm and 200-210 ppm are greatly reduced, and (4) The C=C peaks at 103 and 148 ppm are reduced, while that at 113 ppm is no longer visible.

In source pyrolysis desorption chemical ionization mass spectrometry

A time integrated mass spectrum resulting from in-source pyrolysis of initial dinoflagellate residue under ammonia CI conditions is shown in Figure 4.3. Major peaks in this spectrum clearly reflect the abundance of cellulosic thecal material in the unprocessed culture debris. The base peak at m/z 180 corresponds to the ammonium adduct ion (M^+ + 18) of 1,6-anhydroglucose (levoglucosan). This peak forms the starting point for a prominant ion series, including the monomer (m/z 180), dimer (m/z 342), trimer
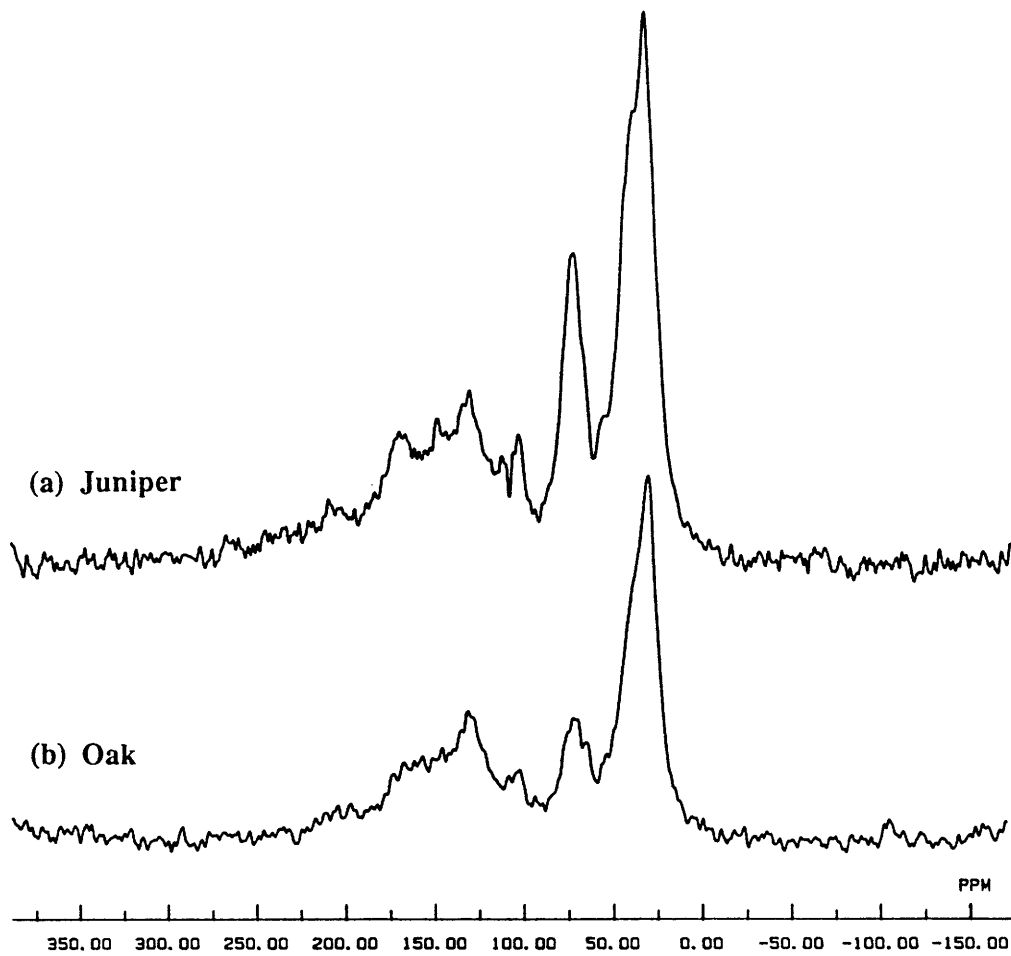
FIGURE 4.2 Solid-state ^{13}C NMR spectra of (a) Juniper (II)R2, and (b) Oak (I)R1.
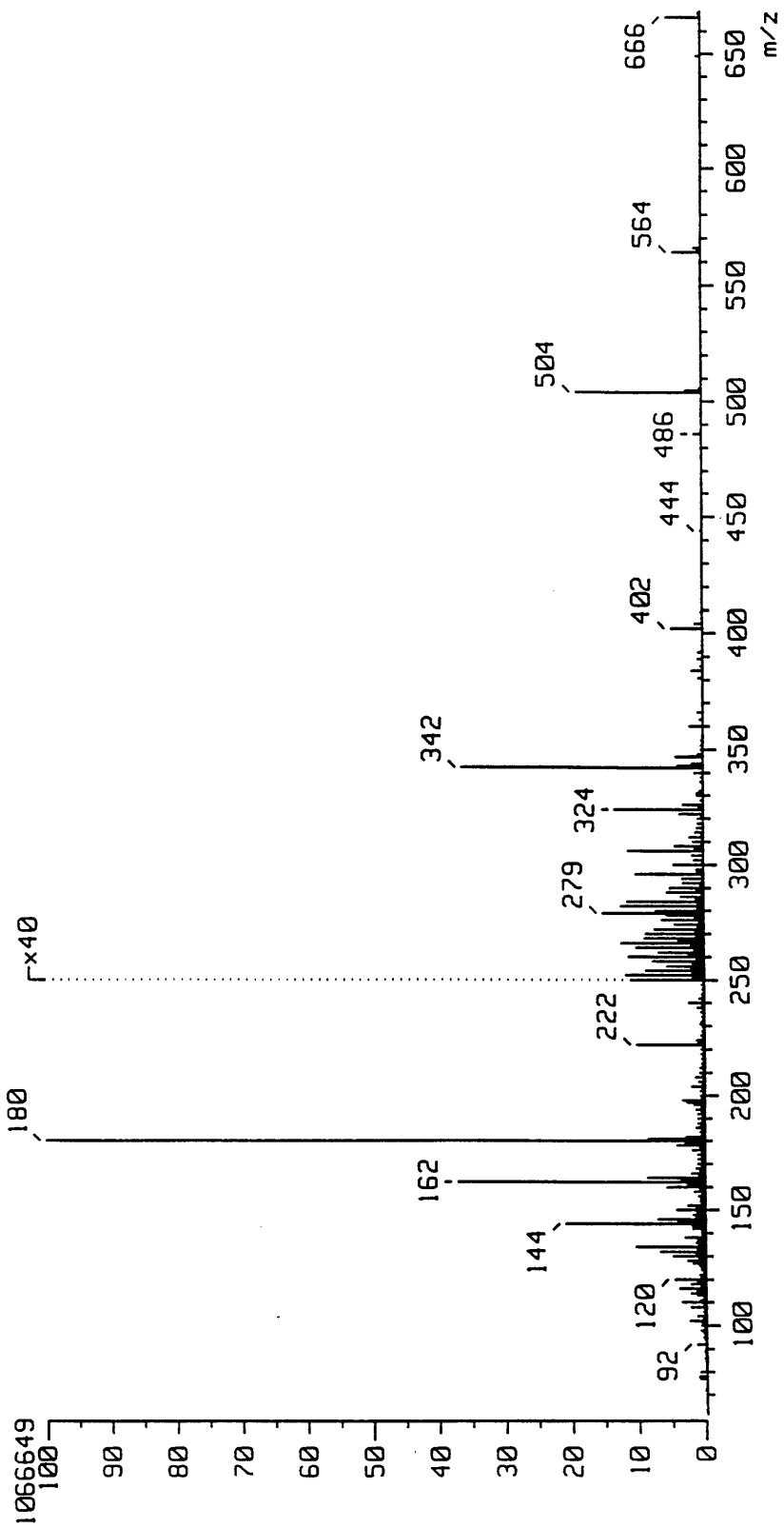
FIGURE 4.3 Time integrated mass spectrum from Py-MS analysis of *L. polyedra* Initial residue under ammonia CI conditions.

(m/z 504), and tetramer (m/z 666). The appearance of such a clear oligomer series was unexpected and points to the presence of well ordered linear glucan chains.

Other mass peaks can be correlated with known pyrolysis products from cellulose. According to Pouwels et al. (1989), the ion at m/z 162 may represent contributions from two compounds having a molecular weight of 144 (1,4-dideoxy-*D-glycero*-hex-1-enopyranos-3-ulose and 1,4;3,6-dianhydro-*a-D*-glucose). Ammonium adducts of a number of furanone and pyranone derivatives could yield the ion at m/z 144, while that at m/z 120 probably consists of contributions from several coumpounds with a molecular weight of 102 (e.g. pyruvic acid methyl ester, methoxytetrahydrofuran, and hydroxybutanedialdehyde). Ions at m/z 146 and 164 probably represent small amounts of deoxyhexoses while those at m/z 132 and 150 relate to the presence of pentoses. Retroaldolization fragments can be identified at m/z 240, 402, and 564.

Figure 4.4 shows time-resolved mass chromatograms of selected ions identified in the above spectrum. Note that dissociation maxima of fragments corresponding to labile pentoses and deoxyhexoses (m/z 164, 146, 150, 132) occur slightly earlier in the temperature profile than those of glucan fragments (m/z 180).

Lipid analysis

The total ion chromatogram (TIC) chromatogram resulting from GC/MS analysis of *L. polyedra* (I)E1 extract is shown in Figure 4.5. Peak numbers correspond to the compounds listed in Table 4.2. The dominant compounds in this chromatogram are a series of fatty acids of even carbon number ranging from C_{14} to C_{24}, with a strong maximum at C_{16} (Peak #3, scan 1125). Other significant components include a full suite of tocopherols (*alpha*-tocopherol, Peak #19, scan 2249; *gamma*-tocopherol, Peak #17, scan 2193; *delta*-tocopherol, Peak #15, scan 2130) listed here in order of decreasing abundance. Sterols are well represented, the most abundant being cholesterol (Peak #12,
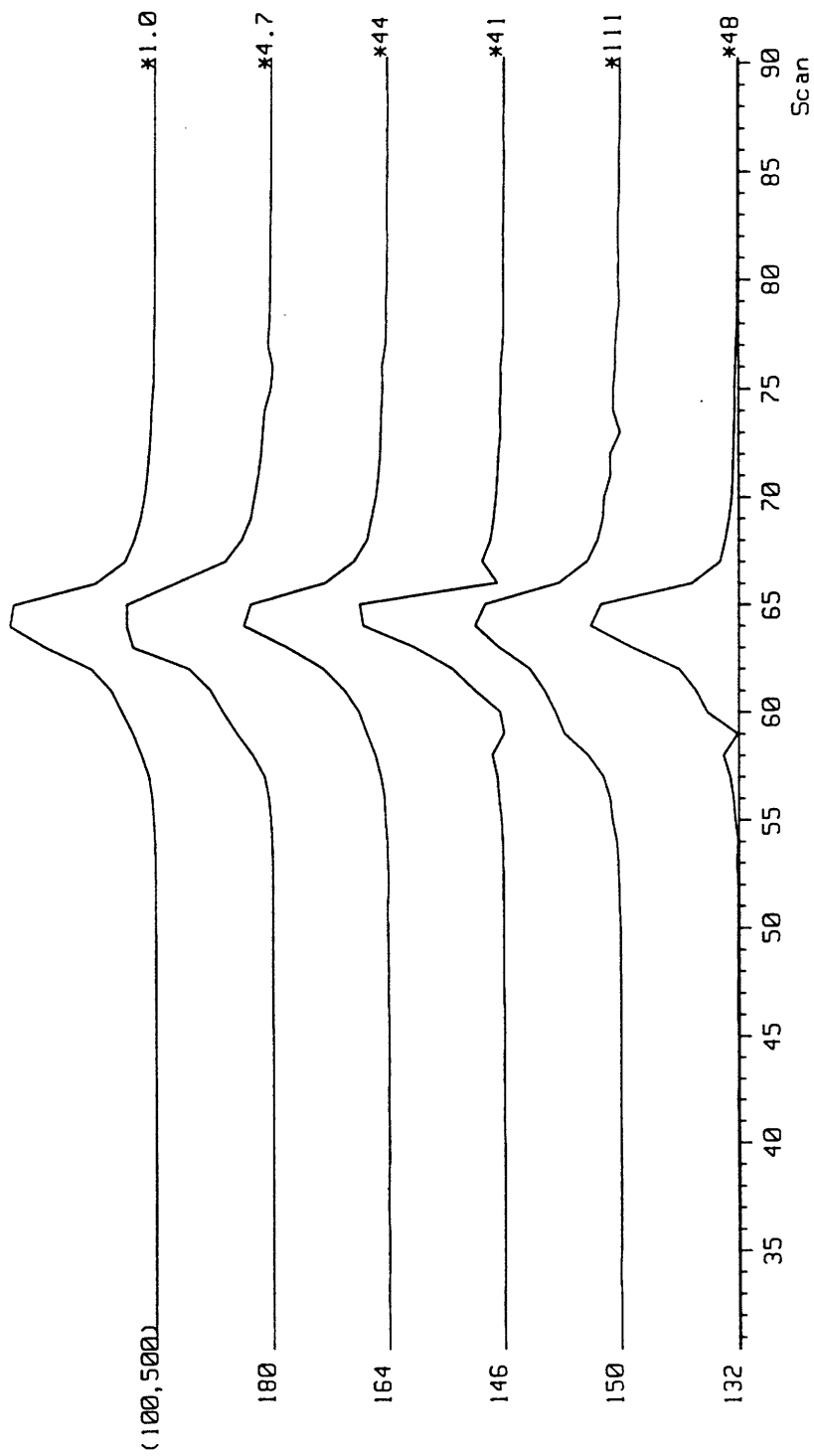
FIGURE 4.4 Time-resolved mass chromatograms of selected ions from Figure 4.3
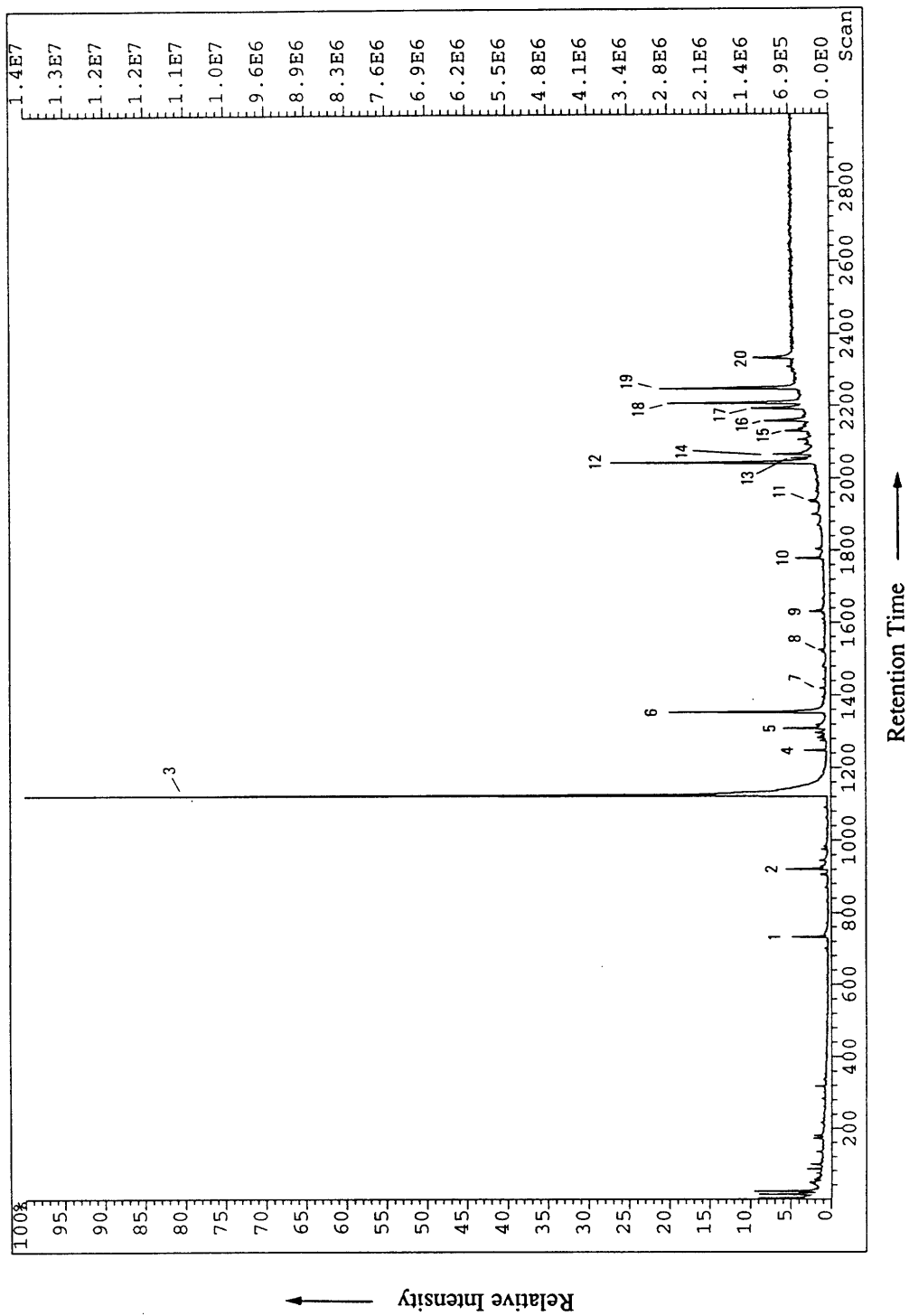
FIGURE 4.5 Total ion current (TIC) chromatogram from GC/MS analysis of *L. polyedra* (I)E1 lipid extract (TMS derivatives). Peak numbers correspond to compounds listed in Table 4.2.

173

TABLE 4.2. *GC/MS data for (I)E1 extracts of* L. polyedra *culture material. Compound numbers refer to peak labels in Figure 4.6.*

Compound Number	Scan Number	Compound Name
1	733	Hydroxy C10 fatty acid or Hydroxy C12 di-acid
2	921	C14 fatty acid
3	1125	C16 fatty acid
4	1248	unknown
5	1309	C18 fatty acid
6	1353	C18 alcohol
7	1419	unknown
8	1525	unknown
9	1630	C22 fatty acid
10	1779	C24 fatty acid
11	1939	unknown
12	2042	Cholesterol
13	2056	C28 alcohol
14	2066	Cholestanol
15	2130	*delta*-tocopherol
16	2158	Demethyldinosterol
17	2193	*gamma*-tocopherol
18	2207	Dinosterol
19	2249	*alpha*-tocopherol
20	2334	Gorgosterol?

scan 2042) and dinosterol (Peak #18, scan 2207). Other sterols tentatively identified include demethyldinosterol (Peak #16, scan 2158) and gorgosterol (Peak #20, scan 2334). Also noteworthy are Peaks #6 and #13 which correspond to C_{18} and C_{28} alcohols, respectively.

As might be expected, components identified in the dinoflagellate (I)E1 extract appear to be consistent with data obtained previously by in-source pyrolysis--mass spectrometry of bulk *L. polyedra* culture material (Chapter 3). In addition to free fatty acids (m/z 228, 256, 284), ions at m/z 522, 550, and 578 in the summed Py-MS spectrum of Dinoflagellate Initial (Figure 3.8) represent M^{+}-18 fragments of bound fatty acids (as diglycerides) incorporating pairs of $C_{16} + C_{14}$, $C_{16} + C_{16}$, and $C_{16} + C_{18}$ units respectively. The presence of these compounds in the initial material thus nicely supports the distribution, and abundance of fatty acids identified in the (I)E1 extract.

DISCUSSION

The present investigation represents a continuation of earlier studies (Chapters 2 and 3) and aims to further elucidate the nature and origin of the resistant outer wall enclosing the *Lingulodinium polyedra* resting cyst. Our transmission electron microscope observations of this cell covering provide the first description of resting cyst cell wall ultrastructure of a living, paleontologically-significant dinoflagellate species. Further chemical analysis (via GC/MS analysis of cupric oxide oxidation reaction products and lipid extracts, in source pyrolysis--desorption chemical ionization mass spectrometry, and solid state ^{13}C NMR spectroscopy) of *L. polyedra* resting cyst wall material togetrher with that derived from pollen standards revealed new insights into the chemical composition of these biopolymers. These data, together with results of Chapter 3 (optical microscopy, FTIR microscopy, elemental analysis, in source pyrolysis--mass spectrometry, and

175

pyrolysis--gas chromatography--mass spectroscopy), represent an unprecedented level of characterization of these resistant cell wall macromolecular substances. Interpretation of chemical and ultrastructural data in view of our previous light microscopical observations suggests a model of formation invoking internal pools of "structural precursor units" rapidly assembled into an outer wall and spines during *L. polyedra* encystment. The present study indicates that tocopherols, fatty acids, and/or aromatic amino acids could be important building blocks in the structure of the resistant biopolymer in the *L. polyedra* resting cyst wall.

Ultrastructure

To date, only a half dozen or so descriptions of dinoflagellate cyst ultrastructure exist in the literature (Bibby and Dodge, 1972; Dürr, 1979; Chapman et al., 1982; Doucette et al., 1989; Fritz et al., 1989; Gao et al., 1989; Buck et al., 1992). Although these investigations provide an important framework for the interpretation of the fine structure of cysts, the species studied have little direct bearing on those structures preserved in the fossil record. With the exception of *Scrippsiella* sp. (Gao et al., 1989) which forms a resting cyst wall of calcite, these species show little or no preservation potential. Although calcitic structures are indeed present in the fossil record, the vast majority of preserved resting cyst walls are of non-mineral (i.e. organic) composition. Published comments on the acetolysis resistance of the resting cyst wall of *Alexandrium tamarense* , the species investigated by both Doucette et al. (1989) and Fritz et al. (1989), are contradictory and difficult to evaluate. Similary, Buck et al. (1992) claim that their Antarctic dinoflagellate hypnozygotes showed some indication of having a resistant cell wall, but apparently this material does not consistently survive acetolysis. The present investigation represents the first look at the ultrastructure of thick-walled resting cysts produced by an extant species with an extensive and well known fossil record.

The scarcity of ultrastructural investigations of paleontologically relevant dinoflagellate resting cysts is largely a reflection of the difficulties encountered in applying traditional TEM methodologies to these unusual biological structures. Most workers invoke a protectional role for the resting cyst cell wall, and thus it is not surprising that these cell coverings are thick and greatly inhibit the penetration of fixatives and embedding resins. As pointed out earlier, successful TEM observation of resting cyst ultrastructure in the present study was constrained by these same problems.

Previous descriptions of living resting cysts of *L. polyedra* and closely related species at the level of the light microscope (e.g. Chapter 2) typically distinguish two components of the cell covering. A conspicuous, clear, and relatively thick layer, generally referred to as the endospore, immediately surrounds the cell cytoplasm. This is enclosed by a much thinner outer wall, spongy or fibrous in visual texture and normally bearing prominent spines. The relationship of wall layers identified in our ultrastructural observations to those described via light microscopy is straightforward: Layer 1 corresponds to the spine bearing outer wall, while Layers 2-3 comprise the endospore.

A light microscope comparison of living *L. polyedra* resting cysts to those specimens (referred to as *L. machaerophorum* in cyst-based terminology) found in the fossil record strongly suggests that only Layer 1 is ultimately preserved. This conclusion is nicely supported by the ultrastructure of fossil *L. polyedra* reported by Jux (1971); his TEM micrographs clearly illustrate specimens consisting only of the spine-bearing outer layer. Jux's description of this wall closely matches that of the present investigation and includes comments on the appressed structural elements, interstitial spaces, basal surface, and spines. One difference, however, concerns the thickness of this layer. Jux's specimens showed a more developed "spongy network" (i.e. structural elements more elaborately branched and interconnected) extending the total thickness of the wall up to ~2.5 μm. He describes this wall as consisting of two zones differing only in terms of density: an inner region showing a more compact structure, merging smoothly into an outer

region characterized by a more open network. Our specimens from laboratory culture appeared to lack a well developed outer region.

Other dinoflagellate cyst species (*Dapsilidinium* [formerly *Hystrichosphaeridium*] *simplex* and *Impletosphaeridium* sp.) studied by Jux (1971) show ultrastructural features similar to those of *L. machaerophorum*. Of special interest is a common wall architecture comprised of closely appressed and/or fused elements more or less rooted on a basal membrane. Dinoflagellate resting cyst walls recovered from the fossil record also occasionally show evidence of being constructed of fused elements; in some cases, these elements or subunits appear highly ordered into crystal-like arrays (N. Albert, personal communication). Interestingly, crystalline or semi-crystalline arrangements of structural units have also been identified as important skeletal components in the cell walls of both modern and fossil megaspores (see Hemsley et al., 1992, for illustrations, discussion, and references). These latter authors suggest that the "sporopollenin" walls of such megaspores may derive from colloidal mixtures which condense into crystalline arrays during "subtle alterations of the chemical and physical environment immediately surrounding the developing spore". Although the structural subunits comprising the *L. polyedra* resting cyst outer wall are neither regular in shape nor position, it is certainly possible to conceive of a developmental mechanism consisting of precursor structural elements which assemble into the wall and spines during encystment.

Consideration of this hypothetical mechanism of wall development invites speculation regarding the function of other elements present in the cell covering of *L. polyedra* resting cysts. For example, one specimen showed discontinuous layers locally present in the outer zone of Layer 2, and these were noted to contain small rounded masses with an electron density similar to the closely-packed elements in Layer 1. The association of these layers with the endospore inclusion bodies was also noted. Given this relationship, and the proximity of these features to the outer wall, one might interpret these as perhaps playing some role in the generation and/or transportation of precursor units.

Although this is purely speculative at present, transportation of wall elements by cytoplasmic vesicles has been previously observed during encystment of other dinoflagellate species. Fritz et al. (1989) described numerous vesicles in the peripheral cytoplasm of *Alexandrium tamarense* which occasionally fused to the inner surface of developing cyst walls; these vesicles were presumed to deposit material along the thickening wall. Another study (Chapmen et al., 1982) documented the presence of electron dense granules within cytoplasmic vesicles and their subsequent deposition on the surface of the developing *Ceratium hirundinella* cyst. Observation of similar cytoplasmic dynamics can also be found among the vegetative stages of dinoflagellate cells. One example is provided by Hansen (1989) who described the production and transportation of organic body scales from golgi cisternae to the cell surface in the unarmored species *Katodinium rotundatum*. Confirmation of the existence of this type of mechanism in the development of *L. polyedra* resting cyst walls, however, will require further ultrastructural studies of both planozygotes preparing to encyst and the various intermediates in cyst formation described in Chapter 2.

The complex ultrastructure of the preservable outer wall of *L. polyedra* resting cysts, described here and by Jux (1971), stands in sharp contrast to fine structure of preservable wall layers among the green algae. Ultrastructural examinations of chlorophycean cell walls (e.g. Atkinson et al., 1972; Puel et al., 1987; Derenne et al., 1992) have pointed out a strong (though not exclusive) correlation between the occurrence of a trilaminar sheath (TLS) and the presence of algaenan, a highly resistant wall biopolymer. In the present study, we did not see any clear evidence of a TLS associated with the preservable wall of *L. polydera* resting cysts. Examination of micrographs of other dinoflagellate resting cyst walls (provided by Jux, 1968 and later) similarly failed to disclose any sign of such a layer. It is interesting to note, however, that a TLS has been identified in the amphiesma of motile cells of some dinoflagellate species (Swift and Remson, 1970), and that this wall component (called the pellicle layer) shows resistance to

acetolysis. This finding has led some authors (e.g. Loeblich, 1970) to speculate that the

resistant resting cyst wall may derive from the pellicle. To date, however, no observations

have confirmed or disproved this hypothesis. At present, therefore, the ultrastructure of

resistant wall layers of dinoflagellate resting cysts appears fundamentally different from that

shown by the algaenan-containing layers of chlorophyte algae.

In spite of the focus of the present study on the resistant outer wall, it seems

appropriate to comment briefly on the nature of the *L. polyedra* endospore. Light

microscope observations of resting cysts produced in laboratory cultures (Chapter 2)

indicate that deposition of this wall layer occurs after the outer wall has formed. When

resting cysts of this species were isolated from natural sediments and exposed to Gram's

Iodine (according to the method of Gürr, 1966), the endospore appeared to test positive for

the presence of cellulose (unpublished data). These results are consistent with those

obtained from other resting cyst species by von Stosch (1973) and Anderson and Wall

(1978). At the level of the electron microscope, the laminated appearance of the *L.*

polyedra resting cysts endospore again appears consistent with observations of other

species; a finely laminated endospore in hypnozygotes of *Alexandrium tamarense* was

illustrated by Fritz et al. (1989).

As mentioned previously, endospore layers 2 and 3 were very similar in

appearance, yet failure of sections during microtomy seemed to consistently occur at the

interface between them. These two charateristics may point to the presence of a fixation

and/or infiltration artifact at this boundary (e.g. a penetration front) rather than a

biologically meaningful interface between discrete wall layers. Alternatively, this interface

may represent a true boundary, but one showing extraordinary effectiveness in halting the

penetration of fixatives or resins.

Finally, it is interesting to consider the cellulosic endospore in light of the

unexpected discovery of highly ordered, hexose-based polysaccharide (reminiscent of

higher plant cellulose) during Py-(DCI)MS analysis of thecal material. The degradation of

thecal plates during *L. polyedra* encystment (see Chapter 2) suggests that some of this material is resorbed by the cell and may be "recycled" into the endospore. Interestingly, the resting cyst endospore of this and several other dinoflagellate species displays a characteristic interference figure when observed under polarized light (see Chapter 2), indicating that this material may also be highly ordered.

Additional chemical characterization of resistant cell wall materials

Aromatic components. In the present investigation, alkaline CuO oxidation was employed to allow comparison of products yielded by chemical degradation to those obtained by thermal degradation (i.e. pyrolysis) in Chapter 3. CuO oxidation is a mild oxidatitive technique that hydrolyzes most ester and ether bonds and oxidatively cleaves some carbon-carbon bonds. As a result, this technique proves especially useful in the analysis of ether and ester linked polyphenolic macromolecules. Although not previously rigorously applied to algal-derived resistant materials, CuO chemolysis has been used extensively to characterize recalcitrant biopolymers such as lignin and cutin which are synthesized by higher plants (e.g. Goñi and Hedges, 1990a,b; 1992, 1993; Goñi et al., 1993). Relative to pyrolytic techniques, CuO oxidation is a more selective form of degradation and tends to give a clearer picture (although perhaps more biased) of the aromatic constituents of complex macromolecules.

To better compare the distribution of CuO products yielded by our pollen and resting cyst residues, composite mass chromatograms were constructed (Fig. 4.6) to selectively enhance peaks representing oxygenated aromatic compounds. The presence of methoxylated compounds (e.g. vanillin, vanillic acid, acetovallinone) among the pollen CuO products indicates that a portion of the aromatic polymer bears some resemblence to lignins found in other tissues of higher plants (e.g. woods, leaves). However, the high
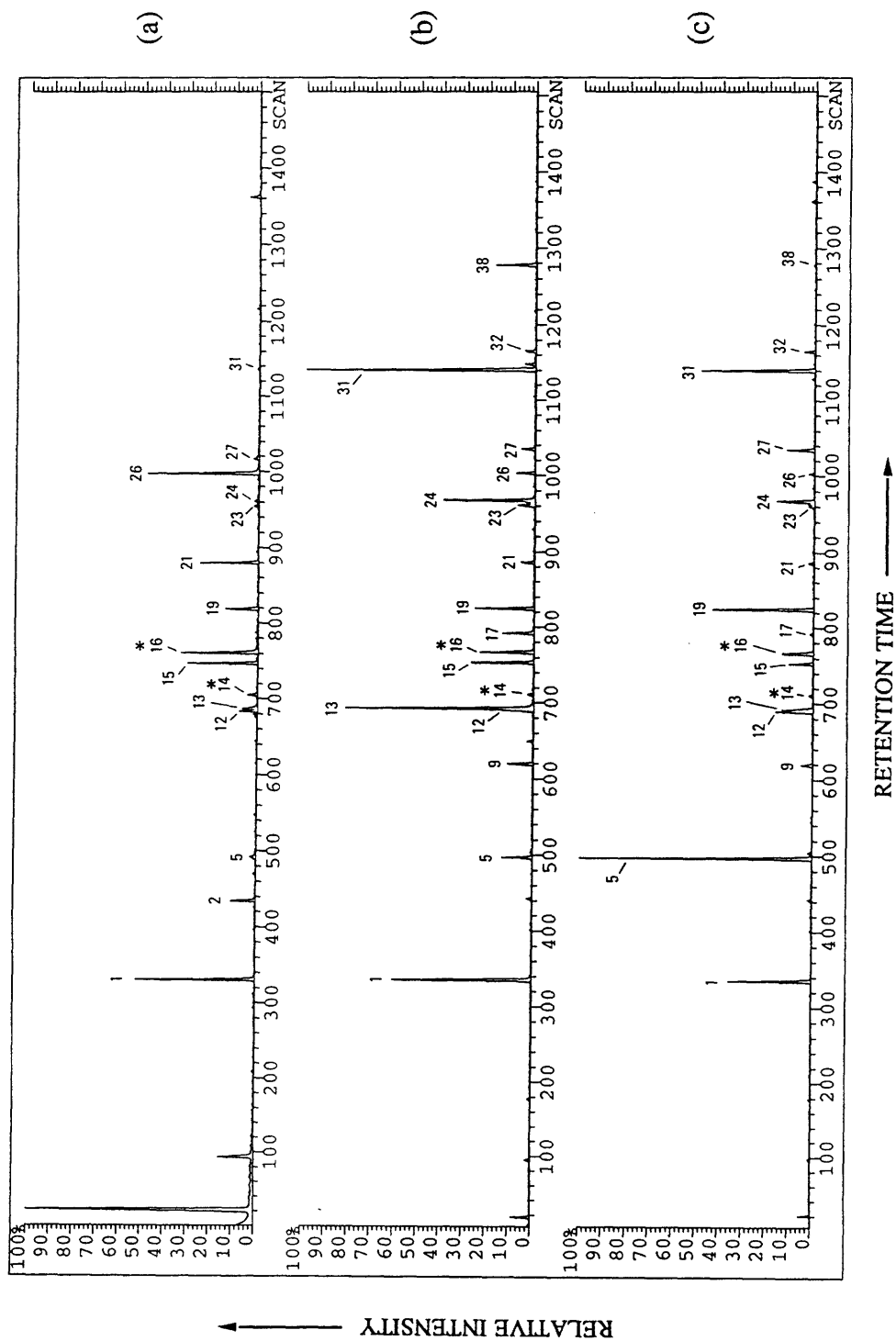
FIGURE 4.6 Partial summed (composite) mass chromatograms from GC/MS analysis of CuO oxidation products: Aromatic compounds (TMS derivatives). (a) *L. polyedra* (II)R2, (b) Juniper (I)R3, and (c) Oak (I)R3. Peak numbers correspond to compounds listed in Table 4.1. Asterisks denote internal standards.

abundance of *p*-hydroxy phenols, particularly *p*-coumaric acid, suggests that a large fraction of the aromatic components in the walls of these pollens are *not* directly related to lignin. As noted earlier, the lack of syringyl compounds in the Oak residue was also unexpected, since these products are typically conspicuous in reaction mixtures resulting from CuO analysis of angiosperm-derived materials, and serves to further distinguish the pollen resistant materials from true lignin.

In the dinoflagellate resting cyst wall material (Fig 4.6a), lignin-derived aromatic CuO components (methoxyphenols and associated aldehydes and acids) are present in only trace amounts, suggesting a further departure from a "classical" lignin structure. In addition, *p*-hydroxy phenols are significantly less abundant relative to the pollens. Instead, major phenolic products yielded by CuO oxidation of resting cyst wall material include an abundance of carboxylated phenols. Interestingly, similar carboxylated phenols have been observed among CuO oxidation products from the outer seed coats of both fossil and extant water plants (van Bergen et al., submitted). The differences in CuO products yielded by pollen and dinoflagellate materials may indicate fundamental differences in the type of linkages present in the macromolecular substances under consideration here. The presence of methoxylated phenols and *p*-hydroxylated components in the pollen CuO reaction mixtures suggests that these aromatic units are primarily ether-linked. On the other hand, the relative abundance of carboxylated phenols among resting cyst CuO products indicates that aromatic structural units in the dinoflagellate material may be largely carbon-linked, most likely directly between aromatic nucleii (as opposed to via alkyl side chains). This latter bond type would imply a more condensed structure and may, in part, be responsible for the extraordinary physical and chemical stability of the *L. polyedra* resting cyst wall biopolymer.

The aromatic CuO reaction products of both Juniper and Oak materials show a marked similarity to those generated by related chemical degradation techniques applied to other pollen materials. Schulze Osthoff and Wiermann (1987) employed saponification,

183

potash fusion, and nitrobenzene oxidation (NBO) to analyze a purified "sporopollenin" fraction derived from *Pinus mugo* pollen. These procedures yielded significant amounts of *p*-coumaric acid, *p*-hydroxybenzoic acid, vanillic acid, vanillin, *p*-hydroxybenzaldehyde, and ferulic acid as degradation products. The fact that main products yielded by nitrobenzene oxidation had a phenylpropane skeleton led these authors to conclude that the structure of *P. mugo* sporopollenin is different from that of lignin-like components. In a similar study, Herminghaus et al. (1987) analyzed resistant wall material isolated from *Corylus avellana* pollen. Degradation of this residue by NBO yielded a suite of main products identical to those listed by Schulze Osthoff and Wiermann (1987). Ultimately, *p*-coumaric acid was identified as the main component of *C. avellana* sporopollenin, and these authors concluded that phenolic compounds are integral constituents of this material. A similar conclusion was reached by Wehling et al. (1989) after subjecting *P. mugo* sporopollenin to both saponification and aluminum iodide (AlI_3) degradation. Both techniques yielded *p*-coumaric acid as the main degradation product, and further analysis suggested that this component might be bound by ether linkages. Interestingly, as a control experiment, these authors also analyzed "synthetic sporopollenin" (a carotenoid polymer) using AlI_3 degradation and found that neither *p*-coumaric acid nor any other phenolic substances could be detected. Overall, chemolysis of pollen materials in both the present study and other investigations seems to confirm a significant aromaticity in the pollen wall structure that is different from that of either lignin or carotenoid-based biopolymers.

Aliphatic components. The distribution of di-acid CuO products yielded by both dinoflagellate resting cyst and pollen residues is illustrated by the composite mass chromatograms shown in Figure 4.7. These types of carboxylic acids are thought to derive from oxidation of aliphatic side chains (perhaps localized at sites of ether cross-linking) during CuO degradation. Dicarboxylic acids have been observed as CuO products of aliphatic rich sediments (Hedges, 1975), kerogens (Goñi, personal communication),
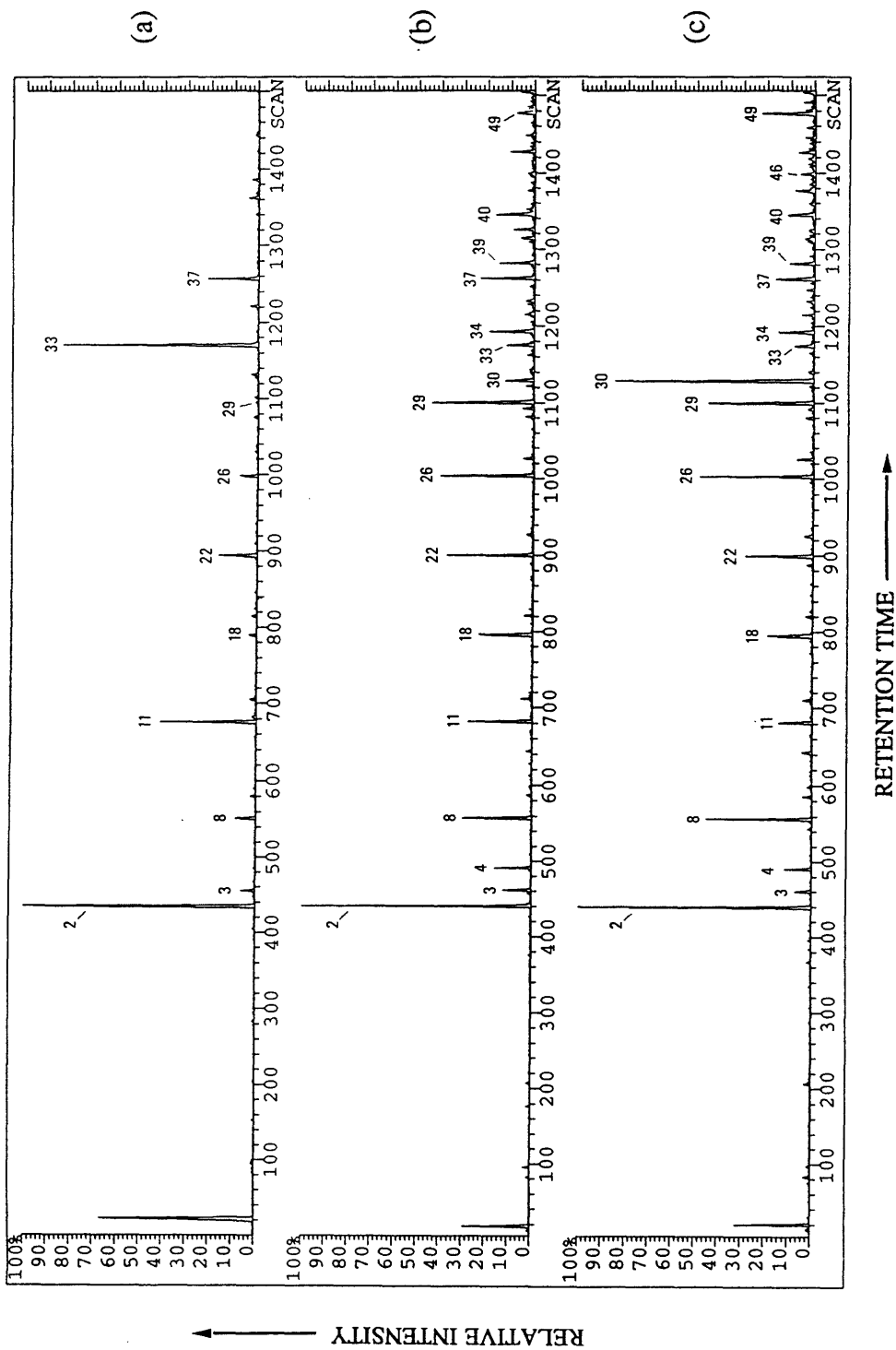
184

FIGURE 4.7 Partial summed (composite) mass chromatograms from GC/MS analysis of CuO oxidation products: Di-acids (TMS derivatives). (a) *L. polyedra* (II)R2, (b) Juniper (I)R3, and (c) Oak (I)R3. Peak numbers correspond to compounds listed in Table 4.1.

185

and plant cuticles (Goñi, 1990a).

Figure 4.7a nicely illustrates the marked truncation of the dinoflagellate CuO di-acid series (extending only up to C_{10}) mentioned earlier. The predominance of shorter chain di-acids among CuO products suggests that the *L. polyedra* resting cyst wall biopolymer is not likely to include extended polymethylenic chains as significant structural components. These results are consistent with those obtained by Py-GC/MS analysis of resting cyst wall material in Chapter 3. In contrast to the dinoflagellate data, both pollen chromatograms (Figs. 4.7b & c) show a continuous di-acid series extending to at least C_{12}, suggesting the presence of longer aliphatic (polymethylenic?) elements in the pollen wall biopolymers. Although these results are consistent with pyrolysis data for the Juniper pollen, this agreement is less apparent for the Oak residue which did not show significant aliphatic components with extended chain lengths in the pyrolyzate.

Interesting in this regard, however, was the occurrence of a suite of *n*-alkanes among the Oak CuO products. The origin of these compounds is unclear. Since bound *n*-alkanes would be released by CuO oxidation as carboxylic acids, these compounds may represent free, yet very tightly trapped, elements of the pollen wall. Interestingly, reexamination of Oak Py-GC/MS mass chromatograms generated to enhance peaks representing *n*-hydrocarbons (Chapter 3) shows the very weak presence of a homologous series of *n*-alkanes ranging from C_{21}-C_{31}. This may be a manifestation of the *n*-alkane series (C_{22}-C_{29}) identified after cupric oxide oxidation. In both CuO and Py-GC/MS analyses, however, corresponding *n*-alkenes could not be detected, suggesting that their saturated counterparts were not derived from pyrolytic degradation of a biopolymer.

The presence of hydroxylated C_{16} di-acids among pollen CuO degradation products may indicate some structural similarity between pollen wall materials and cutin, although the exact relationship is not clear. The monohydroxylated C_{16} di-acids identified in both Juniper and Oak CuO chromatograms are significant, but not major CuO products of cutin. On the other hand, the major OH C_{16} di-acid (dihydroxy hexadecanedioic acid)

186

yielded by CuO degradation of typical cutin is absent from both pollen chromatograms. One interpretation of these differences might invoke formation of the pollen monohydroxy C_{16} di-acids via cleavage of mid-chain ether linkages present within an aliphatic network, a mechanism not likely to be significant during degradation of cutin biopolymers. Shorter chain dihydroxy di-acids (C_{10} and C_{11}) are present in both pollen and dinoflagellate CuO reaction mixtures and may also represent degradation products of aliphatic components characterized by some degree of mid-chain ether bridging.

In the present study, solid state ^{13}C NMR spectroscopy was employed to further assess the relative proportion of aromatic vs. aliphatic components in resting cyst and pollen residues. Unfortunately, while informative spectra were obtained from both pollen materials, the amount of dinoflagellate resting cyst wall residue available for analysis fell below the detection limits of the instrument. Also, it is important to emphasize that, due to restrictions imposed by the amounts of material available for analysis, the pollen residues subjected to ^{13}C NMR analysis were obtained by slightly different isolation techniques (Batch I vs. Batch II; see methods). As a result, some caution needs to be exercised in the discussion of the spectra. Nevertheless, these data provide an interesting framework for the interpretation of other chemical information obtained both previously (Chapter 3) and herein.

Although the large aliphatic resonance in the Juniper ^{13}C NMR spectrum appeared consistent with our earlier data, the presence of a similar, very prominent peak in the Oak spectrum was entirely unexpected. Aside from the elemental analysis and FTIR data, all of our previous analyses seemed to indicate that aliphatic components played, at best, only a minor role in the basic structure of the Oak pollen wall. The NMR spectrum of Oak (I)R3, however, points to an aliphaticity roughly equivalent to that of the Juniper material.

If aliphatic elements are indeed significantly present in the Oak residue, one is left to consider (1) the nature of this component, and (2) why it was not revealed by earlier analyses which exposed aliphatic components in the Juniper pollen material. As to the

187

source of the aliphatic material, one hypothesis might call upon the presence of residual fatty acids in the Oak (I)R3 as was indicated by Py-MS analysis in Chapter 3. If, as speculated above, un-bound but physically trapped n-alkanes are part of the Oak pollen wall residue, these would also make a contribution to the aliphatic NMR resonance. These hypotheses, however, do not properly explain why most other techniques, particularly those involving pyrolysis, fail to expose any clear indication of significant aliphatic structure. Py-GC/MS analysis of Oak (I)R3 does show a homologous series of n-alkanes / n-alkenes, but this is truncated (up to C_{17}) compared to the Juniper series (up to C_{28}) and these compounds do not seem sufficiently abundant to make an important contribution to the aliphatic NMR peak. The existence of long aliphatic chains cross-linked to the point where they resist pyrolitic degradation is unlikely, given our earlier attempts at exposing such networks by systematically increasing the rigorousness of pyrolysis (Chapter 3). A final hypothesis might invoke an abundance of very short ($< C_4$) carbon chains which would elute very early during chromatographic separation, and hence would be incompletely resolved.

The difficulties encountered in reconciling the differing levels of Oak pollen wall aliphaticity predicted by pyrolysis and ^{13}C NMR spectroscopy point out the need for caution when drawing inferences regarding nature of the *L. polyedra* resting cyst wall biopolymer. Resting cyst wall residues did not yield significant aliphatic products during pyrolysis. Alkane/alkene doublets were identified up to C_{12} (a more restricted carbon number range than either pollens) but, above this, the only aliphatic pyrolysis product detected was prist-1-ene (Chapter 3). As just demonstrated for the Oak pollen wall material, however, these results do not rule out the possibility that aliphatic components may play an important structural role in the *L. polyedra* resting cyst wall, especially given the FTIR and elemental analysis data presented in Chapter 3.

Other resistant cell wall biopolymers characterized by solid state ^{13}C NMR spectrometry include those isolated from species in the chlorophycean genera

Botryococcus (Largeau et al., 1984; Kadouri et al., 1988; Zelibor et al., 1988; Derenne et al., 1989), *Chlorella* (Guilford et al., 1988; Zelibor et al., 1988; Derenne et al., 1992), *Dunaliella* (Zelibor et al., 1988), *Nanochlorum* (Derenne et al., 1992), and *Scenedesmus* (Zelibor et al., 1988; Derenne et al., 1991). In addition, ^{13}C NMR spectra of *Lycopodium* spore wall material and that derived from several pollen types (pine, wheat, ragweed) are provided by Guilford et al. (1988). Interestingly, all spectra referred to here are dominated by the aliphatic resonance at about 30 ppm. As might be expected, our Juniper and Oak spectra correspond most closely with those representing pollen of higher plants. These tend to be distinguished from chlorophyte cell wall ^{13}C NMR spectra by showing broader resonances (particularly evident at ~30 ppm) and higher intensity in resonances due to oxygenated carbons (Guilford et al., 1988).

Cellular materials available during assembly of the L. polyedra *resting cyst wall*

Any consideration of potential precursor materials involved in the assembly of the resistant outer wall of the *Lingulodinium polyedra* resting cyst requires awareness of the pool of cellular materials available for this construction. To this end, we first examined unprocessed dinoflagellate culture residue using in-source Py-(DCI)MS, and then analyzed the corresponding (I)E1 lipid extract by GC/MS. As pointed out earlier, the former procedure showed that bulk culture is dominated by the presence of a highly ordered (microcrystalline?) cellulose. This discovery is significant, as this type of polysaccharide is normally thought to be restricted to terrestrial plant tissues.

Major components identified in the dinoflagellate extract were the even numbered (C_{14}-C_{24}) fatty acids, a suite of sterols, two (C_{18} and C_{28}) alcohols, and a series of tocopherols. The abundance of these latter compounds is provocative given the possible role of tocopherols as structural components in the *L. polyedra* resting cyst wall (see Chapter 3). This connection, based on the presence of prist-1-ene among products

189

generated by pyrolysis of *L. polyedra* resting cyst material, does not, however, rule out the involvement of other precursors such as sterols and/or fatty acids. Indeed, the prominence of the 30 ppm peak in ^{13}C NMR spectra of several resistant cell wall residues led Guilford et al. (1988) to conclude that these sporopollenin-like materials were largely based on fatty acid precursors.

A model of outer wall formation during L. polyedra *encystment*

The ultrastructural and chemical data reported here, when considered in light of the observations on morphological development presented in Chapter 2, allow the formulation of a hypothetical model of *L. polyedra* encystment. As described in Chapter 2, the spine-bearing outer wall of the L. polyedra resting cyst is rapidly formed (~10 min.) in a zone fully enclosed by an expanding balloon-like membrane. The extremely short duration of this event suggests that morphogenesis of the resting cyst wall represents an assembly phase rather than a phase involving synthesis *de novo*. As noted above, ultrastructural observations indicate that the spine-bearing outer wall appears to be composed largely of closely appressed structural subunits. If this is indeed the case, precursor subunits probably form prior to the assembly phase and are likely to be synthesized and accummulated in the maturing planozygote.

The chemical investigations carried out both in the present study and in Chapter 3 suggest that precursor units may incorporate tocopherols, sterols, and/or fatty acids. Another possibility, given the aromaticity predicted by CuO analysis, is some contribution by aromatic amino acids (phenylalanine, tyrosine, and tryptophan) in an analogous fashion to lignin biosynthesis. Structural precursor units may form in or be transported to the periphery of developing cyst wall. As described in Chapter 2, the spherical portion of the resting cyst wall appears to be assembled first; precursor units destined for spine formation

190

are then extruded into globules on the cyst surface and/or into the medium filling the widening interstice between cytoplasm and external membrane.

The rapid final assembly of structural subunits suggests that the reaction might be free-radical catalyzed. If this is the case, the selectivity of the process, and hence the uniformity of the resistant material, may be less well ordered relative to biopolymers formed under more controlled conditions (e.g. enzyme-mediated reactions). One consequence of a rapid, free-radical mechanism, therefore, might be some degree of heterogeneity in the composition of the cyst wall. This heterogeneity may, in part, be responsible for the biological resistance of this material.

Borrowing from the hypothesis put forward to explain the ultrastructure of megaspore walls (Hemsely et al., 1992), resting cyst wall precursor units may polymerize from a colloidal mixture present in the globules and/or expansion zone. Deposition of the cyst wall may be controlled, at least in part, by chemical alterations within the expansion zone. Evidence to support this latter mechanism may be found in the fact that (1) both terminal process globules and free floating globules show simultaneous modification during the completion of spine formation, and (2) all wall building events are aborted if the expanding outer membrane is prematurely ruptured.

CONCLUSIONS

To briefly summarize the results of our extensive chemical characterization of the resistant biopolymer in the outermost cell wall of *L. polyedra* resting cysts:

1. Both thermal (pyrolysis) and chemical (CuO oxidation) degradative techniques yielded suites of products consistent with a macromolecular substance composed chiefly of aromatic (phenolic) components. The relative abundance of carboxylated phenols among resting cyst CuO oxidation products indicates that aromatic structural units in the

191

dinoflagellate material may be largely carbon-carbon linked, probably directly via aromatic nuclei. Such a "condensed" arrangement may explain, at least in part, the extraordinary resistance of the *L. polyedra* resting cyst cell wall.

2. Although some short chain carboxylic acids are generated during CuO oxidation, there is little evidence obtained by degradative techniques to suggest the significant presence of extended polymethylenic chains in this macromolecular substance.

3. Lipid analysis of *L. polyedra* culture extract revealed a series of even-carbon-numbered fatty acids (C_{14} - C_{24}), as well as sterols (including dinosterol and cholesterol), and a full suite of tocopherols. These compounds, particularly the latter (in light of the identification of prist-1-ene as a principal pyrolysis product), are present during construction of the resistant outer wall of the resting cyst, and could function as precursors to this material.

4. Using pyrolysis and CuO oxidation techniques, the resistant biopolymer present in the outer wall of *L. polyedra* resting cysts can be clearly distinguished from that in the pollen cell walls examined in this study. In addition, no convincing evidence for a carotenoid-based structure (i.e. traditionally defined "sporopollenin") was obtained during analysis of either dinoflagellate or pollen materials. Furthermore, the resistant biopolymer isolated from *L polyedra* resting cyst walls is fundamentally different from "algaenan", the highly aliphatic resistant substance reported to comprise the cell walls of many green algae. Together, these results support the use of "dinosporin" (see Fensome et al., 1993) as a term to distinguish the dinoflagellate resting cyst wall material from other resistant cell wall biopolymers.

REFERENCES

Anderson, D. M., and Wall, D., 1978. Potential importance of benthic cysts of *Gonyaulax tamarensis* and *G. excavata* in initiating toxic dinoflagellate blooms. *Journal of Phycology*, Vol. 14, No. 2, p. 224-234.

Atkinson, A. W., Jr., Gunning, B. E. S., and John, P. C. L., 1972. Sporopollenin in the cell wall of *Chlorella* and other algae: Ultrastructure, chemistry, and incorporation of ^{14}C acetate, studied in synchronous cultures. *Planta*, Vol. 107, No. 1, p. 1-32.

Bibby, B. T., and Dodge, J. D., 1972. The encystment of a freshwater dinoflagellate: A light and electron microscopical study. *British Phycological Journal*, Vol. 7, No. 1, p. 85-100.

Brooks, J., and Shaw, G., 1978. Sporopollenin: A review of its chemistry, palaeochemistry and geochemistry. *Grana*, Vol. 17, p. 91-97.

Buck, K. R., Bolt, P. A., Bentham, W. N., and Garrison, D. L., 1992. A dinoflagellate cyst from Antarctic sea ice. *Journal of Phycology*, Vol. 28, No. 1, p. 15-18.

Bujak, J. P., and Davies, E. H., 1983. *Modern and Fossil Peridiniineae*. AASP Contribution Series Number 13. American Association of Stratigraphic Palynologists Foundation. 203 p.

Burczyk, J. and Dworzanski, J., 1988. Comparison of sporopollenin-like algal resistant polymer from cell wall of *Botryococcus*, *Scenedesmus* and *Lycopodium clavatum* by GC-pyrolysis. *Phytochemistry*, Vol. 27, No. 7, p. 2151-2153.

Chaloner, W. G. and Orbell, G., 1971. A palaeobiological definition of sporopollenin. *In* Brooks, J., Grant, P. R., Muir, M., van Gijzel, P., and Shaw, G., (eds.), *Sporopollenin*, Proceedings of a symposium held at the Geology Department, Imperial College, London, 23-25 September, 1970, Academic Press, London. p. 273-294.

Chapman, D. V., Dodge, J. D., and Heaney, S. I., 1982. Cyst formation in the freshwater dinoflagellate *Ceratium hirundinella* (Dinophyceae). *Journal of Phycology*, Vol. 18, No. 1, p. 121-129.

Correia, M., 1971. Diagenesis of sporopollenin and other comparable organic substances: Application to hydrocarbon research. *In* Brooks, J., Grant, P. R., Muir, M., van Gijzel, P., and Shaw, G., (eds.), *Sporopollenin*, Proceedings of a symposium held at the Geology Department, Imperial College, London, 23-25 September, 1970, Academic Press, London. p. 569-620.

Derenne, S., Largeau, C., Casadevall, E., and Berkaloff, C., 1989. Occurrence of a resistant biopolymer in the *L* race of *Botryococcus braunii*. *Phytochemistry*, Vol. 28, No. 4, p. 1137-1142.

Derenne, S., Largeau, C., Casadevall, E., and Sellier, N., 1990. Direct relationship between the resistant biopolymer and the tetraterpenic hydrocarbon in the lycopadiene race of *Botryococcus braunii*. *Phytochemistry*, Vol. 29, No. 7, p. 2187-2192.

Derenne, S., Largeau, C., Casadevall, E., Berkaloff, C., and Rousseau, B., 1991. Chemical evidence of kerogen formation in source rocks and oil shales via selective preservation of thin resistant outer walls of microalgae: Origin of ultralaminae. *Geochimica et Cosmochimica Acta*, Vol. 55, No. 4, p. 1041-1050.

Derenne, S., Largeau, C., Berkaloff, C., Rousseau, B., Wilhelm, C., and Hatcher, P. G., 1992. Non-hydrolysable macromolecular constituents from outer walls of *Chlorella fusca* and *Nanochlorum eucaryotum*. *Phytochemistry*, Vol. 31, No. 6, p. 1923-1929.

Doucette, G. J., Cembella, A. D., and Boyer, G. L., 1989. Cyst formation in the red tide dinoflagellate *Alexandrium tamarense* (Dinophyceae): Effects of iron stress. *Journal of Phycology*, Vol. 25, No. 4, p. 721-731.

Dürr, G., 1979. Elektronenmikroskopische untersuchungen am panzer von dinoflagellaten III. Die zyste von *Peridinium cinctum*. *Archives für Protistenkunde*, Vol. 122, Nos. 1 & 2, p. 121-139.

Eisenack, A., 1963. Hystrichosphären. *Biological Reviews of the Cambridge Philosophical Society*, Vol. 38, No. 1, p. 107-139.

Evitt, W. R., 1961. Observations on the morphology of fossil dinoflagellates. *Micropaleontology*, Vol. 7, No. 4, p. 385-420.

Evitt, W. R., 1985. *Sporopollenin Dinoflagellate Cysts: Their Morphology and Interpretation*. American Association of Stratigraphic Palynologists Foundation. 333 p.

Fensome, R. A, Taylor, F. J. R., Norris, G., Sarjeant, W. A. S., Wharton, D. I., and Williams, G. L., 1993. *A Classification of Living and Fossil Dinoflagellates*. Micropaleontology, Special Publication Number 7. Sheridan Press, Hanover, Pennsylvania. 351 p.

Fritz, L., Anderson, D. M., and Triemer, R. E., 1989. Ultrastructural aspects of sexual reproduction in the red tide dinoflagellate *Gonyaulax tamarensis*. *Journal of Phycology*, Vol. 25, No. 1, p. 95-107.

Gao Xiaoping, Dodge, J. D., and Lewis, J., 1989. An ultrastructural study of planozygotes and encystment of a marine dinoflagellate, *Scrippsiella* sp. *British Phycological Journal*, Vol. 24, No. 2, p. 153-165.

Geisert, M., Rose, T., Bauer, W., and Zahn, R. K., 1987. Occurrence of carotenoids and sporopollenin in *Nanochlorum eucaryotum* a novel marine alga with unusual characteristics. *BioSystems*, Vol. 20, No. 2, p. 133-142.

Goñi, M. A., and Hedges, J. I., 1990a. Cutin-derived CuO reaction products from purified cuticles and tree leaves. *Geochimica et Cosmochimica Acta*, Vol. 54, No. 11, p. 3065-3072.

Goñi, M. A., and Hedges, J. I., 1990b. The diagenetic behavior of cutin acids in buried conifer needles and sediments from a coastal marine environment. *Geochimica et Cosmochimica Acta*, Vol. 54, No. 11, p. 3083-3093.

Goñi, M. A., and Hedges, J. I., 1992. Lignin dimers: Structures, distribution, and potential geochemical applications. *Geochimica et Cosmochimica Acta*, Vol. 56, No. 11, p. 4025-4043.

Goñi, M. A., Nelson, B., Blanchette, R. A., and Hedges, J. I., 1993. Fungal degradation of wood lignins: Geochemical perspectives from CuO-derived phenolic dimers and monomers. *Geochimica et Cosmochimica Acta*, Vol. 57, No. 16, p. 3985-4002.

Goodman, D. K., 1987. Dinoflagellate cysts in ancient and modern sediments. *In* Taylor, F. J. R., (ed.), *The Biology of Dinoflagellates*, Botanical Monographs, Vol. 21, Blackwell Scientific Publishers, Oxford. p. 649-722.

Goth, K., de Leeuw, J. W., Püttmann, W., and Tegelaar, E. W., 1988. Origin of Messel Oil Shale kerogen. *Nature*, Vol. 339, No. 6201, p. 759-761.

Guilford, W. J., Schneider, D. M., Labovitz, J., and Opella, S. J., 1988. High resolution solid state ^{13}C NMR spectroscopy of sporopollenins from different plant taxa. *Plant Physiology*, Vol. 86, No. 1, p. 134-136.

Gurr, E., 1966. *The Rational Use of Dyes in Biology*. The Williams and Wilkins Co., Baltimore, Maryland. 422 p.

Hansen, G., 1989. Ultrastructure and morphogenesis of scales in *Katodinium rotundatum* (Lohmann) Loeblich (Dinophyceae). *Phycologia*, Vol. 28, No. 3, p. 385-394.

Hedges, J. I., 1975. *Lignin compounds as indicators of terrestrial organic matter in marine sediments*. Ph.D. Dissertation, University of Texas at Austin, Austin, TX.

Hatcher, P. G., 1988. Dipolar-dephasing ^{13}C NMR studies of decomposed wood and coalified xylem tissue: Evidence for chemical structural changes associated with defunctionalization of lignin structural units during coalification. *Energy and Fuels*, Vol. 2, No. 1, p. 40-58.

Hedges, J. I., and Ertel, J. R., 1982. Characterization of lignin by gas capillary chromatography of cupric oxide oxidation products. *Analytical Chemistry*, Vol. 54, No. 2, p. 174-178.

Hemsley, A. R., and Scott, A. C., 1991. The occurrence and significance of ultrastructure in fossil spores. *Microscopy and Analysis*, Issue 22, 3 p.

Hemsley, A. R., Collinson, M. E., and Brain, A. P. R., 1992. Colloidal crystal-like structure of sporopollenin in the megaspore walls of Recent *Selaginella* and similar fossil spores. *Botanical Journal of the Linnean Society*, Vol. 108, p. 307-320.

Herminghaus, S., Gubatz, S., Arendt, S., and Wiermann, R., 1988. The occurrence of phenols as degradation products of natural sporopollenin--a comparison with "synthetic sporopollenin". *Zeitschrift für Naturforschung*, Vol. 43c, No. 7/8, p. 491-500.

Jux, U., 1968a. Über den feinbau der wandung bei *Cordosphaeridium inoides* (Klump 1953). *Palaeontographica*, Abt. B, Vol. 122, p. 48-54.

Jux, U., 1968b. Über den feinbau der wandung bei *Hystrichosphaera bentori* Rossignol. *Palaeontographica*, Abt. B, Vol. 123, p. 147-152.

Jux, U., 1971. Über den feinbau der wandungen einiger Tertiärer dinophyceen-zysten und achritarcha *Hystichosphaeridium, Impletosphaeridium, Lingulodinium*. *Palaeontographica*, Abt. B, Vol. 132, p. 165-174.

Jux, U., 1976. Über den feinbau der wandungen bei *Operculodinium centrocarpum* (Deflandre and Cookson) Wall 1967 und *Bitectatodinium tepikiense* Wilson 1973. *Palaeontographica*, Abt. B, Vol. 155, p. 149-156.

Jux, U., 1980. Über den feinbau der wandung bei *Oligosphaeridium abaculum* Davey 1979. *Palaeontographica*, Abt. B, Vol. 174, p. 1-6.

Kadouri, A., Derenne, S., Largeau, C., Casadevall, E., and Berkaloff, C., 1988. Resistant biopolymer in the outer walls of *Botryococcus braunii, B* race. *Phytochemistry*, Vol. 27, No. 2, p. 551-557.

Kofoid, C. A., 1911. Dinoflagellata of the San Diego Region, IV. The genus *Gonyaulax*, with notes on its skeletal morphology and a discussion of its generic and specific characters. *University of California Publications in Zoology*, Vol. 8, No. 4, p. 187-286.

Largeau, C., Casadevall, E., Kadouri, A., and Metzger, P., 1984. Formation of *Botryococcus*-derived kerogens--Comparative study of immature torbanites and of the extant alga *Botryococcus braunii*. *Organic Geochemistry*, Vol. 6, p. 327-332.

Largeau, C., Derenne, S., Casadevall, E., Kadouri, A., and Sellier, N., 1985. Pyrolysis of immature Torbanite and of the resistant biopolymer (PRB A) isolated from the extant alga *Botryococcus braunii*. Mechanism of formation and structure of Torbanite. *Organic Geochemistry*, Vol. 10, No. 4-6, p. 1023-1032.

Loeblich, A. R., III, 1970. The amphiesma or dinoflagellate cell covering. *Proceedings of the North American Paleontological Convention, Chicago, September 1969*, (Allen Press, Lawrence, Kansas), Vol. 2, Part G, p. 867-929.

Pfiester, L. A., 1989. Dinoflagellate sexuality. *International Reviews of Cytology*, Vol. 114, p. 249-272.

Pfiester, L. A. and Anderson, D. M., 1987. Dinoflagellate Reproduction. *In* Taylor, F. J. R., (ed.), *The Biology of Dinoflagellates*, Botanical Monographs, Vol. 21, Blackwell Scientific Publishers, Oxford. p. 611-648.

Pouwels, A. D., Eijkel, G. B., Arisz, P. W., and Boon, J. J., 1989. Evidence for oligomers in pyrolysates of microcrystalline cellulose. *Journal of Analytical and Applied Pyrolysis*, Vol. 15, p. 71-75.

Puel, F., Largeau, C., and Giraud, G., 1987. Occurrence of a resistant biopolymer in the outer walls of the parasitic alga *Prototheca wickerhamii* (Chlorococcales): Ultrastructure and chemical studies. *Journal of Phycology*, Vol. 23, No.4, p. 649-656.

Sarjeant, W. A. S., 1986. *Review of* Evitt, W. R., 1985, *Sporopollenin Dinoflagellate Cysts: Their Morphology and Interpretation. Micropaleontology*, Vol. 32, No. 3, p. 282-285.

Schultze Osthoff, K. and Weirmann, R., 1987. Phenols as integrated compounds of sporopollenin from *Pinus* pollen. *Journal of Plant Physiology*, Vol. 131, No. 1/2, p. 5-15.

Spurr, A. R., 1969. A low viscosity epoxy embedding medium for electron microscopy. *Journal of Ultrastructural Research*, Vol. 26, No. 1-2, p. 31-43.

Swift, E., and Remson, C. C., 1970. The cell wall of *Pyrocystis* spp. (Dinococcales). *Journal of Phycology*, Vol. 6, No.1, p. 79-86.

Taylor, F. J. R., (ed.), 1987. *The Biology of Dinoflagellates*. Botanical Monographs, Vol. 21. Blackwell Scientific Publications, Oxford. 785 p.

van Bergen, P. F., Goñi, M. A., Collinson, M. E., Barrie, P. J., and de Leeuw, J. W., (submitted). Chemical and microscopical characterization of outer seed coats of fossil and extant water plants.

von Stosch, H. A., 1973. Observations on vegetative reproduction and sexual life cycles of two freshwater dinoflagellates, *Gymnodinium psuedopalustre* Schiller and *Woloszynskia apiculata* sp. nov. British Phycological Journal, Vol. 8, No. 2, p. 105-134.

Wehling, K., Niester, C., Boon, J. J., Willemse, M. T. M., and Wiermann, R., 1989. *p*-Coumaric acid--a monomer in the sporopollenin skeleton. *Planta*, Vol. 179, No. 3, p. 376-380.

Williams, G. L., and Bujak, J. P., 1985. Mesozoic and Cenozoic dinoflagellates. *In* Bolli, H. M., Saunders, J. B., and Perch-Nielsen, K., (eds.), *Plankton Stratigraphy*, Cambridge Earth Science Series, Cambridge University Press, Cambridge. p. 847-964.

Williams, G. L., Stover, L. E., and Kidson, E. J., 1993. Morphology and stratigraphic ranges of selected Mesozoic-Cenozoic dinoflagellate taxa in the northern hemisphere. *Geological Survey of Canada Paper 92-10*, p. 1-137.

Zelibor, J. L., Jr., Romankiw, L., Hatcher, P. G., and Colwell, R. R., 1988. Comparative analysis of the chemical composition of mixed and pure cultures of green algae and their decomposed residues by 13C nuclear magnetic resonance spectroscopy. *Applied and Environmental Microbiology*, Vol. 54, No. 4, p. 1051-1060.

PLATE 4.1

Transmission electron micrographs illustrating the ultrastructure of the *L. polyedra* resting cyst cell wall. Scale bars in Figures 1, 3, and 4 = 1 μm; scale bar in Figure 2 = 0.5 μm.

Figure 1.　　General view of resting cyst wall. Arrowhead points to region of the wall showing clearest definition of the 3 layers described in the text. Layer 1= outermost layer, dark colored, elaborately sculptured; Layer 2 = middle layer, lighter in color, thickest portion of wall; Layer 3 = innermost wall, similar in color to Layer 2, but significantly thinner. Near arrowhead, inner and outer zones of Layer 2 very faintly defined by change in color (inner zone slightly darker). Two additional features occasionally found in Layer 2 are both illustrated here. Below the arrowhead (lower left of photo), the outer zone of Layer 2 contains a discontinuous layer, generally lighter in color, but showing darker-colored elements internally. Above and to the right of the arrowhead, a prominent endospore inclusion body (EIB) is present within Layer 2. Asterisk denotes a starch body in the cytoplasm.

Figure 2.　　Portion of resting cyst wall at higher magnification (scale bar = 0.5 μm), with individual layers labeled. Transition from inner to outer zone of Layer 2 occurs at point marked by "L2" symbol. Outer zone of Layer 2 includes the discontinuous lighter-colored layer described in text. Note: (1) the "fused element" structure of the outer wall, and (2) varying definition of endospore laminae shown by Layers 2 and 3.

Figure 3.　　Endospore Inclusion Body. Note internal structure, including suggestion of fibrous mass near the upper boundary (~12 o' clock). Multiple, weakly defined lighter-colored layers are located between EIB and outer wall. Presence of EIB causes inward bulging of endospore; note that laminae in Layer 2 (inner zone) follow contour of the EIB. Also note structural elements of Layer 1 and the network of interstitial channels defined by these masses.

Figure 4.　　Portion of spine. Spine wall similar in electron density to the outer wall described above.

198

199
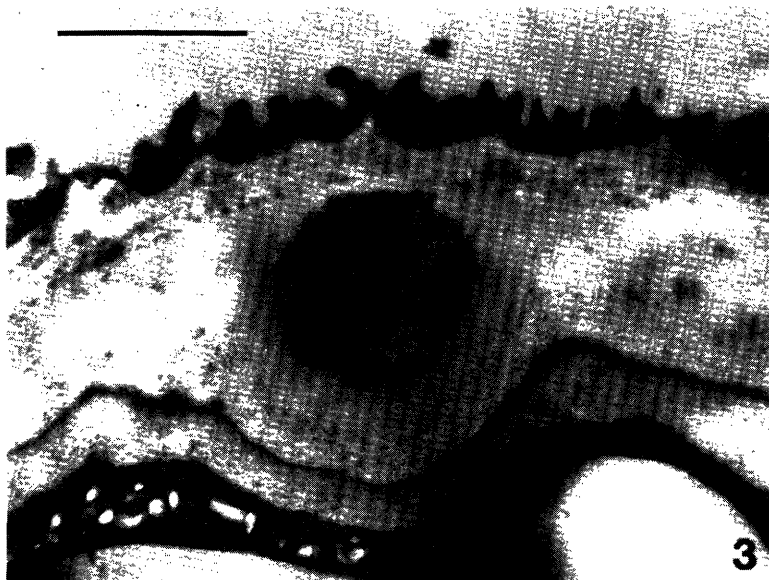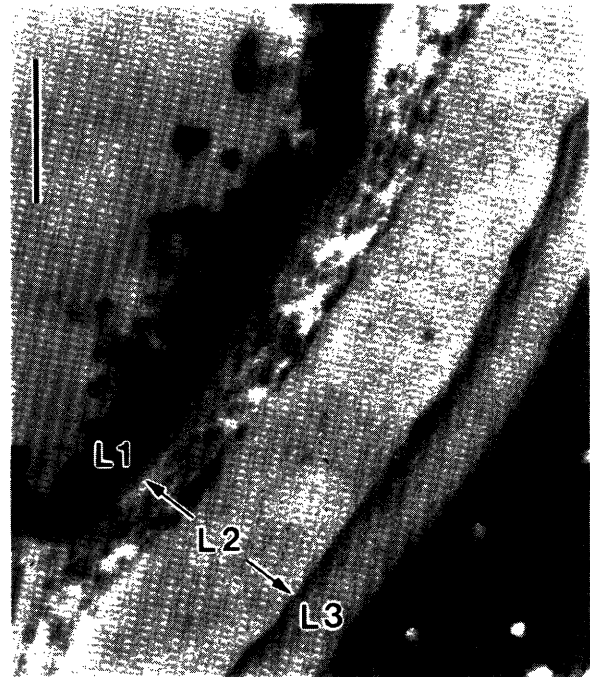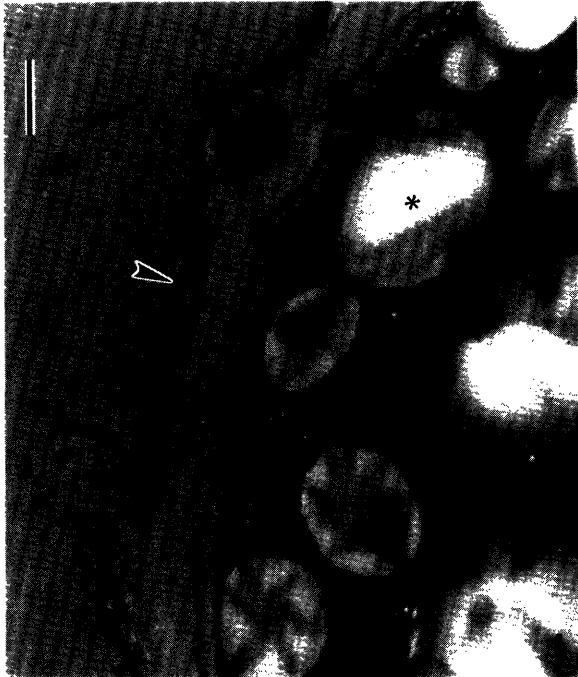
CHAPTER 5

Conclusions and Future Work

CONCLUSIONS

The main conclusions of this dissertation are outlined in the following paragraphs which are organized according to the three themes presented in the introduction: morphological development, ultrastructure, and chemical composition.

The description of *Lingulodinium polyedra* encystment recorded in Chapter 2 represents a major step forward in our understanding of both the paleontology and biology of dinoflagellates. Although resting cyst formation has been reported in other species, this thesis documents for the first time the morphological development of resting cysts having "fossilizable", morphologically complex cell walls. In laboratory cultures of *L. polyedra*, resting cyst formation is an extremely rapid phenomenon; the transition from thecate, actively swimming planozygote to spine-bearing, morphologically mature hypnozygote occurs within 10-20 minutes. The basic mechanism consists of dramatic cell expansion resulting from the widening of an interstice between the planozygotic cytoplasm and a balloon-like membrane external to the theca. Key morphological events in the development of the distinctive *L. polyedra* resting cyst cell covering occur within this interstice. These include early dissociation and outward migration of the theca, formation of the resistant endophragm, and growth of spines from globules on the surface of the cytoplasm.

The direct observation of these developmental events has shed much light on several issues regarding resting cyst morphogenesis. First, growth of *L. polyedra* resting cyst spines is clearly centrifugal (i.e. growing radially outward). Although not necessarily representative of spine growth in all species, this mode of formation provides a useful preliminary framework for interpreting some of the "histrichosphaerid" morphologies present in the fossil record. Second, in this species at least, the theca plays no direct role in influencing the morphology of spines. Finally, considerable variation in resting cyst morphology, particularly in relation to the length and distribution of spines, is possible within one biologically-defined species. This last point has considerable significance for

cyst-based (i.e. paleontological) taxonomy, especially in regards to the not-uncommon practice of using spine morphology in delineating fossil taxa. Overall, these insights point to the enormous potential of using culturing studies of extant, cyst-producing dinoflagellates to address issues of paleontological significance.

Ultrastructural examination of *L. polyedra* resting cysts formed in laboratory culture has shown, for the first time, the fine structure of the cell walls enclosing a living, paleontologically-significant resting cyst. Unfortunately, difficulties associated with fixation and infiltration of these thick-walled structures precluded an in-depth investigation of the ultrastructural dynamics underlying the morphological development described above. Preliminary results, however, confirm earlier speculation that only the outermost wall of the *L. polyedra* resting cyst is normally preserved in the fossil record. This outer wall (including spines) appears constructed of closely appressed structural units, an ultrastructural style apparently widespread among species related to *L. polyedra*.

Results from the extensive chemical characterization of the resistant biopolymer in the outermost cell wall of *L. polyedra* resting cysts are presented in Chapters 3 and 4. These studies represent the first rigorous analysis of the "fossilizable" biopolymer(s) produced by dinoflagellates. Both thermal (pyrolysis) and chemical (CuO oxidation) dissociation techniques yielded suites of products consistent with a macromolecular substance composed significantly of aromatic components. In addition, the relative abundance of carboxylated phenols among resting cyst CuO oxidation products indicated that aromatic structural units in the dinoflagellate material may be largely carbon-carbon linked, probably directly through aromatic nuclei. Such a "condensed" arrangement may be, in part, responsible for the remarkable resistance of the dinoflagellate resting cyst wall biopolymer. Overall, the aromatic signature of *L. polyedra* resting cyst wall material can be clearly distinguished from that of both pollen wall "sporopollenin" and classical lignin.

Although some short chain carboxylic acids are generated during CuO oxidation, there is little evidence obtained by dissociation techniques to suggest the significant

presence of extended polymethylenic elements in this macromolecular substance. As a result, the dinoflagellate material appears fundamentally different from the highly aliphatic "algaenans" recently identified in the cell walls of several chlorophyte species. Interestingly, pyrolysis (Py-GC/MS) of resting cyst wall material produced an abundance of prist-1-ene. This strongly suggests the presence of bound tocopherols which may play an important structural role in the resistant cell wall biopolymer. Analysis of lipids extracted from *L. polyedra* culture containing mostly vegetative cells revealed a series of even carbon numbered fatty acids (C_{14} - C_{24}), as well as sterols (including dinosterol and cholesterol), and a full suite of tocopherols. These compounds are present during construction of the resistant outer wall of the resting cyst, and could function as precursors to the resting cyst wall biopolymer. Another possibility, given the strong aromaticity predicted by the results of pyrolysis and CuO oxidation, is some contribution by aromatic amino acids in an analogous fashion to lignin biosynthesis.

Together, the analyses described in Chapters 3 and 4 represent an unprecedented level of chemical characterization of a resistant algal cell wall biopolymer, and ultimately point to a unique macromolecular substance. As a result, these studies provide the first chemical justification for the term "dinosporin", previously proposed to distinguish the highly resistant material comprising dinoflagellate resting cyst walls from other resistant cell wall biopolymers.

FUTURE WORK

Culturing

Over the course of this thesis, I have spent 6 years working intimately with laboratory cultures of *L. polyedra*. The many hours invested at the light microscope have afforded me a fairly detailed look at the nature of these cells in the laboratory environment. Ultimately, I am struck by how many fundamental questions remain unanswered. For example, at any given time during the growth curve (but particularly during plateau), one can observe cells exhibiting a variety of morphologies, sizes, and behavior. Sometimes it is extremely difficult, if not impossible, to reconcile these cell types with any of the predicted life cycle stages described in traditional models. A convenient answer, of course, is that these cells are stressed by the culturing environment and are hence unrepresentative of natural systems, but this does not seem to be the case in all circumstances. Although neither easy nor inexpensive, a fascinating study would be a cell-by-cell analysis via SEM, TEM, and LM of these various "stages" and perhaps comparison to cells isolated from field populations.

Another observation stemming from culturing dinoflagellates in laboratory batch cultures was a sometimes disturbing inconsistency of basic growth curve profile. This inconsistency could be due to a number of reasons, all of which seem to demand some level of future investigation. First, the natural seawater based media used during all phases of my thesis are relatively uncharacterized and undoubtedly show some seasonal variability. To compound this uncertainty, some of my early culturing efforts (prior to the work directly resulting in this thesis) involved experimenting with the addition of soil extract to the growth medium, a procedure which sometimes seemed to "make them grow better", but the cause of this enhancement was never determined. Although special pains were taken to maintain cultures in a stable physical environment (i.e. with respect to light

206

intensity, temperature, etc.), it is not known to what extent subtle changes in these conditions (i.e. *exact* position in the incubator, amount of mechanical disturbance resulting from occasionally moving culture tubes, length of time tubes sat on the bench during fluorescence measurement, etc.) might affect culture performance.

A good illustration of the sensitivity of batch cultures to unknown parameters relates to the growth of *Alexandrium tamarense* in carboy cultures, a routine operation in the WHOI dinoflagellate culturing facility. When this facility was located at the Clark Lab, these carboy cultures achieved maximum densities in the neighborhood of 10-12,000 cells per mL. In 1990, the facility (complete with walk-in incubators) was relocated to the Redfield Lab. Since the move, carboy cultures regularly reach densities of 30,000 cells per mL (D. Kulis, personal communication). Since the only difference between these culturing environments seems to be the source of air used to bubble through the carboys, "Redfield Air" has been (unofficially) attributed to have special growth properties. Although these observations suggest that physical and/or chemical "growth factors" exist, a systematic search for such factors would likely be lengthy (and extremely tedious). At the very least, however, such observations seem to encourage the consideration of fully defined, artificial seawater based media for use in future culturing efforts.

Cyst production in culture

If basic culturing still encompasses some degree of uncertainty, the phenomenon of resting cyst production appears to represent another order of magnitude of "unpredictability". Consider the following:

1. Only about 25% of the laboratory strains of *L. polyedra* established during the present work formed resting cysts in batch culture.

2. The "efficiency" of cyst production seemed to vary considerably among those cyst-producing strains. Similarly, with any given strain, this efficiency varied from transfer to transfer.

3. All initially cyst-producing strains eventually stopped producing cysts--some after only a month or two, others after two years.

4. In one case only, did a non-cyst-producing strain suddenly begin to generate resting cysts.

What triggers *L. polyedra* resting cyst formation in batch culture and in nature? What external and/or internal controls regulate this process after triggers have been activated? Some work has been done to answer these questions for other species (see Chapter 2 for references), but much remains to be done. For example, although *A. tamarense* cells (perhaps the most thoroughly studied species in terms of encystment behavior) grown in nutrient depleted media routinely produce resting cysts, this phenomenon seems to reliably occur only when batch cultures are confined to 50 mL culture tubes. If identical conditions are employed, with the exception of using flasks instead of tubes, batch cultures either fail to produce resting cysts, or the production is significantly reduced (D. Kulis, personal communication). On the other hand, natural plankton samples containing this and other species, when concentrated and placed in flasks with nutrient enriched medium, often produce resting cysts in significant amounts. From these "anecdotal" results and my own observations, cyst production in culture does not appear to be a simple, predictable phenomenon.

Why do cultures stop producing resting cysts? To what extent do cultures experience selection pressure against encystment? To what extent is resting cyst production influenced by "internal clocks" of the organism? These questions all deserve further inquiry. It is important to emphasize here that resting cyst formation requires certain basic conditions (all mating types present; cells physiologically healthy, etc.) and ultimately is the end product of a complex chain of events, including: (1) an initial trigger and trigger

reception, (2) initiation and successful completion of gametogenesis within the vegetative population, (3) gamete encounter and recognition, (4) successful gamete pairing and fusion, (5) development of planozygote, and (6) initiation of the planozygote to hypnozygote transition. A proper investigation into resting cyst formation would explore each of these steps in detail, since many (most?) are poorly understood at present.

Morphological development of resting cysts

Regarding the mechanism(s) of resting cyst formation employed by paleontologically-significant extant dinoflagellates, the work presented here represents the *only* description of this process, and this is limited to one species. As stated in Chapter 2, the existence of multiple developmental mechanisms among a group as diverse as the dinoflagellates is entirely possible and it remains for continued investigation of encystment in living species to shed more light on this issue. Logical targets are those species forming *Spiniferites*-type resting cysts (see Table 1.1). These morphotypes bear ornamentation (gonal / intergonal processes) which is fundamentally different from that of the *L. polyedra* resting cyst (nontabular processes) and very likely result from different cyst-building mechanisms.

Ultrastructure

The detailed account of *L. polyedra* resting cyst morphogenesis, as observed with the light microscope, provided in Chapter 2 raises numerous questions regarding the "internal workings" of the cell as it undergoes such a dramatic change in morphology, structure, and composition. What is the nature of the balloon-like membrane? How does it relate to the plasmalemma and/or vesicular membranes of the motile cell amphiesma? How/when does the planozygotic theca degrade? What is the source of the material

forming the outermost (preservable) resting cyst wall layer? How do the process globules originate? What is occurring *inside* the globules during spine formation? What rearrangements take place in the cytoplasm during these processes? How is the endospore deposited?

To properly answer these questions, one must examine the ultrastructure of cell stages intermediate in this developmental process, as well as the starting point (planozygotes) and final product (resting cysts). As mentioned previously, however, there are several obstacles in this endeavor. In the batch culture system described in Chapter 2, encystment was observed on a cell-by-cell basis. Additionally, the transition from planozygote to hypnozygote (especially the flurry of activity during the initiation stages) was very rapid. Finally, because of the nature of the cell covering, resting cysts are difficult subjects to prepare for transmission electron microscopy. Thus, although such a project is not impossible, it ultimately did not fit into the time frame of the present investigation. As a result, these studies remain for the future.

(Bio)chemistry

Isolation of resistant materials. As outlined in Chapters 3 and 4, nearly all of the chemical analytical techniques described in this thesis were applied to the solid residues obtained after solvent extraction, saponification, and acid hydrolysis (see Figure 3.1). Liquid extracts were investigated in only one case, the lipid analysis of *L. polyedra* (I)E1 (Chapter 4). To further assess the isolation procedures employed here, the remaining extracts of both dinoflagellate and pollens should be examined. "Fluff" materials also remain to be characterized, preferably by both optical and chemical means. Together, these additional studies would provide a more complete picture of all materials partitioned during the isolation procedures.

Another promising direction for future isolation work is the use of alternative processing strategies, particularly those which apply enzyme treatments to remove unwanted cellular materials. These methods have been employed by some pollen workers (see Chapter 3 for references) and show great potential for obtaining pure cell wall fractions while avoiding aggressive acid and base treatments.

Future culturing studies. Our inability to obtain a solid-state ^{13}C NMR spectrum from *L. polyedra* resting cyst wall material due to insufficient sample size was mentioned in Chapter 4. Because such NMR data would be extremely complimentary to the results already obtained, some additional effort in this direction is warranted. A potentially very fruitful study would involve culturing the organism in a ^{13}C-enriched environment. Incorporation of this isotope into the resting cyst wall would greatly enhance the sensitivity of the analysis, allowing a spectrum to be obtained from very small sample sizes.

Results from the various chemical analyses performed in this thesis have pointed towards several compounds (fatty acids, tocopherols, and aromatic amino acids) which may serve as precursors to the resistant biopolymer in the *L. polyedra* resting cyst cell wall. Other biochemicals (e.g. pigments, proteins), might also contibute in some way to cyst wall construction. To explore these possibilities, a number of investigations come to mind. First, the abundance and availability of potential precursors should be assessed over the growth curve of the organism, with special attention focused on cultures just prior to encystment. Second, suspected precursors could be labeled, and their incorporation by encysting cultures ascertained. Finally, it may be possible to synthesize wall analogs by polymerizing various mixtures of precursors; these synthetic polymers could then used as "standards" during subsequent chemical evaluation of natural materials.

Another avenue for exploring the formation of resting cyst wall biopolymer(s) in culture systems might involve the production of antibodies against this material. Ideally, both cell wall materials and their precursors could be labeled and visualized (via TEM

and/or Scanning Confocal Microscopy) in developing cysts, ultimately illuminating the fine-scale temporal and spatial dynamics of resting cyst wall formation.

Finally, since statements in the literature regarding the level of resistance displayed by dinoflagellate pellicle layers are somewhat ambiguous, these components of the motile cell amphiesma seem to invite future investigation. By inducing *pellicle cyst* formation among motile cell populations at various stages during the growth curve, quantities of wall material sufficient for analysis would potentially be obtainable if adequate isolation methods could be developed.

Resistant components of the *L. polyedra* cytoplasm. One of the more unexpected results of our chemical work was the discovery of what appear to be cytoplasmic components which survive the harsh treatments used to isolate resting cyst cell walls from other culture debris. What exactly are these bodies and what makes them so chemically resistant? The possible origin of these features as "accumulation bodies" is discussed in Chapter 3, and the suggestion of using electron microscopy to investigate their structure is mentioned briefly. Another possibility might involve using size fractionation techniques, possibly even flow cytometry, to obtain a pure fraction of these bodies for chemical analysis. Alternatively, the adaptation of analytical techniques to the microscopic scale (as has been done with IR spectroscopy) might eventually lead to analysis of individual particles. In this regard it is interesting to note that laser pyrolysis systems are currently being developed both at WHOI and elsewhere.

Chemotaxonomy. A primary motivation for undertaking the chemical analysis of dinoflagellate and pollen "sporopollenin-like" materials was to evaluate the possible development of a chemotaxonomy for "palynomorphs" (highly resistant, organic-walled microfossils, e.g. dinoflagellates, spores, pollen, acritarchs). The fact that resistant cell walls isolated from *L. polyedra* culture and pollen materials could be clearly distinguished from each other in the present investigation lends preliminary support to this notion. Important future studies, however, would extend these analyses to additional species of

dinoflagellates as well as other palynomorphs. If consistent (and useful) chemical differences can be established between materials produced by extant taxa, the next step would explore how these relationships change as materials are exposed to conditions of diagenesis and fossilization. Ultimately, it may be possible to apply a chemotaxonomy towards the many unresolved issues surrounding fossil palynomorphs. For example, based on our current understanding of the fossil record, the origin of the dinoflagellates is somewhat obscure. Most workers feel that a considerable number of the morphotypes regarded as acritarchs may in fact represent dinoflagellates, but this cannot be established on morphological criteria alone. If chemical differences between algal cell walls persist in the fossil record, future application of a chemotaxonomy may go a long way towards illuminating the origin and evolution of important algal groups.

Appendices

APPENDIX 1

Preparation of Isolated Resting Cysts for TEM

1. Isolate single cells from observation chamber using micropipette.

2. Transfer cells to 1 mL primary fixative in well of depression slide which is supported over ice in a covered glass petrie dish. Primary fixative: 2.5% glutaraldehyde, 2.0% paraformaldehyde, 0.25 M PIPES buffer, ph 7.2, Osmolarity approx. 1200. Total fixation time: 4 hrs. with frequent agitation (i.e. using micropipette to circulate fixative around cells).

3. Transfer cells to cold rinse buffer in a second well of depression slide. Rinse buffer: 0.4 M PIPES + 0.1 M sucrose; pH 7.2, Osm. 1200. Rinse time = 10 min. with gentle agitation.

4. BSA encapsulation. For each cell: (a) Chill 1" X 3" glass microscope slide on ice, (b) Deposit 2 drops of cold BSA solution (10% in rinse buffer) on slide, (c) Add 3 drops cold primary fixative which has been diluted 5-fold using rinse buffer, (d) Thoroughly mix BSA and fixative, (e) Quickly introduce single cell from rinse buffer: mix any carry-over buffer into BSA/fixative with eyelash probe while viewing under the microscope, (f) Keep slide on ice; allow 20-30 min. for aldehydes to fully cross-link the BSA.

5. Trim excess BSA with razor, leaving cells in small blocks.

6. Place each BSA block in its own carrier assembly. These assemblies are homemade versions of Pelco's "Tissue Carrier Sets" (page 120 of Pelco Catalog 8). My version utilizes lengths of glass tubing which fit into notched segments of teflon tubing. The teflon ring holds a piece of nitex mesh which supports the BSA cube. Three of these assemblies fit into one 20 mL glass scintillation vial. All subsequent processing involves adding agents to vial as a whole; specimen carriers prevent any direct mechanical disturbance of encapsulated cells.

7. Three 10 min. post-encapsulation washes in rinse buffer. This step and those following (up to resin infiltration) accomplished with vials rotating on Pelco Infiltron kept in refrigerator.

8. Post fix: 1.5 hrs in 1% OsO_4, 0.3 M PIPES, 0.4 M sucrose (pH 7.2, osm. 1200).

9. One wash (10 min.) with rinse buffer.

10. Three washes (10 min. each) with Milli-Q water.

11. En bloc stain (1.5 hrs.) with saturated aqueous uranyl acetate.

12. Three washes (10 min. each) with Milli-Q water.

13. Dehydration in graded ethanol series. 7 min. each in 25%, 50%, 70%, 85%, 95%, 100%, 100%, 100%.

14. Infiltration in Spurr resin (medium hardness formulation). Initial treatments in Spurr without addition of DMAE hardener.

10%	Spurr without DMAE	6 hrs.
25%	" "	6 hrs.
50%	" "	12 hrs.
75%	" "	24 hrs.
100%	" "	24 hrs.
100%	with DMAE	12 hrs.
100%	" "	12 hrs.

NOTE: Starting with the 12 hr. 50% treatment, vials alternated (every few hrs during the day) between rotation on the Infiltron, and a vacuum dessicator kept at approximately half an atmosphere.

15. Embedding. Each infiltrated BSA block individually flat-embedded in a thin layer of fresh Spurr's between two glass microscope slides previously treated with liquid release agent.

16. Polymerization. 12 hrs. at 70 degrees C.

17. After polymerization, glass slides pried apart. Excess resin trimmed away (accomplished with a razor slightly heated in a bunsen burner flame) leaving each specimen in thin wafer about 1 cm. square.

18. Resin wafers super-glued to blank resin cylinders (formed by polymerizing Spurr's resin in modified BEEM capsules). Trim blocks with razor to prepare for sectioning.

APPENDIX 2

Acetolysis of *L. polyedra* Resting Cyst and Pollen Materials: Methods and FTIR spectra

Methods: Initial materials (*L. polyedra* culture, Juniper pollen, and Oak pollen; see Chapter 3) were washed in glacial acetic acid, recovered by centrifugation, and then boiled with stirring for 20 minutes in concentrated H_2SO_4 / acetic anhydride (approx. 1/10 v/v). Samples were then centrifuged, and the supernatant discarded. Subsequently, residues were washed again in glacial acetic acid, followed by 3 washes in ddH_2O. After pollen samples were sonified in ddH_2O (20 minutes at room temperature), the above procedure was repeated for all samples. Residues were analyzed by optical microscopy, FTIR microscopy, and Py-MS as described in Chapter 3. Time contraints during the final stages of thesis preparation allowed only the inclusion of FTIR results (Figures A.1, A.2, and A.3) in this appendix.
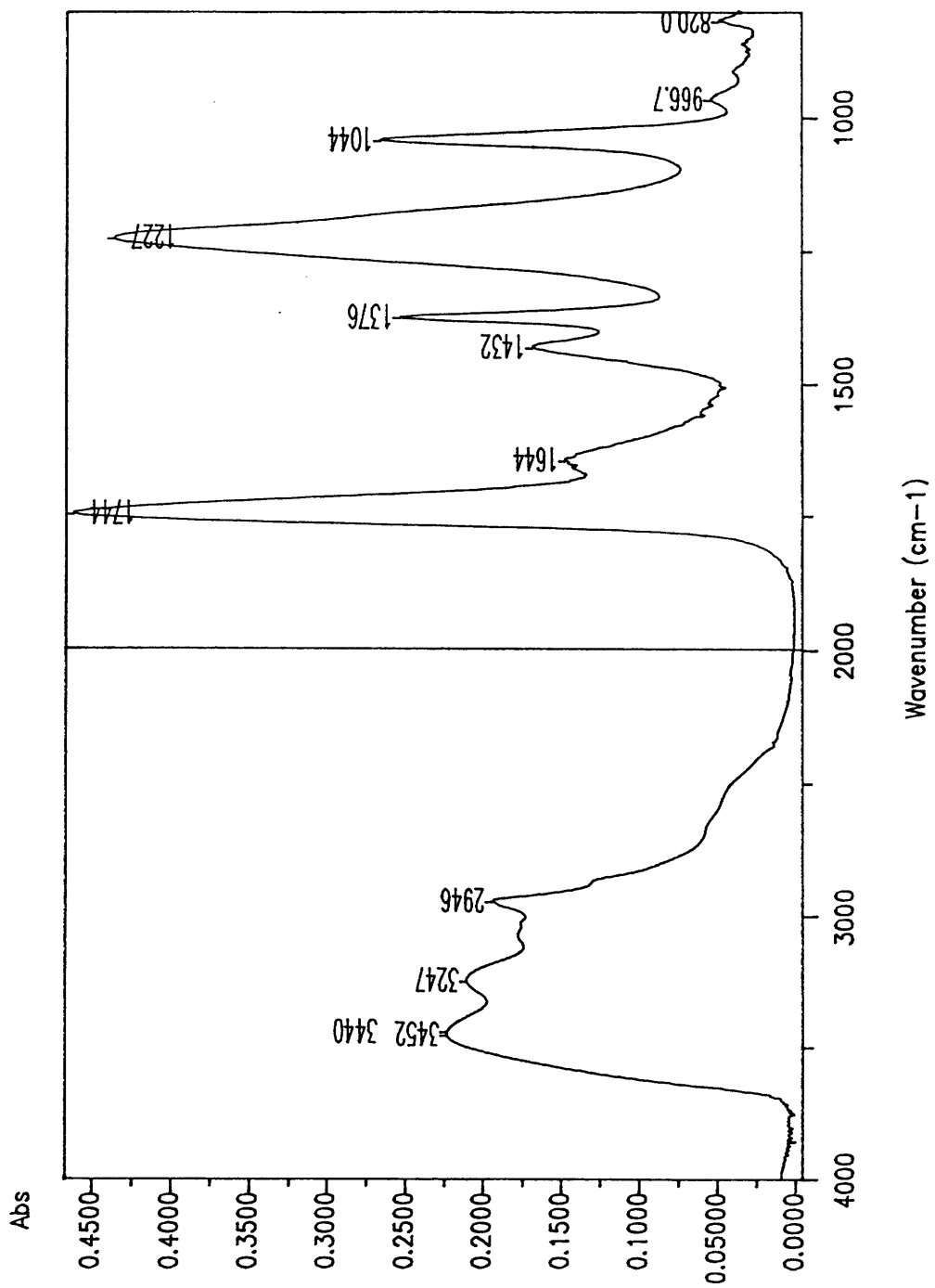
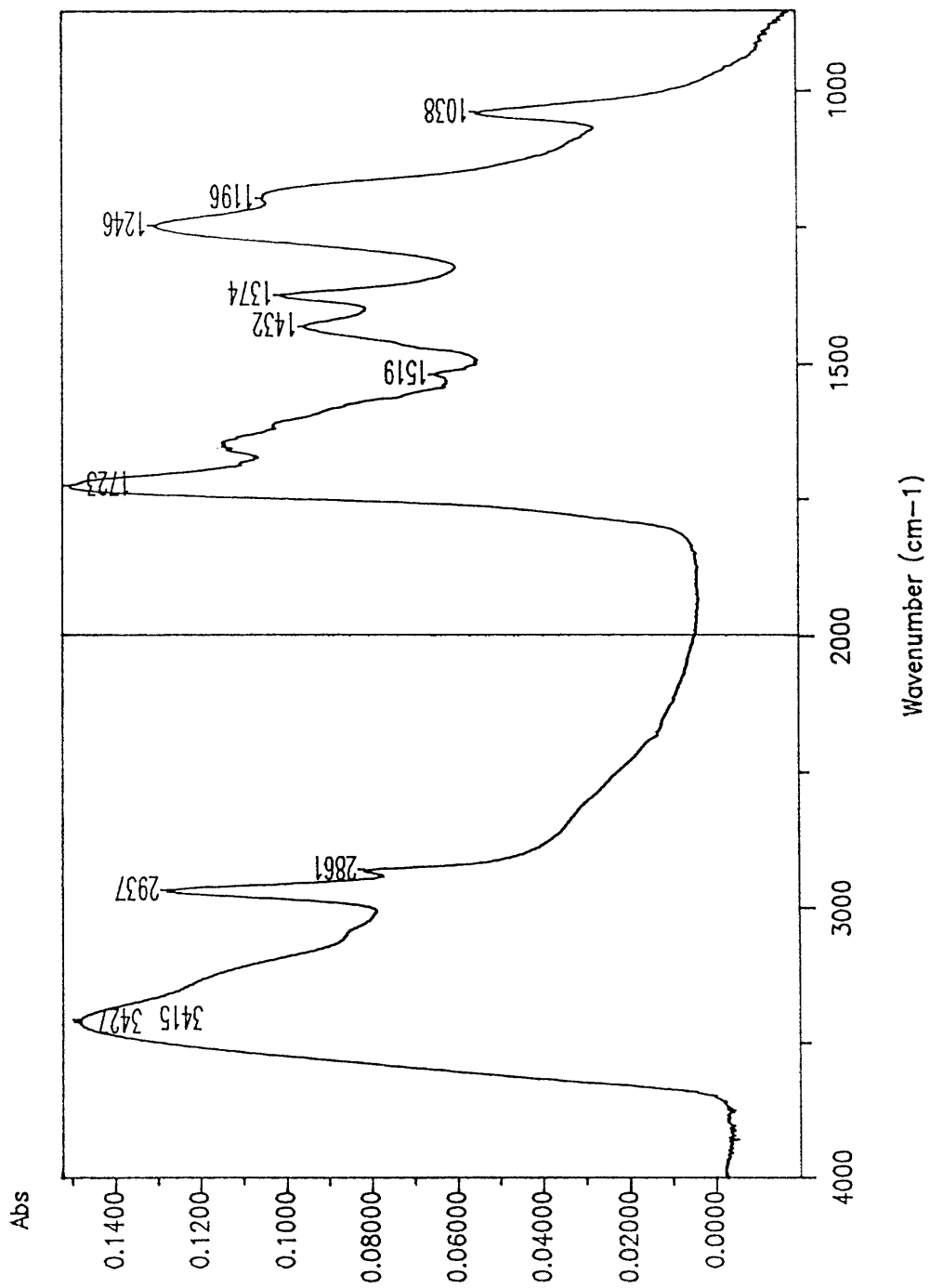FIGURE A.1 FTIR spectrum of acetolyzed *L. polyedra* resting cysts
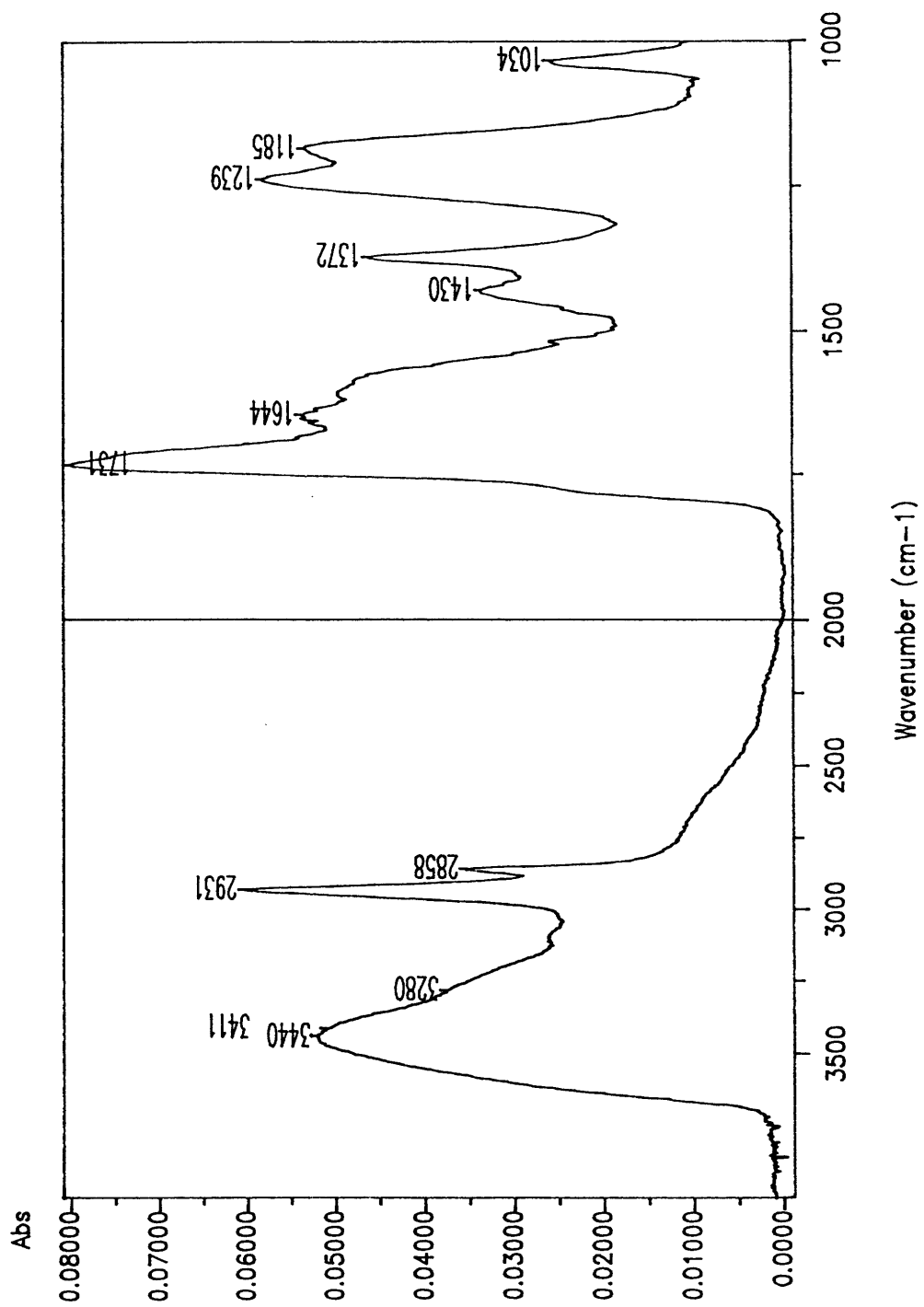
FIGURE A.2 FTIR spectrum of acetolyzed Juniper pollen

FIGURE A.3 FTIR spectrum of acetolyzed Oak pollen